CONTROLLERS FOR THE PERFORMANCE ENHANCEMENT OF AN ISOLATED ASYNCHRONOUS GENERATOR

THESIS

Submitted in fulfillment of the requirement of the degree of

DOCTOR OF PHILOSOPHY

to

YMCA UNIVERSITY OF SCIENCE & TECHNOLOGY
by

SHAKUNTLA

Registration No: YMCAUST/PH 01/2010

Under the Supervision of

Professor S. K AGARWAL
Deptt. of Electronics Engineering
YMCAUST, Faridabad

Professor K. S SANDHU
Deptt. of Electrical Engineering
National Institute of Technology
Kurukshetra

DEPARTMENT OF ELECTRICAL ENGINEERING

Faculty of Engineering & Technology
YMCA University of Science & Technology
Sector-6, Mathura Road, Faridabad, Haryana, India

SEPTEMBER 2018

DECLARATION

I hereby declare that this thesis entitled "**CONTROLLERS FOR THE PERFORMANCE ENHANCEMENT OF AN ISOLATED ASYNCHRONOUS GENERATOR**" by **SHAKUNTLA**, being submitted in fulfillment of the requirements for the Degree of Doctor of Philosophy in **ELECTRICAL ENGINEERING** under faculty of Engineering & Technology, YMCA University of Science & Technology Faridabad, during the academic year 2018-2019, is a bona fide record of my original work carried out under guidance and supervision of **Dr. S. K AGARWAL**, Professor, Department of Electronics Engineering, YMCA University of Science and Technology, Faridabad and **Dr. K. S SANDHU**, Professor, Department of Electrical Engineering , National Institute of Technology (NIT), Kurukshetra and has not been presented elsewhere.

I further declare that the thesis does not contain part of any work which has been submitted for the award of any degree either in this university or in any other university.

(Shakuntla)

Registration No: YMCAUST/PH01/2010

CERTIFICATE

This is to certify that this Thesis entitled **"CONTROLLERS FOR THE PERFORMANCE ENHANCEMENT OF AN ISOLATED ASYNCHRONOUS GENERATOR"** by **SHAKUNTLA**, being submitted in fulfillment of the requirements for the Degree of Doctor of Philosophy in **ELECTRICAL ENGINEERING** under faculty of Engineering & Technology YMCA University of Science & Technology Faridabad, during the academic year 2018-2019, is a bonafide record of work carried out under our guidance and supervision.

We further declare that to the best of our knowledge, the thesis does not contain part of any work which has been submitted for the award of any degree either in this university or in any other university.

Professor S. K Agarwal
Department of Electronics Engineering
YMCA University of Science & Tech.
Faridabad, INDIA

Professor K. S Sandhu
Department of Electrical Engineering
National Institute of Technology
Kurukshetra, INDIA

(Professor Rajesh Ahuja)
Chairman, Department of Electrical Engineering
YMCA University of Science & Technology
Faridabad, INDIA

The Ph.D. viva-voce examination of Shakuntla Research Scholar has been held on …….

(Signature of Supervisors) (Signature of Chairman) (Signature of External Examiner)

ACKNOWLEDGEMENT

I would like to take this opportunity to express my heartfelt gratitude to my guide **Prof. S. K Agarwal**, Professor, Department of Electronics Engineering, YMCA University of Science & Technology and **Prof. K. S Sandhu**, Professor Dept. of Electrical Engineering, National Institute of Technology (NIT), Kurukshetra who gave me a lifetime opportunity to undertake my PhD work under their guidance. They have been my guide in all true senses from the very beginning of the research to its completion. They constantly motivated me and offered invaluable suggestions during my research work. Their support and constant motivation has been a source of inspiration to me throughout this research.

I also express my sincere thanks to Dr. Rajesh kumar Ahuja, Chairperson Electrical Engineering department, YMCA University of Science and Technology for providing all necessary research facilities in the department.

I am also thankful to Mr. Rambhajan (M. Tech Student) and Mr. Avinish Gaur (Lab Technician) and all other Laboratory staff that has helped me performing the experiments in the lab. Their co-operation and support was instrumental in findings of the research.

My thanks are due to my family members who have constantly encouraged me to complete the research work. I have no words for my husband Mr. Om Parkash Boora, and my dear sons Samarth and Krishav who have made huge sacrifices to make my PhD dream come true. Without their support, I could not have accomplished this work. My parents were equally the driving force behind this endeavor, who has always taught me to work hard in life. I also thank to all those who helped me directly or indirectly in the completion of my thesis.

Lastly but not the least, I am indebted to my University, YMCA University of Science and Technology, Faridabad for supporting me throughout the PhD program.

(Shakuntla)

Registration No: YMCAUST/PH01/2010

ABSTRACT

It is an established and very well known fact that an ordinary asynchronous motor can operate as a generator when it is mechanically rotated by a prime mover and a.c capacitor bank of appropriate size and configuration (Y or Δ) is connected across its stator terminals. Machine under such operation is called self-excited induction generator (SEIG). The purpose of using the capacitor bank is to provide adequate reactive power needed for excitation of the generator to produce the rotating nature magnetic field as well as for meeting the reactive var demand of the load. Alternatively, the generator can be connected to an infinite bus or grid supply to draw reactive power from the grid. The voltage and frequency of a grid connected asynchronous generator are fixed and depends upon the grid voltage and frequency. Thus, the analysis of a grid connected generator becomes much easier and hence does not require any kind of numerical technique or optimization based technique to evaluate its performance. On the other hand, The SEIG operates in isolation from the grid and hence is also termed as isolated asynchronous generator (IAG). The voltage and frequency of an IAG are not fixed but are affected by various factors such as prime mover speed, no-load characteristics (magnetization characteristic), excitation capacitor, load etc. Hence the analysis of an IAG is much more complex, tedious and difficult than that of a grid connected generator. It is realized that the analysis of IAG during self-excitation phenomenon, steady state and transient conditions is of utmost importance from practical aspects. This preliminary study provides the data requisites for the design of controllers for an IAG for voltage and frequency support.

In the earlier published research work, the performance of IAG under steady state analysis of IAG has been computed using the concepts of loop (loop impedance) and node (nodal admittance) for problem description and various numerical techniques like Newton Raphson method, secant method, golden section method etc has been recommended for the solution of non-linear equations attained after problem formulation. Both methods prove to be quite efficient in determining the steady state performance of the IAG. But these methods sometimes demand lengthy calculations in evaluating the coefficients of higher degree polynomial. Moreover, these coefficients are model specific and get modified even with slight modification in the equivalent

circuit model. Also, the degree of the polynomial varies on insertion of some elements in equivalent circuit model e.g. core loss resistance R_{cl}, series and shunt capacitance X_{sc}. Hence, these methods prove to be system specific, inflexible and are time consuming also.

In the present thesis, the steady state performance of three-phase IAG furnishing 3-phase has been analyzed and investigated using a MATLAB based optimization technique fsolve for the solution of non linear equation. The problem formulation for a 3-phase IAG furnishing 3-phase load is based on loop impedance method. The experimental investigations have been attained on a laboratory available asynchronous machine set of 3.73 kW coupled with a dc shunt machine (prime mover). The good association between the analytical and experimental investigations authenticates the implementation of the proposed technique. The results under transient condition are captured using Fluke-435-B power analyzer.

Above 3.73 kW (5HP), 3-phase IAG is preferred due to economical advantages over single-phase IAG of the equivalent rating. These advantages includes low cost, more readily available and possesses higher efficiency that of single-phase machine of equivalent rating.

It is concluded from the literature that the existing conventional and optimization based analysis of 3- Φ IAG furnishing 1- Φ load demanded lengthy calculations and algorithm implementation of numerical techniques in software. But in this thesis, a simple optimization technique fsolve is implemented to analyze the steady state performance of 3- Φ IAG for meeting 1- Φ load in remote off-grid rural sites. The simulated results have been verified experimentally on a 5 HP asynchronous machine available in the laboratory.

The IAG however suffers from certain drawbacks. The main disadvantages involved are change in supply frequency at resistive loads and poor voltage regulation under varying load conditions even for fixed prime mover speed. Voltage regulation may be corrected by the use of voltage regulators. Hence, there is a need of some simple and cost effective controller which can support both voltage and frequency under load conditions.

Most of the voltage and frequency controllers for IAG reported in literature employed traditional PI type controllers because of their simple design. The major drawback was in attaining the optimal performance when the control criteria consist of more than one PI controllers. But, today different types of intelligent controllers are fetching the attention of researcher due to its enormous advantages over traditional PI controllers. In the present thesis, a fuzzy logic based Mamdani type approach is discussed and implemented because such controllers can handle non-linearity, uncertainty, noisy signals and also do not require any kind of mathematical model of the system. In this thesis, an attempt is made for the first time to accomplish the performance of an IAG using both PI and FL based controller to support its voltage and frequency under balanced/ unbalanced operating conditions.

The designing, implementation and testing of PI and fuzzy logic (Mamdani type FIS) based Electronic generator load controller (EGLC) has been carried out in MATLAB for an IAG subjected to varying static load situation. The transient and the steady state behavior of IAG-EGLC system has been examined and tested under different operating condition of resistive, R-L and non-linear load to demonstrate the efficacy of FLC controller as compared to traditional PI controller. The performance enhancement of IAG has been attained relating to rise time, settling time, overshoot and THD values of generated current and voltage, voltage and frequency support using the planned FLC.

A PWM IC-3524 based EGLC for an IAG furnishing 1-phase load has been practically designed, tested and implemented in the laboratory for a 5 HP asynchronous machine. The outcomes have been verified using a hardware model of the IC-3524 based EGLC developed in laboratory to testify the expected results. This work provides a practical experience of installing EGLC for field applications.

It is observed that mostly conventional PI controllers are suggested for IAG to provide voltage and frequency support. The main aspiration behind its use is its simplicity only. The main problem encountered with these controllers is in attaining the optimized values of the gains of the PI controllers considered in the control strategy to attain desired performance while the system is having uncertainty.

Whereas in the present work, the designing and implementation of a Mamdani and Sugeno type Non conventional FL based 3-legged VSI controller for voltage and frequency support of an IAG has been elaborated. The simulated outcomes of the performance characteristics of an IAG have been obtained using Mamdani and Sugeno type FL based controller. Then the comparison of various outcomes based on conventional PI and both FL based controllers has been made to testify that the recommended controller is superior to the PI method and is well suited for electrical power generation (EPG) in grid isolated areas .

The work carried out motivates the use of more and more intelligent controllers for attaining the performance enhancement of IAG in terms of voltage and frequency so that IAG acts as a good quality voltage source for meeting the increased load requirement using renewable energy potential in near future and for electrifying the remote sites.

TABLE OF CONTENTS

LIST OF TABLES

LIST OF FIGURES

LIST OF SYMBOLS

d	Direct axis
q	Quadrature axis
s	Stator variable
r	Rotor variable
F_{ij}	Flux linkage (i=q or d & j=s or r)
V_{qst}, V_{dst}	q and d- axis stator voltage (V)
V_{qro}, V_{dro}	q and d-axis rotor voltages (V)
F_{md}, F_{mq}	q and d-axis magnetizing flux linkages (V)
i_{qst}, i_{dst}	q and d-axis stator currents (A)
i_{qro}, i_{dro}	q and d-axis rotor currents (A)
P	No of poles
J	Moment of inertia
T_e	Electrical output torque (N-m)
T_L	Load torque (N-m)
w_e	Stator angular electrical frequency
w_b	Motor angular electrical base frequency
w_{rs}	Rotational speed of the prime mover
X_{sc}	Shunt capacitor reactance
X_{mg}	Magnetizing reactance (Ω)
C_{sc}	Shunt connected capacitor (µF)
C_{scu}, C_{scl}	Upper and lower limits for shunt connected capacitor
v	Speed (rpm)
Z_{si}	Stator input impedance (Ω)
Z_{ri}	Rotor input impedance (Ω)
Z_{li}	Load input impedance (Ω)
I_{ro}	Rotor current (A)
I_{lo}	Load current (A)
P_{out}	Output power (kW or W)
Y_{la}, Y_{lb}, Y_{lc}	Admittance of load across winding a, b and c
G, G_{la}, G_{lb}, G_{lc}	Conductance, conductance of load across winding a, b and c

$\varkappa$, $\varkappa_{ca}$, $\varkappa_{cb}$, $\varkappa_{cc}$	Susceptance, capacitive susceptance of phase a, b and c
V_{wa}, V_{wb}, V_{wc}	Voltage of winding a, b, c
I_{wa}, I_{wb}, I_{wc}	Current of winding a, b, c
V_{os},V_{ps},V_{ns}	Zero sequence voltage, positive sequence voltage and negative sequence voltage.
k	$e^{(j2\Pi/3)}$
Z_{ps}, Z_{ns}	Positive and negative sequence impedance (Ω)
V_{ps}, V_{ns}	Positive and negative sequence voltage (V)
I_{ps}, I_{ns}	Positive and negative sequence current (A)
K_{vuf}	Voltage unbalance factor
X_{mg1}	Positive sequence magnetizing reactance (Ω)
X_{mg2}	Negative sequence magnetizing reactance (Ω)
V_{g1}	Positive sequence air-gap voltage (V)
V_{g2}	Negative sequence air-gap voltage (V)
F_y	Generated frequency (Hz)
f_{bv}	Base value of frequency (Hz)
P_{out}	Power delivered to the load by the IAG (kW or W)
n	No of phases
N_{bv}	Base value of speed (rpm)
Z_{bv}	Base value of impedance (Ω)
V_{bv}	Base value of voltage (V)
I_{bv}	Base value of current (A)
Z_{li}	Load impedance (Ω)
Z_{si}	Stator impedance (Ω)
Z_{ri}	Rotor impedance (Ω)
X_{lst}, X_{lro}	Stator reactance, Rotor reactance (referred to stator)
R_{st}, R_{ro}	Stator resistance, Rotor resistance (referred to stator)
X_{le}	Leakage reactance (Ω)
X_{mg}	Magnetizing reactance (Ω)
X_{sc}	Excitation reactance at base frequency (Ω)
C_{sc}	Shunt excitation capacitance (μF)
V_{gp}	Air-gap voltage (V)

T_{ec}	Electromagnetic torque (N. m)
N	Prime-mover speed (rpm)
P_{iag}	Power generated by the IAG (kW or W)
P_{dld}	Dump load power (kW or W)
P_{cld}	Consumer load power (kW or W)
$\mathbf{V}_{dco}$	dc output side voltage (V)
$V_{abcg\ (L\text{-}L)}$	R.m.s value of the line-to-line voltage (V)
V_{pk}	Peak value of three-phase ac input side voltage (V)
I_{pk}	Peak value of three-phase ac input side current peak value (A)
I_{aca}	Active component of three-phase ac input side current (A)
I_{dac}	Three-phase ac input side current of EGLC (A)
R_{dld}	Dump load resistance (Ω)
C_{dcl}	Filtering capacitor (μF)
V_{abcg}	Three-phase IAG voltage (V)
I_{abcg}	Three-phase IAG current (A)
I_{al}, I_{bl}, I_{cl}	Resistive load currents (A)
I_{ac}, I_{bc}, I_{cc}	EGLC currents (A)
V_{ter}	IAG ac voltage magnitude (V)
V_{pac}	IAG peak ac voltage (V)
S_{ap}	Apparent power (kVA)
P_{ap}	Active power (kW)
Q_{ap}	Reactive power (kVAR)
I_s	Peak value of VSI curent (A)
$I_{Lripplepk\text{-}pk}$	Current ripple through filter inductor L (A)
V_{db}	dc voltage for VSI (V)
m_i	Modulation index
L_{af}, L_{bf}, L_{cf}	Filtering inductance of line a, b and c for VSI (mH)
$V_{dbripple}$	Voltage ripple in V_{db} (V)
I_{avg}	Average value of current flowing through the 3-legged VSI (A)
C_{db}	Dc capacitance (μF)
f_s	Carrier frequency (kHz)

LIST OF PHOTOGRAPHS

ACRONYMS

IAG	Isolated Asynchronous Generator
SEIG	Self-excited induction generator
ELC	Electronic Load Controller
STATCOM	Static compensator
EGLC	Electronic Generator Load Controller
VFC	Voltage and frequency controller
FIS	Fuzzy inference system
FL	Fuzzy logic
VSI	Voltage source inverter
CC-VSI	Current controlled voltage source inverter
IELC	Improved electronic load controller
SRF	Synchronous reference frame
SVC	Static var compensator
TCR	Thyristor controlled reactor
TSC	Thyristor switched capacitor
STATCON	Static condenser

CHAPTER 1

INTRODUCTION

1.1 GENERAL

Electrical energy was generated earlier in 1930's using conventional energy sources with synchronous generator. But after 1947, due to depletion, exploitation and ever increasing rates of non-renewable energy sources, the use of renewable energy sources with asynchronous generator for electrical power generation has been recommended by the energy experts. Today, the electrical energy is generated with the help of asynchronous generator by utilising the renewable energy potential freely available in the remote and off-grid areas. The conventionally used synchronous generator is being replaced by the asynchronous generator because it possesses various critical features. A simple asynchronous machine can be utilised as an asynchronous generator by simply connecting capacitor bank of suitable value across its stator terminals. The various critical features of asynchronous machine (squirrel cage) are its robust construction, design simplicity, economical, reliability, self-starting and high efficiency has attributed to its day to day popularity for its use in industrial and household applications [1-4]. Hence, to understand the concept of working of asynchronous generator, one should model it mathematically in different reference frames.

Dynamic modelling is requisite for carrying out the analysis of an asynchronous machine in order to understand its behaviour when subjected to steady state and transient phenomenon. This analysis is also requisite for accessing the performance of the asynchronous motor drives with the various control techniques like vector control or DTC (direct control) drives.

During starting conditions, the asynchronous motor draws very high starting currents which results into voltage drops, fluctuating nature torques and injects harmonics in the system [5]. Therefore, it is requisite to model the asynchronous machine in order to investigate the various undesirable phenomenons occurring during starting. The d-q model has been tested and proven accurate and reliable for investigating the behaviour of the machine under transient state [5, 6]. The d-q axis

rotation preferably depends on the three speeds or three different types of reference frames:

- When the d-q axes are stationary i.e. do not rotate and hence it is termed as stationary reference frame.
- When the d-q axes are rotating at the rotor speed and hence are termed as rotor reference frame.
- When the d-q axes rotating at the synchronous speed and hence are termed as synchronously rotating reference frame [7].

In synchronously rotating frame, the variables are constant under steady state and do not follow sinusoidal variation with time. In this chapter, the modelling of the asynchronous machine is carried out in synchronously rotating frame [8] and the impact of changing load torque in steps on output variables are visualised.

1.2 MODELING OF ASYNCHRONOUS MACHINE IN D-Q AXIS [8]

The equivalent circuit representation of the asynchronous machine (AM) in d^e-q^e axis is illustrated in Fig. 1.1. The flux linkage based modelling equation after rearranging can be represented as:

$$dF_{qst}/dt = \omega_b\left[V_{qst} - (\omega_e/\omega_b)\,F_{dst} - (R_{st}/X_{lst})\left(F_{qst} - F_{mq}\right)\right] \tag{1.1}$$

$$dF_{dst}/dt = \omega_b\left[V_{dst} - (\omega_e/\omega_b)\,F_{qst} - (R_{st}/X_{lst})(F_{dst} - F_{md})\right] \tag{1.2}$$

$$dF_{qro}/dt = -\omega_b\left[\{(\omega_e - \omega_r)/\omega_b\}F_{dro} + (R_{ro}/X_{lro})\left(F_{qro} - F_{mq}\right)\right] \tag{1.3}$$

$$dF_{qro}/dt = -\omega_b\left[\{(\omega_e - \omega_r)/\omega_b\}F_{qro} + (R_{ro}/X_{lro})\,(F_{dro} - F_{md})\right] \tag{1.4}$$

$$F_{mq} = X^*_{mg}\left[(F_{qst}/X_{lst}) + (F_{qro}/X_{lro})\,\right] \tag{1.5}$$

$$F_{md} = X^*_{mg}[(F_{dst}/X_{lst}) + (F_{dro}/X_{lro})\,] \tag{1.6}$$

$$i_{qst} = (1/X_{lst})\left(F_{qst} - F_{mq}\right) \tag{1.7}$$

$$i_{qro} = (1/X_{lro})\left(F_{qro} - F_{mq}\right) \tag{1.8}$$

$$i_{dst} = (1/X_{lst})\,(F_{ds} - F_{md}) \tag{1.9}$$

$$i_{dro} = (1/X_{lro})\,(F_{dro} - F_{md}) \tag{1.10}$$

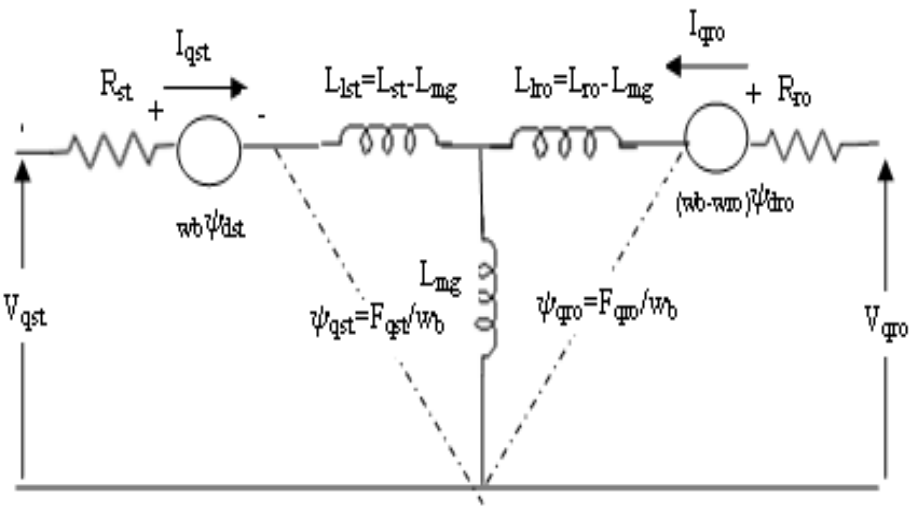

(a)

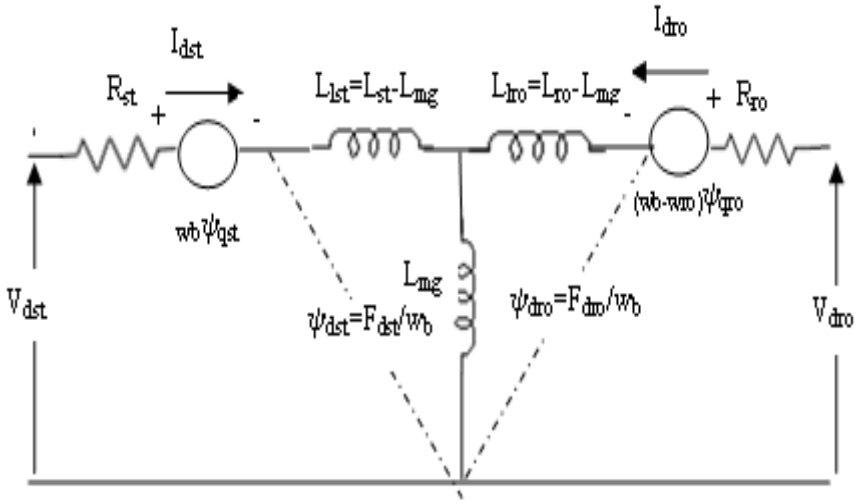

(b)

Fig. 1.1 Dynamic d^e- q^e axis based equivalent circuit representation of asynchronous machine (a) q^e-axis, (b) d^e – axis circuit.

$$T_e = \frac{3}{2}(P/2)\,(1/\omega_b)\left(F_{dst}i_{qst} - F_{qst}i_{dst}\right) \tag{1.11}$$

$$T_e - T_L = J(2/P)\,dw_r/dt \tag{1.12}$$

In case of a squirrel cage rotor type asynchronous machine the q-axis and d-axis voltages of the rotor (v_{qro} and v_{dro}) in Eq. (1.3) and (1.4) are equated or substituted to zero. The complete d-q model of the asynchronous machine is constituted with the aid of five differential equations. The state space approach is

adopted here for the solution of differential equations.For attaining the equations in state space representation form substitute the values of F_{mq} and F_{md} from Eq. (1.5) and Eq. (1.6) into Eq. (1.1-1.4) and combining the identical terms together. Then, the state space representation form of Eq. (1.1-1.4 and 1.12) becomes

$$dF_{qst}/dt = \omega_b \left[V_{qst} - \frac{\omega_e}{\omega_b} F_{dst} + \frac{R_{st}}{X_{lst}} \left(\frac{X^*_{mg}}{X_{lro}} F_{qro} + \left(\frac{X^*_{mg}}{X_{lst}} - 1\right) F_{qst}\right)\right] \quad (1.13)$$

$$dF_{dst}/dt = \omega_b \left[V_{dst} + \frac{\omega_e}{\omega_b} F_{qst} + \frac{R_{st}}{X_{lst}} \left(\frac{X^*_{mg}}{X_{lro}} F_{dro} + \left(\frac{X^*_{mg}}{X_{lst}} - 1\right) F_{dst}\right)\right] \quad (1.14)$$

$$dF_{qro}/dt = \omega_b \left[-\frac{(w_e - w_r)}{\omega_b} F_{dro} + \frac{R_{ro}}{X_{lro}} \left(\frac{X^*_{mg}}{X_{lst}} F_{qst} + \left(\frac{X^*_{mg}}{X_{lro}} - 1\right) F_{qro}\right)\right] \quad (1.15)$$

$$dF_{dro}/dt = \omega_b \left[\frac{(w_e - w_r)}{\omega_b} F_{qro} + \frac{R_{ro}}{X_{lro}} \left(\frac{X^*_{mg}}{X_{lst}} F_{dst} + \left(\frac{X^*_{mg}}{X_{lro}} - 1\right) F_{dro}\right)\right] \quad (1.16)$$

$$(dw_r)/dt = (P/(2 * J))(T_e - T_L) \quad (1.17)$$

1.2.1 Implementation of Dynamic (d-q) Modelling of Asynchronous Machine

The 3-phase voltages, its frequency and the load torque (T_L) acts as the inputs of an asynchronous machine whereas the 3-phase currents, the electromagnetic torque (T_e) and the rotor speed acts as the outputs of the machine.

The d-q model of asynchronous machine is depicted in Fig. 1.2 and is constituted with the aid of five blocks (B.1 to B.5):

B. 1. Conversion block (o-n)

$$\begin{bmatrix} V_{an} \\ V_{bn} \\ V_{cn} \end{bmatrix} = \begin{bmatrix} 2/3 & -1/3 & -1/3 \\ -1/3 & 2/3 & -1/3 \\ -1/3 & -1/3 & 2/3 \end{bmatrix} \begin{bmatrix} V_{ao} \\ V_{bo} \\ V_{co} \end{bmatrix} \quad (1.18)$$

B. 2. Unit vector evaluation block

$$\theta_e = \int w_e \, dt \quad (1.19)$$

B. 3. Conversion block (abc - syn)

$$\begin{bmatrix} V^s_{qst} \\ V^s_{dst} \end{bmatrix} = \begin{bmatrix} 1 & 0 & 0 \\ 0 & -1/\sqrt{3} & -1/\sqrt{3} \end{bmatrix} \begin{bmatrix} V_{an} \\ V_{bn} \\ V_{cn} \end{bmatrix} \quad (1.20)$$

$$\begin{Bmatrix} V_{qst} & = V^s_{qst}\cos\theta_e - V^s_{dst}\sin\theta_e \\ V_{dst} & = V^s_{qst}\sin\theta_e + V^s_{dst}\cos\theta_e \end{Bmatrix} \quad (1.21)$$

B. 4. An asynchronous machine q-d model block is built using Eq. (1.5-1.10) and Eq. (1.13-1.17)

B.5. Conversion block (syn - abc) is built using the following equations

$$\begin{Bmatrix} i^s_{qst} & = V_{qst}\cos\theta_e + V_{dst}\sin\theta_e \\ i^s_{dst} & = -V_{qst}\sin\theta_e + V_{dst}\cos\theta_e \end{Bmatrix} \tag{1.22}$$

$$\begin{bmatrix} i_a \\ i_b \\ i_c \end{bmatrix} = \begin{bmatrix} 1 & 0 \\ \frac{-1}{2} & -\frac{\sqrt{3}}{2} \\ \frac{-1}{2} & \frac{\sqrt{3}}{2} \end{bmatrix} \begin{bmatrix} i^s_{qst} \\ i^s_{dst} \end{bmatrix} \tag{1.23}$$

1.2.2 Simulation Based Performance Outcomes

Asynchronous machines of 3 HP and 2250 HP [Appendix-A] are simulated using the dynamic model thus obtained. The simulated outcomes of the 3 HP are illustrated in Fig. 1.3-1.6. The 3HP asynchronous machine is comparatively a machine of high slip value and the rated torque in such machines is produced at a rotor speed lower than the synchronous speed [Fig. 1.3].

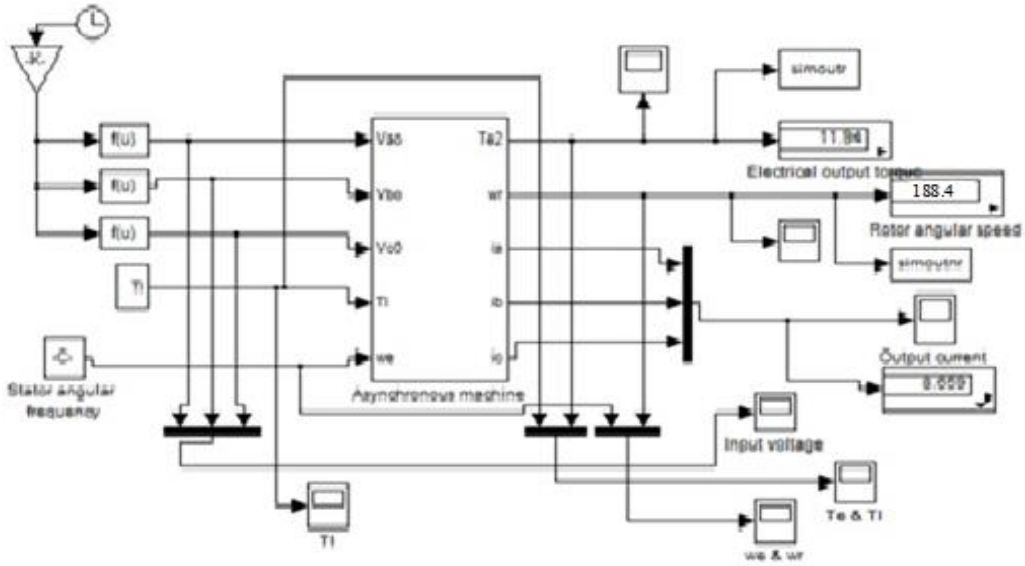

Fig. 1.2 The complete asynchronous machine simulink model

During stall condition, the input impedance of the asynchronous motor represents the sum of the stator resistance, its leakage reactance, rotor resistance and its leakage reactance. With the application of rated voltage directly to the machine terminals, the starting current flowing is very high (8 to 10 times the full-load rated current) and can produce heat loss in the winding. This heat loss may rupture the

insulation of the winding and hence can damage the windings of the motor. This is the major drawback of DOL (Direct on-line) starting and is depicted in Fig. 1.4(a) and 1.8(a). Hence, it is advisable and preferable to opt for reduced voltage based starting methods i.e. star/delta starter, autotransformer starter and soft start methods to limit the very high current at starting.

It is visualised from Fig. 1.4(c) that the rotor starts from stall condition and attains synchronous speed with zero value of load torque as friction and windage losses are not neglected. The initial transient phenomenon of the machine gets over within few seconds and the machine attains its steady state in just 4 sec. The load torque is increased from 0 Nm to 11.87 Nm at 0.5 sec. The load torque remains 11.87 Nm from 0.5 to 0.9 sec. During this simulation period, the electromagnetic torque raises to the load torque of 11.87 Nm as depicted in Fig. 1.4(b) and the speed drop sharply from 188.4 rad/sec to 172.4 rad/sec as depicted in Fig.14(c). It is visualised from Fig. 1.5 that the stator q-axis voltage is equal to 179.6V which is equal to the magnitude of supply side voltage and the stator d-axis voltage is equal to 0. It indicates that the stator d-q voltages appear as dc type quantities throughout the complete simulation time of 1.5 second. It is visualised from Fig. 1.6 that the stator q-axis and d-axis currents appear as dc type quantities in the steady state at 0.4 sec.

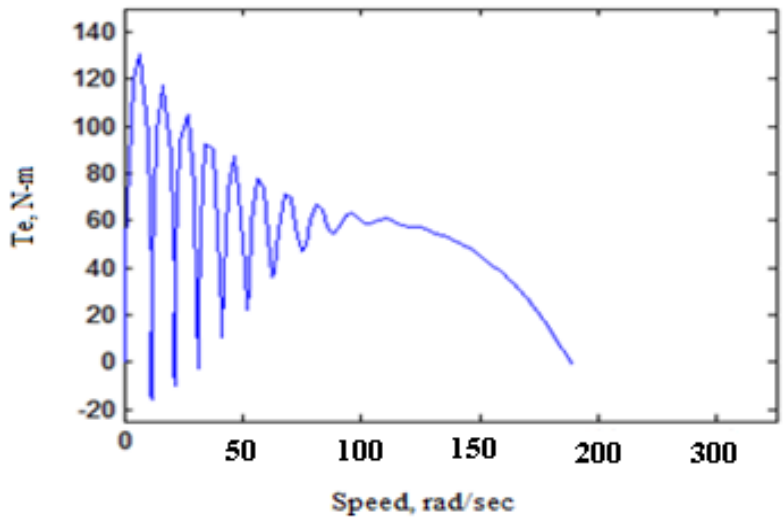

Fig. 1.3 Variation of electromagnetic torque (T_e) with speed for a 3 HP Asynchronous motor during free acceleration

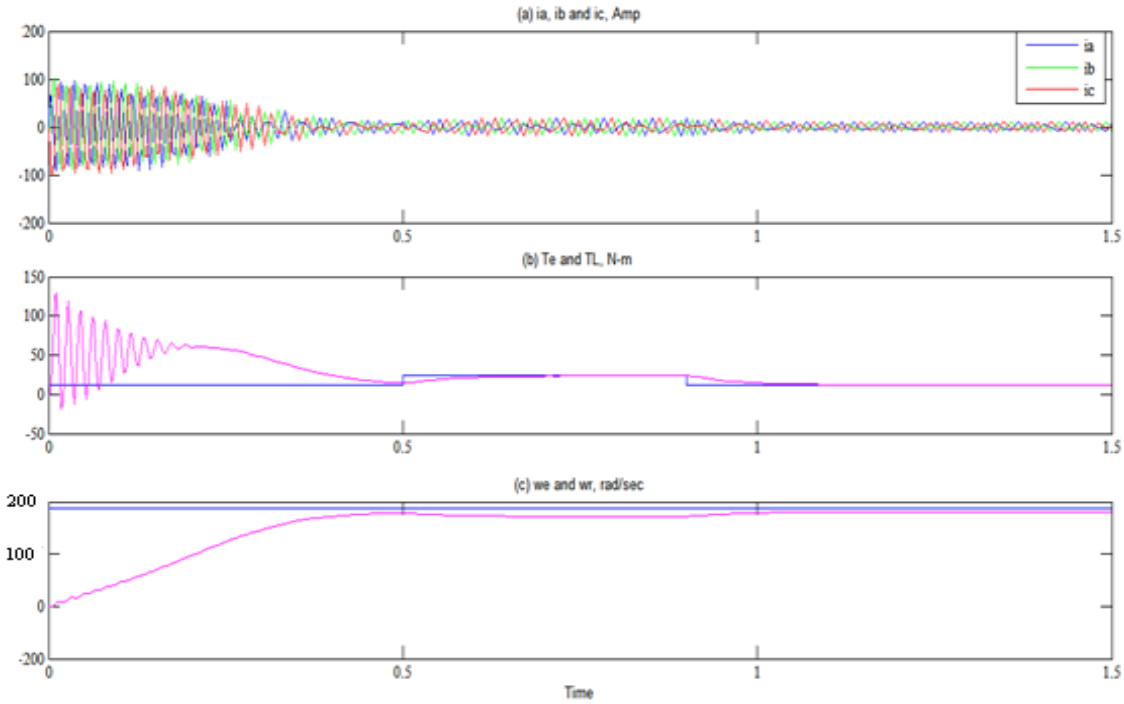

Fig. 1.4 Simulation based performance outcomes for (a) 3-phase stator currents (i_a, i_b and i_c) (b) electromagnetic torque (T_e) , load torque (T_L) and (c) rotor speed when T_L is increased (0 to 11.87N-m) and then decreased (11.87N-m to 0) in steps

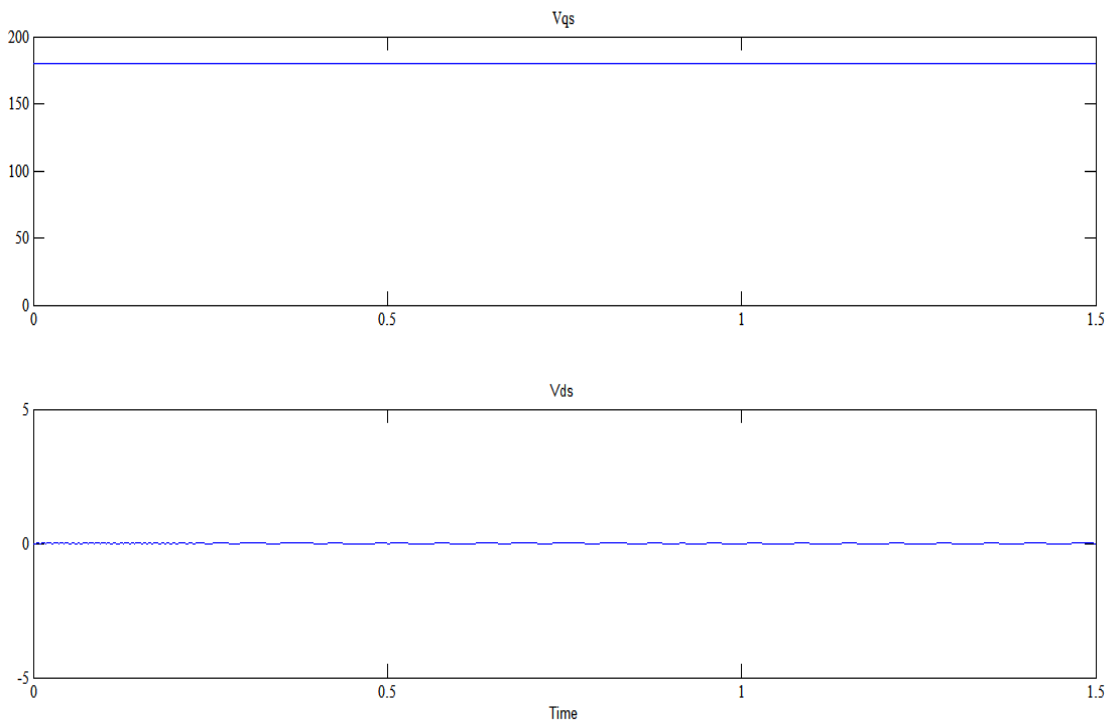

Fig. 1.5 Simulation based performance outcomes for stator q-d voltages when T_L is increased (0 to 11.87N-m) and then decreased (11.87N-m to 0) in steps

The application of 11.87 Nm load torque at 0.5 seconds as illustrated in Fig.1.6 results in slight increase in dc currents. After removal of load at 0.9 sec, the stator d-q currents again appear as dc type quantities.

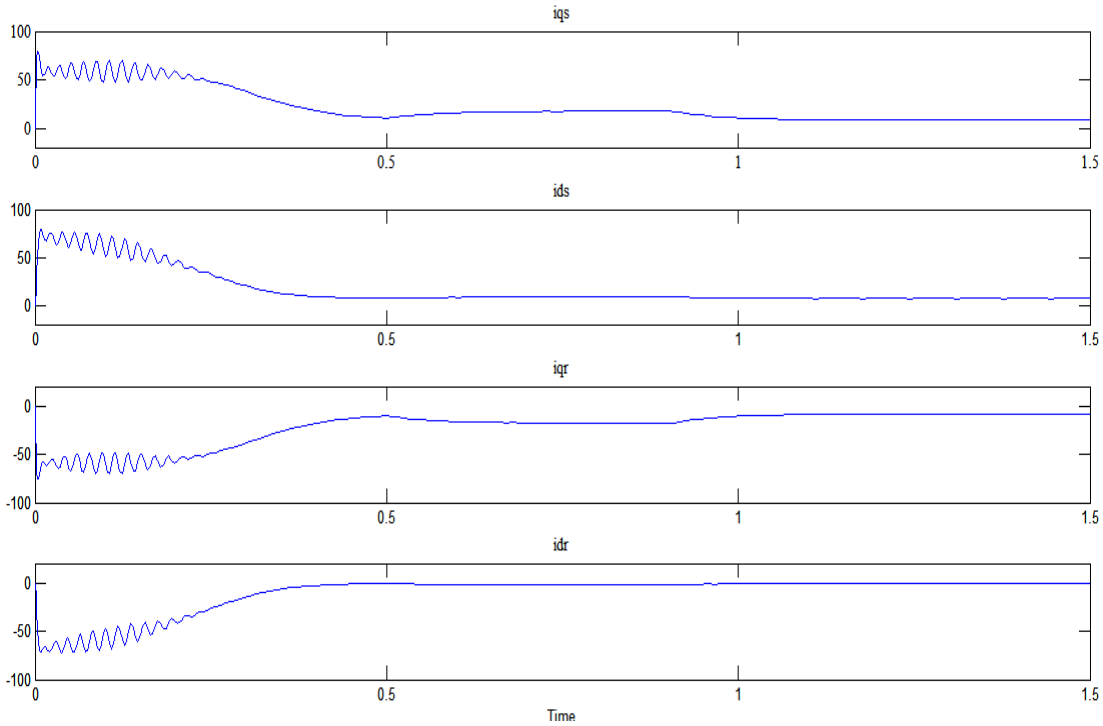

Fig. 1.6 Simulation based performance outcomes for stator and rotor q-d currents when T_L is increased (0 to 11.87N-m) and then decreased (11.87N-m to 0) in steps

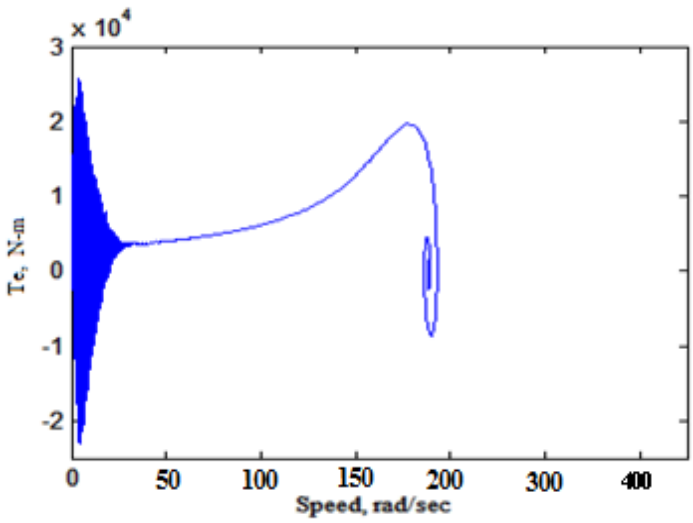

Fig. 1.7 Variation of electromagnetic torque (T_e) with speed for a 2250 HP Asynchronous motor during free acceleration

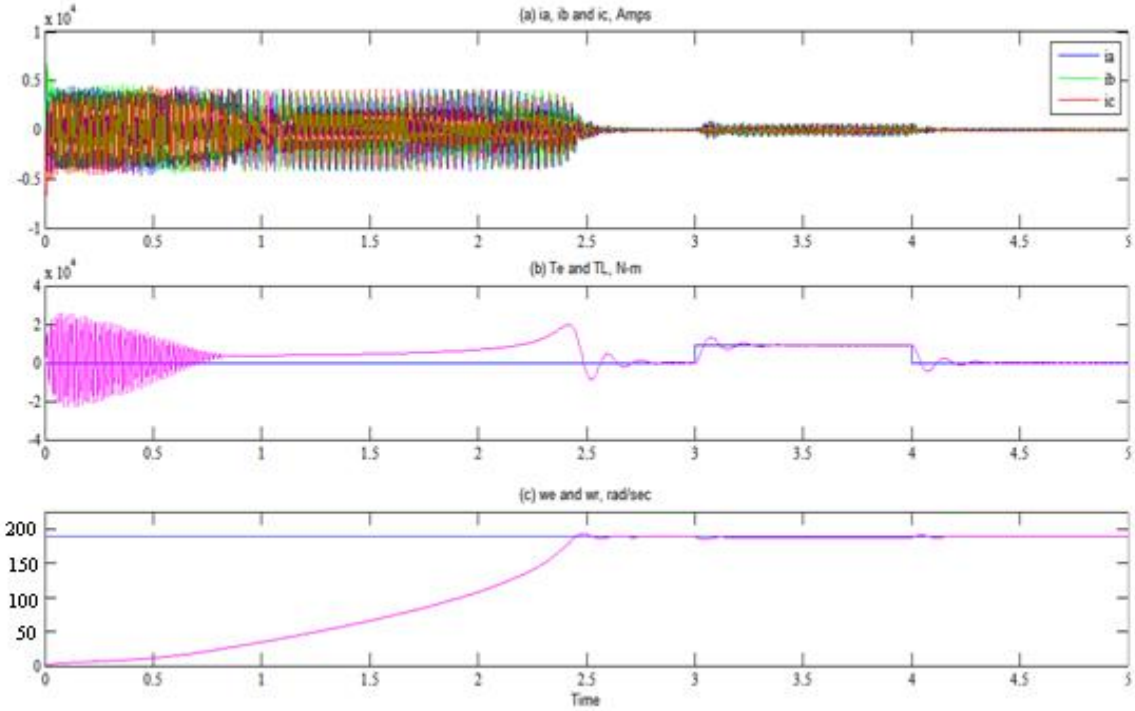

Fig. 1.8 Simulation based performance outcomes for (a) 3-phase stator currents (i_a, i_b and i_c), (b) electromagnetic torque (T_e), load torque (T_L) and (c) rotor speed when T_L is increased (0 to 8900 N-m) and then decreased (8900 N-m to 0) in steps

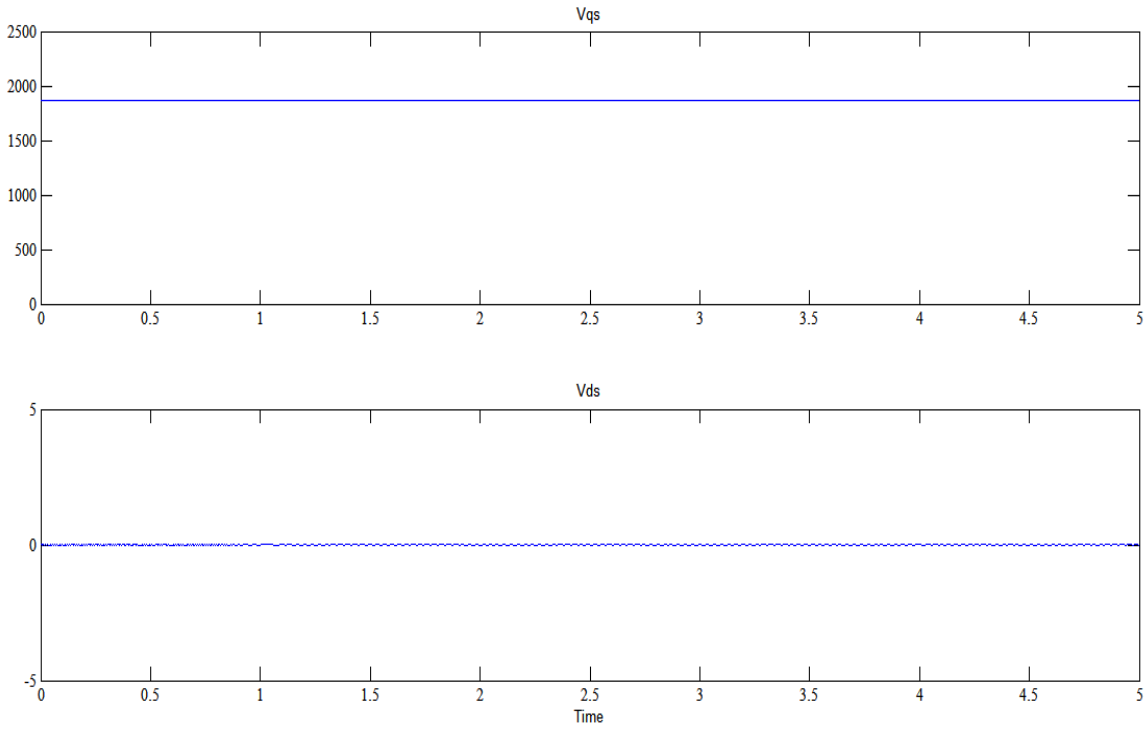

Fig. 1.9 Simulation based performance outcomes for stator q-d voltages when T_L is increased (0 to 8900 N-m) and then decreased from (8900 N-m to 0) in steps

The simulation outcomes are also illustrated for the asynchronous machine of 2250 HP machine. It is a low slip value machine and the rated torque in such machines is produced at synchronous speed as illustrated in Fig. 1.7.

It is visualised from Fig. 1.8(c) that the rotor starts from stall condition and attains synchronous speed with zero value of load torque as friction and windage losses are not neglected. The initial transient phenomenon of the machine gets over within few seconds and the machine attains its steady state in just 2.8 sec. The load torque is increased from 0 Nm to 8900 Nm at 3 sec. The load torque of 8900 Nm is applied from 3 to 4 sec. During this simulation period, the electromagnetic torque rises to the load torque of 8900 Nm as depicted in Fig. 1.8(b) and results in the same motor speed as synchronous speed of Fig.1.8(c).

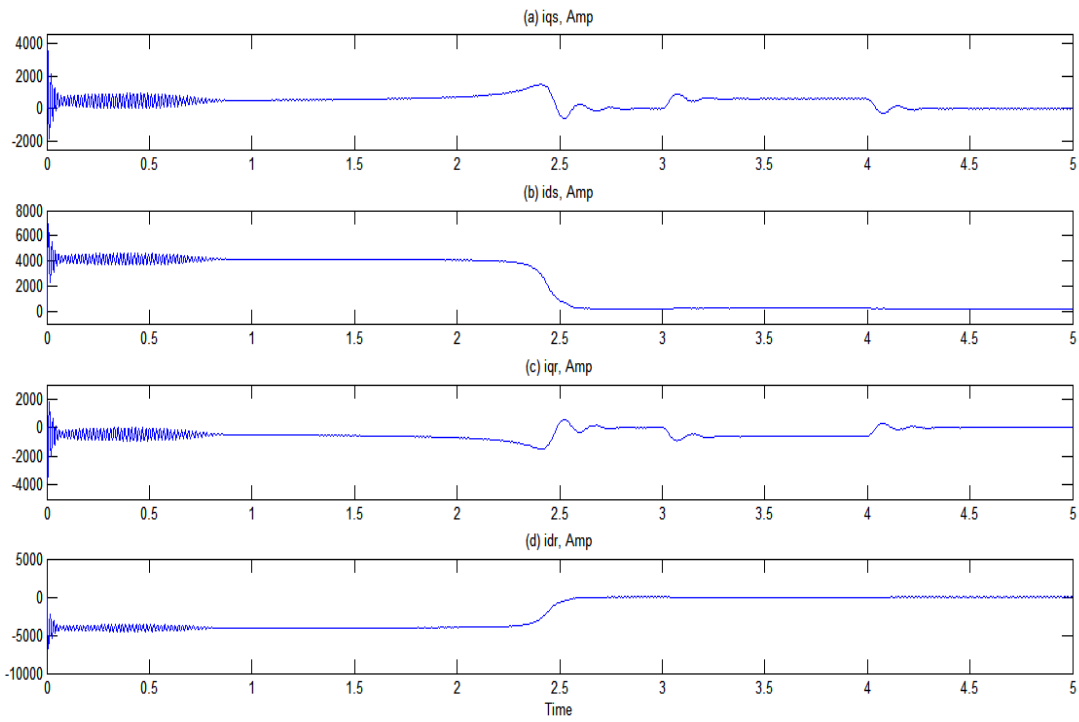

Fig. 1.10 Simulation based performance outcomes for stator and rotor q-d currents when T_L is increased (0 to 8900 N-m) and then decreased from (8900 N-m to 0) in steps

It is visualised from Fig. 1.9 that the stator q-axis voltage is equal to 1877.7V which is equal to the supply side voltage and stator d-axes voltage is equal to 0. It implies that the stator q-d axes voltages appear as dc type quantities.

It is visualised from Fig. 1.10 that the stator q-d axes currents appear as dc type quantities in the steady state at 2.8 sec. The application of 8900 N-m load torque at 3 seconds as illustrated in Fig. 1.8, results in very slight increase in currents. After removal of load at 4 sec, the stator q-d currents again appear as dc type quantities.

1.3 DIFFERENT OPERATING MODES OF AG

There exist two phenomenons through which an asynchronous machine operates as an Asynchronous Generator i.e. through regeneration and self-excitation phenomenon. Based on these phenomenon's, the Asynchronous Generator are classified as

- Externally excited Asynchronous Generator
- Self-excited Asynchronous Generator or Isolated asynchronous generator (IAG)

1.3.1 Externally Excited Asynchronous generator

Externally excited asynchronous generator are excited from an external power source or infinite bus of known voltage and frequency and its rotor is mechanically rotated at a speed more than the synchronous speed with the help of prime-mover. In this case the asynchronous machine draws magnetising current (lagging current) from the source to set rotating nature magnetic field rotating at synchronous speed in the air-gap requisite for regeneration process. This synchronously rotating field induces a voltage in the rotor winding and current will flow if the rotor circuit is closed. The difference in speed of the rotating nature magnetic field and rotor is negative and hence slip is negative. The machine operates as an externally excited asynchronous generator and now it sends active power back (P_p) to the infinite bus and take reactive power (Q_p) to produce the required rotating magnetic field. In externally excited asynchronous generator, the generator side voltage and its associated frequency are same as voltage and frequency of the source or grid or infinite bus to which it is connected or through which it is excited. Hence, the voltage and frequency of the generator are known and hence its analysis becomes quite simple and the performance equations related with analysis can be attained from the equations derived from the equivalent circuit. The phasor diagram of asynchronous motor under load is illustrated in Fig. 1.12.

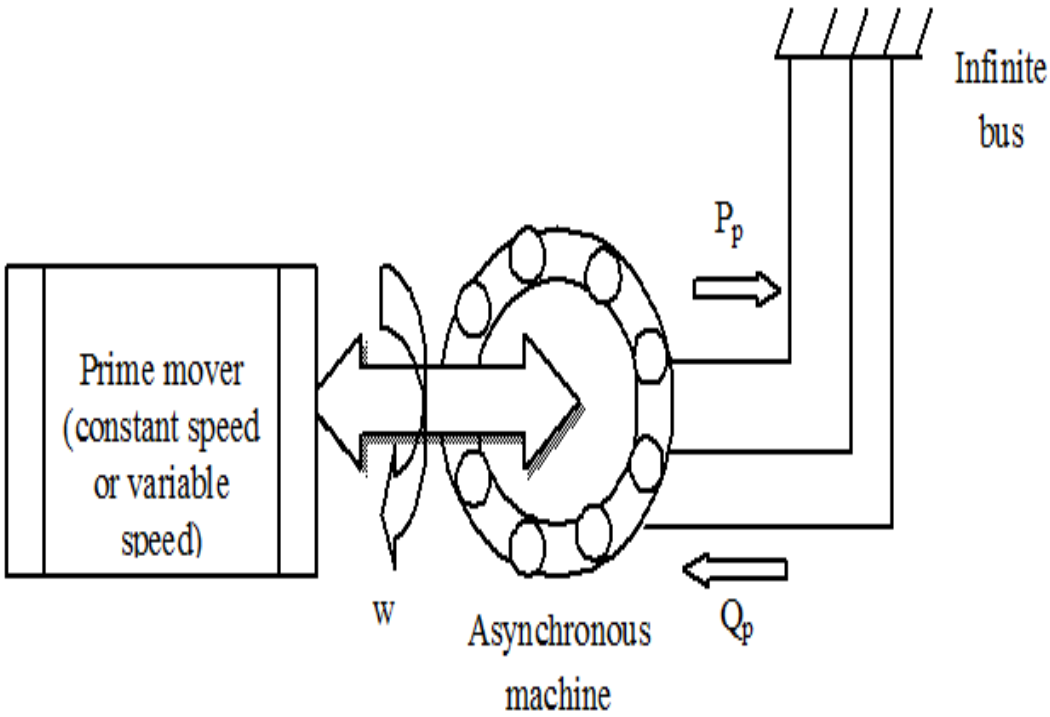

Fig. 1.11 Block diagram of externally excited asynchronous generator

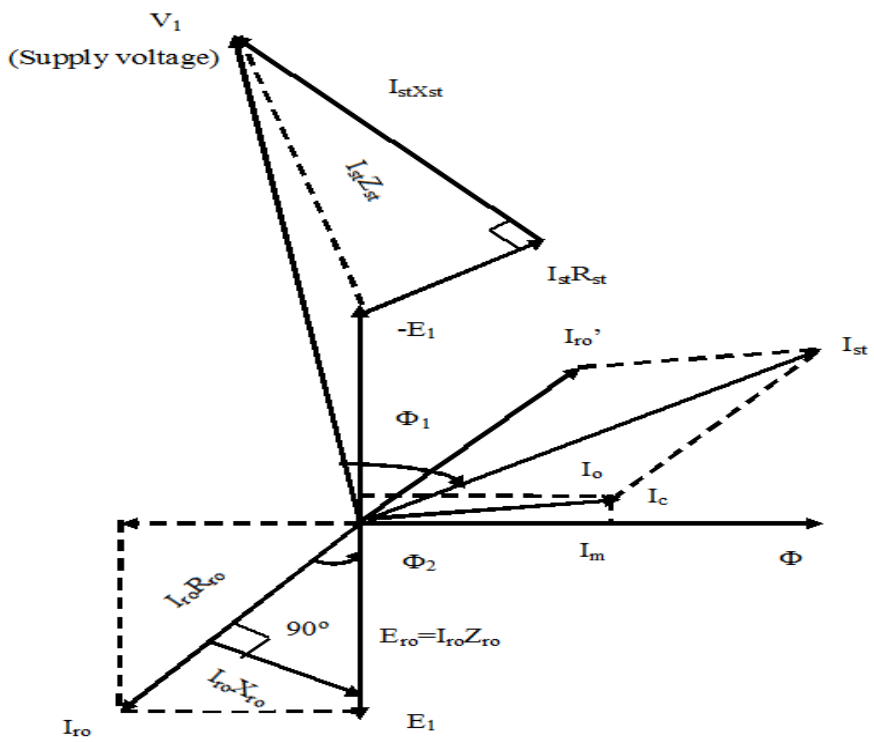

Fig. 1.12 Phasor diagram representation of externally excited asynchronous generator for unity power factor load.

The stator current is the phasor sum of no-load current I_o and I_{ro}' (reversal of rotor current I_{ro}) and voltage fed to the stator of AM is given by the following mathematical expression

$$V_1 = -E_1 + I_{st}R_{st} + I_{st}X_{st}$$

1.3.2 Self-Excited Asynchronous Generator (SEIG) or Isolated Asynchronous Generator (IAG)

An asynchronous machine can be made to operate as an asynchronous generator through self-excitation phenomenon. Such generators are termed as self-excited induction generator or IAG. The working of self-excited induction generator requisites two fundamental conditions which should be met:

- Availability or existence of residual magnetism in the rotor circuit
- Permanent source of reactive power i.e. a.c capacitor bank

Now if the 3-phase asynchronous machine is rotated mechanically at more than the synchronous speed and a 3-phase capacitor bank is permanently held across the stator terminals of the machine under no-load conditions, Fig. 1.13(a), then a voltage appears across the machine terminal. Now the difference in speed of the rotor and rotating magnetic field is negative and hence the slip is negative. It is a known fact that some small voltage is always available in the stator winding due to existence of residual flux in the core. This small voltage appears across the capacitor and produces a lagging current to flow through the stator winding of the asynchronous machine. This lagging current is requisite for the production of rotating magnetic field in air-gap. This rotating nature magnetic field further builds up the voltage across the stator winding of the machine. The voltage across the stator terminals keeps on building up and its final value is restricted by the magnetic saturation of the core of the machine, Fig. 1.13 (b). Such generators are called self-excited asynchronous generator and operates independent of power source. As these generators operate independent of power source, these generator are also termed as Isolated Asynchronous Generator (IAG). The block diagram of IAG is depicted in Fig. 1.14. The capacitor bank is a source of reactive vars and is supplying lagging nature reactive vars to both IAG and the consumer load.

$$Q_{pc} = Q_{pg} + Q_{pl}$$

Here Q_{pc} is reactive var of capacitor, Q_{pg} is the reactive var supplied to the generator by capacitor bank or reactive var consumed by IAG and Q_{pl} is the reactive var supplied to the load by the capacitor bank or reactive var consumed by consumer load. The equivalent circuit diagram representation of IAG is shown in Fig. 1.14

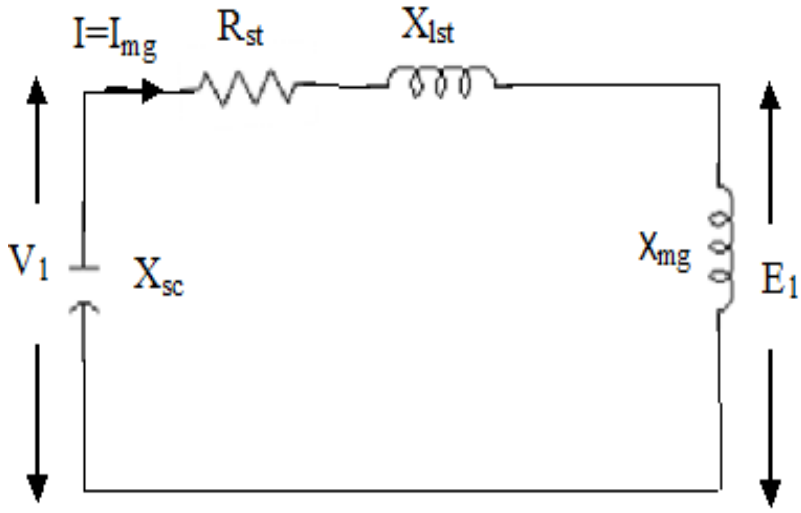

(a)

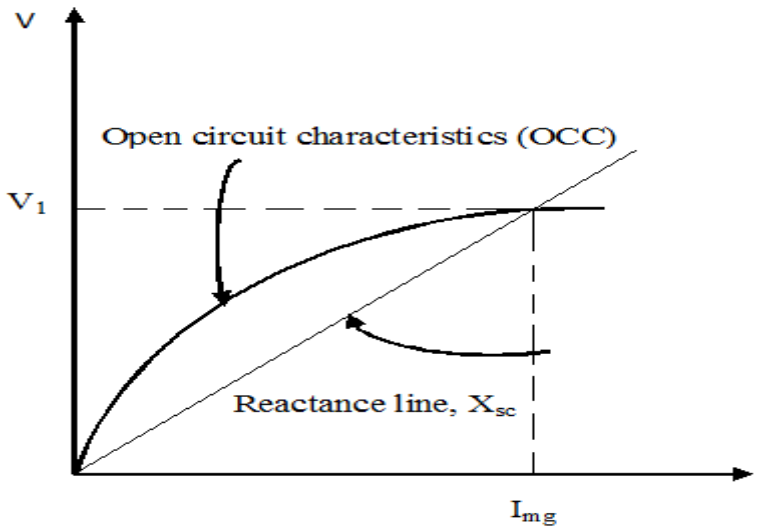

(b)

Fig. 1.13 (a) Equivalent circuit diagram of IAG under no-load conditions (b) OCC and reactance line

The equivalent circuit is similar to asynchronous machine equivalent circuit but with additional capacitors connected across the stator terminals.

In the phasor diagram, Fig. 1.16, the direction of in-phase component of current I_{2r} changes, while the direction of quadrature current remains same as that of asynchronous motor phasor diagram, Fig. 1.12.

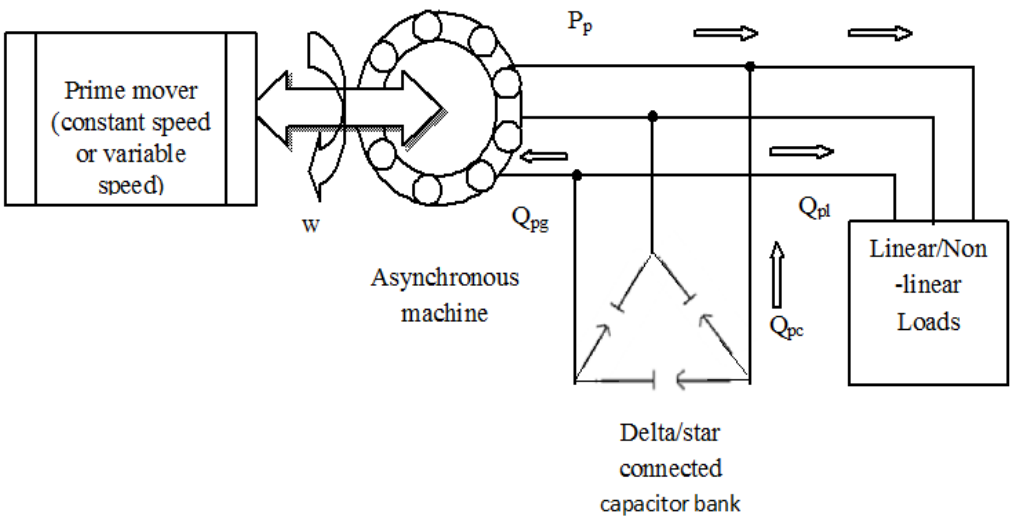

Fig. 1.14 Schematic diagram of isolated asynchronous generator (IAG)

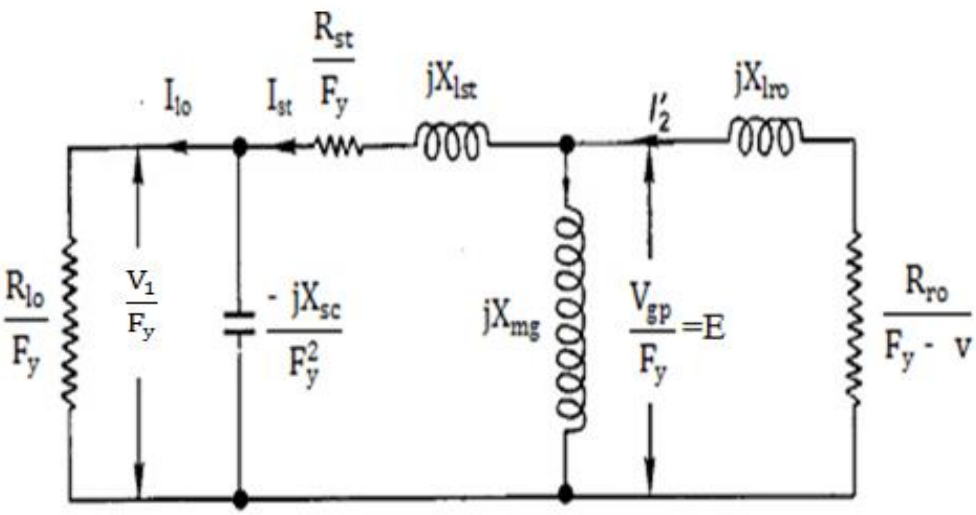

Fig. 1.15 Equivalent circuit diagram of IAG

The effect of the change in in-phase component of I_{2r} results in reversed direction of rotor e.m.f. E_{ro} and the angle Φ between V_1 and I_1 is more as compared to asynchronous motor phasor diagram. Hence, the asynchronous machine starts operating as a generator and supplying power to the stator. It operates independent of grid or source of electrical power and hence termed as isolated asynchronous generator.

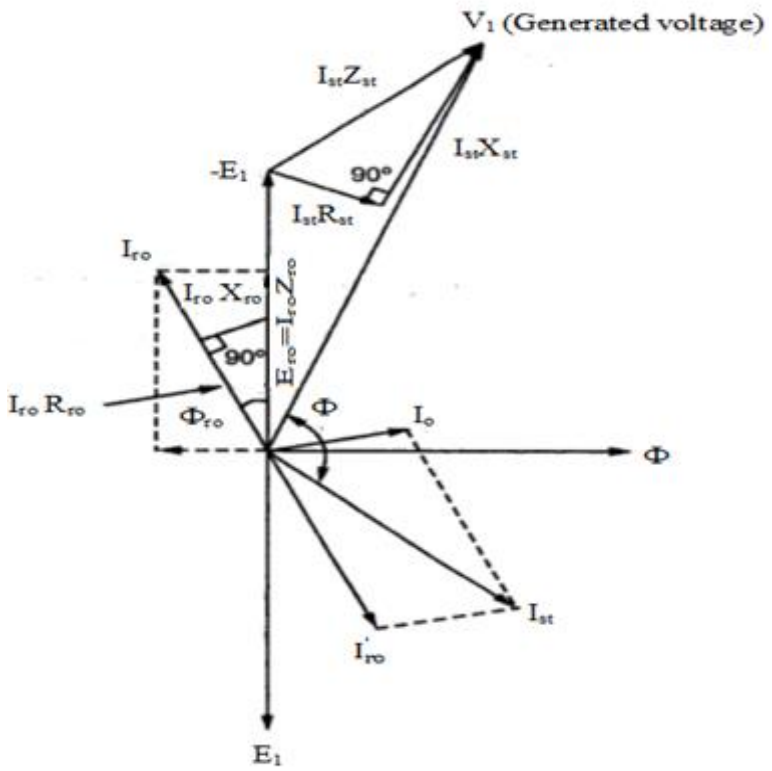

Fig. 1.16 Phasor diagram of IAG

1.3.3 Advantages of IAG

1. It possesses robust construction and thus requiring less maintenance and repair work.
2. It has small size per KW output power.
3. It can efficiently operate in parallel for meeting the increased load requirement in near future without causing hunting problem.
4. It operates at wide range of speeds.
5. No synchronization to the supply line is required like a synchronous generator.
6. It does not need any commutator and brushes as required in synchronous generator. Hence it is an economical and cheaper option for electrical power generation as compared to conventional synchronous generators.
7. It inherently provides protection under overload and short circuit conditions.

1.3.4 Limitations of IAG

It cannot generate reactive volt amperes. It requires reactive volt amperes from the supply line or capacitor bank to furnish its excitation requisites for the production of

rotating magnetic field. A continuous source of lagging reactive var is required for its operation. Due to lack of required lagging reactive var, the issue of poor voltage and frequency regulation arises and restricts its use for commercialisation purpose.

1.3.5 Applications of IAG

These generators are used with constant speed (micro-hydro turbines) and variable speed prime-movers (wind mills) to generate electrical power for electrifying the grid isolated remote sites.

1. 4 OBJECTIVE OF STUDY / PROBLEM FORMULATION

As the poor voltage and frequency regulation is a major bottleneck in its commercialization. These controllers have been investigated either for a three-phase, 3-wire, or single-phase power applications of SEIG. Analysis, design and control aspects of self-excited induction generators (SEIG) are dealt in several papers. A crucial aspect in this area is the development of appropriate control mechanism to achieve desired output in terms of voltage, frequency and waveforms at different loads with different types of prime movers.

1.5 METHODOLOGY ADOPTED

- The transient/steady-state analysis of three -phase self-excited induction generator (SEIG) or IAG furnishing 3-phase/1-phase/static or dynamic load with an appropriate controller has been carried out.
- A composite mathematical model of the total system has been developed by combining the modeling of the prime mover, SEIG or IAG, controller and load.
- The dynamic model of the SEIG or IAG using a three phase asynchronous machine has been developed based on stationary reference frame.
- Simulated results have been compared with the experimental results attained on hardware set-up of IAG system.

The following steps have been adopted or followed to achieve the above mentioned objectives:

Step1: Literature survey

Step2: Dynamic d-q modelling of the asynchronous machine

Step3: Experimental and Optimization based analysis of 3-phase IAG furnishing 3-phase balanced load.

Step4: Analysis of 3-phase IAG furnishing unbalanced and single-phase load using symmetrical component theory.

Step5: An electronics generator load controller (EGLC) has been designed and simulated in MATLAB/SIMULINK to support voltage and frequency of an IAG furnishing three-phase balanced and unbalanced consumer load for constant power applications.

Step6: Design and Implementation of conventional PI and fuzzy logic (FL) based EGLC for voltage and frequency support of an IAG subjected to varying consumer load.

Step7: Hardware implementation of PWM IC-3524 based EGLC for an IAG furnishing single-phase load.

Step8: Design and Implementation of 3-legged PI and Fuzzy logic (FL) based VSI controller for an IAG.

1.6 ORGANISATION OF THE THESIS

The whole work related to thesis is covered in ten chapters.

CHAPTER 1 first briefed about the research topic. Then it covers the brief theory of asynchronous machine and its d-q modelling in different reference frames. This chapter also described the dynamic modelling of 3-phase asynchronous motor in synchronously rotating frame. The influences of the step change in load torque on the motor output variables are examined. Then it discusses the various conditions under which an asynchronous machine starts working as an asynchronous generator along-with its advantages, disadvantages and its applications.

CHAPTER 2 covers the literature review of various issues related to an IAG i.e. self-excitation phenomenon, analysis of IAG furnishing 3-phase and 1-phase load using various techniques. It also highlights the problem of poor voltage and frequency regulation and provides the state of art of various voltage and frequency controllers or regulators available in the past along-with its advantages and disadvantages.

CHAPTER 3 This chapter covers the analytical and optimization based analysis of IAG under balanced conditions. This chapter envisages or examines initially the basic phenomenon of voltage build-up and the steady state analysis of 3-phase IAG furnishing three phase balanced resistive load. This preliminary study forms the foundation or basis of the design of future controllers. The conventional Newton Raphson technique and a MATLAB based optimization technique fsolve is elaborated in detail along-with advantages and disadvantages for attaining the solution of simultaneous non linear equation. The fsolve technique is adopted in this chapter for the solution of non-linear equations due to its advantages over conventional method. The solution of these equations yields the saturated value of magnetizing reactance X_{mg} and frequency F_y. Then the performance can be accessed from equivalent circuit using these values of X_{mg} and F_y. The effect of excitation capacitance on the different performance characteristics under no load and resistive load on the IAG is also investigated here. The experimental results outcomes are investigated on laboratory available induction machine set of 3.73 kW coupled with a dc shunt machine (prime mover). The analytical and the experimental investigations outcomes exhibit a very good association. The good association between the two outcomes authenticates the implementation of the proposed technique. The results under transient condition are captured using Fluke-434 Power Quality Analyzer.

CHAPTER 4 In this chapter, an optimisation based performance analysis of 3-phase IAG furnishing unbalanced load and 1-phase load is performed. The equations representing the behaviour of the IAG subjected to balanced/unbalanced operating conditions of load is derived mathematically based on theory of symmetrical components. Finally, the two non-linear equations with X_{mg} and F_y as unknowns are obtained. The fsolve technique is recommended for the solution of these equations. The desired values of X_{mg} and F_y are attained for carrying out the performance evaluation of IAG corresponding to steady state situation. The experimental investigations are carried out in laboratory to validate the analytical attained outcomes.

CHAPTER 5 This chapter covers the design and simulation of an EGLC in MATLAB/SIMULINK to support IAG voltage and its frequency subjected to 3-phase balanced/unbalanced consumer load for constant power applications. The EGLC

comprises of a six-pulse diode based bridge rectifier, IGBT switch, filtering capacitor, PI controller and a dump load (resistive). The transient behaviour of IAG-EGLC system is investigated and studied, operating under varying load conditions to demonstrate the capabilities of EGLC.

CHAPTER 6 This chapter covers the basic details regarding the fuzzy logic based controller approach It also provides information based on different types of Fuzzy Inference System (FIS) along with its advantages and disadvantages. Two types of FIS i.e. Mamadani and Sugeno type FIS for the performance enhancement of the system. It is observed that Mamdani type FIS is globally acceptable whereas the Sugeno type FIS works efficiently with linear, optimization and adaptive techniques.

CHAPTER 7 This chapter explored the designing, realization and testing of conventional PI and fuzzy logic (FL) based EGLC for an IAG subjected to varying load. The performance of IAG-EGLC system subjected to varying load is accomplished corresponding to transient and the steady. The enhancement in performance of an IAG is accomplished relating its voltage and frequency support, rise time, settling time, and overshoot and THD in generated voltage and current values using the suggested FL based controller as inferred from the results.

CHAPTER 8 explains the hardware implementation of EGLC for an IAG furnishing single-phase loads in the laboratory. The voltage support at consumer terminals is required in remote areas. This voltage support should be provided economically. The study carried out in this chapter emphasis on the designing methodology and implementation of an EGLC for an asynchronous generator feeding single-phase loads. The driving signals for the IGBT based chopper switch is generated using IC-3524. The generator is providing power to the two loads connected in shunt across each other. The objective of the controller is to maintain constant load or power on the generator during the entire operation of the generator. The outcomes have been verified using a hardware model of the IC-3524 based controller developed in laboratory to testify or justify the expected results. The outcomes have been also evaluated and verified using MATLAB. Both results have been verified and justified its applications for feeding single-phase loads in remote areas.

CHAPTER 9 In this chapter, two types of Fuzzy logic (FL) controllers (one for ac generated voltage and another for dc capacitor voltage control) are recommended to formulate template based algorithm for yielding reference supply currents. The recommended controller controls both reactive and active (kW) power parallely for retaining the IAG voltage and its frequency at the desired level under varying loads. The designing part of 3-legged VSI controller is also elaborated. The controller used here is formed by integrated various electronic components: 3-legged IGBT type current controlled VSI, high carrier frequency (10 kHz) DC type chopper and a capacitor across 3-legged VSI to filter out ripples in dc voltage. In this chapter, first the simulated outcomes of the performance characteristics are accomplished using Mamdani and Sugeno type FL based controller. Then, the comparison of various outcomes based on conventional PI and FL is made to testify that the recommended controller is superior to the conventional PI method and is well suited for power generation in isolation mode. Here, the whole electrical system and the controller are modelled using Simpower system and Fuzzy logic toolbox of MATLAB (version 7.8) software package.

CHAPTER 10 The various analysis or investigations made in the research work have been concluded in this chapter. It also highlights the scope for future work.

1.7 PROPOSED OUTCOME OF THE RESEARCH AND SCOPE OF FUTURE WORK

As the poor voltage and frequency regulation are the two constraints of IAG under load condition and restricted its use for the commercialization purposes. In almost all the published literature, mainly conventional PI controllers are employed for voltage and frequency support. The main aspiration behind its use is its simplicity.

But on the counterpart, there is difficulty in achieving the fine tuning of the gains to obtain desired performance particularly when more than one PI controllers are used. The second biggest drawback is encountered when the system is having both non-linearity and uncertainty.

The traditional PI and fuzzy logic (FL) based controllers are designed and implemented for EGLC and 3-legged VSI for an IAG for accomplishing its steady state and transient performance. It is shown that the enhancement in performance

characteristics of IAG is accomplished using FL based EGLC than the conventional PI based method.

The enhancement in performance characteristics of an IAG with a 3-legged VSI is accomplished using Mamdani and Sugeno type fuzzy logic (FL) based controller. The comparison of various outcomes based on conventional PI and FL proved that the recommended controller is superior to the conventional PI method and is well suited for power generation in isolation mode.

In the present work, the performance enhancement of IAG is achieved using fuzzy logic approach based EGLC and three-legged VSI controller. In future work, an ANFSI based EGLC and 3-legged VSI controller will be developed for further enhancement in performance characteristics of an IAG.

The difficulties faced during the experimental work are:

- Loss of residual magnetism in the core at lower values of operating speeds.
- Implementation of IC-3524 based control strategy for IAG.

The hardware implementation of the control circuit of the controller can be realized using DSPACE and Controller HIL (C-HIL) Typhoon HIL. The Controller HIL (C-HIL) testing can be performed using Typhoon ultra high fidelity Typhoon HIL Simulator.

1.8 SUMMARY

The concept of d-q modelling and different types of reference frame is requisite for getting the better understanding of the analysis of an asynchronous machine under steady state and transient phenomenon and for the performance assessment of the asynchronous motor drives with the various control techniques like vector control or DTC (direct control) drives.

This chapter discussed the concept of different reference frames and modelling and digital simulation of asynchronous machines (3 HP and 2250 HP) in synchronously rotating frames. It also highlighted the phenomenon of self excitation in asynchronous generator or working of an asynchronous machine as an asynchronous generator along with its advantages, disadvantages and applications. It

furnishes an outline of the whole work covered in separate chapters and also brief about the proposed outcomes and scope for future work in the concerned area.

CHAPTER 2

LITERATURE REVIEW

2.1 GENERAL

If the stator of an asynchronous machine is energised or excited by an ac system, a rotating nature magnetic field revolving at synchronous speed is established in the air-gap. This rotating magnetic field induces a voltage in the stator as well as rotor winding. The current will flow if the rotor circuit is closed. The rotor attains a speed lower than the speed of the rotating nature magnetic field. The relative speed of the rotating field is positive and hence the slip value is positive and the asynchronous machine works as an asynchronous motor.

The same asynchronous machine can be operated as a generator. There are two basic conditions which should be met: presence of residual magnetism and capacitor bank to furnish reactive power. The asynchronous machine is mechanically rotated at a speed higher than the synchronous speed with the aid of prime-mover. Now the difference between the speed of the rotor and rotating field is negative and hence slip is negative. Now the asynchronous machine starts operating as a generator. It starts feeding power to the grid and acts as a source of supply for feeding 3-phase or 1-phase loads. The shaft torque is conveyed to the stator via air-gap. The net available power at output depends on the value of slip, s. The asynchronous generators are categorised as an isolated asynchronous generator (IAG) as these generators operates independent of grid or infinite bus-bar. The voltage and frequency parameters of these generators are not fixed and known. Moreover, the voltage and frequency are also affected by the value of excitation capacitor, load, machine parameters and speed of the prime-mover. Also, the magnetising reactance varies with the operating point even at fixed rotor speed. Therefore the performance analysis of IAG under steady state and transient conditions is requisite from practical application point of view.

2.2 ANALYSIS OF IAG FEEDING BALANCED /UNBALANCED LOAD

2.2.1 Performance Analysis of 3-Phase IAG Feeding 3-Phase Load

The analysis aspect of IAG furnishing 3-phase or 1-phse load provides basis for designing various control strategies for IAG. Hence, the analysis aspect is requisite

for designing the controllers. Many scientists and researchers have analyzed the steady state based performance of 3-phase Isolated Asynchronous Generator (IAG) feeding three-phase load using equivalent circuit [9-28].

A tremendous number of research papers examined the performance characteristics of IAG based on equivalent circuit using loop analysis technique [9-20]. The performance analysis of IAG under the steady state and transient conditions are also investigated using admittance method [21-28].

B. C Doxey [9] enlightened the concept of how a induction machine operates as an induction generator in grid isolated mode. It is shown that the performance characteristics of IG are slightly different from the induction machine. The performance of IG attained using both theoretical concepts and test results are found quite satisfactorily and are in close resemblance with each other. It also discussed about the various practical applications related to induction motor and induction generator. Use of saturable reactors is discussed here for to achieve better voltage regulation. For attaining the voltage regulation more precisely, the use of magnetic amplifiers is recommended. The main disadvantage of IG with only excitation capacitor is of overload and short circuit situation. It is shown that IG is a viable option for brushless based electrical power generation.

R. Holland [10] discussed about two person's i.e Surendra Mathema (Nepal Engineer) and his colleague Akkal Man Nakarmi. They both fabricated small hydro turbines in Kathmandu. They tried to curtail the cost of micro-hydro based electric plants. They manufactured and installed such plants in remote areas. It is discussed that they built around 30 micro-hydro sets in Nepal only. They used asynchronous generators instead of synchronous generators because of its low cost. But the main problem with IG was poor voltage regulation under varying load conditions. So, they designed and installed an electronic load controller in Nepal which allows a voltage variation within ± 10%.

S. S Murthy et.al [12] described the Newton Raphson method of analytically determining the values of X_m (magnetising reactance) and F (frequency) for analysing the performance of three- phase type SEIG corresponding to steady state. The values of X_m and F are attained for the defined values of X_c, speed and the load. The effect of

varying various parameters i.e. stator and rotor resistance, its leakage reactance, X_m on the steady state performance are studied or analysed. This study provided the guidelines for the proper design of such systems. The results obtained from analytical and experimental study showed good degree of correlation and testified the feasibility of the proposed method.

A. K AI Jabri et.al [13] discussed that the SEIG output voltage and frequency depend on various factors i.e. speed, terminal capacitance and load. These factors have imposed certain constraints on its performance. In this paper, the performance analysis of 3-phase SEIG is carried out under different operating conditions i.e. controlled speed, excitation capacitance reactance and load. It is inferred from the results that for fixed value of speed and load impedance, there has been certain values of upper and lower limits of excitation capacitance C. The value of C should be within limits for self-excitation phenomenon. There is mentioned the lower and upper limits for speed for given values of R_L and X_c, outside the limits the machine fails its self-excitation phenomenon. The proposed scheme helped in selecting the optimum values of speed, excitation capacitance and load for obtaining maximum power output.

N. H Malik et.al [14] reported the performance analysis of SEIG feeding balanced R-L load under steady state conditions. In the analysis, machine core losses are included. The value of excitation capacitance is estimated under no load and load conditions in order to maintain self-excitation phenomenon and terminal voltage. Few analytical outcomes are verified experimentally and a good correlation is noticed.

S. P Singh et.al [15] presented the performance characteristics of 3-phase SEIG. For performance evaluation, the values of frequency F and excitation reactance X_c are analytically obtained using Newton Raphson method. An analytical procedure i.e. described to evaluate the number of switching capacitors needed to support the terminal voltage at the desired level and to load the generator upto its rated capacity. It is concluded from the analytical results that only four numbers of switching capacitors are sufficient to support the desired terminal voltage within ± 6%. It is also noticed that the use of switching capacitors for terminal voltage regulation and for achieving maximum power output is a economical and viable option. The proposed

scheme of voltage regulation and the analytical results are validated experimentally on a 3.7 kW asynchronous machine.

M. H Hague [16] explored a novel method for accessing the performance of 3-phase SEIG subjected to different operating conditions. The values of X_m and F for performance evaluation purpose are obtained using 'fsolve' routine of MATLAB. In addition to no-load and load characteristics of generator, the performance characteristics relating to fixed terminal voltage and stator current are obtained. Some of the performance characteristics analytically attained are verified experimentally on an induction machine of 1.5 kW and both results are closely related.

A. H A. L Bahrani et.al [17] presented the steady state analysis of a single capacitor excited 3-phase IAG furnishing single-phase load. For performance evaluation, the values of X_m and F have been using Newton-Raphson method. For sustaining self-excitation, the variation range for various parameters i.e. excitation capacitance, speed and load impedance are defined in the paper mentioned. The influence of various parameters i.e. speed, excitation capacitance and load is observed on the performance characteristics of Y and Δ-connected IAG. It is observed that these characteristics are strongly affected by value of C. This paper provided the guidelines for proper selection of C for both configurations. The analytical results obtained using the proposed scheme is validated experimentally using a test machine.

M. H Haque et.al [18] discussed a method of evaluating the value of X_c for initiating the voltage rise phenomenon at no load for grid isolated operation of 3-phase SEIG. The equivalent circuit model (per-phase) of the SEIG under no load behaved like an L-C circuit provided its stator copper losses are neglected. The proposed scheme is based on the phenomenon of L-C resonance and non-linear magnetization characteristics of SEIG. Firstly, the value of X_m is evaluated by solving a 4th order polynomial in X_m for given values of voltage and speed. Then, the value of X_c is evaluated using the condition of L-C resonance. The voltage build up phenomenon under transient condition is also reported in this paper. Analytical results obtained from the proposed scheme are validated through experiments on a 1.5 kW rating asynchronous machine.

S. S Murthy et.al [19] discussed the theory of symmetrical components for the performance analysis of 3-phase SEIG furnishing three-phase unbalanced and 1-phase load. The analysis was little bit complicated due to effect of unbalance in operating conditions and magnetic saturation. This paper helped in designing a capacitor for a given motor rating. The performance characteristics of SEIG feeding unbalanced load is analysed both analytically and experimentally on a 7.5 kW machine. The close resemblance between the analytical and experimental outcomes validates the considered scheme.

A. H A.L-Bahrani et.al [20] discussed the analysis of SEIG (3-phase) connected in parallel and feeding a balanced load. It is concluded from the results that the machine with same or different parameters and speed can be operated successfully in parallel. A Newton Raphson method is considered for obtaining the values of F and X_m for the performance assessment of SEIG corresponding to steady state. The performance characteristics are strongly affected by the various parameters of machine, excitation capacitance, speed, and load nature and magnetizing characteristics. The analytical outcome obtained using the proposed schemes are validated experimentally.

A. H A. L-Bahrani et.al [21] emphasized on the two techniques of controlling common bus voltage control for any number of SEIG's operating in parallel under balanced steady state conditions. The control of voltage is provided by capacitance C and machine speeds. The proposed scheme may be suggested for a single SEIG or a number of SEIG's of same or different ratings operating at equal or different speeds. The effects of various electrical parameters on the voltage control are reported for a number of SEIG's operating in parallel. The theoretical investigations made from the two techniques are verified experimentally.

A. H AL-Bahrani [22] derived the various conditions for the self-excitation phenomenon for various types of generator and load connections with the application of theory of symmetrical component and sequence circuit models. The performance analysis is performed on a 3-phase SEIG supplying balanced/ unbalanced loads with balanced and unbalanced excitation schemes. The theoretical investigations made from the proposed models are verified experimentally under different balanced and unbalanced operating conditions.

N. H Malik [23] promoted a Newton Raphson method to evaluate the values of X_m and F for deriving the performance related equations of SEIG furnishing balanced load. The effects of X_c on the different performance characteristics related with SEIG are analysed. The conditions for the existence of self-excitation in terms of capacitance, speed and load impedance are explained.

Y. H. A Rahim [24] investigated the performance analysis of SEIG using a single capacitor configuration. This single capacitor may be used for line and phase excitation and one or two loads are connected across the free terminals. The two non linear nature equations containing F and X_m are formed using the application of symmetrical component theory in the circuit model of SEIG. The values of F and X_m for the performance analysis are attained using Newton Raphson method. The analytical calculations are verified experimentally. The close resemblance between both results proved that a 3-phase SEIG could be satisfactorily excited by a single capacitor.

K. S Sandhu et.al [25] introduced a new approach to analyse the performance of SEIG subjected to different operating conditions under steady state. A Nodal analysis method is applied in the equivalent circuit of SEIG to access the values of slip s and the magnetizing reactance X_m for the complete performance analysis of SEIG. A second degree polynomial in slip s is obtained on equating the real part of admittance equal to zero. A low order polynomial in slip‘s’ is made the analysis simpler and comprehensive. The analytical results are verified experimentally.

T. F Chan [26] described an iterative method based performance analysis of SEIG corresponding to steady state. A Nodal admittances method is applied across the air-gap node to obtain the values of X_m and F for the performance analysis corresponding to steady state. The proposed scheme made the problem formulation into simple algebraic calculations. Both the rate of convergence and accuracy are shown to be rapid and accurate. Effect of core loss is included. The analysis of the SEIG with long shunt and short shunt compensation are carried out. The computed results are verified experimentally on a 2kW induction machine.

K. S Sandhu [27] implemented an improved iterative technique to evaluate the values of F and X_m for the analysis of SEIG corresponding to steady state. For the

analysis purpose, a different equivalent circuit is proposed in place of conventionally used equivalent circuit. The final values of F and X_m are obtained in just 4 to 5 iterations only. Using the proposed scheme, the performance analysis of SEIG is carried out under different operating conditions. The theoretical and experimental outcomes close association confirmed the validity and applicability of the betrothed scheme.

A. L Alolah et.al [28] focused on the optimization technique of evaluating the values of F and X_m for the analysis of SEIG corresponding to steady state. The two MATLAB inbuilt functions “fmin” and “constr” are employed to simplify the total impedance of the equivalent circuit (per-phase) to evaluate the values of F and X_m for the analysis purpose. The theoretical and experimental results are shown to be closely related.

D. Joshi et.al [29] introduced a GA based control technique for attaining voltage and frequency regulation of the SEIG. The speed and excitation capacitance are chosen as the control variables frequency and voltage regulation. The optimized values of these control variables are attained by evaluating the performance index. Using these optimized values of the control variable, the desired performance of the SEIG under steady state conditions is obtained. GA modelling based analytical results of the SEIG is validated experimentally. The close resemblance between the two results proved the validity of the proposed scheme.

T. F Chan [30] emphasized on the analysis of 1-phase SEIG feeding a resistive nature load. Application of nodal admittance method in the equivalent circuit yielded the value of F and X_m. A 9th degree polynomial in F is obtained on equating the real part of the total admittance to zero. The value of X_m is obtained on equating the imaginary part of the admittance equal to zero. A conventional Newton Raphson (N-R) method is discussed for evaluating the values of F and X_m for the analysis purpose of SEIG. Experiments are performed to verify the theoretical predictions. This paper also provided the guidelines on how to select the proper value of excitation capacitance in order to attain optimum utilization and better performance of the machine.

T. F Chan [31] envisaged the performance analysis of 3-phase SEIG rotated by both regulated and unregulated turbines. The desired values of F and X_m are accomplished on equating the total admittance of the circuit to zero. For regulated turbines, two modes i.e. constant speed and frequency operation are analysed. For constant speed mode, the value of F is evaluated using a simple iterative algorithm. For constant frequency mode, the value of p.u. speed is evaluated by a quadratic equation solution. For unregulated turbine, a two-level iteration technique is adopted to evaluate the values of torque and speed. Secant method is included for fast convergence and for providing additional iteration.

L. Quazene et.al [32] discussed a method of evaluating the squirrel cage IG output voltage and its frequency when subjected to resistive load under steady state. The SCIG output voltage and its frequency are varied for a wide range of speeds. The effect of excitation capacitance, speed and load on the performance characteristics is considered. The operating slip remained small during the analysis and hence made the system efficient. The analytical outcomes are verified experimentally.

J. L Bhattacharya et.al [33] covered the symmetrical component theory based analysis of a 3-phase SEIG furnishing unbalanced load particularly 1-phase load. A C-2C excitation scheme is opted for furnishing a 1-phase load in order to obtain maximum power output of a machine and to make the system balanced. An optimization technique is used for evaluating the values of F and X_m for carrying out performance analysis. The proposed scheme also helped in calculating the derating factor and voltage regulation under unbalanced conditions. Analytical outcomes are validated experimentally.

Li Wang et.al [34] presented the eigen values based transient performance of the SEIG furnishing dynamic load (IM) using short and long shunt connections. The effect of both types of connections on the voltage variation and dynamic performance of SEIG with or without dynamic load is carried out. It is concluded from the results that the long shunt connection resulted into distorted generated voltage while the short-shunt connection provided better voltage variation. The analytical results are validated experimentally using a 1.1kW induction machine.

2.2.2 Performance Analysis of 3-Phase IAG Furnishing a 1-Phase Load

Isolated Asynchronous generators (IAG) may be utilized for furnishing single-phase load [29-38] because of its very simple protection scheme, economical and almost maintenance less operation.

Above 5 HP, 3-phase IAG is preferred due to economical advantages over 1-phase IAG of the same rating. These advantages are low cost and have higher efficiency than the equivalent rating single-phase machine. Hence, it encourages the researchers to use three-phase IAG for furnishing single-phase load [41-53]. To minimize the adverse effects of phase unbalancing, a lot of research has been focused on three-phase IAG furnishing 1-phase load.

B. Singh et.al [35] attempted to analyse the performance of 1-phase SEIG furnishing 1-phase lighting load on a hardware set-up of 1 HP induction machine in the laboratory. The experimental study is carried out in order to check the suitability of 1-phase SEIG for feeding lighting loads. It is inferred from experimental outcomes that it is possible to maintain the terminal voltage at the desired level within ± 5% range by only a two-step capacitor switching circuit. The capacitor switching circuit operation is totally based on voltage. This switching circuit provides the guidelines to the design engineers for designing voltage regulation scheme for SEIG. The capacitor switching proves to be economical and can be easily implemented for supplying power in off-grid areas. Such cost effective generating units may be utilised for electrical power generation in remote sites and off- grid areas for meeting lighting load requirement.

S.S. Murthy et.al [36] detailed experimental study to carry out to check the feasibility of Self-excited self-regulated single-phase IG for its practical use. The performance analysis of 1-phase SEIG is carried out at constant speed for maintaining terminal voltage at desired level. The effect of various parameters i.e. speed, load, power factor and shunt and series capacitances on the performance characteristics have been analyzed. It is observed that due to speed drop, the voltage regulation was little bit poorer and its value could be improved either by using a saturable core reactor or by doing speed regulation.

T. F Chan [37] described the performance characteristics of 1-phase SEIG

subjected to no load and resistive load condition. For the performance evaluation, the values of frequency F and magnetizing reactance X_m are obtained from admittance based equivalent circuit. Upon equating the real part of total admittance across air-gap node equal to zero, a 9th degree polynomial in frequency F is obtained. Upon equating the imaginary part of the total admittance across air gap node equal to zero, the value of X_m is obtained. The solution of the polynomial by Newton Raphson method yields the value of F. By using this known value of F, X_m is obtained. Using the known value of X_m, the air-gap voltage (V_g) is evaluated from the no-load curve obtained from synchronous speed test. With the attained values of F, X_m and V_g of the asynchronous machine, the complete performance of the SEIG is attained using the equivalent circuit. The analytical outcomes are tested and verified experimentally and validate the proposed scheme. This study helps the design engineers in selecting the proper size of capacitor according to the machine rating so that optimum performance and optimum utilization of the machine can be made.

Y. H. A Rahim et.al [38] presented analysis of 1- phase IG corresponding to steady state situation. The excitation capacitor is inserted in one winding (auxiliary winding) and the load is inserted in the second winding (main winding). The application of the symmetrical component theory in the equivalent circuit finally resulted into two non-linear equations having two unknown variables X_m and F. A numerical technique i.e. Newton Raphson technique is used to evaluate the values of X_m and F. Based on these analytical values, the complete performance of the machine is determined. The analytical results are validated experimentally. A study based on the effect of various parameters on the machine performance is carried out.

B. Singh et.al [39] identified a method of selecting the value of excitation capacitance to attain optimum excitation of 1-phase SEIG. For performance evaluations of SEIG under steady state condition, the values of frequency F and magnetizing reactance X_m are evaluated using SUMT and Rosenbrock's method of rotating coordinates. After knowing the values of F and X_m, the complete performance of the SEIG is accomplished using no-load characteristics and the equivalent circuit. The analytical and experimental results of SEIG under steady state condition are illustrated for three types of excitation capacitor schemes: fixed shunt, fixed and variable, shunt and series. It is investigated that a fixed shunt excitation

capacitor scheme produces lower output at reduced voltage and it finds limited practical applications. With fixed and variable shunt excitation capacitor scheme, the SEIG can be loaded to 150% rating of the machine provided winding currents should lies within the rated value. With shunt and series excitation capacitor scheme, the SEIG can be loaded safely to 140% rating of the machine. Thus it is finally concluded that that a shunt and series excitation scheme is the most attractive and preferred option for small scale 1-phase power generation.

T. F Chan et.al [40] focussed on the analysis of a single-phase SRSEIG based on symmetrical component theory. A pattern search optimisation method is used to evaluate the value of X_m and F for the analysis purpose. Finally the effect of series capacitance on various aspects i.e. voltage regulation, phase balancing capability, capacitance calculation for perfect phase balance, voltage unbalance factor, output power and efficiency is demonstrated.

T. F Chan et.al [41] explained the analysis of 3-phase SEIG with the asymmetrical connected X_c and load with the aid of symmetrical components. In this paper, a function based on scalar impedance is minimized using pattern search based optimisation method. The search strategies for attaining the optimum value of X_m and F for the performance evaluation is based on exploratory and pattern moves. Moreover, a scheme for accomplishing almost exact phase balancing based on MSC is implemented in this discussed paper.

S. N Mahto et.al [42] discussed the way of evaluating the optimal value of excitation capacitance required for obtaining maximum power output of three-phase SEIG (star connected) for furnishing 1-phase inductive and capacitive load. The values of X_m and F are attained using Sequential Unconstrained Minimization Technique (SUMT). It is observed that the developed algorithm helps in evaluating the values of series connected capacitances (C_p and C_s) for accomplishing maximum power output and its value related to maximum power output. The effect of power factor of load and speed (prime-mover) on the maximum power output is illustrated. It is noticed that the voltage related to maximum power output is found to within the defined and acceptable bounds. Also, the voltage regulation is found to be small due to presence of two series connected capacitances. The close association of the experimental and simulated outcomes validates the discussed scheme.

T. F Chan et.al [43] explored a secant method to obtain the values of X_m and F for finding the minimum value of C for three-phase SEIG furnishing single-phase load. In this paper, the Steinmetz connection is adopted for a 3- phase generator excited by a single capacitor and feeding a 1-phase load. For voltage build or self-excitation phenomenon, the sum of the generator impedance using loop analysis has been equated to zero. This complex equation is separated into real and imaginary parts and equated individually to zero to attain the value of F and X_c using Secant method for the analysis purpose. The various results showing the effect of speed, load impedance and power factor on the excitation is demonstrated. The minimum and maximum values of speed, load impedance and power factor required to sustain self-excitation is provided. An iterative technique is adopted for evaluating the value of excitation capacitance requisite to support terminal voltage under load conditions. The analytical results are validated using an experimental set-up of 2 kW asynchronous machines.

A. I Alolah et.al [44] discussed an optimization technique to evaluate the value of excitation capacitance for the 3-phase SEIG furnishing 1-phase load. Two capacitors (C-2C) configuration are connected across the SEIG terminals to feed 1-phase load. The C-2C configuration is chosen to ensure the existence of self excitation phenomenon and to minimize voltage unbalances in stator voltages. The values of X_m and F for the performance analysis are attained using a gradient solver initiated by a sequential generic (GA) is used to minimise a cost function of the sum of equivalent impedances plus the voltage unbalance factor.

Y. J Wang et.al [45] investigated the performance of three-phase SEIG with the aid of symmetrical component theory and two-port network. The unbalanced loads are modelled using the concept of two-port network. The performance characteristics are obtained under three operating conditions of load and excitation capacitance: balanced excitation capacitances and loads, unbalanced excitation capacitances and balanced loads etc. The analytical results are verified experimentally on a 0.5 Hp asynchronous machine. Both results are closely related and validate the proposed scheme.

T. F Chan et.al [46] focused on several phase balancing schemes for a three-phase SEIG furnishing single phase load or single phase power system. Perfect phase

balance is obtained using modified Steinmetz connection. The proposed schemes are based on phase converters consisted of passive circuit elements. Symmetrical component theory is adopted for carrying out steady state performance analysis and for attaining the perfect phase balanced operation. Experimental investigations are carried out on an asynchronous machine to verify the feasibility of theoretical investigations.

L. Wang et.al [47] derived the dynamic equations of the three-phase SEIG furnishing 1-phase resistive load with single capacitor excitation. This paper focussed on three types of stator connection: 1-phase connection, Steinmetz connection I and II. The lower and upper value of excitation capacitance corresponding to no load and load conditions for the three types of stator connections are evaluated using the concept of Eigen value and Eigen value sensitivity. It is observed that the single phase connection has slightly larger value of C_{min} than the two connections under no load and load conditions. Also, the single phase connection has larger value of C_{max} than other two connections under no load conditions and smaller value of C_{max} than the other two connections under load conditions. The analytical results achieved using the proposed scheme for the three types of stator connection are validated experimentally on a 1.1 kW an asynchronous machine.

T. F Chan [48] presented the symmetrical component theory based steady state performance characteristics of a 3-phase SEIG with a one capacitor excitation and feeding a 1-phase load. For performance evaluation, the values of F and X_m are evaluated using pattern search method proposed by Hooke's and Jeeve's. Steinmetz connection is used here for feeding 1-phase load. Steinmetz connection with excitation capacitor connected across the lagging phase results into better voltage regulation and better performance characteristics relating to output power, efficiency and voltage unbalance factor. Experimental investigations are performed on asynchronous machine (2.2 kW) to validate analytical investigations and the proposed scheme.

T. F Chan et.al [49] revealed the symmetrical component theory based steady state performance analysis of 1-phase SRSEIG using a 3-phase asynchronous machine. For performance assessment, the values of F and X_m are evaluated using Hooke's and Jeeve's method (Pattern search method). The Steinmetz connection is

used in single phase SRSEIG. This generator improved the voltage regulation, increased power output and provided better phase balance. The close resemblance of the experimental and theoretical outcomes confirmed the validity of the suggested scheme.

T. F Chan et.al [50] presented the symmetrical component theory based performance analysis of a 3-phase IG feeding 1-phase load using Smith connection (SMIG). Further, the conditions for achieving the perfect phase balance are derived. Under perfect phase balance condition, the mathematical expression for line power factor and line current are derived from the phasor diagram. Also, the effect of speed and phase balancing excitation capacitance on the performance characteristics are analysed. It is noticed that when the IG impedance angle lies between $2\pi/3$ rad and $5\pi/6$ rad then only phase balance is achieved using excitation capacitance. The proposed phase balancing scheme and analytical results are validated experimentally on a 2.2kW induction machine.

T. F Chan [51] suggested a novel excitation scheme for a three-phase SEIG furnishing single-phase load. The Smith connection is opted here for excitation capacitor and phase winding connection. This novel excitation scheme is called SMSEIG. This excitation capacitor provided phase balancing in addition to the self excitation phenomenon. Symmetrical component theory is used for the performance analysis of SMSEIG. For accessing performance analysis, the values of F and X_m are evaluated using Pattern search method (Hooke's and Jeeve's). With the help of phasor diagrams, the conditions for achieving perfect phase balance and the value of excitation capacitance is deduced. The proposed scheme resulted into higher efficiency, larger power output and noise free operation of the generator due to perfect phase balance. The theoretical aspects of SMSEIG are validated through experiments on a induction machine of 2.2 kW

T. F Chan et.al [52] discussed four different schemes for phase balancing for 3-phase IG energised by a 1-phase system. These four schemes are realized or implemented using phase converters consisting of passive elements only. The steady state analysis of IG and condition for attaining the perfect phase balance is carried out using symmetrical component theory. From the results, it is concluded that the values of converter elements for attaining perfect phase balance are the function of positive

sequence conductance and susceptance and the power factor is the function of the positive sequence impedance angle. The effect of phase balancing on the system power factor, power and its efficiency has been illustrated. The theoretical outcomes are validated experimentally on a 2kW induction machine set.

S. N Mahato et.al [53] presented the analysis of a 3-phase SEIG (Y-connected) excited by a three capacitor connection. Two series connected capacitors are held across the generator and the remaining capacitor is connected across the 1-phase load. The d-q modelling of the generator including cross-saturation effect has been done using stationary reference frame. The complete performance is accessed during the starting of self-excitation phenomenon, load application and perturbation and short circuit load terminals under transient conditions. For performing analysis, the values of X_c and F are evaluated using SUMT along with Rosenbrock's method of rotating coordinates. Finally the simulation based results are validated experimentally. Both results showed good resemblance. It is inferred from the outcomes that good voltage regulation, sustained self-excitation phenomenon and sinusoidal nature output voltage and current are achieved using the proposed scheme.

Y. J Wang et.al [54] revealed or stated that when a 3-phase SEIG feeds unbalanced load then an unbalance in generator voltage and current takes place which finally results into overheating and derating of the machine. This paper explores a 3-capacitor circuit scheme and evaluates the values of excitation capacitor that balance the 3-phase SEIG system supplying 1-phase load. The 3-capacitor scheme is formed by using one fixed capacitor scheme and two variable capacitor schemes. The fixed capacitor scheme provides the requisite reactive power whereas the two variable capacitor schemes help in balancing the SEIG system feeding 1-phase resistive and inductive load. The two variable capacitor schemes is formed by using two SVC's, a parallel combination of a fixed capacitor and a TCR. This paper proposed a two port model for evaluating the values of 3 capacitors to balance the SEIG system. The analytical results attained using two port networks are verified experimentally on a 0.375 kW induction generator.

2.3 VOLTAGE AND FREQUENCY REGULATION SCHEMES OF IAG FEEDING BALANCED/UNBALANCED LOADS

The fundamental problem with IAG is concerned with its poor voltage and frequency regulation when subjected to varying load. Owing to the problem of poor voltage regulation of the machine, the rating of the machine is not wholly utilised. The desired voltage and frequency of IAG is accomplished using the VFC and an additional source of reactive var.

2.3.1 Electronics Generator Load Controller (EGLC) for an IAG

An extensive literature related with the design, testing and development of the VFC's for an IAG is available. The challenging task is to accomplish the desired performance of IAG related with its voltage and its frequency at different loads. These VFC controllers are reviewed one by one in the following section:

J. M Elder et.al [55] discussed the ways to minimize the cost of micro-hydro based stand-alone power generation scheme (upto 100kW). This paper analyzed the stability of both conventional synchronous generator and induction generator using switching of capacitor in steps under varying load condition. The integral cycle control method proves less costly and is highly recommended for small power generation schemes. Results are presented to validate the proposed scheme for micro-hydro based power generation.

R. Bonert et.al [56] presented an impedance controller based on the principle of electric load governing for better voltage and frequency regulation of the SEIG. The suggested controller comprises of a phase controlled bridge connected in series with a IGBT switch and a resistor. The aforementioned controller provided the real and imaginary parts of the current for a defined ac voltage. These real and imaginary current components depends on α (control angle) and δ (pulse width).The value of α and δ have been produced by the control algorithm. These are given as inputs to the controller. The controller provided the desired compensating current to keep constant load on the SEIG. Hence the recommended controller maintained both voltage and frequency constant. To validate the proposed scheme, the analytical results are verified experimentally.

R. C Bansal [57] reviewed the various research papers related to SEIG: initiation of self-excitation phenomenon, various modeling techniques of SEIG, Performance analysis of SEIG under steady state and transient condition, various voltage regulation strategies and finally the parallel operation of SEIG.

B. Singh et.al [58] elaborated or explained in detail the modeling of various components of the composite system. The composite system consists of IAG or SEIG modeling in stationary reference frame, ELC modeling along-with control scheme, load. The combined modeling finally results into non-linear differential equations whose solutions are achieved using Runga Kutta method of numerical integration. The modeled system are then tested both using simulations and experiments for standalone applications.

B. Singh et.al [59] described the designing part of 3-phase and 1-phase electronic load controller (ELC) for a 3-phase SEIG of 7.5 kW rating. The results achieved under steady state and transient conditions showed that the suggested ELC can keep the voltage constant under varying load condition.

T. S Chandra et.al [60] discussed how a 3-phase induction machine (IM) works like an induction generator (IG) with the help of capacitor bank connected across the machine terminals. It needs reactive power for producing the rotating magnetic field and adjustable or varying reactive power under varying load conditions for voltage support. It also discussed the various types of voltage controllers i.e. series capacitor scheme, power electronics controllers: thyristor switched capacitor bank, AC/DC converters, thyristor controlled inductors with fixed capacitor bank, ELC, STATCOM and magnetic amplifier along-with its advantages and disadvantages. This paper also discussed the effect of excitation capacitance and loads on the performance characteristics of induction generator and finally introduced about the various voltage regulation schemes of SEIG using Magnetic amplifier, ELC and STATCOM.

S. Gao et.al [61] addressed the design aspects of microcontroller based ELC feeding 1-phase load for pico hydro based electrical power generation. The control signal to the ELC is provided by PIC18F252 microcontroller. Both hardware and software outcomes are illustrated to demonstrate the feasibility and effectiveness of the proposed controller.

J. M. Ramirez [62] discussed the designing procedure to design a dump load resistance for a 3-phase ELC furnishing a 3-phase consumer load for the SEIG. The dump load has been controlled using two IGBT based switches in anti parallel /phase. The recommended system performance is analyzed under different loads. A THD analysis is performed to examine the harmonic content in voltage and current. It is noticed that the recommended controller supports the SEIG voltage and its frequency under various critical conditions of load.

E. G Marra et.al [63] proposed a voltage source PWM inverter for the performance enhancement of IG. The performance enhancement of IG relating to voltage regulation, frequency regulation and reactive power compensation is achieved using the proposed controller. This paper elaborated in detail two distinct schemes. In one scheme, generator speed is controlled. The other scheme does not contain speed governor and is known as cogenerator scheme. The power produced in this scheme is used for agricultural purpose, manufacturing process and for feeding 1-phase load. In both schemes the voltage and frequency regulation is provided by PWM based inverter. The obtained result outcomes illustrated that the system is robust, stable and can act as a regulated 3-phase power source.

B. Singh et.al [64] focussed in his research paper on the improvement of power quality of voltage and current of six-pulse ELC using 24-pulse ELC for an IAG. The design calculations for autotransformer (polygon connected) have been provided in detail. Both topologies of ELC have been tested experimentally and analytically using SIMULINK and Sim Power System toolbox of MATLAB. The results obtained of the topologies of ELC have been compared. It has been concluded that 24-pulse ELC provided better performance. But the autotransformer based ELC increases the cost of the whole generating system. Moreover, the control to the ELC has been provided using conventional PI controller.

S. Mbabazi [65] provided a review of the already available literature, existing technology and already available research on ELC for micro-hydro based power generation. This paper discusses various aspects of micro-hydro generation in detail covering: Introduction and working principle of micro-hydro, components of micro-hydro system, control systems related to micro hydro, Introduction to different load

regulation techniques and finally introduction and details of various already existing ELC's.

B. Singh et.al [66] provided detailed modelling of isolated asynchronous generator (IAG) and 1-phase ELC feeding 1-phase load. The composite modelling of generator, ELC and load are validated using software and hardware approach.

B. Singh et.al [67] focussed on the stationary frame based d-q modelling of Δ-connected SEIG, modelling of Δ-connected capacitor, modelling of dynamic load (Induction motor) and unity p.f. load, modelling of 3-Φ ELC, modelling of control scheme of ELC, modelling of prime mover. The performance is examined under transient condition. Star-delta (Y-Δ) starter is used here for starting the induction motor in order to avoid the flow of in-rush current through the winding. A hardware set-up is constructed for SEIG-ELC system to validate the simulated outcomes. The simulated and experimental results show less discrepancy. The THD based analysis is carried out to check the power quality of generated voltage and current of the SEIG.

S. N Mahato et.al [68] conveyed about the performance analysis of three-phase SEIG feeding lagging power factor loads under transient conditions. The complete system is modelled using: d-q modelling of Y-connected SEIG (saturation effect included), modelling of 1-phase ELC, modelling of control scheme of 1-phase ELC, modelling of consumer load. To validate modelling based results, a hardware set-up of SEIG-ELC is developed. Finally, a comparison is made between the results obtained from modelling and experimental, both results are closely related. Hence, such systems can be adopted for micro-hydro based generation.

B. Singh et.al [69] provided information about the performance analysis of SEIG-ELC under occurrence of steady state for varying loads. It consists of rectifier circuit, chopper switch in series with auxiliary load R_{ad}. It supplies or injects harmonics on the generator side of the SEIG. So, a harmonic analysis of ELC is carried out to illustrate its effects on performance under steady state conditions. The harmonic analysis formed the basis for designing aspects of capacitor and various types of VFC's.

B. Singh et.al [70] discussed the control strategy, designing and implementation of an EVFC for a 1-phase IAG. The EVFC is deployed here for

supporting IAG voltage and its frequency under varying load. The dynamic behaviour of IAG-EVFC under transient phenomenon subjected to different conditions of load injection and load rejection for 0.8 p.f load is analysed or examined experimentally to prove the feasibility of designed EVFC.

S. C Kuo et.al [73] discussed the CC-VSI for voltage regulation and harmonic elimination of a 3-phase IAG feeding balanced/unbalanced resistive, inductive and non-linear loads. A hybrid model of the induction machine based on the two types of reference frames (3-phase a-b-c and d-q axis) is considered to accomplish the transient performance of the IAG and CC-VSI system. Both the 3-phase ac voltage of the generator and dc voltage of the CC-VSI are controlled by two PI controllers. From the simulated results, it is noticed that the IAG performance under unbalanced condition of non-linear loads is effectively enhanced by the proposed controller.

E. Suarez et.al [74] introduced or explored a new strategy for supporting SEIG voltage and its frequency. It is assumed here that the generator should operate in the linear part of the no-load curve. The dynamic model of the SEIG is suggested here to provide guidelines for designing of the controller and its analysis under transient conditions subjected to change in consumer load. Voltage and frequency regulation is based on Variable Structure Control Criteria. Dynamic performance is analyzed using computer based simulations.

S. S Murthy et.al [75] shared a field experience of establishing standalone generating systems using SEIG driven by hydro turbines with two different types of ELCs. Two types of ELC's (back to back thyristor based ELC and uncontrolled rectifier chopper operated ELC) are designed, developed and established in the Asolli villiage (Karnataka) to maintain power balance under varying consumer load. Field data related to SEIG and both types of ELC is provided to check the feasibility and viability of the suggested scheme. Finally the performance attained using SEIG with both controller is compared. It is observed that uncontrolled rectifier chopper operated ELC provides better voltage regulation than thyristor based ELC.

B. Singh et.al [76] covered the dynamic d-q modelling of the SEIG in stationary reference frame with an improved ELC. The Improved ELC consists of 3-phase IGBT type current controlled VSI (CC-VSI), DC type chopper switch and a

load Rd. The dynamic behaviour of SEIG-IELC is examined under the situation of balanced and unbalanced load. Tested simulated outcomes show that the IELC is efficiently or effectively working as voltage and frequency regulator or supporter, harmonic minimize.

I. Serban et.al [77] focussed entirely on the analysis part of an ELC. The ELC is represented here as a dump load. A lot of attempts are made through simulations and experiments to check the validity and feasibility of ELC.

B. Singh et.al [78] discussed about an IAG-IELC system designed for furnishing 3-Φ, 4-W linear and non-linear nature loads for constant power based applications. The IELC circuitry is formed by various electronic components: four-lagged IGBT based VSC, IGBT based chopper switch, dump load resistance, capacitor on dc side and filtering inductors on ac side. A template based control strategy is adopted here for producing the driving signals for IELC. The mathematical modelling of the complete system is developed in MATLAB and simulated results prove the capability of IELC as a supporter of voltage and frequency of IAG.

B. Singh et.al [79] investigated an ELC for Islanded Asynchronous Generator. The generating system circuitry includes Asynchronous Generator, AC capacitors, consumer loads, VSC module with dc type capacitor, IGBT based chopper switch, three-phase transformer (star/delta) and a dump load. SRF based control theory is adopted here for producing gating signals for ELC. A hardware module of ELC is designed and implemented for 3.7 kW asynchronous machine using DSPACE DSP in the machine laboratory. The performance of IAG-ELC feeding balanced/unbalanced non-linear loads is investigated experimentally under steady and transient condition. An insight into the experimental investigations reveals that the regulation of voltage, harmonic minimization and frequency support is satisfactorily controlled by ELC.

V. Rajagopal et.al [80] portrayed the information regarding the implementation of ELC for IG based hydro power generation system. The IcosinΦ based algorithm is implemented here to yield or generate or produce reference currents for voltage and frequency power quality improvement and its control. The ELC is constituted by a T-connected transformer (non-isolated) 3-legged IGBT based CC-VSC, filtering capacitor, chopper switch, dump load. This system of IG-ELC is

basically implemented for furnishing 3-phase 4-wire loads with the added advantage of providing neutral current compensation. A hardware set up is made of the proposed IG-ELC of 3.7 kW rating in the laboratory to testify the performance under the condition of balanced/unbalanced non-linear loads.

E. Torres et.al [81] highlighted the designing of an improved version of an ELC for an SEIG for stand alone or micro-hydro based applications. A dump load is found out to maintain constant power at consumer terminals under varying load. Per-phase two IGBT type switches are connected in series and are inverted. These switches are used for the purpose of ON/OFF of dump load. The performance analysis is done when the SEIG-ELC system is subjected to various operating conditions. It is observed that the proposed controller provided better voltage and frequency support under balanced/unbalanced conditions. A harmonic analysis is performed to evaluate the THD of the generated voltage, controller (dump load) and consumer load current.

S. S Murthy et.al [82] rendered the performance (steady-state and dynamic) of SEIG with an ELC (digitally controlled) furnishing both 3-phase and 1-phase loads. The detailed mathematical modelling of the whole system includes: (i) dynamic d-q modelling of SEIG (considering saturation effect), (ii) excitation capacitor modelling, (iii) load modelling, (iv) ELC modelling. After modelling, a no of differential equations are obtained and are analytically solved using Runge-Kutta method. The proposed controller is fabricated and tested for field applications for voltage regulation of SEIG.

D. K Palwalia et.al [83] proposed a DSP based VFC for a 3-phase SEIG rotated by an unregulated micro-hydro turbine and feeding 1-phase load (resistive or reactive load). The input power is maintained constant by micro-hydro turbines but the output power of SEIG is varying under load. To maintain constant power output, the two loads (dump and consumer) are connected in shunt. The DSP based controller helps in maintaining the generator load constant. Hence constant SEIG voltage and its frequency operation is obtained. A hardware set-up of DSP operated controller for an SEIG is developed in the laboratory to check its operation, validity, effectiveness and feasibility. The transient performance characteristics of a DSP based SEIG under different operating conditions (load application and removal) are illustrated. It is noticed that the SEIG voltage and its frequency are constant under varying load

condition and hence validates the proposed controller for an SEIG. Moreover the DSP operated controller reduces hardware complexibility, cost and increases reliability.

S. S Murthy et.al [84] accessed the complete behaviour or performance of the IAG feeding 1-phase load with digitally controlled ELC (DCELC) under transient or dynamic and steady state condition. The compete model of generating system is constructed here by combining the dynamic or d-q model of SEIG with saturation effect, excitation capacitor model, 1-phase load model , electronic load controller model. The digital driving or control signals are fed to the ELC through PIC18F252 microcontroller. This controller provided better voltage regulation and is found to be more reliable, economical and compact for practical applications.

S. Gao et.al [85] addressed the design aspects of microcontroller based ELC for SEIG for feeding single-phase load for pico hydro based electrical power generation. The control signal to the ELC has been provided by PIC18F252 microcontroller. Both hardware and software results have been presented to demonstrate the feasibility and effectiveness of the proposed controller.

S. Sharma [86] emphasized on the designing and implementation of Fuzzy logic approach based two PI controllers for supporting the IAG voltage and its frequency for variable speed applications (wind). The control strategy is operated on power balance theory. The system comprises of IAG, load, three-legged VSC, battery energy storage system. A 3-phase zig- zag connected transformer connection is employed here to feed 3-Φ, 4-wire WECS system. The simulated outcomes revealed that better dynamic performance is achieved in fuzzy based PI controllers rather than conventional PI controllers.

Y. Sofian et.al [87] elucidated the design of ELC, design of ELC using fuzzy logic approach based on microcontroller ATMega32. A C-2C capacitor connection is adopted with Δ-connected SEIG for feeding 1-Φ loads. The proposed ELC consists of various types of electronic components: rectifier, voltage sensor, MOSFET type chopper switch, microcontroller ATMega32, opto-coupler and dump load. The suggested controller is tested both analytically and experimentally for a 3-Φ SEIG furnishing 1-phase load for step change in load.

D. Henderson [88] explained the original research on the development of microprocssor based binary weighted ELG (Electronic load governer). A hardware set-up of microprocessor based ELG is developed and tested in hydraulic laboratory of Napier University. The response of the governer is based improved using proportional control based advanced algorithm. Finally a comparative study is carried out between original and advanced algorithm. From comparative study, it is noted that there is a significant improvement i.e. reduction in frequency magnitude rise on full load removal and a significant improvement i.e. is reduction in transient duration period itself. Thus the better performance is attained using advanced algorithm than the original ELG.

D. K Palwalia et.al [89] aimed at designing and execution of a DSP (TMS320F2812) VFCs for a three-phase SEIG furnishing 1-phase load (resistive and reactive load. The proposed controller works on the concept of constant load on the generator to support its voltage and frequency subjected to varying load. The proposed controller is tested in the laboratory hardware set up of 3.73 kW asynchronous machines. From the test results, it is inferred that the recommended controller supports voltage and frequency of SEIG with a THD related to voltage and current of generator and load within defined acceptable bounds.

V. Verma et.al [90], analyzed the performance of the SEIG subjected to various critical operating conditions of load i.e. full application and full removal of load. This paper recommended a VSC for providing support to SEIG voltage and its frequency under varying load. The voltage and frequency regulation is achieved by controlling active and reactive power through VSC. The control algorithm of SEIG voltage and its frequency regulation by VSC is operated on indirect current control strategy modeled in d-q reference frame. The simulated outcomes illustrated the generator voltage and its frequency support operating under varying load with the help of VSC.

S. Gao et.al [91] proposed an efficient and low cost microcontroller operated ELC for supporting voltage of 3-phase SEIG furnishing 1-phase load (resistive and inductive load) in remote sites. The proposed ELC is realized using uncontrolled rectifier, a capacitor on dc side, IGBT type chopper switch and a dump load. The PWM signals of appropriate duty cycle for driving the IGBT switch are produced

using microcontroller (dsPIC30F6010). This controller helps in proper switching of consumer load and dump load in such a way that the entire load on the SEIG becomes constant. Hence the proposed controller maintains fixed load on the generator and hence the SEIG voltage and its power remains constant when subjected to variable load conditions. The experimental results are obtained from the developed hardware to validate the simulated results. Such microcontroller based system proves cost effective and efficient as a source of electrical power generation in grid isolated remote areas.

2.3.2 CC-VSI Based Controller for an IAG

Different types of voltage and frequency controllers IAG feeding 3-phase 3-wire and 3-phase 4-wire type loads have been designed developed and are reported in literature [51-58]. But, today the traditional controllers (PI) are replaced by FL based controllers for the performance enhancement of IAG [59].

S. S Murthy et.al [92] discussed the development and practical implementation of the three electrical power generation schemes using three different configurations of the SEIG: 3-phase SEIG supplying 3-phase load and 1-phase load, 1-phase SEIG supplying 1-phase load with electronic load controller and VAR compensator. The complete performance of the 3-phase (7.5 kW, 415V) and 1-phase (220 V, 750W) SEIG are analysed for testifying the validity and feasibility of the proposed scheme for field installation of micro - hydel units (upto 100kW). Based on the proposed and developed laboratory schemes, a unit of 6 kW is planned for field installation of such schemes in Kerala with the joint efforts of IRTC (Integrated Rural Technology Centre), Kerala.

S. S Murthy et.al [93] provides the detailed review of the operation of various types of var controllers with different types of prime-movers. Few results related with the var requirement of the SEIG with prime-mover speed and load are illustrated and this analytical data provides the foundation of designing different control strategies. It is also discussed that the var controllers for wind turbines are complicated owing to varying speed and power. A broad list of var controllers is discussed and these controllers can be tested and realised for practical field applications.

S. K Jain et.al [94] presented the dynamic d-q axes based modelling of the SEIG in stationary reference frame. A set of seven differential equations representing d-q components of stator currents, rotor currents, stator voltages and speed are obtained. The matrices [B] and [C] gets modified under balanced, unbalanced and fault conditions. The effect of symmetrical and unsymmetrical load and excitation capacitor connection can be included in the model. The performance of SEIG subjected to load perturbations is investigated considering the saturation effect of both main flux and cross flux. The performance of SEIG is accessed under various operating conditions: 3-phase and L-L short circuit, removal of any one or two capacitors, single line availability at load and at capacitor bank, removing of 1-phase and 2-phase load. The experimental outcomes are obtained on a 3.7 kW machine in the laboratory. The close resemblance between the experimental and simulated outcomes indicates the validity of the proposed scheme.

M. B Brennen et.al [95] explored the static exciters for an IG for autonomous power generation. The 1-phase static exciters are composed of fixed capacitors in parallel with thyristor controlled variable inductors. The control of exciter is based on integrated voltage error. The control circuit of exciter provides compensation to the IG under unbalanced load and varying non unity power factor loads. The feasibility of the proposed static exciter is verified experimentally on a hardware set-up of 15 Hp asynchronous machines. This paper also discussed the various applications of static exciters such as in rolling mill power factor correctors, transmission line stabilizers, high speed air craft generator etc.

R. K Mishra et.al [96] developed a voltage controller for a 5HP, 3-phase self-excited cage induction generator feeding various types of static (resistive and inductive load) and dynamic loads (3 H.P Induction motor). The proposed controller consists of a saturable core reactor in shunt with fixed value capacitors. The steady state and dynamic performance characteristics of the whole system are analysed under different operating conditions and different types of loads. Finally a comparison of the proposed controller with the thyristor based voltage regulator is made. From the experimental outcomes, it is inferred that the recommended voltage controller is able to maintain constant terminal voltage irrespective of operating conditions, nature and type of the load. From the comparative study, it is concluded that the proposed

controller for cage induction generator is found to be better than the thyristor based voltage controller relating to cost, reliability, robustness and dynamic performance. It is suggested that the complete system can be treated as an electric power source for remote areas electrification.

L. Shridhar et.al [97] covered in detail the transient performance characteristics of both simple shunt and short shunt SEIG (3.7 kW) including cross saturation effect under different operating conditions: voltage build-up, load perturbation, short circuit and loss of excitation etc. From the obtained results, it is observed that a short shunt SEIG possesses a very good voltage regulation, higher overload capability and better transient performance as compared to simple shunt SEIG. It also automatically regains the self-excitation phenomenon after the removal of faulted conditions. Thus, the short shunt SEIG proves as a simple, rugged and a self-regulated generating system for electrifying grid isolated areas.

T. Ahmed et.al [98] discussed the steady state analysis of a 3-phase SEIG driven by wind turbine easily available in remote or isolated areas for feeding inductive load. An impedance approach is used for problem formulation and for carrying out steady state analysis for performance evaluation. The generator voltage and its frequency variation with the excitation capacitance, output power and prime-mover speed are observed. Moreover this paper discussed an SVC based voltage regulator for a 3-phase IAG driven by a VSPM. The SVC comprises of a TSC in parallel with a TCR and a fixed capacitor (FC). A hardware set-up of 3-phae SEIG with SVC is established in the laboratory for validating results obtained from simulations. The experimental investigations are closely related with the simulation outcomes and prove the effectiveness of the proposed scheme for rural electrification.

T. Ahmed et.al [99] discussed the steady state performance of 1-phase SEIG. The analysis of 1-phase SEIG is carried out on the basis of per-unit frequency and per-unit slip frequency using nodal admittance method under varying prime-mover speed and inductive load. A 1-phase SVC along-with a PI controller is used here for providing voltage support to IAG under varying load conditions. A SVC consists of TCR, TSC and fixed capacitors (FC). The simulated results are validated through experimental results obtained on a hardware set up of 1-phase SEIG with SVC. A

close resemblance between the two outcomes validates the proposed scheme for electrification purpose for rural applications.

B. Singh et.al [100] explored a static condenser (STATCON) based voltage controller for a 3-phase SEIG. STATCON works as a synchronous condenser similar to SVS (synchronous voltage source). It operates in both inductive and capacitive modes. It also protects the SEIG from loss of excitation problem under varying load conditions. It consists of a 3-phase CC-VSI and a dc type electrolytic capacitor. The modelling of the SEIG-STATCON system i.e. modelling of SEIG (stationary reference frame), STATCON and control scheme for voltage regulation is done in order to access the dynamic performance. From the simulated outcomes, it is concluded that the STATCON supports terminal voltage under varying load. The proposed SEIG-STATCON system can be used to harness the electrical energy using non-conventional energy sources in remote sites.

S. C Kuo et.al [101] discussed the CC-VSI for voltage regulation and harmonic elimination of a 3-phase SEIG feeding balanced/unbalanced resistive, inductive and non-linear loads. A hybrid model of the induction machine based on the two types of reference frames (3-phase a- b-c and d-q axis) is considered to accomplish the dynamic performance evaluation of the SEIG and CC-VSI system. Both the 3-phase ac voltage of the generator and dc voltage of the CC-VSI are controlled using two PI type controllers (PI-AC and PI-DC). It is observed from the simulated results that the performance of the SEIG under unbalanced condition of non-linear type loads is effectively enhanced by the proposed controller.

S. C Kuo et.al [102] focused on the performance analysis of a 3-phase SEIG (1.1 kW) feeding rectifier loads only under transient state and steady state conditions. The performance is evaluated using hybrid induction machine model. The complete system is modelled by combining the modelling of the SEIG stator voltage in abc coordinates, rotor variables in qd0 coordinates, modelling of controlled rectifiers (semi and full converters) using switching functions. The performance of the SEIG subjected to variable load is analysed. Under steady state, the THD in generated voltage and current is evaluated using FFT analysis tool. The simulated results are verified experimentally on a hardware set-up and validate the effectiveness of the proposed scheme.

B. Singh et.al [103] presented the performance analysis of an SEIG-STATCOM system feeding balanced and unbalanced non-linear nature loads. The modelling of the complete system i.e. control scheme for STATCOM, STATCOM itself, SEIG (stationary reference frame) and four circuit configurations of non-linear loads is detailed here for carrying out the transient analysis of the IAG-STATCOM system feeding balanced/unbalanced 3-phase and 1-phase non-linear (uncontrolled and controlled rectifier type). From the simulated results, it is noticed that STATCOM balances the unbalanced load current and hence maintains the generator current and voltage constant, sinusoidal and harmonic free. Hence STATCOM works as a load balancer, voltage controller and harmonic eliminator. Thus SEIG with STATCOM can be treated as an ideal generating system for grid isolated locations.

B. Singh et.al [104] explained the design criteria of STATCOM device controlled SEIG. The designed criterion of the system (STATCOM-SEIG) for full rating and reduced rating for five machines of different ratings feeding different types of load is explained. The desired voltage regulation is accomplished using the designed controllers. The modelling of the system consists of (i) SEIG stator voltages in abc model, (ii) rotor variables in qd0 coordinates and (iii) the controlled rectifiers using the concept of switching functions. The performance of the SEIG subjected to variable load is analysed. Under steady state condition, THD in generated voltage and current is evaluated using FFT analysis. The simulated results are verified experimentally on a hardware set-up and simultaneously validate the effectiveness of the proposed schemes.

M. Bašić et.al [105] proposed two different types of techniques for SEIG terminal voltage control using a vector control system. An IRFO based control algorithm for terminal voltage regulation is executed in real time by MATLAB Simulink and DS1104 R and D controller board. An experimental set up of SEIG control strategy is implemented for experimental verification of the simulated outcomes. The performance of the SEIG is accessed using both conventional PI and fuzzy logic approach (Mamdani and Sugeno) and finally the performances attained from both methods are compared. From the results, it is concluded that better performance regarding rise time, settling time and robustness are attained using FL controllers than the conventional PI controllers.

B. Singh et.al [106] covered the modelling aspects of the combined generator and STATCOM system (STATCOM-SEIG) for static R and R-L load under unbalanced load situation. It is noticed from the simulated outcomes that the STATCOM-SEIG system supports the voltage and reduces the harmonics under unbalanced situation.

B. Singh et.al [107] analysed the performance of SEIG for feeding various types of loads using a voltage regulator STATCOM. The STATCOM based SEIG provided the voltage regulation under balanced or unbalanced loads. Dynamic modelling (d-q) of the complete system i.e. SEIG, Load, CC-VSI is done using stationary reference frame. The simulated outcomes revealed that the STATCOM worked as a voltage supporter and minimised harmonics under balanced or unbalanced conditions.

B. Singh et.al [108] presented a STATCOM controlled SEIG system supplying dynamic load (induction motor).Good quality and controlled nature voltage is attained using the aforementioned controller with a fast dynamic response.

Y. K Chauhan et.al [109] elaborated the designed procedure of cost effective static compensator (STATCOM) and full-rating static compensator (STATCOM). The performance of the SEIG-STATCOM for R-L and dynamic load is observed under transient conditions. The cost-effective static compensator is proposed for remote applications. Using the designed controllers, the performance improvement in characteristics regarding various parameters i.e. starting time, voltage dip, generator current and total THD is attained.

T. Ahmed et.al [110] firstly focussed on the performance analysis of SEIG corresponding to steady state using impedance based approach model. Here, both VSPM and CSPM are used for driving SEIG for producing clean electrical energy for benefitting rural sites. The operating conditions are created by changing prime-mover speed and inductive load variations. The performance characteristics in terms of voltage and frequency are accomplished at fixed capacitance. A hardware set-up of SEIG-SVC is developed in the laboratory for voltage generation and its regulation. The developed SEIG-SVC system proved to be cost effective can be utilised for

feeding rural sites. The simulated outcomes are closely resembled with the experimental outcomes.

S. Tiwariet.al [111] presented the performance characteristics of a fuzzy logic approach (Mamdani type FLC) based SAPF for voltage support of a 3-phase IAG feeding 3-phase static loads (linear and non-linear). The IAG is driven with the aid of some prime-mover at constant speed and is feeding 3-phase load. Under loaded conditions, IAG alone is not able to control the voltage of the source and load. Under loaded condition, SAPF along-with IAG can maintain both source and load voltage constant. SAPF consists of a 3-phase IGBT based VSC and dc capacitor. The whole system consists of IAG, constant speed prime-mover, excitation capacitor, load, SAPF and interfacing transformers. SAPF is modelled, designed and simulated for a generating system of 7.5 kW in MATLAB software. The performance characteristics are also accomplished using conventional PI controller. Finally, a comparison of the performance characteristics using both PI and Fuzzy logic based SAPF is made. It is concluded that better transient performance relating to settling time and overshoot is attained using fuzzy logic than PI based SAPF. Moreover it also maintains constant and sinusoidal voltage of IAG and load under varying load condition.

A. Banerji et.al [112] proposed a BESS operated VFC for an autonomous asynchronous generator (AAG) feeding load and is driven by a uncontrolled pico-hydro turbine. The extra need of the reactive var of an IAG and load under loading conditions is met by the VFC. This VFC is modelled using a 3-phase IGBT based CC-VSC and a battery on the dc side. A Sinusoidal PWM control scheme is used for the control of CC-VSC. The control algorithm of the SPWM control strategy is based on IRPT (Instantaneous reactive power theory). The recommended control scheme is easy to implement on the hardware set-up and software as it consists of only linear type PI controllers. It is inferred from the simulated outcomes that the proposed controller is efficiently working as a load leveller, voltage and frequency controller for an AAG furnishing various types of balanced/unbalance linear and non-linear loads. Such systems can be opted for autonomous power generation using pico-hydro turbines.

S. Sharma et.al [113] focussed on the implementation of fuzzy logic based PI controllers for supporting IAG voltage and its frequency. The IAG is mechanically

rotated with the aid of wind turbine. To improve the dynamic characteristics of an IAG, two FPI regulators are used in place of PI regulators in the VFC control strategy which works on power balance theory. A 3-phase four wire WECS system is implemented by using a zig-zag transformer at load bus. The whole FPI based WECS system is modelled, designed and tested in MATLAB software package. Better steady-state and dynamic performance characteristics of IAG under varying are attained using FPI controller than PI controller. It is inferred from the simulated outcomes that FPI controller worked satisfactorily as a load supporter, generator voltage and frequency supporter and a harmonic eliminator.

A. Banerji et.al [114] explained the operation of DSTATCOM in the defined window range with fuzzy logic controller operated TSC for an autonomous power generation using AAG. It is stated in the paper that for large rating inductive load, large rating of DSTATCOM is needed to generate the required amount of reactive power of the load. Large rating of DSTATCOM indicates higher cost of the system. This paper suggested that the base reactive power is met by the TSC and DSTATCOM provides both inductive and capacitive reactive power within a window. The DSTATCOM operates in the window range and provide the continuous and smooth control of varying reactive power instantly. For attaining the optimal performance of the whole system TSC are operated using fuzzy logic based controller. It is noticed that the suggested controller helps in providing regulated good quality power under varying load at a faster rate and avoids hunting problem.

2.4 SUMMARY

This chapter covered the literature review of various issues related to an Isolated Asynchronous Generator (IAG) i.e. self-excitation phenomenon in an Isolated Asynchronous Generator (IAG), analysis of isolated 3-phase IAG furnishing 3-phase loads and 1-phase loads using various techniques. It also highlights the problem of poor voltage and frequency regulation and provides the state of art of electronic load controller and 3-legged CC-VSI based voltage and frequency regulators available in the past. It provides immense information required for carrying out the research on the topic of my PhD entitled “Controllers for the performance enhancement of an Isolated Asynchronous Generator”. It is observed from the literature that the analysis and performance enhancement of 3-phase IAG is mostly carried out using conventional

numerical methods and the conventional controllers. In the present thesis, the analysis of 3-phase IAG furnishing 3-phase and 1-phase load is accomplished using optimisation technique “fsolve” and the performance enhancement of IAG is attained using Fuzzy logic (FL) based controllers.

CHAPTER 3

ANALYTICAL AND EXPERIMENTAL INVESTIGATIONS OF ISOLATED ASYNCHRONOUS GENERATOR (IAG) FURNISHING 3-PHASE LOAD

3.1 GENERAL

The self-excitation or voltage build-up phenomenon related to an asynchronous machine is identical with the dc shunt type generator and is still a topic of research although it is well known for more than a half century [9-10]. When an asynchronous machine is mechanically rotated above the base speed and is connected across reactive source of power (AC capacitor bank), the residual magnetism existing in the rotor part of the asynchronous machine induces an electromotive force (emf) in the stator winding. The frequency of emf induced in the stator winding depends on the rotor speed. This emf produces a lagging nature reactive current to flow in the stator windings. Hence a magnetizing flux is induced in the machine is established. This small residual voltage keeps on building up and reaches to the rated voltage. The final value of stator voltage is limited by the magnetic saturation within the machine. Hence, the asynchronous machine works as an asynchronous generator without a grid supply [11]. Hence, the complete analysis of such machines under initial transient phenomenon and steady state is of great practical interest. A lot of research is already done but still a topic of research. Many researchers have analyzed the steady state performance of IAG using equivalent circuit. In the earlier published research work, mainly two methods based on KVL (loop impedance) and KCL (nodal admittance) laws have been recommended for the solution of simultaneous non-linear equations [12-34].

A vast number of research papers covered the aforementioned two techniques of evaluating or investigating the performance characteristics of IAG based on equivalent circuit using loop analysis technique [12-25]. The problem formulation consists of two simultaneous non-linear equations in terms of two unknown variables (frequency F_y and excitation capacitor reactance X_{sc}). These equations are attained after disintegrating real and imaginary parts of the total loop impedance and equating

them individually to zero. Then these equations are evaluated using various numerical techniques like Newton Raphson method, secant method, golden section method etc. The solution of these equations yields the value of frequency F_y and excitation capacitance X_{cs}. With the aid of the attained value of F_y and X_{sc} and the magnetization characteristics, the equivalent circuit of the IAG can be completely solved. Hence, the complete performance of the IAG under steady state conditions can be analytically attained.

The steady state and transient analysis is also investigated using admittance method [26-33]. Li Wang et.al [34] presented the eigen values based dynamic performance of the IAG feeding dynamic load (IM) using short shunt and long shunt connections.The problem formulation results into an equivalent circuit in terms of admittances. This method accounts the admittance of the air-gap voltage branch node of the equivalent circuit. Two simultaneous non-linear equations in terms of F_y and X_{sc} are attained after disintegrating real and imaginary parts of the total admittance and then equating them individually to zero. A higher degree polynomial in F_y is attained after equating the sum of real parts of total admittance equal to zero. Solution of this higher order polynomial output the value of F_y. The value of X_{sc} can be attained by using the aforementioned value of F_y and equating the sum of imaginary parts of the total impedance equal to zero.

Both methods are quite efficient in determining the steady state performance of the IAG. But these methods require lengthy calculations in deriving the coefficients of high order polynomials. Moreover, these coefficients are system or model specific and vary with even slight change in the equivalent circuit. Also, the order of the polynomial changes on addition of some elements in equivalent circuit e.g. core loss resistance R_{cl}, series and shunt capacitance X_{sc}. Hence, these methods are model specific, inflexible and are time consuming also.

This chapter emphasis on the implementation of MATLAB based optimization technique “fsolve” to obtain analytical results. It is a built-in function available in optimization toolbox and does not require mathematical manipulations; deep knowledge of programming and debugging in MATLAB environment; handles complexity with ease, less computational time and is highly flexible. This method

proves quite efficient in attaining the performance of IAG under steady state conditions.

3.2 ANALYTICAL AND OPTIMIZATION BASED ANALYSIS OF IAG

3.2.1 Analytical Technique

The equivalent circuit of an IAG comprises of stator winding (represented by stator resistance and reactance), rotor winding (represented by rotor resistance and reactance), resistive load and an excitation capacitance depicted in Fig. 3.1(a).

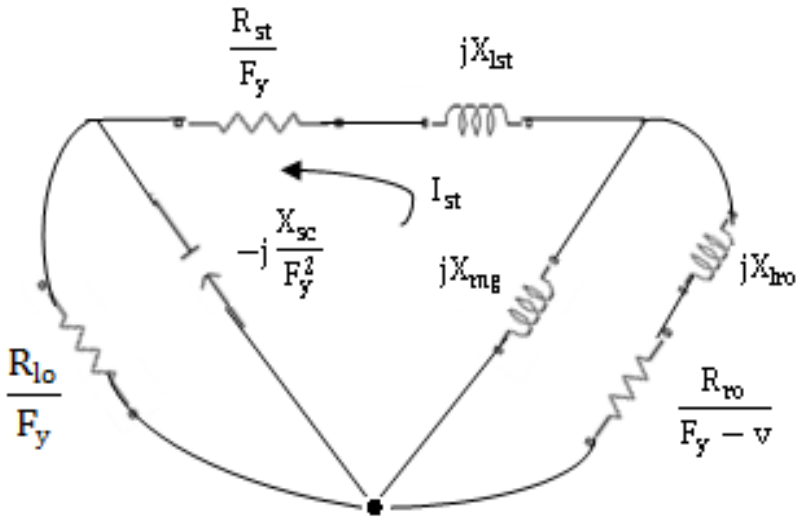

Fig. 3.1 (a) Equivalent circuit of asynchronous machine with core loss neglected

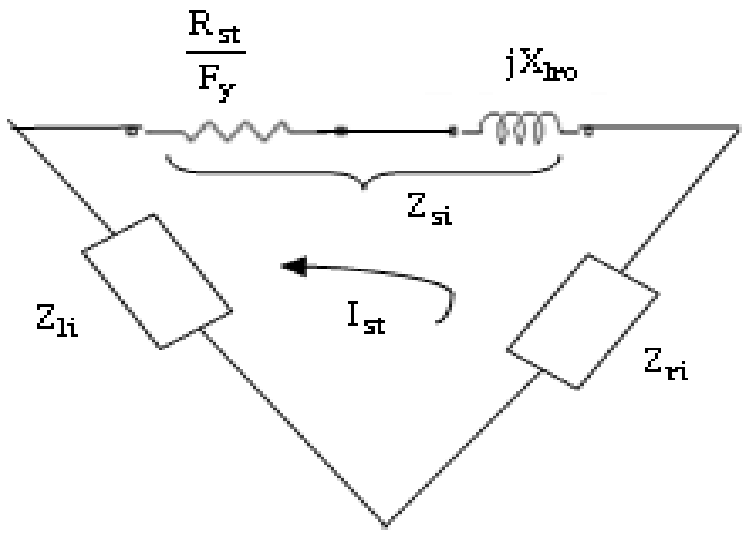

Fig. 3.1 (b) Simplified impedance based equivalent circuit of an asynchronous machine.

All the parameters of the equivalent circuit are regarded as constant and only the parameter magnetizing reactance X_{mg} is considered to be effected by the magnetic

saturation [33]. The simplified impedance based equivalent circuit is drawn in Fig. 3.1(b). Loop analysis application in Fig. 3.1(b) results into the formation of the following equations:

$$Z_{st}I_{st} = 0 \tag{3.1}$$

$$Z_{st} = Z_{li} + Z_{si} + Z_{ri} \tag{3.2}$$

Consequently,

$$Z_{li} = \left(-jX_{sc}\, R_{lo}/F_y^2\right)/\left(R_{lo}/F_y - j\, X_{sc}/F_y^2\right) \tag{3.3}$$

$$Z_{si} = (R_{st}/F_y) + jX_{lst} \tag{3.4}$$

$$Z_{ri} = [jX_{mg}\{R_{ro}/\left(F_y - v\right) + jX_{lro}\}]/\{R_{ro}/(F_y - v)\} + j\left(X_{mg} + X_{lro}\right) \tag{3.5}$$

For the operation of IAG, the stator current I_{st} must not be equal to zero. Therefore, the total stator impedance (Z_{st}) must have essentially a zero value. Equating real and imaginary parts of Z_{st} separately equal to zero. Assuming $X_{lst} = X_{lro} = X_{le}$, the following two nonlinear simultaneous equations with two unknown variables X_{mg} and F_y are obtained or formulated or evaluated or described or represented as

$$H_1\left(X_{mg}, F_y\right) = \left(M_1X_{mg} + M_2\right)F_y^3 + \left(M_3X_{mg} + M_4\right)F_y^2 + \left(M_5X_{mg} + M_6\right)F_y + \left(M_7X_{mg} + M_8\right)F_y = 0 \tag{3.6}$$

$$H_2\left(X_{mg}, F_y\right) = \left(N_1X_{mg} + N_2\right)F_y^2 + \left(N_3X_{mg} + N_4\right)F_y + N_5 = 0 \tag{3.7}$$

The Jacobian matrix (J_{BM}) is formulated as

$$[J_{BM}] = \begin{bmatrix} J_{11} & J_{12} \\ J_{21} & J_{22} \end{bmatrix} \tag{3.8}$$

Here

$$J_{11} = \frac{\partial H_1}{\partial X_{mg}};\ J_{21} = \frac{\partial H_2}{\partial X_{mg}}$$

$$J_{12} = \frac{\partial H_1}{\partial F_y};\quad J_{12} = \frac{\partial H_2}{\partial F_y}$$

$$\begin{bmatrix} p \\ q \end{bmatrix} = [\,J_{BM}\,]^{-1}\begin{bmatrix} -H_1 \\ -H_2 \end{bmatrix} \tag{3.9}$$

These coefficients M_1-M_8 and N_1-N_5 are evaluated using symbolic mathematics toolbox available in MATLAB.

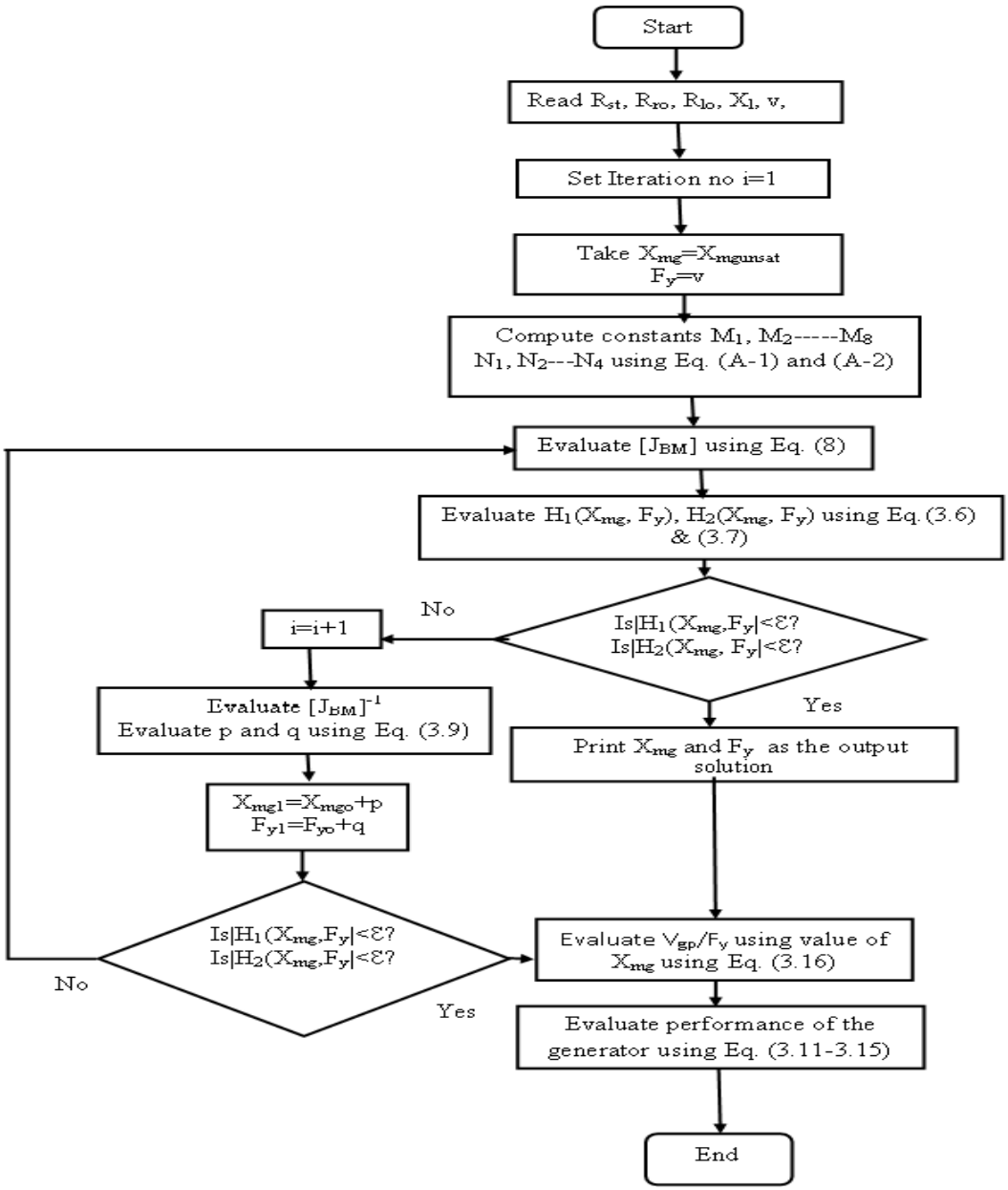

Fig. 3.2 Flowchart depicting the algorithm of Newton Raphson method

Fig. 3.2 illustrates the complete implementation procedure of Newton Raphson method wherein it is inferred that the algorithm implementation of Newton Raphson method requisites: Evaluation of function value, its derivatives (Jacobian matrix) and its inverse at the end of iteration, starting and stopping criteria, more no of iterations.

3.3 OPTIMISATION TECHNIQUE TO SOLVE NON-LINEAR EQUATIONS

Equations (3.6) and (3.7) are the two nonlinear simultaneous equations with two unknowns.

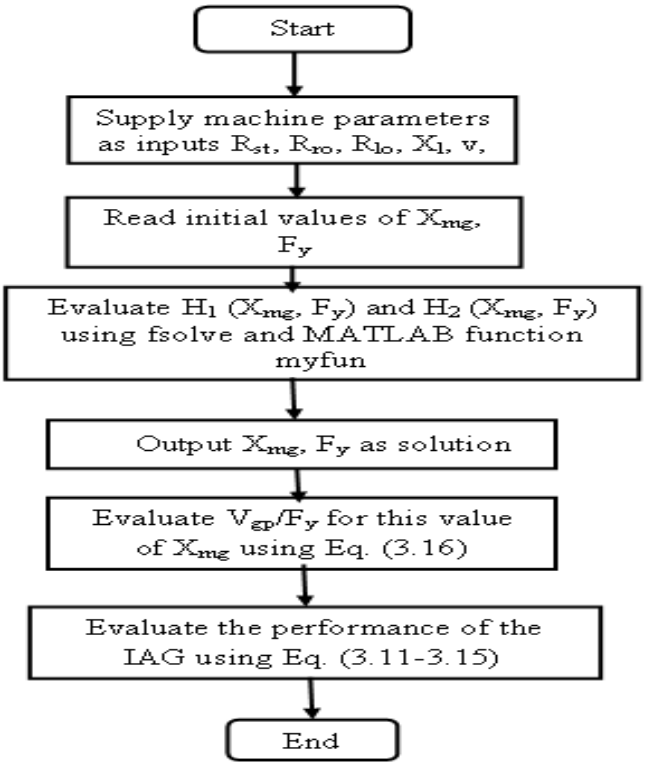

Fig. 3.3 Flowchart depicting procedure of fsolve technique

These equations are not easily solvable and require some numerical technique or optimization technique to find out their solutions. These equations are solved to find out the values of X_{mg} and F_y for the given values of machine parameters, speed v, R_{lo} and X_{sc}. Most of the numerical methods require lengthy and tedious calculations, partial derivatives, higher order polynomials even 6th to 10th degree algebraic polynomials. These equations can be easily and conveniently solved using fsolve technique of MATLAB optimization tool box. The flowchart is illustrated in Fig. 3.3. Eqs. (3.6) and (3.7) can be written as

$$H(x) = 0 \text{ for } x \tag{3.10}$$

Here x is a vector and H(x) is a function that returns a vector value.

Here H= $[H_1, H_2]^T$ and x is an unknown vector of two variables $[X_{mg} \;\; F_y]^T$. It uses trust-region-dogleg, trust-region-reflective, Levenberg - Marquardt and an algorithm based on Gauss-Newton for solving non-linear equations of n variables.

The algorithm is simple and easy to implement. The small section of the MATLAB code for “fsolve” is given below:

%% Take initially the unsaturated value of magnetizing reactance and the value 1 for the generated frequency F_y %%

X_o = [X_{mg} ; F_y]

x = fsolve (@myfun3, [X_{mg}; F_y])

options = optimset ('Display', 'iter')

[x, fval] = fsolve (@myfun3, [X_{mg}; F_y], options)

The desired solution is just achieved in 3 to 4 iterations as compared to conventional Newton Raphson method.

The solution of Eq. (3.6) and (3.7) furnishes the value of X_{mg} and F_y. The various performance characteristics of the IAG can be analytically attained from the magnetization characteristics (Eq. 3.16) and the equivalent circuit depicted in Fig. 3.1.

$$I_{st} = (V_{gp}/F_y)/[(R_{st}/F_y) + jX_{lst} - (jX_{sc}R_{lo}/F_y^2R_{lo}) - jF_yX_{sc}] \quad (3.11)$$

$$I_{ro} = (-V_{gp}/F_y)/\{ R_{ro}/(F_y - v)\} + jX_{lro} \quad (3.12)$$

$$I_{lo} = [(-jX_{sc}/R_{lo}) - jX_{sc})].I_{st} \quad (3.13)$$

$$V_t = I_{lo}R_{lo} \quad (3.14)$$

$$P_{out} = n|I_{lo}^2|R_{lo} \quad (3.15)$$

3. 4 IAG LABORATORY HARDWARE SET UP

The MATLAB based optimization technique is recommended in this manuscript due to easy problem formulation and other added advantages mentioned above. The IAG was spinned by a dc shunt machine. The hardware structure embody a delta connected three-phase asynchronous machine of 380/660V, 8.2/4.75A, 50Hz, 3.73 kW, 4-pole, 1450 rpm [Appendix B]. A three-phase capacitor bank (balanced excitation) was interfaced to the stator terminals to examine or obtain self-excited phenomenon in IAG. A 3-Φ variable resistance bank was used to load the asynchronous generator as shown in Fig. 3.5. The various electrical parameters of the machine were accessed or accomplished or obtained experimentally from no-load, blocked rotor test and

synchronous speed test [Appendix B]. The data required for the analytical and experimental investigations was evaluated from equivalent circuit.

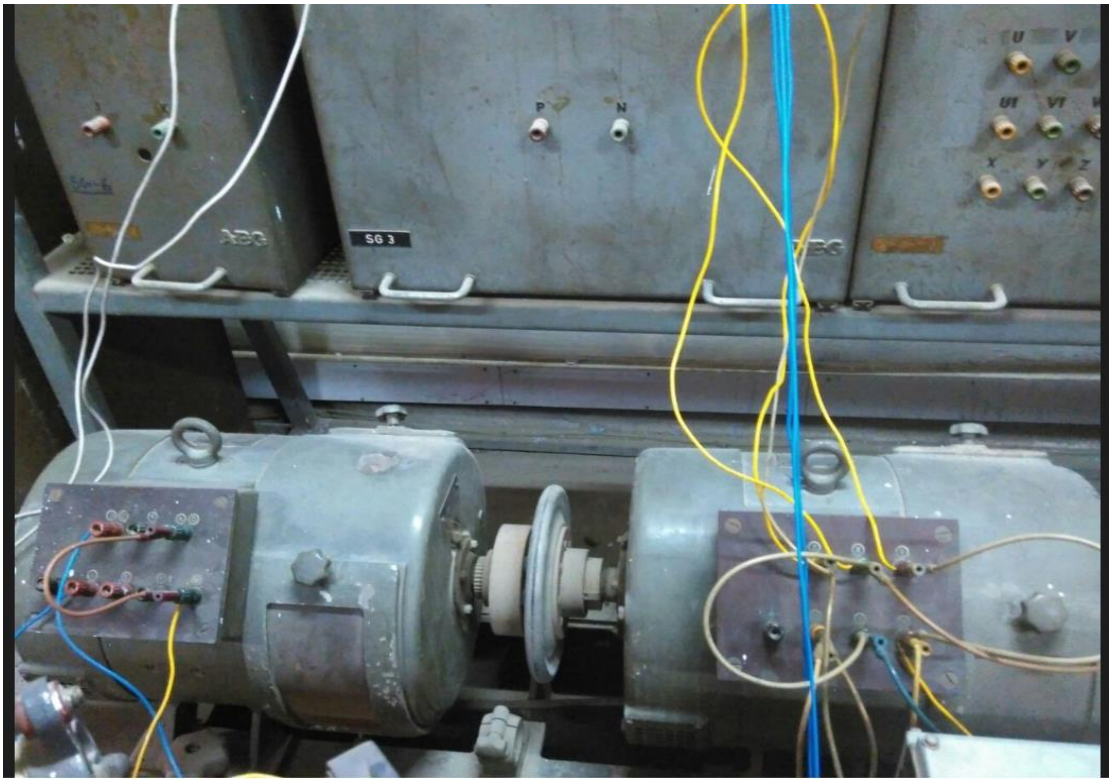

Photo 1 Experimental hardware set-up of the prime-mover and Asynchronous machine

Photo 2 Experimental laboratory hardware setup of IAG

3.5 ANALYTICAL AND EXPERIMENTAL INVESTIGATIONS

3.5.1 Effect of Excitation Capacitor on the Performance of IAG under no-load conditions

For initiating the self-excitation phenomenon, an excitation capacitance of value above the minimum value is required. The delta connected asynchronous machine was driven above synchronous speed by the dc machine and at the same time the machine is excited by the delta connected capacitor bank. The asynchronous machine starts generating the voltage. The value of excitation capacitance depends on various parameters of the machine, its rotational speed, load impedance and its power factor. Also, there is maximum limit of excitation capacitance outside which machine fails or loses its excitation. So the value of C_{sc} should be within the limit $C_{scu} \leq C_{sc} \leq C_{scl}$. This fact is verified both analytically and experimentally and is illustrated in Fig.3.4. The analytical and experimental variation of the value of excitation capacitance (C_{sc}) with IAG speed at no load at constant value of generated voltage (380V) is shown in Fig. 3.4. It is observed that the excitation capacitance rises with drop in speed. Also there is a minimum value of speed (i.e. 650 rpm) below which the machine loses its excitation.

Fig. 3.5 presented the variation of generated voltage with speed for four different values of C_{sc}. At C_{sc} = 20 µF, the generator generates 380 V at 1628 rpm and 220 V at a speed of 1332 rpm. At C_{sc} = 40 µF, the same 380 V is generated at a still lower speed of 1408 rpm and the generator generates 200 V at a speed of 1009 rpm. At C_{sc} = 60 µF, again the same voltage of 380 V is generated at further lower speed of 1310 rpm and a minimum voltage of 200 V at a speed of 912 rpm which is the critical speed or cut-in or threshold below which there is loss of excitation and the generator is not able to generate further. At C_{sc} = 80 µF, again the same voltage of 380 V is generated at further lower speed of 1241 rpm and a minimum voltage of 200 V at a speed of 845 rpm which is the critical speed below which there is loss of excitation and the generator is not able to generate further. It is observed from the results that the minimum voltage is around 200 V at 800 rpm for all the four values of capacitance. There exists a very good degree of correlation between both analytically and experimentally achieved results. There is indication of discrepancy between

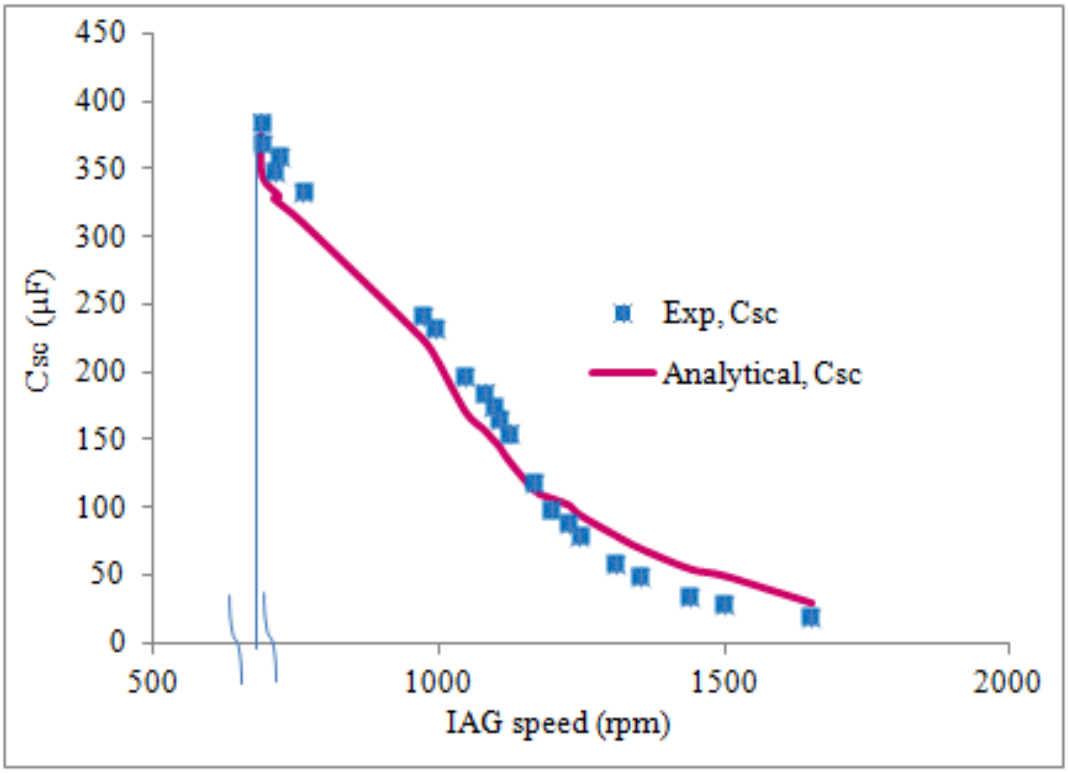

Fig.3.4 Variation of shunt capacitor excitation (C_{sc}) with speed at no load with generated voltage as 380V

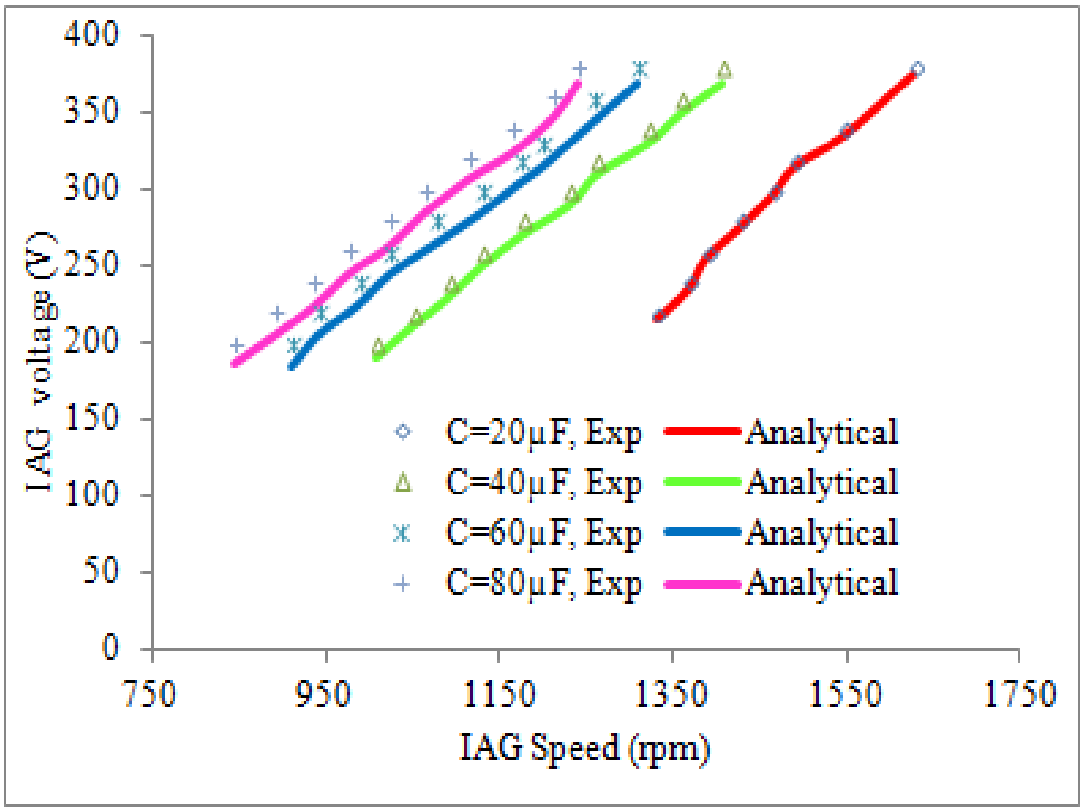

Fig. 3.5 Variation of IAG voltages with speed at no load for different values of shunt capacitors (C_{sc})

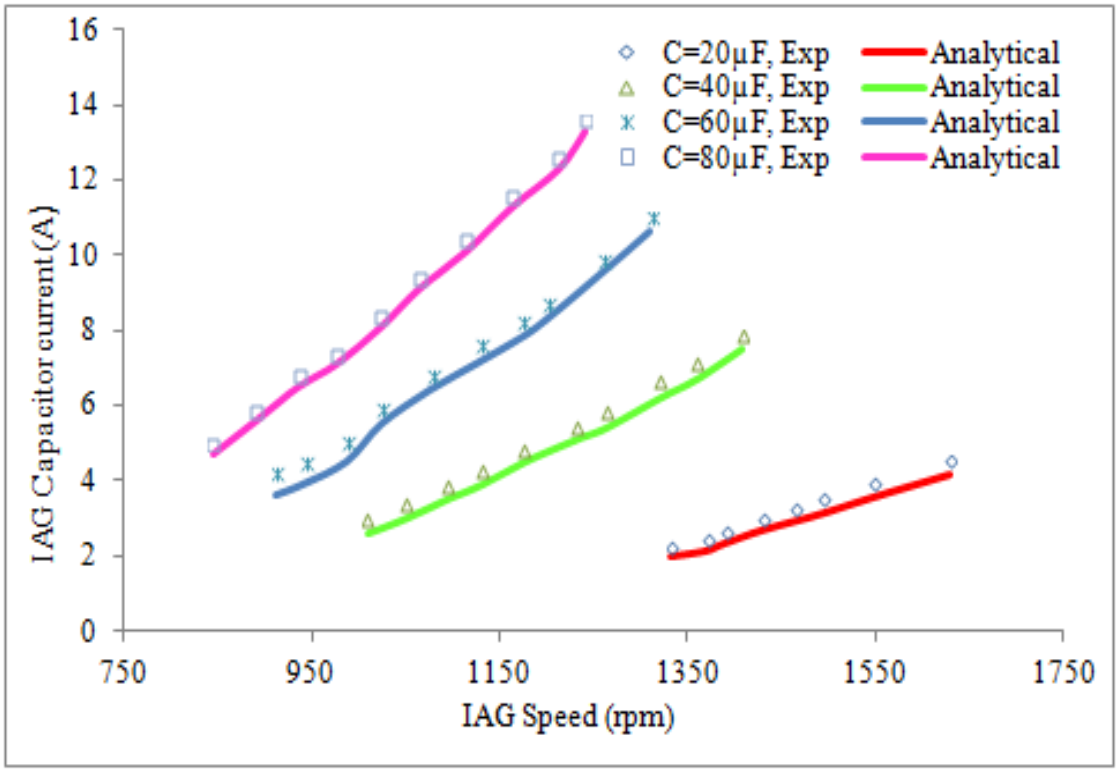

Fig. 3.6 Variation of IAG capacitor current with speed at no load for different values of C_{sc}

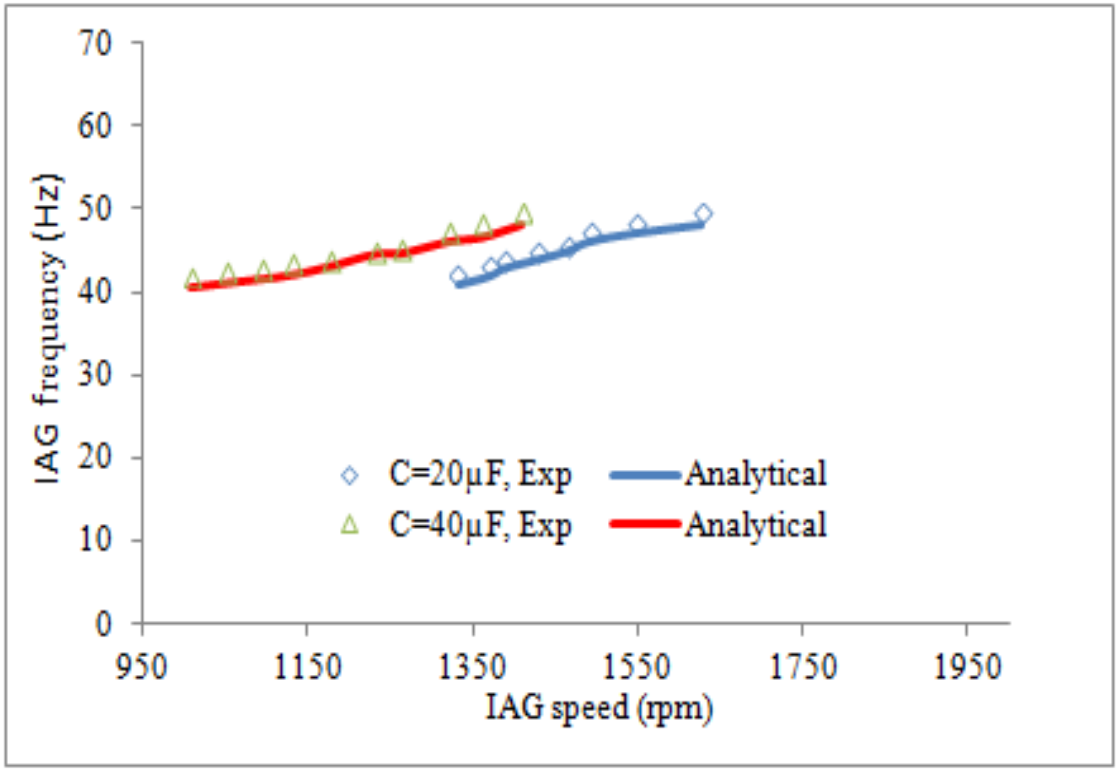

Fig. 3.7 Variation of generated frequency with speed at no load for different values of C_{sc}

analytically and experimentally attained values at higher speeds due to linear approximation of highly saturated non-linear magnetizing curve.

Fig. 3.6 shows the variation of capacitor current with speed for different values of C_{sc}. At C_{sc} = 20 µF, the capacitor provides a minimum current of 2.2 A at 1332 rpm (220 V) and a maximum current of 4.5 A at 1628 rpm (380 V). With increase in capacitance from C_{sc} = 20 µF to C_{sc} = 80 µF, the capacitor current increases and the speed decreases. Hence, the capacitor current is also greatly affected by both capacitance and speed of the IAG.

Fig. 3.7 presented the variation of generated frequency with speed for different values of C_{sc}. For C_{sc} = 20 µF, the generator frequency varies from 42.5 Hz to 49.8 Hz when the speed varies from 1332 rpm to 1628 rpm. Whereas for C_{sc} = 40 µF, frequency regulation is from 42 Hz to 49.6 Hz when the speed varies from of 1009 rpm to 1428 rpm. It means that the frequency increases linearly with speed and is affected by the excitation capacitance C_{sc}.

3. 5. 2 Effect of Excitation Capacitor on the Performance of IAG under resistive load conditions

Fig. 3.8 presents the variation pattern of excitation capacitance with power conveyed to the load by the IAG at unity power factor and at constant terminal voltage of 380 V. It is envisaged that with increase in power delivered to the load, the shunt connected capacitance increases to retain constant voltage of 380 V. There is good resemblance between analytically and experimentally accomplished results.

Fig. 3.9 presented the variation of IAG terminal voltage with power conveyed to the load by the IAG for different values of C_{sc}. It is inferred from this figure that IAG voltage decreases with increase in power conveyed to the load. This decrease in voltage is attributed due to the adverse effect of armature reaction phenomenon, resistance drop and leakage reactance drop. This characteristic at different excitation capacitances seems similar to the load characteristic of dc shunt generator at different field resistances. With increase in excitation capacitance, the voltage generated by IAG increases and also power delivered to the load by IAG increases [16]. The analytical and experimental results are closely related for the highest value of C_{sc}. At C_{sc} = 30 µF, maximum power obtained experimentally is lower than the analytically

obtained value. The discrepancy or deviation in the maximum power conveyed to the load by the IAG for 30µF, 40 µF and 50 µF capacitors are investigated as 7.33%,

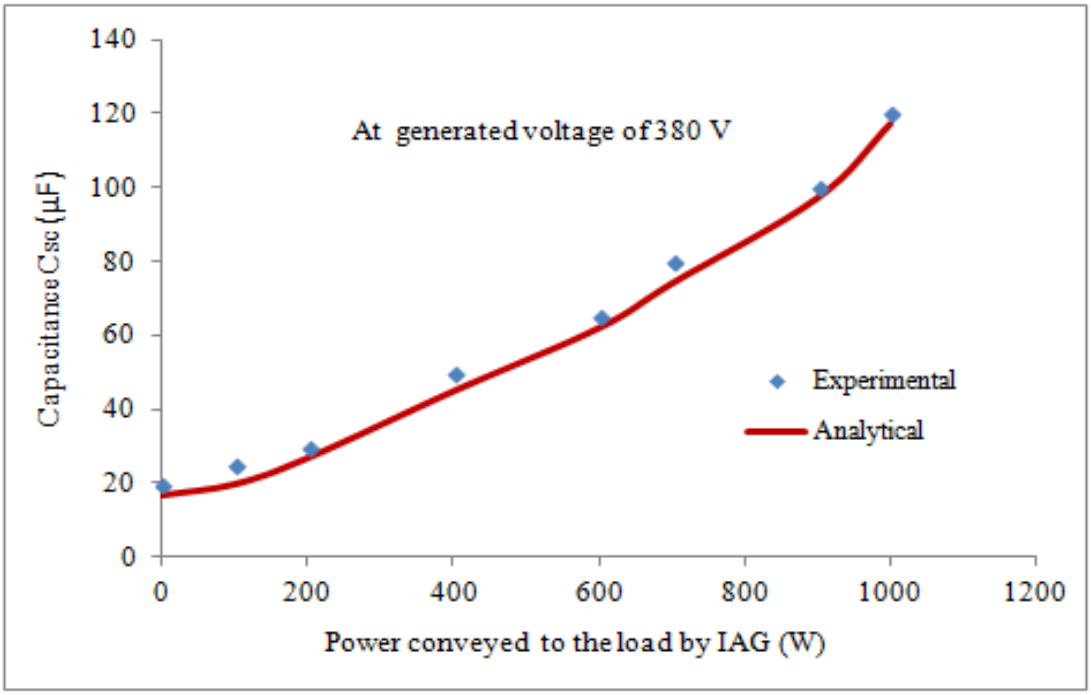

Fig. 3.8 Variation of Excitation capacitance with power conveyed to the load (W) at constant generated voltage.

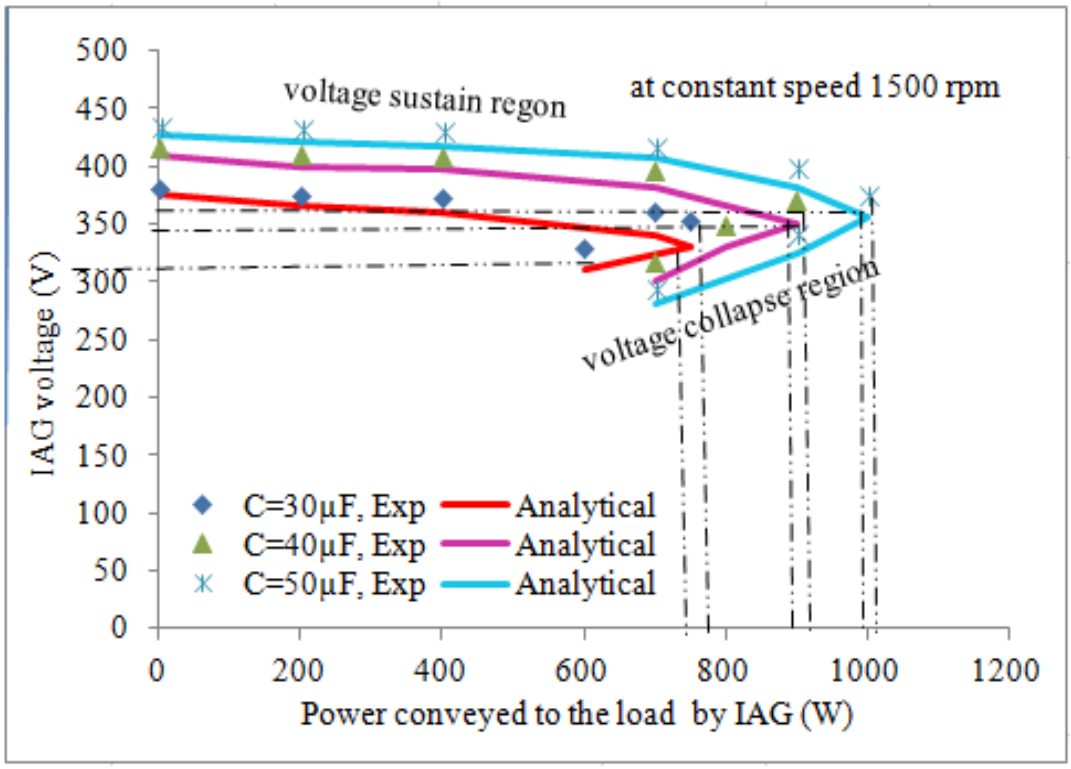

Fig. 3.9 Variation of IAG terminal voltages with power conveyed to the load (W) at unity p.f and at constant speed.

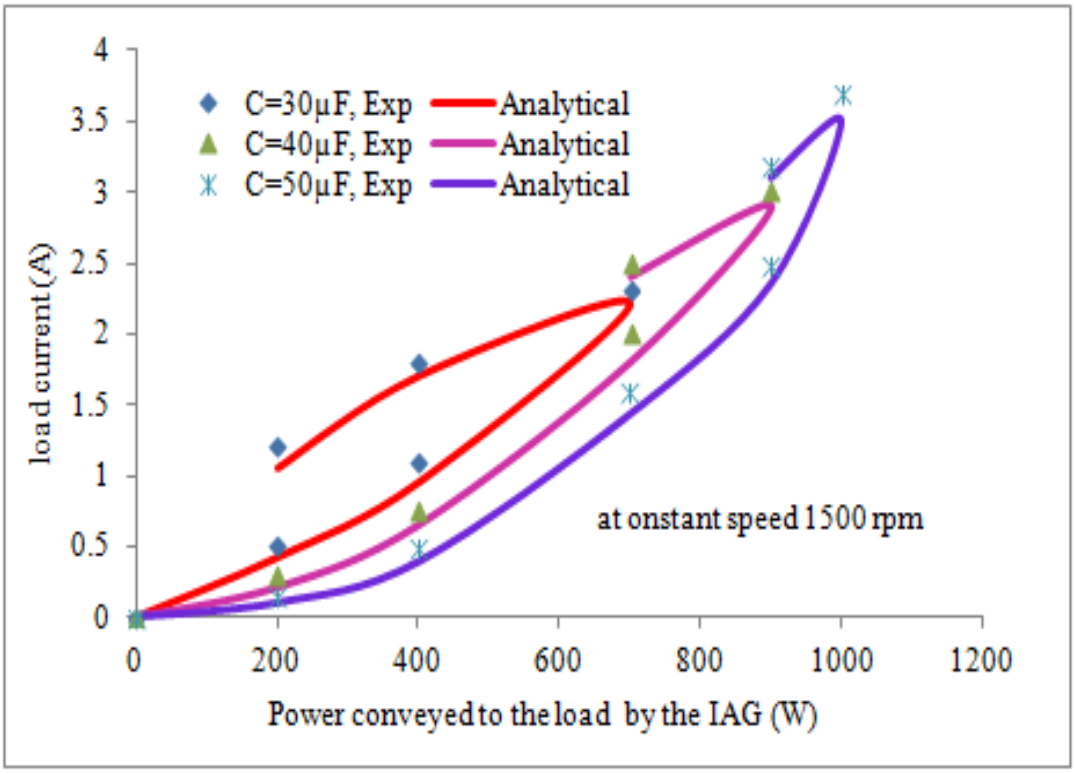

Fig. 3.10 Variation of load current with power conveyed to the load (W).

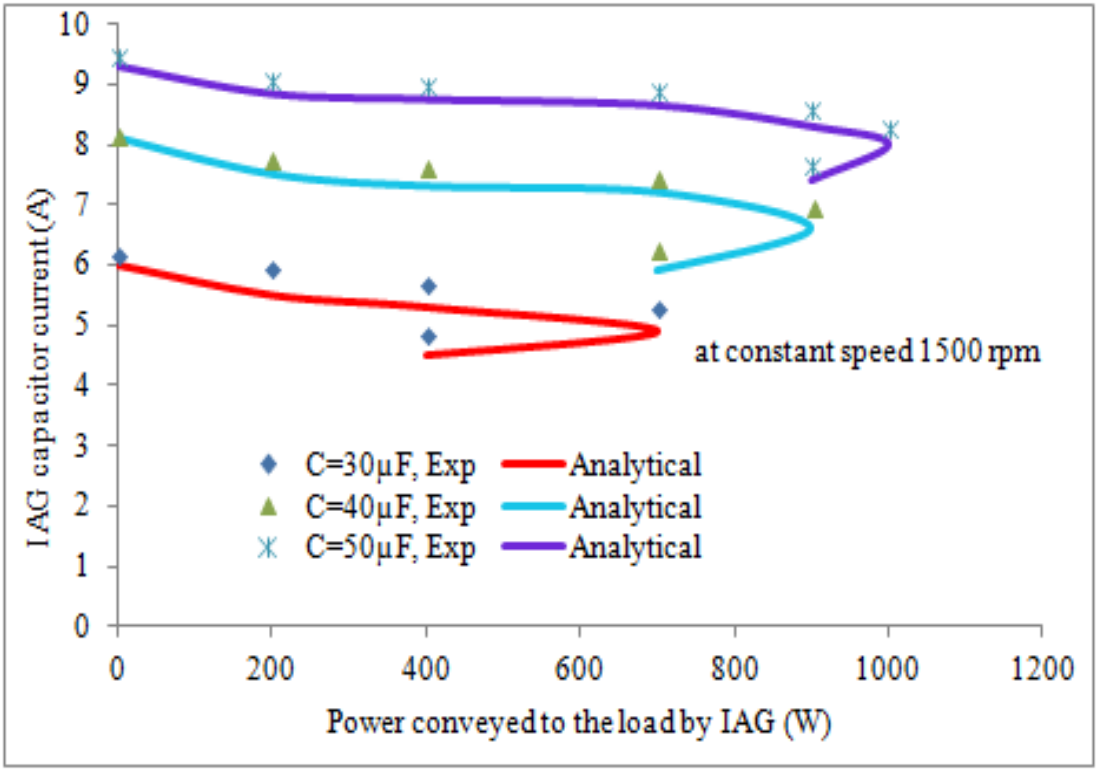

Fig. 3.11 Variation of IAG capacitor currents with power conveyed to the load (W) at constant speed.

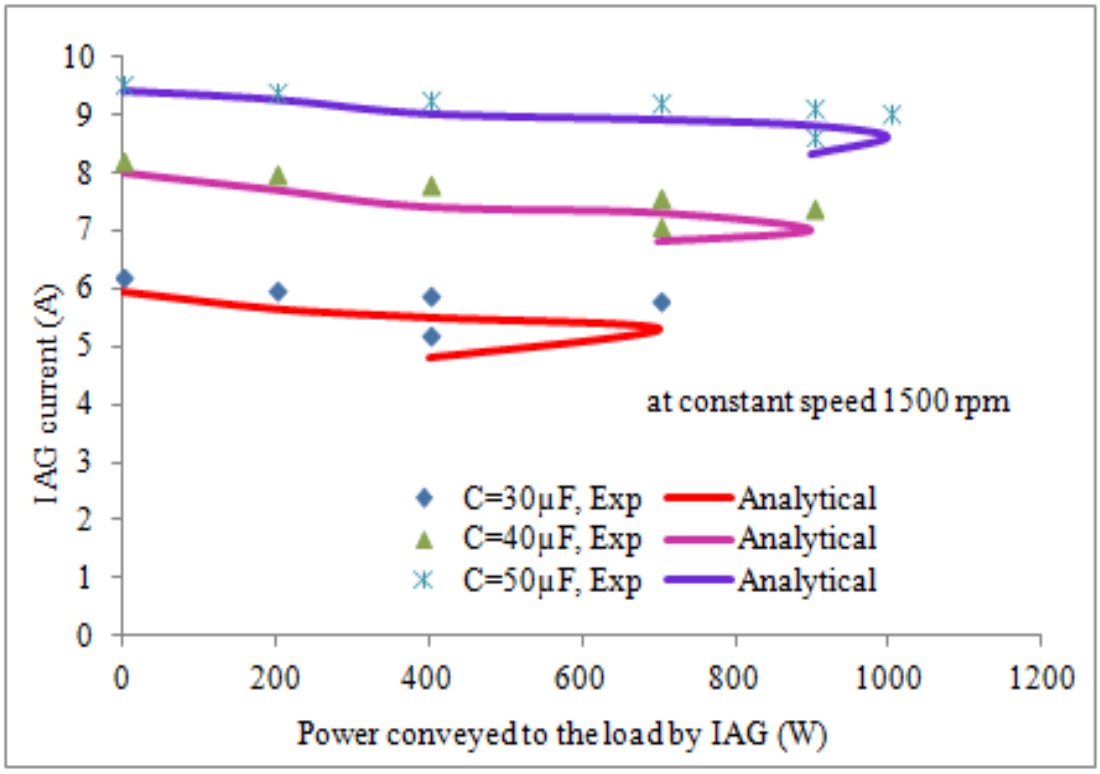

Fig. 3.12 Variation of IAG current with power conveyed to the load (W) by IAG for different values of Excitation Capacitance C_{sc}.

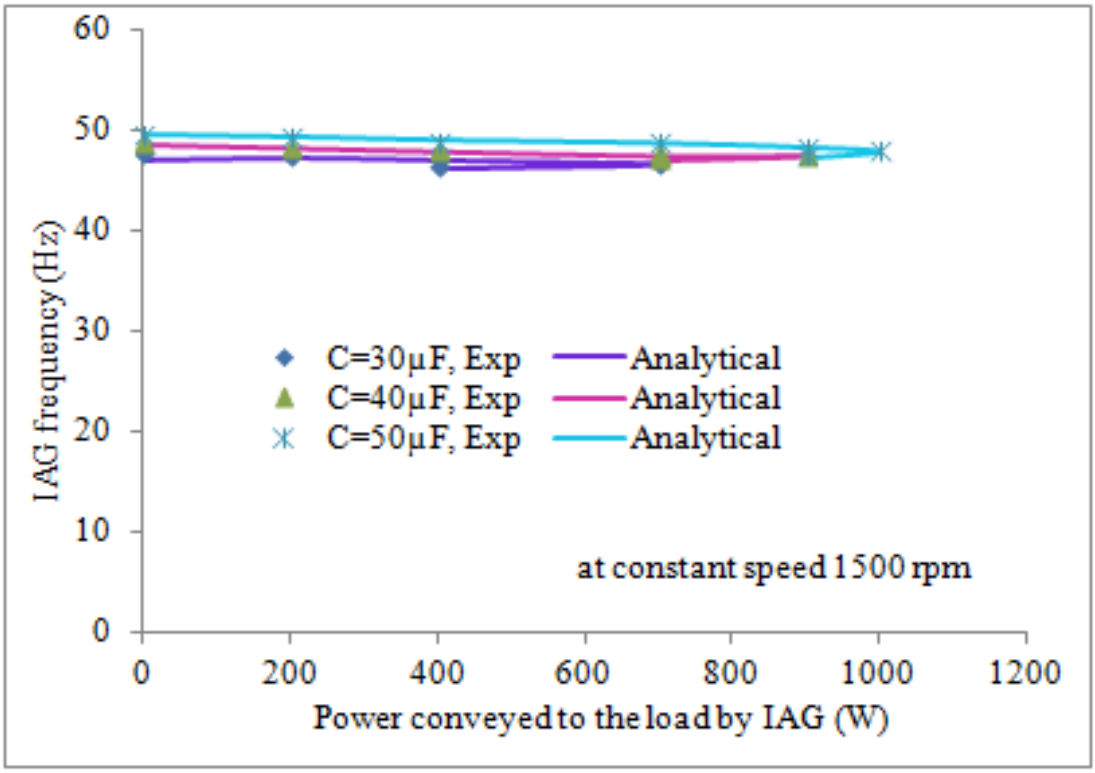

Fig. 3.13 Variation of IAG frequency with power conveyed to the load (W) by IAG for different values of Excitation Capacitance C_{sc}.

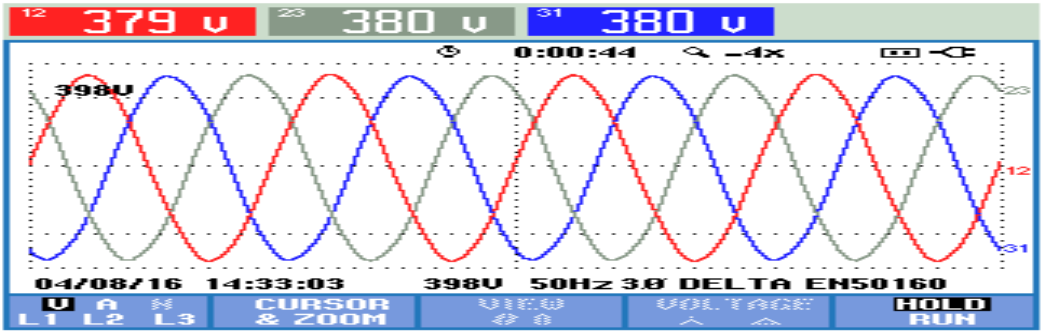

(a)

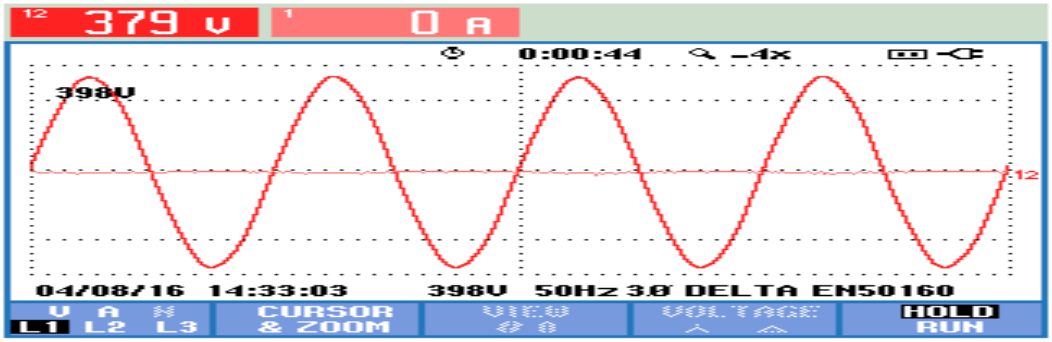

(b)

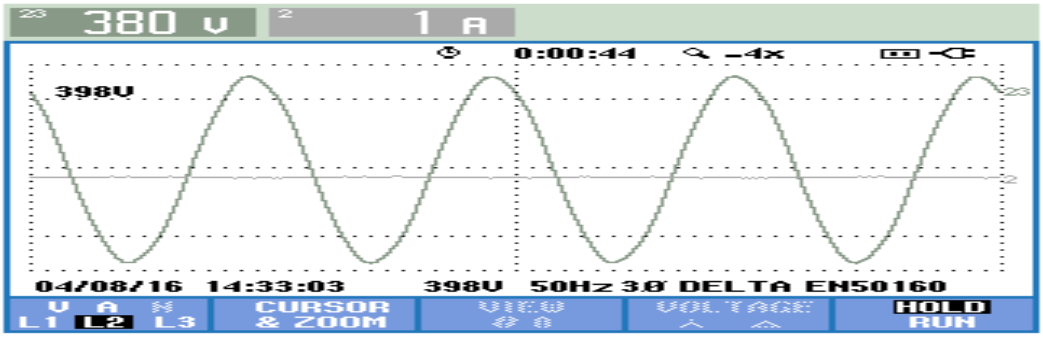

(c)

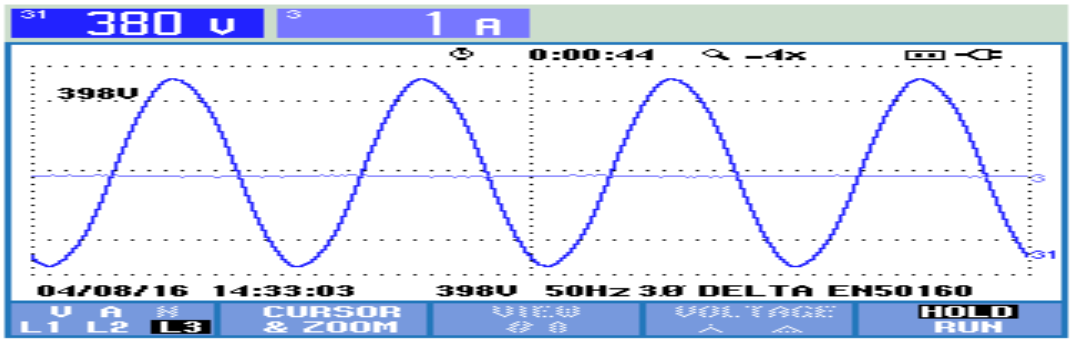

(d)

Fig. 3.14 (a) Three phase generated voltage (b) voltage generated in phase 'a' (c) voltage generated in phase 'b' (d) voltage generated in phase 'c' for C_{sc} = 40μF.

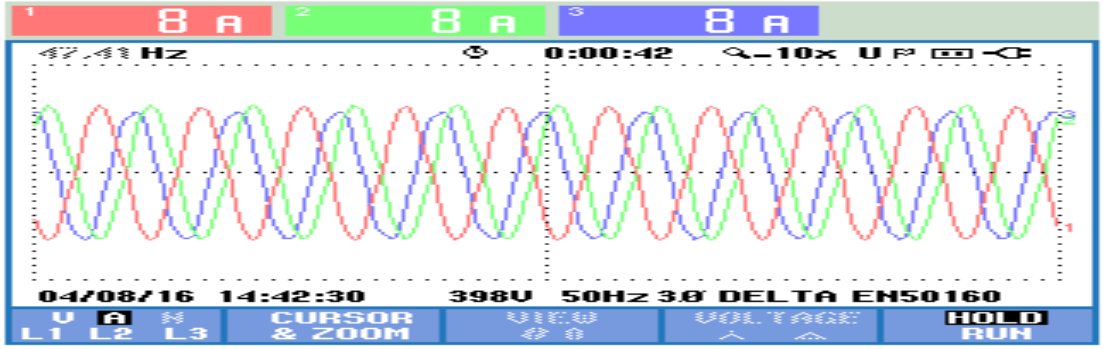

(a)

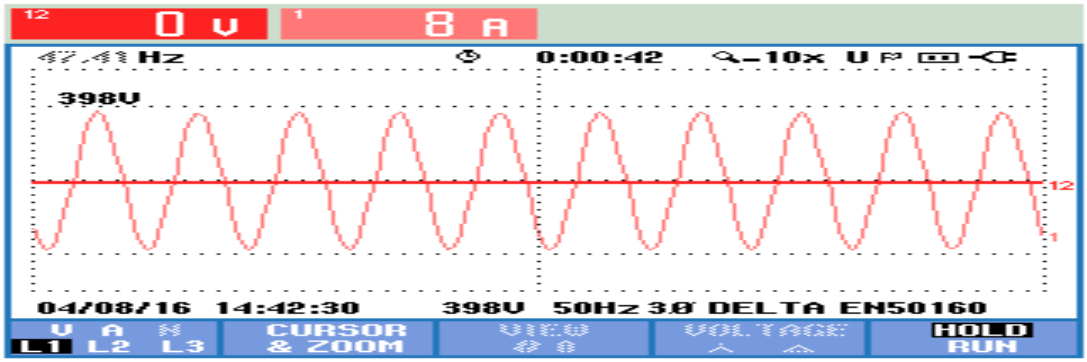

(b)

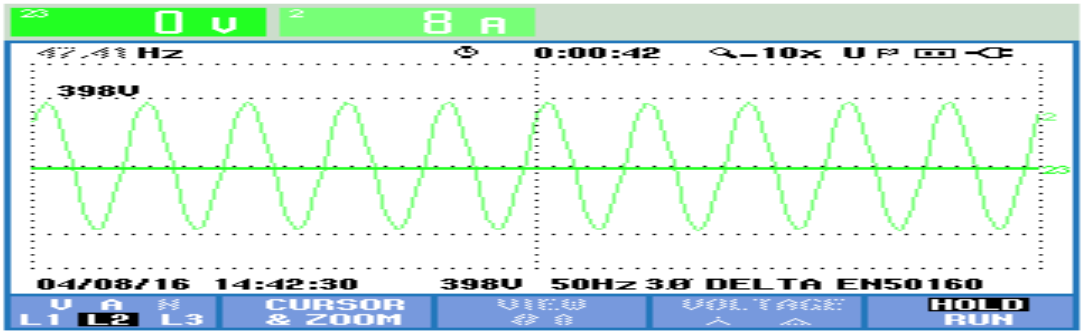

(c)

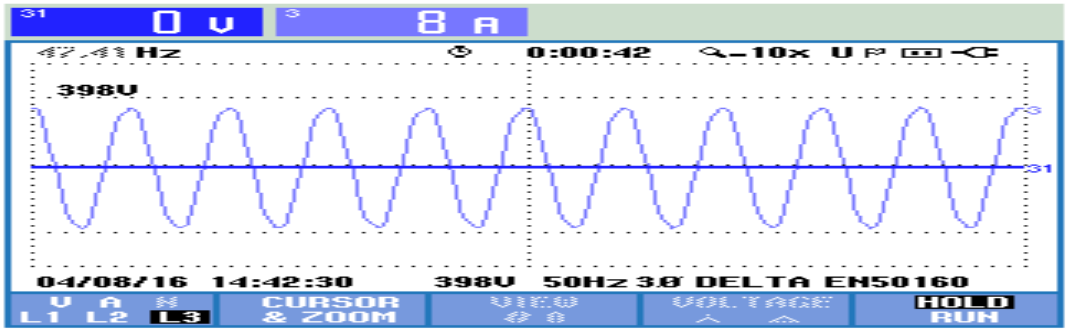

(d)

Fig. 3.15 (a) three phase capacitor current (b) capacitor current in phase a (c) capacitor current in phase b (d) capacitor current in phase c for C_{sc} = 40µF

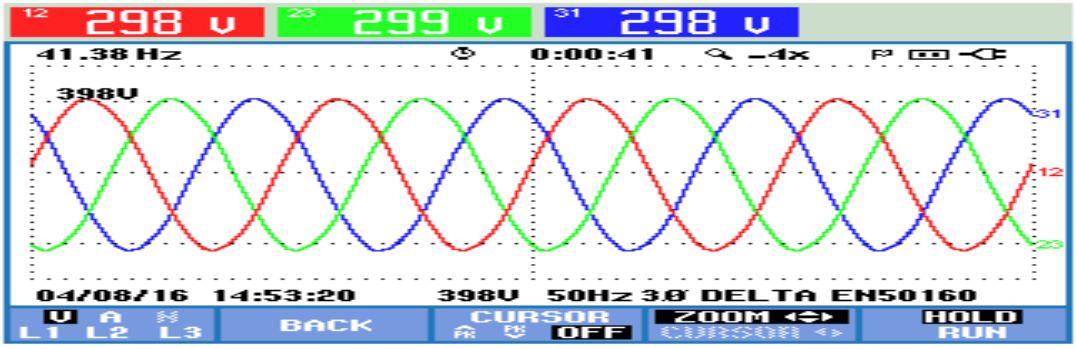

(a)

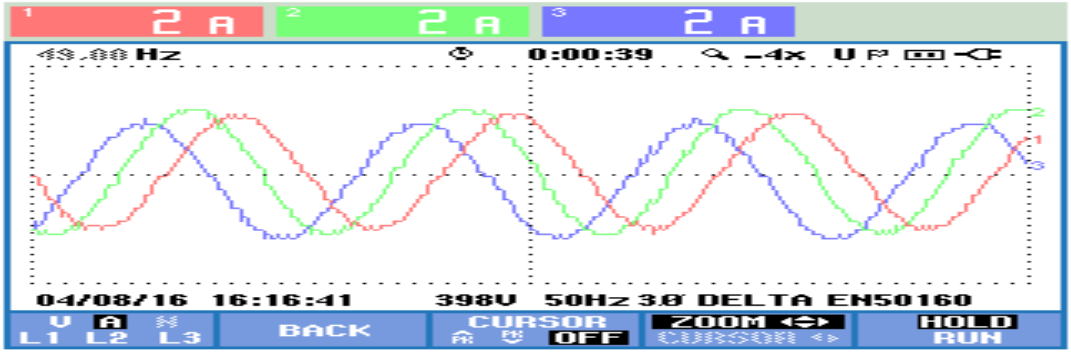

(b)

Fig. 3.16 (a) three-phase voltage across the load (b) three-phase current through the load for R_{lo} = 500W and C_{sc} = 40μF.

3.88% and 1.5% respectively. These discrepancies in maximum power calculations are within acceptable bounds and can be corrected by increasing the values of C_{sc}.

Fig. 3.10 presents the set of curves of load current with power conveyed to the load by IAG drawn at different excitation capacitances. As assumed, the load current increases with increase in power conveyed to the load by IAG.

Fig. 3.11 presents the set of curves of IAG capacitor current with power conveyed to the load by IAG for different excitation capacitances. As expected, the capacitor current decreases with increase in power conveyed to the load by IAG. This decrease is attributed to the decrease in terminal voltage. This decrease in capacitor current is compensated or neutralized by the increase in load current. Hence, the stator current remains almost constant.

Fig. 3.12 presents the set of curves of IAG stator current with power conveyed to the load by IAG for different excitation capacitances. Analytically the stator current is the phasor sum of the load current and the capacitor current [16]. This current is highly insensitive with the variation of power delivered to the load. Its variation is highly effected by the value of C_{sc}.

Fig. 3.13 presents the set of curves of frequency with power conveyed to the load by the IAG for different values of C_{sc}. For C_{sc} = 30 µF, the generator frequency varies from 49.6 Hz to 48.4 Hz. It is concluded that with increase in C_{sc}, the IAG delivers more power to the load and the frequency drops down. As predicted, the frequency decreases with increase in power delivered to the load by the IAG.

Fig. 3.14 (a) presents the three-phase ac voltage-build up by the IAG at no-load for C_{sc} = 40µF. These results are captured using Fluke 43 B power analyzer. Fig. 3.14 (b), (c) and (d) shows the per-phase voltage of phase a, b and c. From these results it is inferred that the voltage generated by the IAG are balanced and sinusoidal in all the three-phases a no-load.

Fig. 3.15 (a) presents the three-phase capacitor current at no-load at C_{sc} = 40µF. Fig. 3.15 (b), (c) and (d) shows the per-phase capacitor current of phase a, b and c. From these results it is inferred that the capacitor current in all the three-phases under are of equal magnitude.

Fig. 3.16(a) illustrates the three-phase voltage across the load (b) three-phase current through the load for R_{lo} = 500W and C_{sc} = 40µF. Under load condition situation the voltage drops from 380 V to 298 V. As anticipated, the voltage across the load decreases with increase in load. This investigation strikes towards the need of some controller to maintain the load voltage constant. The hardware part of the controller needs to be developed.

3.6 SUMMARY

A numerical technique (Newton Raphson method) and a MATLAB based optimization technique (fsolve) has been elaborated for assessing the performance of IAG under steady state conditions. However, the optimization technique has been

desired and recommended to evaluate the value of X_{mg} and F_y for steady state analysis investigations. The following inferences have been made:

- Under no load conditions, the performance regarding the IAG voltage, capacitor current and frequency has been strongly influenced by both speed and capacitor C_{sc}. The close resemblance between analytical and experimental investigations outcomes has been noticed and validated the results.

- Under resistive load condition, the performance regarding IAG voltage, load current, IAG capacitor current has been strongly influenced by both power conveyed to the load and capacitor C_{sc}. However IAG stator current and frequency are highly insensitive to the power conveyed to the load but is strongly influenced by the value of C_{sc}. The best results have been attained for highest value of C_{sc}. For lower values of C_{sc}, small discrepancies between the analytical and experimental investigations outcomes of some performance characteristics have been noticed. But these discrepancies have been shown within the tolerable range. The variation pattern of the set of the curves was as predicted.

- The steady state and transient state analysis revealed that the IAG generates successfully the desired rated voltage of 380 V at no load for different values of Capacitor C_{sc}. There was drop in voltage and frequency when the IAG was loaded. As the devices are designed to operate satisfactory at its rated voltage, hence there is need of voltage controllers for IAG under varying load conditions.

CHAPTER 4

OPTIMIZATION BASED PERFORMANCE EVALUATION OF 3-PHASE IAG FURNISHING 1-PHASE LOAD FOR RURAL SITES

4.1 GENERAL

The per-capita of energy consumption of a particular country is the direct indication of the economic development or growth of that country. It is estimated by the energy engineers that by the 21st century fossil fuels will be depleting or diminishing. The significance or relevance of non-conventional energy sources was recognized in India in 1970's. For people living in remote areas such type of generating systems proves to be more cost effective or economical than connecting or extending a power line to the electricity grid. Such types of generating systems are also preferred by the people living in the vicinity of the grid and willing to get independence from the power providers or whose inclination is towards non-polluting energy sources. Energy experts predicted renewable energy as the upcoming energy of future for energy generation. The energy generation using renewable energy techniques is more environmentally friendly and addresses the local demand of energy at the point of need. Use of such generating systems results in reduced transmission losses. This advantage fetches the attention of the researchers towards the use of renewable energy sources.

Isolated asynchronous generators (IAG's) may be opted as a single-phase generating unit for furnishing single-phase distribution unit because of its very simple protection scheme, low cost and almost maintenance free operation. In [35, 36], the author has done experimental investigations on a 1-Φ IAG to show its applicability for feeding lighting loads in rural areas. In [37, 38], the performance of 1-Φ IAG feeding 1-Φ load has been accessed using conventional Newton Raphson method. The optimum value of excitation capacitance for the voltage build-up in 1-Φ SEIG feeding 1-Φ load has been described [39]. Chan and Lai [40] described the symmetrical component theory based steady-state analysis of self-regulated self-excited induction generator. Such systems [35-40] suffers from

- Worse performance because these asynchronous machines were only designed initially for motor operation.

- More economical advantages for machine rating less than 3.73 kW (5hp) only.
- Complicated self-excited phenomenon in 1-phase asynchronous generator owing to the presence of backward rotating field.
- The backward rotating field attributes to the additional rotor losses and hence, the single-phase IAG proves to be less efficient than the corresponding 3-phase IAG.
- Unbalanced operation leads to voltage stresses and may overheat the machine.
- Due to unbalanced currents, the rated three-phase power output cannot be obtained.
- Low power factor.
- Mechanical vibrations.

Above 5 Hp, 3-phase IAG is preferred due to economical advantages over 1-Φ IAG of the same rating. These advantages are low cost, more readily available and have higher efficiency than the equivalent rating single-phase machine. Hence, it motivates the researches to use three-phase IAG for generating single phase power for feeding single-phase distribution system [41-51]. T.F Chan et.al [41] explained the method of symmetrical components for the analysis of 3-Φ IAG with the asymmetrical connected excitation capacitance and load. Moreover, a phase balancing scheme using modified Steinmetz connection (MSC) has been proposed in this paper. The optimum value of excitation capacitor needed for obtaining max power output of 3-Φ IAG feeding 1-Φ capacitive and inductive nature load has been evaluated [42]. In this paper [43], author suggested secant method for evaluating the minimum of capacitance for a 3-Φ IAG feeding 1-Φ load. An optimization based method has been discussed to determine the value of capacitance of a 3- Φ IAG feeding 1- Φ load [44]. In [45], method of symmetrical components and two-port network has been used for the analysis of 3- Φ IAG excited by unbalanced capacitor and feeding unbalanced load. T.F Chan et.al [46] discussed several phase balancing schemes for a 3-phase IAG feeding 1-phase load to attain perfect phase balance using modified Steinmetz connection. Wang and Cheng [47] suggested an Eigen value based scheme for evaluating the performance of IAG.

Symmetrical component theory and optimization technique have been used for the performance analysis under steady state conditions [48-51]. T. F Chan et.al [50,

51] suggested the smith connection for operating 3-phase IAG for feeding single phase load. T. F Chan et.al [52] discussed the steady state analysis of IAG and derived the condition for achieving perfect phase balance using symmetrical component theory. S. N Mahato et.al [53] discussed the steady state performance analysis of IAG using sequential unconstrained minimization technique (SUMT) along with Rosenbrock's method of rotating coordinates. Y. J Wang et.al [54] proposed a two port model for evaluating the values of 3 capacitors to balance the IAG system. With passage of time or due to failure of one or two capacitors from the balanced excitation scheme of the machine, the drop in power output and voltage will not be highly affected and the machine continues to be operated as an IAG with the left over capacitors of the excitation scheme. The little bit unbalance in generating voltages and currents is visualized. To minimize these adverse effects, a lot of research has been focused on three-phase IAG feeding 1- Φ load. This unbalanced operation is of utmost practical importance in remote sites low power applications where balanced operations are not desirable. The various applications of IAG in remote sites are 1- Φ emergency supplies, as a portable source for construction sites, the isolated line repeaters etc.

It is observed that the conventional and optimization based analysis of 3- Φ IAG feeding 1- Φ load available in literature required lengthy calculations and algorithm knowledge implementation in software. But in this chapter, a simple optimization technique 'fsolve' is implemented to analyze the steady state performance of 3- Φ IAG for meeting 1- Φ load in inaccessible rural sites. This chapter highlights (ii) Symmetrical component theory based analysis of IAG under balanced and unbalanced load conditions (iii) Solution technique (iv) Algorithm for performance evaluation (v) Results (vi) Conclusion.

4.2 SYMMETRICAL COMPONENT THEORY BASED ANALYSIS OF IAG UNDER BALANCED/UNBALANCED LOAD CONDITIONS [19]

The considered system for study consists of the delta connected asynchronous machine (AM), delta connected capacitor bank, delta connected load. The capacitor bank and load are coupled or combined together and connected in parallel with the asynchronous machine (AM). The symmetrical component theory is used here for deriving the conditions under balanced and unbalanced operating conditions [19].

$$Y_{la} = G_{la} - j\varkappa_{la} + j\varkappa_{ca} \tag{4.1a}$$

$$Y_{lb} = G_{lb} - j\varkappa_{lb} + j\varkappa_{cb} \tag{4.1b}$$

$$Y_{lc} = G_{lc} - j\varkappa_{lc} + j\varkappa_{cc} \tag{4.1c}$$

From symmetrical component theory

$$V_{wa} = V_{os} + V_{ps} + V_{ns} \tag{4.2a}$$

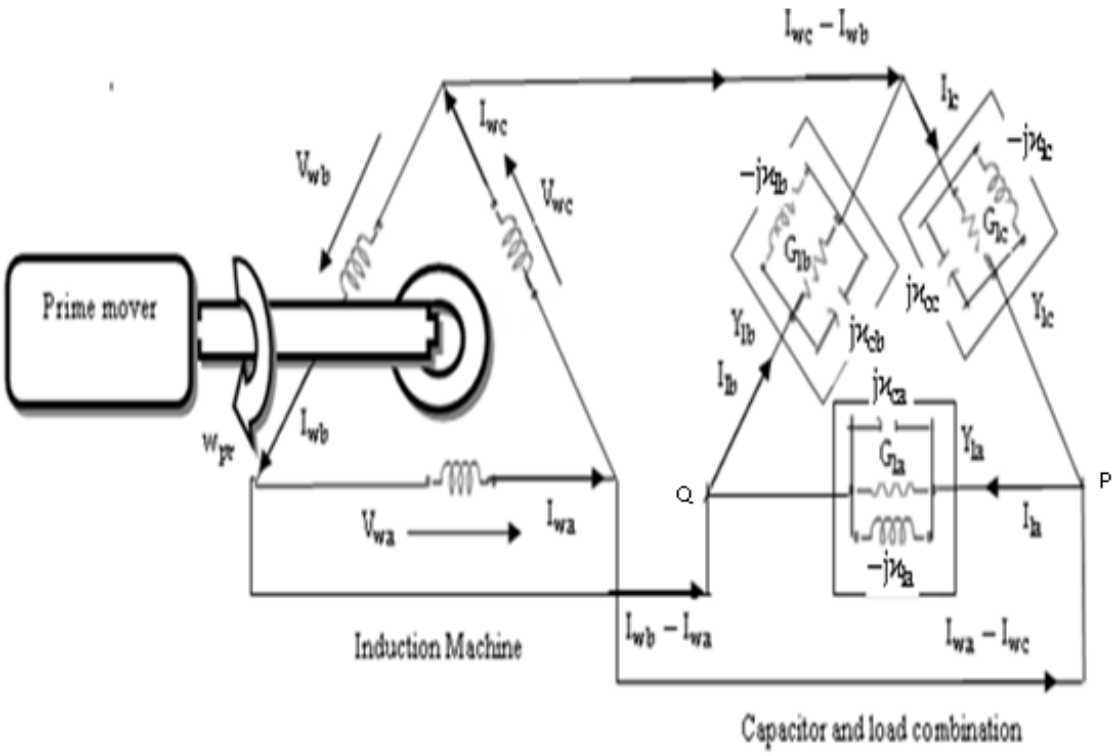

Fig. 4.1 Three-phase IAG feeding three-phase load

$$V_{wb} = V_{os} + k^2V_{ps} + kV_{ns} \tag{4.2b}$$

$$V_{wc} = V_{os} + kV_{ps} + k^2V_{ns} \tag{4.2c}$$

For the delta connected system

$$V_{wa} + V_{wb} + V_{wc} = 0 \tag{4.3}$$

From Fig. 4.1, the load current and winding currents are evaluated by applying KCL at node P and Q gives

$$I_{la} - I_{lc} = I_{wa} - I_{wc} \tag{4.4a}$$

$$I_{la} - I_{lb} = I_{wa} - I_{wb} \tag{4.4b}$$

Symmetrical component theory yields the following winding current equations for the generator

$$I_{wa} = I_{ps} + I_{ns} = -(V_{ps}Y_{ps} + V_{ns}Y_{ns}) \tag{4.5a}$$

$$I_{wb} = k^2 I_{ps} + kI_{ns} = -(k^2 V_{ps}Y_{ps} + kV_{ns}Y_{ns}) \tag{4.5b}$$

$$I_{wc} = kI_{ps} + k^2 I_{ns} = -(kV_{ps}Y_{ps} + k^2 V_{ns}Y_{ns}) \tag{4.5c}$$

The load currents in terms of winding voltages V_{wa} and V_{wb} can be formulated as

$$I_{la} = V_{wa}Y_{la} = (V_{ps} + V_{ns})Y_{la} \tag{4.6a}$$

$$I_{lb} = V_{wb}Y_{lb} = (k^2 V_{ps} + V_{ns})Y_{lb} \tag{4.6b}$$

$$I_{lc} = V_{wc}Y_{lc} = (kV_{ps} + k^2 V_{ns})Y_{lc} \tag{4.6c}$$

Substituting from Eq. (4.4) and (4.5) into (4.3)

$$I_{la} = AV_{ps} + BV_{ns} \tag{4.7a}$$

$$I_{la} = CV_{ps} + DV_{ns} \tag{4.7b}$$

Here

$$A = (k-1)Y_{ps} + kY_{lc} \tag{4.8a}$$

$$B = (k^2 - 1)Y_{ns} + k^2 Y_{lc} \tag{4.8b}$$

$$C = (k^2 - 1)Y_{ps} + k^2 Y_{lb} \tag{4.8c}$$

$$D = (k-1)Y_{ns} + kY_{lb} \tag{4.8d}$$

From Eq. 4.6(a) and 4.6(b) and

$$K_{vuf} = (A - C)/(B - D) = V_{ns}/V_{ps} \tag{4.9}$$

Defining voltage unbalance factor as $K_{vuf} = V_{ns}/V_{ps}$ and eliminating Y_{ps} from Eq. (4.6) through Eq. (4.7)

$$K_{vuf} = -(Y_{la} + kY_{lb} + k^2 Y_{lc}/3Y_{ns} + Y_{la} + Y_{lb} + Y_{lc}) \tag{4.10}$$

Evaluate I_{al} from both Eq. (4.3) and Eq. (4.5a) and then equate I_{al} got from the two equations to evaluate Y_1

$$1 + k + k^2 = 0;\ k^3 = 1;\ k^4 = k;$$

Combination of Eq. (4.2a) and (4.6) yields

$$V_{wa} = I_{la}|Z| \tag{4.11}$$

Here

$$Z = \{(A + D) - (B + C)\}/(AD - BC) \tag{4.12}$$

From Fig. 4.1, the phase a voltage is given by

$$V_{wa} = I_{la}Z_{la} \tag{4.13}$$

On equating Eq. (4.11) and (4.13),

$$I_{la}(Z - Z_{la}) = 0 \tag{4.14}$$

For generator operation, I_{st} should not be equal to zero, hence

$$Z - Z_{la} = 0 \tag{4.15}$$

Substituting from Eq. (4.12) and Eq. (4.8) into Eq. (4.13) yields the following condition of self-excitation under balanced/unbalanced conditions

$$3 + \left(Z_{ps} + Z_{ns}\right)(Y_{la} + Y_{lb} + Y_{lc}) + Z_{ps}Z_{ns}(Y_{la}Y_{lb} + Y_{lb}Y_{lc} + Y_{la}Y_{lc}) = 0 \tag{4.16}$$

The general condition for self-excitation for delta-connected machine and delta-connected load can also be expressed in terms of Z, G, B and some other constants P_1 and P_2 after substituting the values of Y_{la}, Y_{lb} and Y_{lc} from Eq. (4.1) into Eq. (4.16):

$$3 + \left(Z_{ps} + Z_{ns}\right)(G_4 + j\varkappa_4) - (T_1 - jT_2)Z_{ps}Z_{ns} = 0 \tag{4.17}$$

Here

$$G_4 = G_{la} + G_{lb} + G_{lc} \tag{4.18a}$$

$$\varkappa_4 = \varkappa_{ca} + \varkappa_{cb} + \varkappa_{cc} - \varkappa_{la} - \varkappa_{lb} - \varkappa_{lc} \tag{4.18b}$$

$$T_1 = \left\{\begin{matrix} G_{la}G_{lb} + G_{lb}G_{lc} + G_{la}G_{lc} - (\varkappa_{ca} - \varkappa_{la})(\varkappa_{cb} - \varkappa_{lb}) - (\varkappa_{cb} - \varkappa_{lb}) \\ (\varkappa_{cc} - \varkappa_{lc}) - (\varkappa_{cc} - \varkappa_{lc})(\varkappa_{ca} - \varkappa_{la}) \end{matrix}\right\} \tag{4.18c}$$

$$T_2 = \left\{\begin{matrix} G_{la}(\varkappa_{cb} + \varkappa_{cc} - \varkappa_{lb} - \varkappa_{lc}) + G_{lb}(\varkappa_{ca} + \varkappa_{cc} - \varkappa_{la} - \varkappa_{lc}) + \\ G_{lc}(\varkappa_{ca} + \varkappa_{cb} - \varkappa_{la} - \varkappa_{lb}) \end{matrix}\right\} \tag{4.18d}$$

4.2.1 Balanced R-L load

Under this operating condition, external admittances are equal. Let

$$G_{la} = G_{lb} = G_{lc} = G_l$$

$$\varkappa_{la} = \varkappa_{lb} = \varkappa_{lc} = \varkappa_l$$

$$\varkappa_{ca} = \varkappa_{cb} = \varkappa_{cc} = \varkappa$$

$$Y_{la} = Y_{lb} = Y_{lc} = j\varkappa + G_l - j\varkappa_l$$

The values of various constants are modified as:

$$\left.\begin{aligned} G_4 &= 3G_l; \quad \varkappa_4 = 3\varkappa - 3\varkappa_l \\ T_1 &= -\left\{3G_l^2 - 3(\varkappa - \varkappa_l)^2\right\} \\ T_2 &= \{6G_l(\varkappa - \varkappa_l)\} \end{aligned}\right\} \tag{4.19}$$

4.2.2 Balanced R Load

Under this operating condition, the values of external admittances are defined as:

$$G_{la} = G_{lb} = G_{lc} = G_l$$

$$\varkappa_{la} = \varkappa_{lb} = \varkappa_{lc} = \varkappa_l = 0$$

$$\varkappa_{ca} = \varkappa_{cb} = \varkappa_{cc} = \varkappa = 0$$

$$Y_{la} = Y_{lb} = Y_{lc} = G_l$$

$$G_4 = 3G_l; \quad \varkappa_4 = 0$$

$$T_1 = -\left\{3G_l^2\right\}; \quad T_2 = 0$$

Equation (4.17) is simplified as

$$3 + 3\left(Z_{ps} + Z_{ns}\right)G_l + 3G_l^2 Z_{ps} Z_{ns} = 0 \tag{4.20}$$

4.2.3 Single-Phase R-L Load

A three-phase IAG can feed single-phase load using two-capacitor connection topology depicted in Fig. 4.2. To minimize the unbalance in winding voltages and currents, the two capacitors are connected across phases ‘a’ and ‘c’ of the asynchronous machine and the capacitor connected across third capacitor is removed i.e. $\boldsymbol{\varkappa}_{cb} = 0$.

The various parameters of Fig. 4.2 are

$$Y_{la} = j\varkappa_{ca} + G_{la} - j\varkappa_{la}$$

$$Y_{lb} = 0$$

$$Y_{lc} = j\varkappa_{cc}$$

Also,

$$\varkappa_{cb} = G_{lb} = \varkappa_{lb} = 0$$

$$G_{lc} = \varkappa_{lc} = 0$$

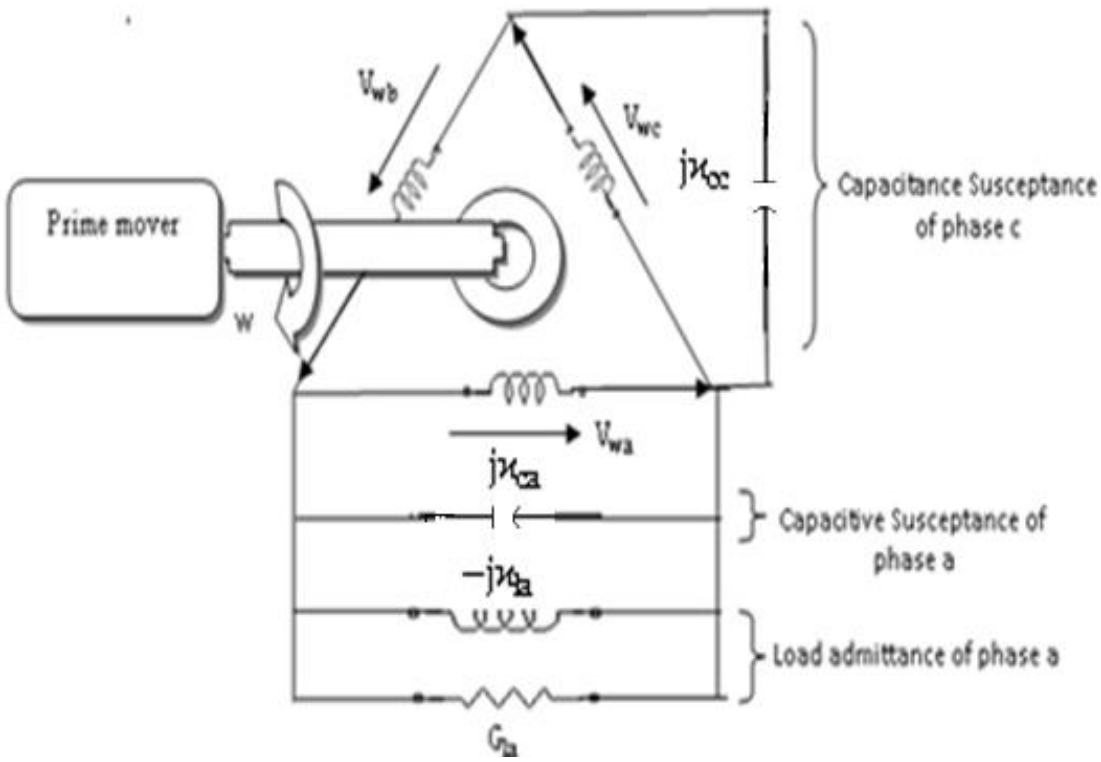

Fig. 4.2 Capacitor connection or topology for 3-phase IAG feeding single-phase load

The various constants of Eq. (4.18) are modified as:

$$\left.\begin{aligned} G_4 &= G_{la} \\ \varkappa_4 &= \varkappa_{ca} + \varkappa_{cc} - \varkappa_{la} \\ T_1 &= -\varkappa_{cc}(\varkappa_{ca} - \varkappa_{la}) \\ T_2 &= G_{la}(\varkappa_{cc}) \end{aligned}\right\} \qquad (4.21)$$

4.2.4 Single-Phase Resistive Load

The various parameters of Fig. 4.2 are

$$Y_{la} = j\varkappa_{ca} + G_{la}$$

$$Y_{lb} = 0$$

$$Y_{lc} = j\varkappa_{cc}$$

Also,

$$\varkappa_{cb} = G_{lb} = \varkappa_{lb} = 0$$

$$G_{lc} = \varkappa_{lc} = 0$$

The various constants of Eq. (4.18) are modified as:

$$\left.\begin{aligned} G_4 &= G_{la} \\ \varkappa_4 &= \varkappa_{ca} + \varkappa_{cc} \\ T_1 &= -\varkappa_{cc}\varkappa_{ca} \\ T_2 &= G_{la}(\varkappa_{cc}) \end{aligned}\right\} \tag{4.22}$$

4.3 SOLUTION TECHNIQUE

The process of self-excitation can be estimated using Eq. (4.18) for the defined or given values of machine parameters, speed, load, capacitances and considering saturation effect. The positive sequence equivalent circuit of asynchronous machine is shown in Fig. 4.3(a), where all the reactance's referred or corresponds to base frequency and X_{mg1} represents the saturated value and corresponds to the forward rotating air-gap field.

The negative sequence equivalent circuit is shown in Fig. 4.3(b). In this circuit, the term (F_y-v) in the rotor circuit is replaced by the term (F_y + v). Moreover, in this circuit, the magnetizing reactance is removed as its value is very high compared to R_{ro} / 2 in the rotor circuit. For analysis purpose, assume $X_{lst} = X_{lro} = X_{le}$ and F_y = v except the term (F_y - v) in the rotor circuit.

From the simplified equivalent circuit of Fig. 4.3(b),

$$Z_{ps} = R_{st} + jvX_{le} + jX_{mg1}[vR_{st}/(F_y - v) + jX_{le}]/[vR_{ro}/(F_y - v) + jX_{le} + jX_{mg1}] \tag{4.23a}$$

$$Z_{ns} = R_{st} + R_{ro}/2 + jvX_{le} \tag{4.23b}$$

Substitute the value of Z_{ps} and Z_{ns} in Eq. (4.17). Eq. (4.17) is a non-linear complex equation. Rearranging all the terms and separating the real and imaginary parts and equating individually to zero to get the value of X_{mg1} and F_y. The following two equations are obtained.

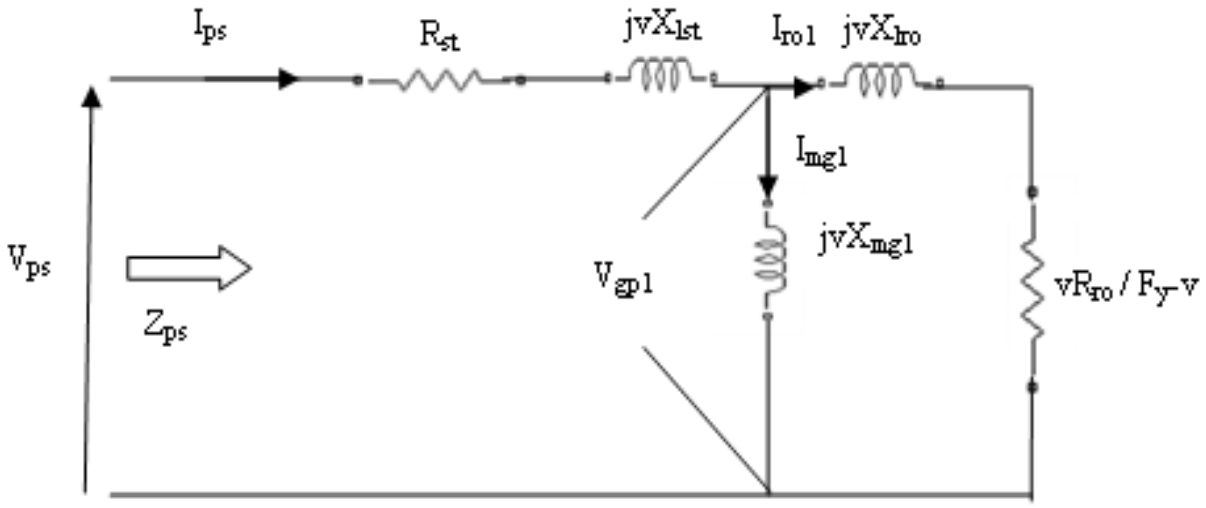

Fig. 4.3(a) Simplified positive sequence equivalent circuit of three-phase asynchronous machine

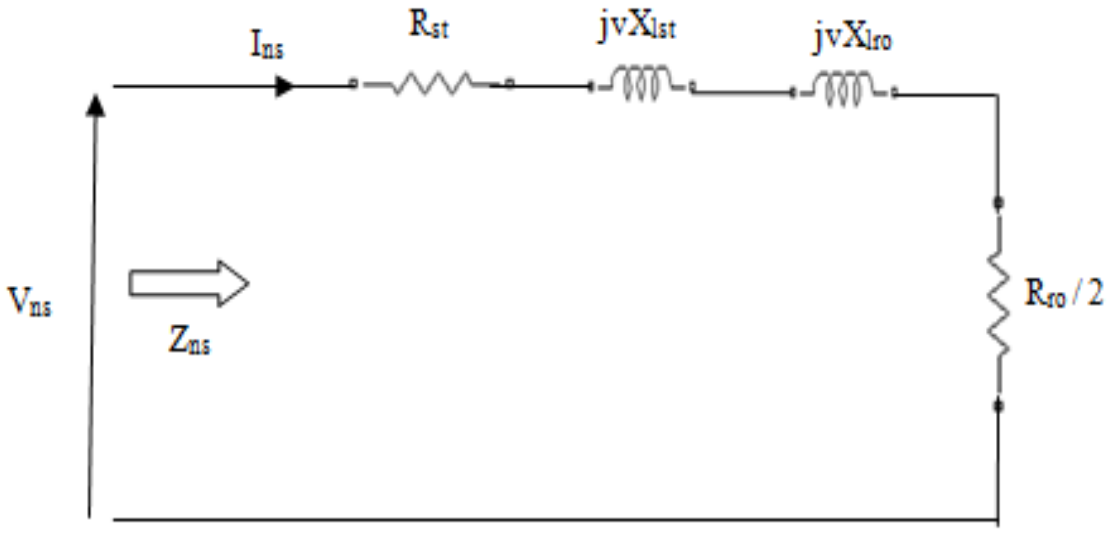

Fig. 4.3(b) Simplified negative sequence equivalent circuit of an asynchronous machine

$$F(S_1X_{mg1} + S_2) + (S_3X_{mg1} + S_4) = 0 \qquad (4.24a)$$

$$F(S_5X_{mg1} + S_6) + (S_7X_{mg1} + S_8) = 0 \qquad (4.24b)$$

The values of the constants S_1-S_8 are provided in appendix C. These equations are solved using 'fsolve' a built in function available in MATLAB Optimization toolbox

4.3.1 Algorithm for Performance Evaluation

Step-1: Solve Eq. 4.24 (a) and 4.24 (b) using 'fsolve' routine of MATLAB optimization toolbox to evaluate the saturated values of X_{mg1} and F_y.

Step-2: Evaluate the complete performance of the generator using the magnetizing characteristics [57] and the following equations:

$$I_{ps} = \left(V_{gp1}/jF_yX_{mgl}\right) + V_{gp1}/[\left(F_yR_{ro}/(F_y\text{-}v\right)] + jF_yX_{le} \quad (4.25)$$

$$V_{ps} = V_{gp1} - \left(R_{st} + jF_yX_{le}\right)I_{ps} \quad (4.26)$$

$$V_{ns} = K_{vuf}V_{ps} \quad (4.27)$$

$$I_{ns} = V_{ns}/Z_{ns} \quad (4.28)$$

Here K_{vuf} is defined in Eq. (4.10)

Step-3: Using these obtained sequence quantities, phase voltages and currents can be computed using Eq. (4.2). The current and power equations relating with the load can be evaluated as:

$$I_{alo} = V_{a,}/\left(R_{alo} + jF_yX_{alo}\right) \quad (4.29)$$

Similarly, I_{bL} and I_{cL} can be evaluated.

$$P = (I_{alo})^2R_{alo} + (I_{blo})^2R_{blo} + (I_{clo})^2R_{clo} \quad (4.30)$$

The modified current and power equations for single-phase load can be evaluated as:

$$I_{alo} = V_a/(R_{alo}) = V_1/(R_{alo}) \quad (4.31)$$

$$P = (I_{alo})^2R_{alo} \quad (4.32)$$

Step-4: Compare results obtained from analytical and experimental investigations or findings.

4. 4 RESULTS

4. 4. 1 Case Study

A case study has been carried out using different capacitor combinations to achieve the desired voltage regulation under varying load conditions. The three capacitor combinations tested in the laboratory are: C_a-C_b-0 (two balanced capacitor in and one

capacitor out of circuit), C_a-2C_c-C_{bf} (two balanced capacitor and one fixed capacitor in the circuit), C_a-2C_c (two capacitor connected in 1:2 ratio) are presented in Table.1. With C_a-C_b-0 capacitor connection, the voltage regulation varies from 51.31% to 26.34% as the capcitance in the capacitor configurtion varies from 40 – 40 - 0 µF to 80 – 80 - 0 µF. With C_a-2C_c-C_{bf} capacitor connection, the voltage regulation varies from 28.69% to 17.35% as the capacitance in the capacitance configuration varies from 20- 30- 60µF to 20-50-100µF.

With C_a-2C_c capacitor connection, the voltage regulation varies from 6.67% to 3.75% as the capacitance in the capacitance configuration varies from 30-60 µF to 50-100 µF. It has been observed from the experimental investigations that the value of voltage regulation in case of C_a-2C_c capacitor connection is smaller than the other capacitor connection schemes and its value is minimum for capacitor combination 50- 100µF. Hence it is inferered that better volatge regulation is attained in case of C_a-2C_c capacitor connection and the best voltage regulation has been attained for 50 - 100 µF. Hence the performance analysis under steady state has been acomplished for 50 - 100 µF(C_a-2C_c).

4.4.2 Result Interpretation on Generator Side

When a three phase IAG is feeding single-phase load, an unbalance occurs in three-phase generated voltages and currents of the IAG. To avoid or minimize this unbalance a C_a-2C_c capacitor connection is suggested in available literature [35-53]. A voltage of 380 V is generated with the help of a delta-connected IAG at no load first. Then to feed single-phase load a capacitor connection of type C_a-2C_c is used here. The voltage across capacitor C is first fed to autotransformer for stepping down to 230 V for single-phase load. Fig. 4.4 graphically demonstrates the variation pattern of excitation capacitance with power across 1-Φ load at constant voltage (380 V). To maintain constant voltage across load terminals, it is visualized that both C_a and C_c almost increases linearly with the power across single-phase load.

Moreover, this capacitance combination minimizes voltage unbalance on the generator side and maintains almost perfect phase balance between the three-phase voltages [Fig. 4.4]. The noise free operation of IAG is an indication of almost perfect phase balance on the generator side.

Fig. 4.5 illustrates the variation pattern of per-phase voltages and frequency of

Table 1: Different Capacitance values combinations for balanced/ unbalanced/single-phase excitation schemes.

Case study 1 3-phase IAG for 3-phase loads	Operating condition	Excitation capacitance Values	Load voltages	Voltage Regulation
	Distrubed balanced condition or failure of one capacitor from balanced excitation C_a-C_b-0	C_a=40µF C_b=40µF C_c=0µF	V_o=380V V_f=185V	51.31%
		C_a=60µF C_b=60µF C_c=0µF	V_o=380V V_f=230V	39.47%
		C_a=80µF C_b=80µF C_c=0µF	V_o=380V V_f=280V	26.31%
Case study 2 3-phase IAG for single-phase loads	C_a-2C_c-C_{bf} with one fixed capacitor across third winding	C_a=20µF C_b=30µF C_c=60µF	V_o=237V V_f=169V	28.69%
		C_a=20µF C_b=40µF C_c=80µF	V_o=240V V_f=184V	23.33%
		C_a=20µF C_b=50µF C_c=100µF	V_o=242V V_f=200V	17.35%
Case study 3 3-phase IAG for 1-phase load with phase balance	C_a-2C_c	C_a=30µF C_c=60µF	V_o=240V V_f=224V	6.67%
		C_a=40µF C_c=80µF	V_o=240V V_f=226V	5.83%
		C_a=50µF C_c=100µF	V_o=240V V_f=231V	3.75%

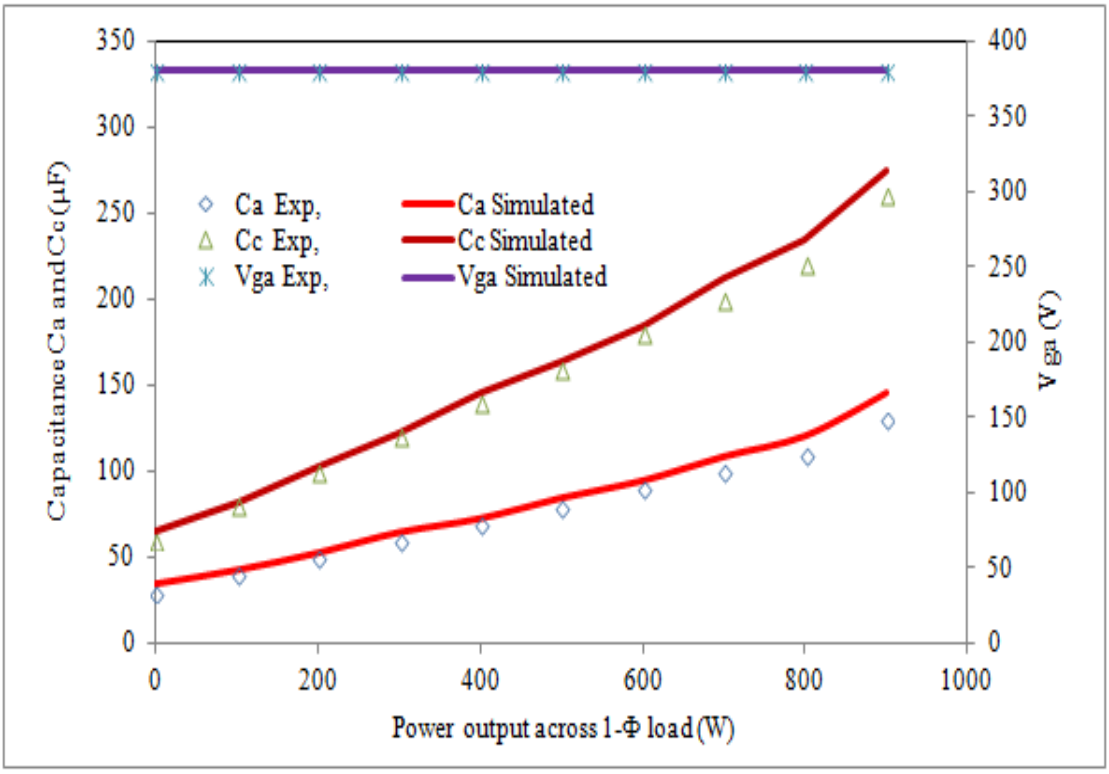

Fig. 4.4 Variation pattern of capacitance with power output at unity power factor and at constant voltage (380 V) for C_a = 50µF and C_c = 100µF.

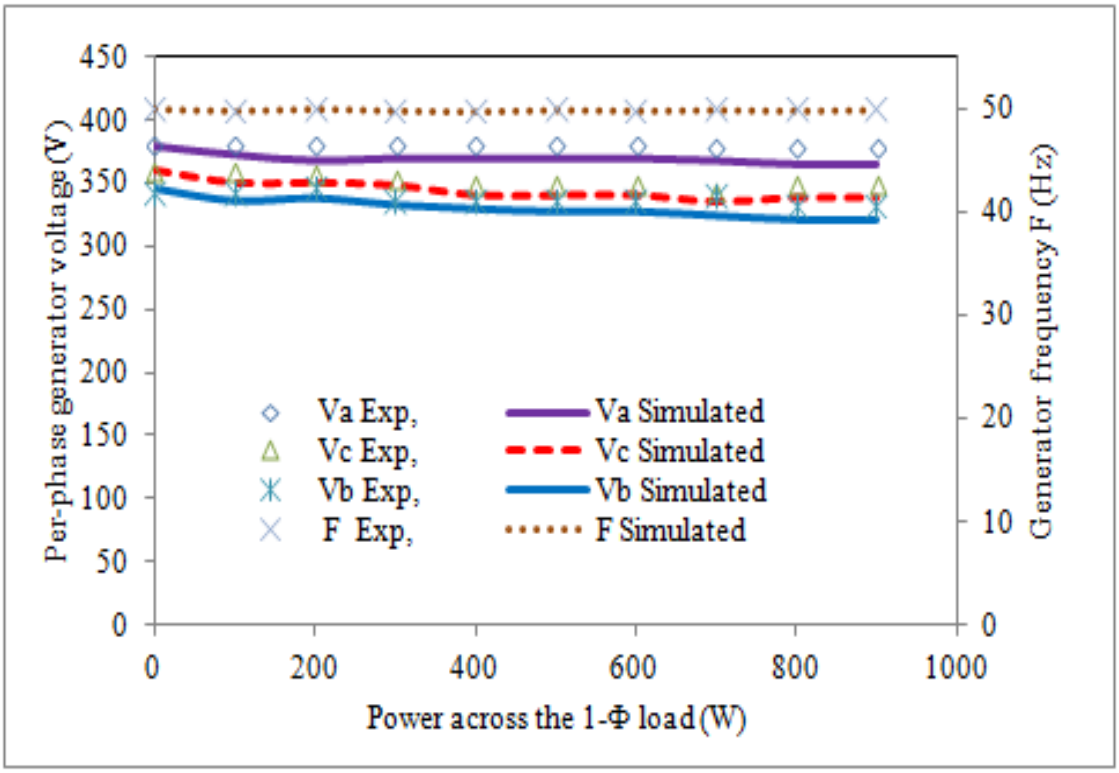

Fig. 4.5 Variation pattern of per-phase generator voltage and frequency with power across the 1-Φ load (W) at unity p.f and at constant speed for C=50µF and 100µF.

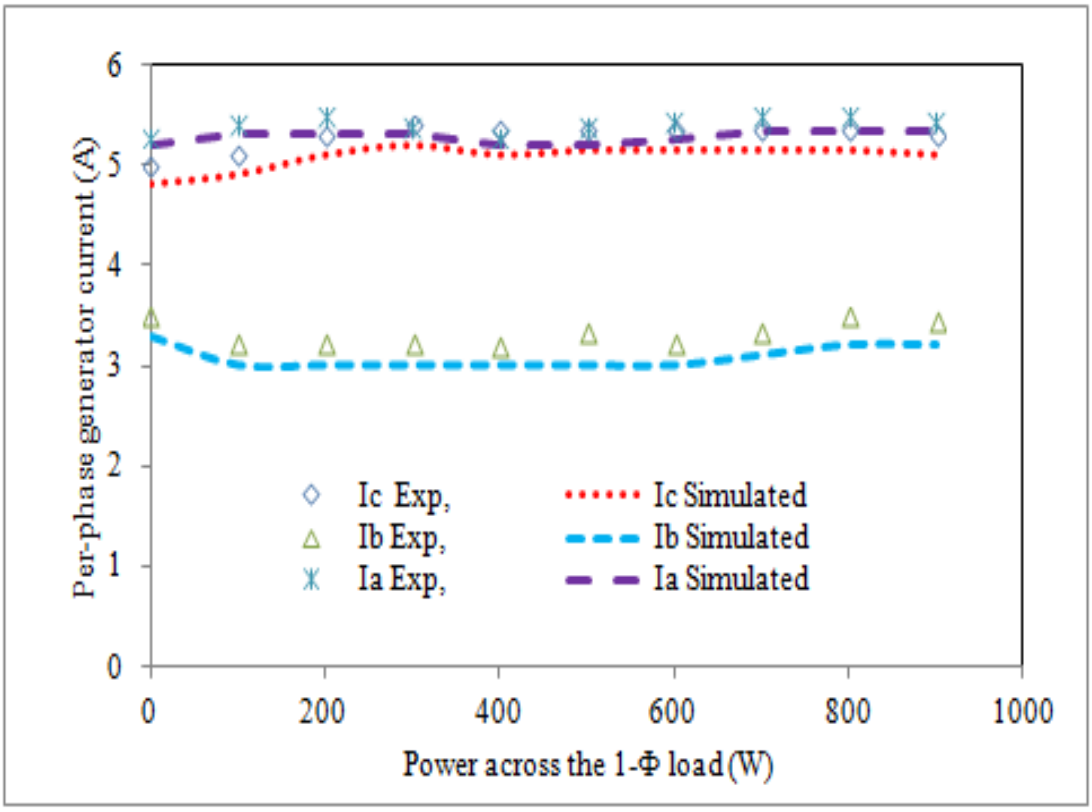

Fig. 4.6 Variation pattern of per-phase generator current with power across 1-Φ load (W) at unity p.f and at constant speed (1068 rpm) for C=50μF and 100μF

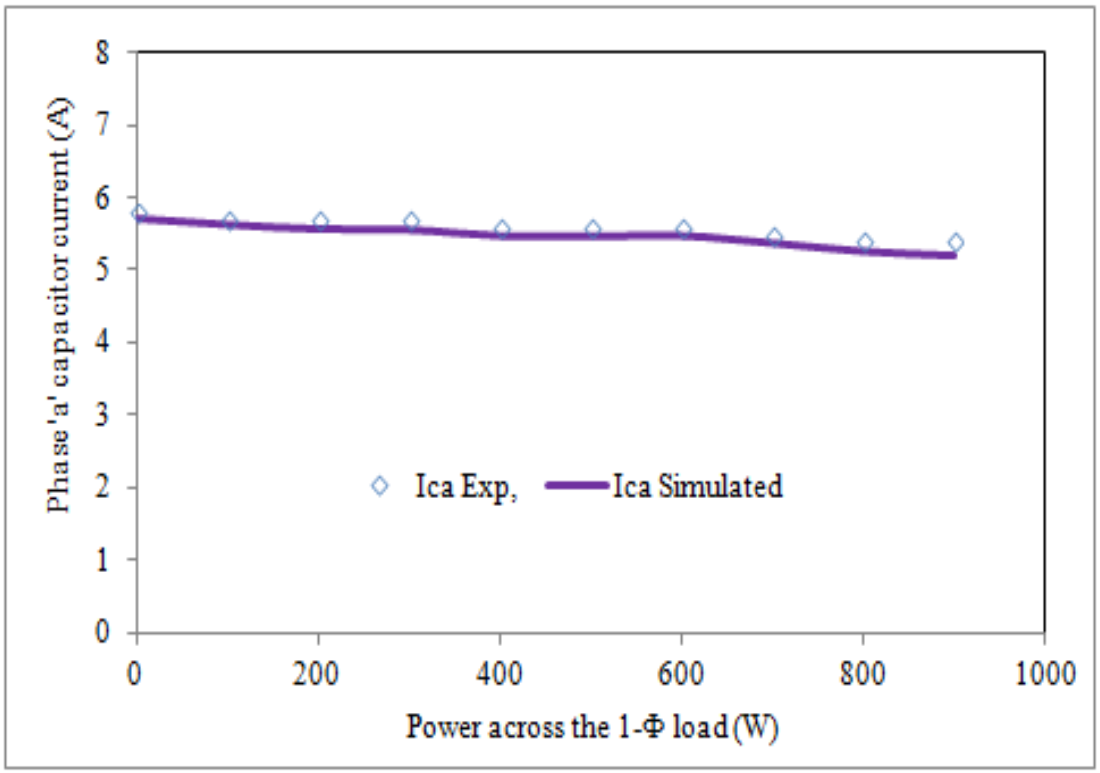

Fig. 4.7 Variation pattern of phase-a capacitor current with power across 1-Φ load (W) at unity p.f and at constant speed (1100 rpm)

the generator with power output at constant speed for capacitance combination of C_a=50µF and C_c=100µF. The generator voltages are almost perfectly balanced. As the load is increased from 0 W to 900 W, the generator frequency is almost constant.

Fig. 4.6 shows the variation pattern of per-phase generated current of IAG with power output at constant speed for C=50µF and 100µF. Below 300 W power output, the current in phase c is slightly unbalanced but after 300 W currents in both phase 'a' and 'c' seems to be balanced and constant also.

Fig. 4.7 shows the variation pattern of capacitor current with power across the 1-Φ load at constant speed and at unity power factor load. The capacitor current from no load to 900W is almost constant and is unaffected by both power output and the value of capacitance C_a and C_c.

4.4.3 Result Interpretation on Single-Phase Load Side

Fig. 4.8 shows the effect of power across single-phase load and capacitances (C_a and C_c) on the voltage across single-phase load. A voltage of 240 V is maintained across the single - phase load as the power across it varies from 0 W to 900 W.

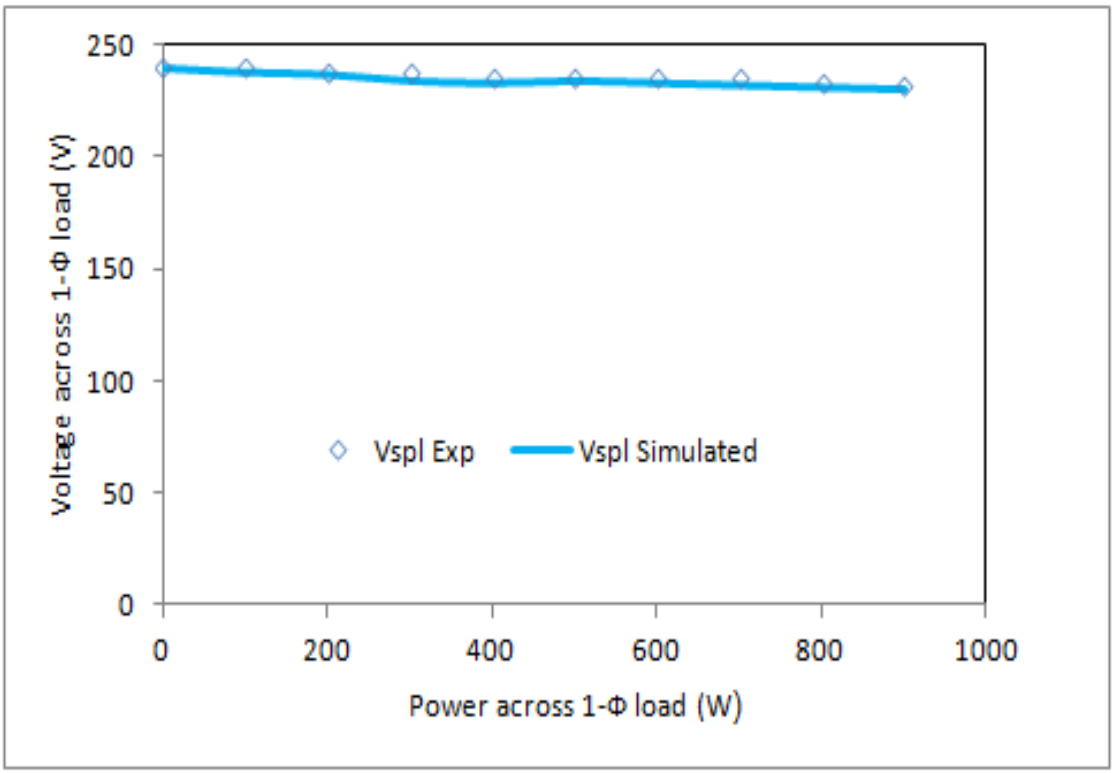

Fig. 4.8 Variation pattern of 1-Φ load voltage with power across 1-Φ the load (W) at unity p.f and at constant speed (1100 rpm)

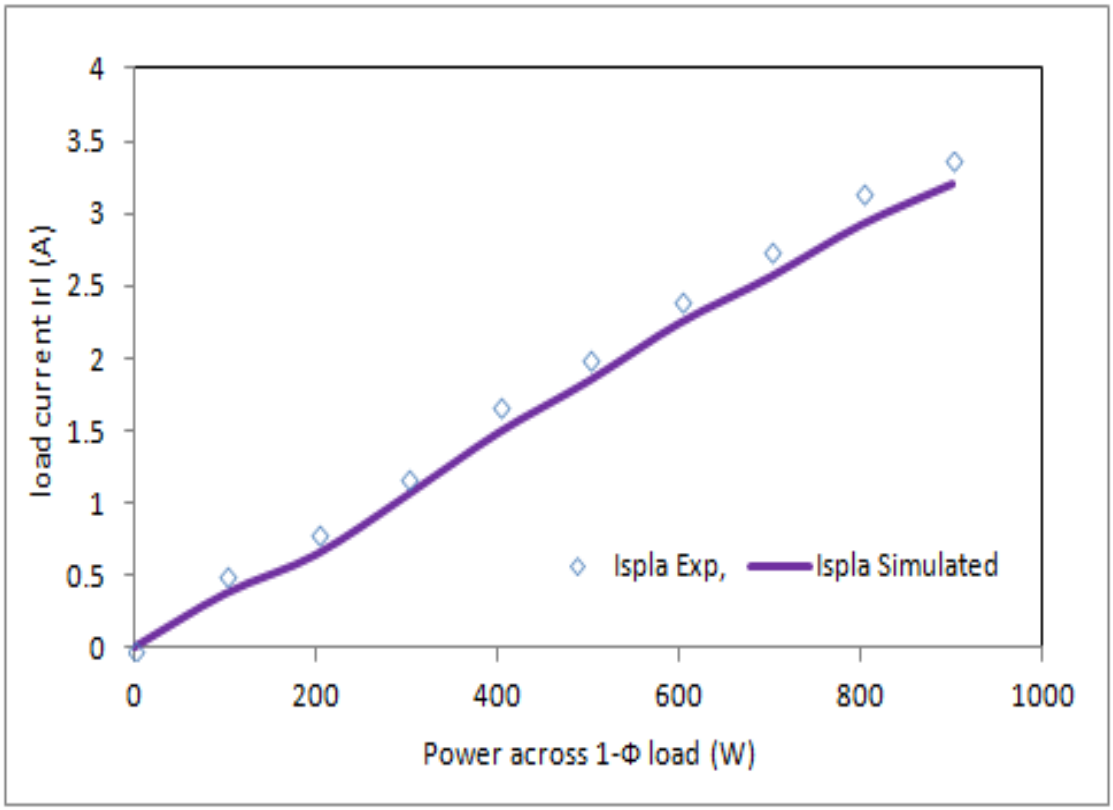

Fig. 4.9 Variation pattern of load current with power across 1-Φ load (W) at unity p.f and at constant speed (1100 rpm)

Fig. 4.9 shows the effect of power across single-phase load and capacitances (C_a and C_b) on the load current. The load current increases with increases in power output across single-phase load. The little bit decrease in capacitor current is compensated by increase in load current so that the total loads on the generator remains constant. Hence, voltage and frequency are constant for constant speed operation.

4.5 SUMMARY

The optimization technique 'fsolve' has been employed for the evaluation of steady-state performance equations of the 3-phase IAG feeding unbalanced and single phase loads in remote sites. Symmetrical component approach as explained by S.S Murthy et.al [42] has been adopted for the application of 'fsolve' technique. This type of unbalanced operation or single-phase load is often encountered and finds practical application in remote areas.

The Equations representing the self-excitation condition for the delta-connected generator and load configuration were non-linear equations in terms of F_y

and X_{mg1}. These equations have been solved to evaluate the values of X_{mg1} and F_y using 'fsolve' routine. From results, it has been revealed that a C_a- $2C_c$ capacitor connection provide a supply system with minimum phase unbalance and maintains almost constant load voltage when fed from constant speed prime mover. Here the constant speed prime mover is emulated with the dc machine. Such systems can be adopted for meeting the electrical requirements of people residing in grid isolated areas.

CHAPTER 5

ELECTRONIC GENERATOR LOAD CONTROLLER (EGLC) FOR AN ISOLATED ASYNCHRONOUS GENERATOR (IAG)

5.1 GENERAL

Decentralized or stand-alone power generation has attracted attention of researchers in recent years for its use in off grid areas due to the reduced amount of energy lost in transmitting electricity, reduced size and exemption from installation, testing maintenance and commissioning of new transmission lines for meeting the enhanced demand. Thus, a decentralized power generation system is considered as an up gradation of the existing conventional electric power generation system. Today, the IAG's are integrated with locally available renewable energy sources (solar, wind and small hydroelectric plants) for electrical power generation rather than fossil fuels for some socio-technical and economical reasons. An IAG was preferred and recommended over a conventional synchronous generator due to its numerous advantages listed as: no brushes in the rotor circuit, reduced unit size, no dc excitation, singly excited, ruggedness, almost maintenance free, protection under abnormal conditions of overloads and short-circuits etc. Owing to the recent research related with non conventional energy sources and off grid systems, the IAG emerges as one of the most promising and favored renewable sources of energy [55-70]. J.M Elder et.al [55] discussed an integral cycle control method to reduce the cost of stand-alone micro-hydro based power generation scheme (upto 100kW). R. Bonert et.al [56] presented an impedance controller for accomplishing better voltage and frequency regulation of the IAG. R.C Bansal [57] detailed the overview of the various practical aspects related to IAG: self-excitation phenomenon, modeling of IAG, performance analysis of IAG, voltage regulation strategies and lastly discussed the parallel operation of IAG. Various types of electronics based ELCs for IAG have been reported in literature along-with its advantages and disadvantages [58-70]. B. Singh et.al [58] discussed in detail the modeling of various components of the complete generating system. B. Singh et.al [59] provided an insight of the designing aspects of

3-phase and 1-phase electronic load controller (ELC) for a 3-phase IAG. T.S Chandra et.al [60] briefed about the various types of voltage controllers and discussed their suitability for various types of application. S. Gao et.al [61] and Juan M. Ramirez [62] described the design criteria of three-phase ELC feeding 1-phase and 3-phase load. E. G. Marra et.al [63] emphasized on PWM based VSI for the performance improvement of the IAG. B. Singh et.al [64] discussed in his research paper how the improvement of power quality of voltage and current of six-pulse ELC can be done using 24-pulse ELC for an asynchronous generator. S. Mbabazi [65] elaborated in detail about the micro-hydro based generation using ELC and its control aspects for providing voltage and frequency support. B. Singh et.al [66-67] enlightened the modelling aspects of isolated asynchronous generator (IAG), ELC and load. S. N Mahato et.al [68] dealt with the transient performance analysis of three-phase SEIG. B. Singh et.al [69] aimed on the steady state performance analysis of the integrated system of IAG-ELC subjected to varying consumer loads. B. Singh et.al [70] researched on the designing and control aspects of the composite system of IAG-EVFC with load and presented its performance under transient phenomenon.

For power rating less than 100kW, uncontrolled hydro based turbines are preferred for driving IAG. These turbines also assists in maintaining the hydropower potential constant, thus requisites the IAG output power held at constant level when subjected to varying load situation. This requisite some Electronic Generator Load Controller (EGLC) for absorbing the difference in generated and load power and hence maintains the constant load on the IAG. In this chapter, a simple EGLC is designed, developed and tested for a 5 HP asynchronous machine (AM) which maintains constant load on the IAG.

5.2 SYSTEM CONFIGURATION

A block diagram of the 3-phase EGLC-IAG system is represented in Fig. 5.1. The suggested system comprises of a star-connected asynchronous machine (AM), permanent source of reactive var (ac capacitors), delta-connected three-phase consumer load and EGLC. The system is constructed using a diode bridge rectifier (six-pulse), IGBT switch, a dc link capacitor (C_{dcl}), a dump load resistance (R_{dld}). The diode bridge rectifier basically helps in converting the three-phase IAG voltage into dc type voltage. This dc output voltage has the ripples and hence some capacitive

filter is requisite to make this dc voltage ripple free and smooth. An IGBT switch assists in switching in and out of R_{dld} in the EGLC circuit. This switch also provides the variable dc voltage across the R_{dld}. Initially the consumer load and the EGLC are not introduced in the system and the IAG generates the desired rated voltage with the aid of ac capacitors (delta connected). After attaining the desired voltage level, the EGLC with the driving signal fed to IGBT switch is introduced in the system and extracts whole of the IAG power (P_{iag}) and this power is utilised for various low power practical applications. Next the consumer load is introduced in the system, now the IAG is facing two loads in shunt. The IAG is providing power to both loads and now the EGLC extracts the difference in power (P_{iag}-P_{cld}) to maintain P_{iag} constant. The constant power is the indication of constant load on IAG. Hence, the EGLC supports the IAG voltage and its frequency when subjected to varying load situation. The IAG-EGLC system works on the principle of experiencing the constant load on the IAG subjected to varying load. The load is supported on the IAG with the aid of EGLC connected across the consumer load. The input power of the IAG must be held constant at varying consumer loads.

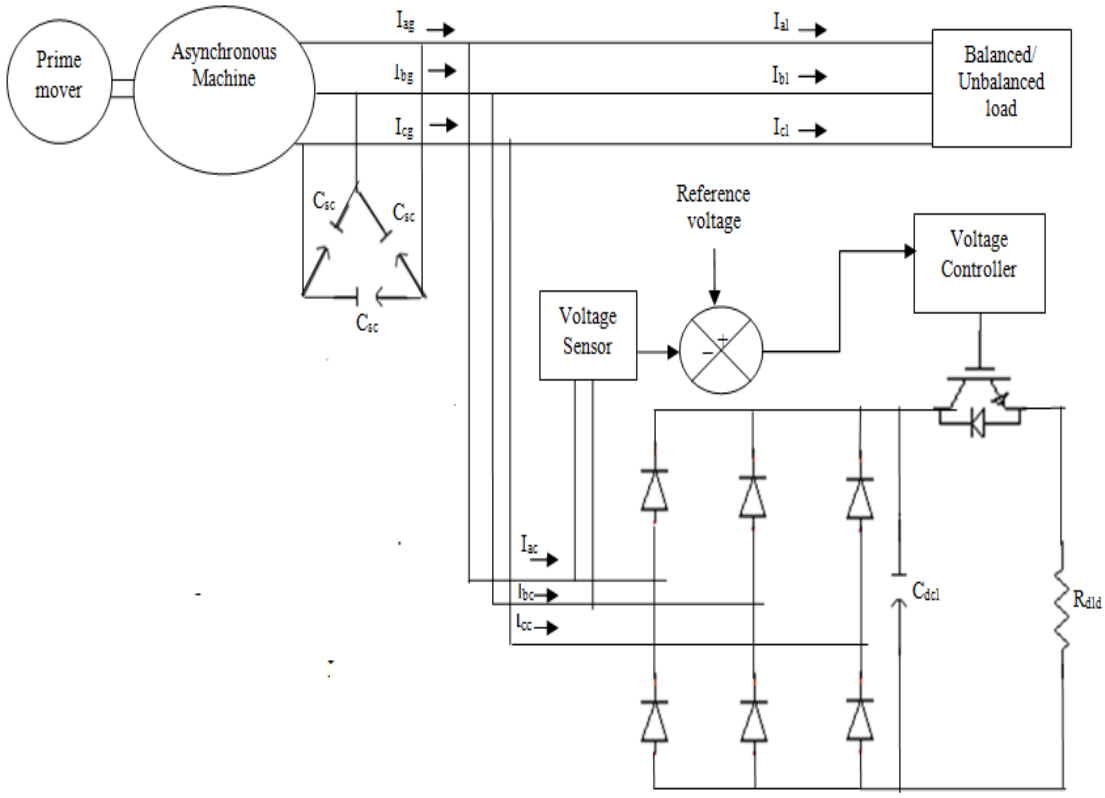

Fig. 5.1 Schematic diagram of IAG with EGLC

The IAG power amounts to the sum of dump load power and the consumer load power and is defined as

$$P_{iag} = P_{dld} + P_{cld} \tag{5.1}$$

Here P_{iag} represents the power generated by the IAG (which should remain constant). P_{cld} represents the consumer load power and P_{dld} represents the dump load power .The dump load power (P_{dld}) may be utilised for various practical applications like space heating, lighting loads, water pumping, cooking, fireworks, heating elements, battery charging etc.

5.3 DESIGN OF THREE-PHASE EGLC

For the proper operation of EGLC, proper design and selection of the various components used in EGLC is required. A design procedure is given for the three-phase EGLC for a three-phase IAG of 3730 W, 460 V [Appendix D]. The volt rating of the diode and IGBT switch will be the exactly same and depends on the r.m.s value of three-phase ac input side voltage and average value of the dc output side voltage. The dc output side voltage is obtained as

$$V_{dco} = \frac{\sqrt{2}\ V_{abcg}(L-L)}{\pi} = (1.35)V_{abcg}(L-L)$$

Here V_{abcg} (L-L) represents the r.m.s value of the line-to-line voltage of the IAG. For 3730W IAG, the line voltage is 460V i.e. V_{abcg} (L-L) = 460V

$$V_{dco} = (1.35) * 460 = 621V$$

For transient phenomenon, a 10% overvoltage is considered. The r.m.s value of three-phase ac input side voltage will be (506V) and its peak value is

$$V_{Pk} = \sqrt{2} * 506 = 715.484V$$

The ampere rating of the diode and IGBT switch is based on the active component of three-phase ac input side current and is obtained as

$$I_{aca} = \frac{P_{iag}}{\sqrt{3}V_{abcg}(L-L)}$$

Here P_{iag} represents the power rating of an IAG. The active component of three-phase ac input side current of an IAG is evaluated as

$$I_{aca} = \frac{3730}{\sqrt{3} * 460} = 4.68 \text{ A}$$

The 3-phase diode based bridge rectifier fetches a current (quasi-square current) having a distortion factor (DF) of 0.955. The three-phase ac input side current of EGLC may be evaluated as

$$I_{dac} = \frac{I_{aca}}{0.955} = \frac{4.68}{0.955} = 4.9 \text{ A}$$

The crest factor (CF) of the three-phase ac input side current fetched by a diode based bridge rectifier having a capacitive type filter lies from 1.4 to 2.0. Hence, the three-phase ac input side current peak value may be evaluated as

$$I_{Pk} = 2I_{dac} = 2 * 4.9V = 9.8 \text{ A}$$

So, for the diode of the bridge rectifier, the maximum voltage may be 715.484V and peak current may be 9.8A. The commercial available rating of the diode and IGBT switch is 900V and 9.8A. Therefore, rating of the diode and IGBT switch has been selected as 900V and 9.8A

The value of the resistance (R_{dld}) is evaluated as

$$R_{dld} = \frac{(V_{dco})^2}{P_{iag}} = \frac{(621)^2}{3730} = 103.38901\ \Omega$$

The value of the capacitance (C_{dcl}) of the EGLC depends on the value of the ripple factor (RF) and these are related to each other by the following mathematical expression

$$C_{dcl} = \left\{\frac{1}{(12fR_{dld})}\right\}\left\{1 + \frac{1}{(\sqrt{2}RF)}\right\}$$

Considering 5% RF in the average value of output dc side voltage then the capacitance is evaluated as

$$C_{dcl} = \left\{\frac{1}{(12 * 60 * 103.389)}\right\}\left\{1 + \frac{1}{(\sqrt{2} * 0.05)}\right\} = 151.442\mu F$$

Based on the described design procedure the values of various parameters of EGLC unit have been evaluated. The designed data thus obtained is used for the simulation studies under balanced and unbalanced three-phase resistive, reactive and non-linear nature consumer load. The designed and the selected data of the 3-phase EGLC for the 3-phase IAG are provided in Table 2

Table 2: Three-phase EGLC designed parameters

KW rating of motor (W)	Volt rating of the diode (V)	Ampere rating of the diode (I)	Volt rating of the IGBT switch (V)	Ampere rating of the IGBT switch(I)	Rating of Dump load resistance (Ω)	Rating of filtering capacitor (μF)
3730	900V	9.72574A	900V	9.72574A	103	151

5.4 PI BASED CONTROL SCHEME OF EGLC

The control circuit of EGLC consists of a voltage sensor for sensing the 3-phase IAG voltage, a comparator circuit for comparing the sensed 3-phase IAG voltage with the set a.c voltage (treated as reference voltage) and a discrete PI controller. This difference of 3-phase IAG voltage and the set a.c voltage is treated as an input to the PI controller. The PI controller output is now compared with a saw tooth waveform of frequency 1 kHz to generate the driving signal for the IGBT switch. The driving signal of varying duty cycle is obtained with the aid of discrete PI controller.

5.5 SIMULATED RESULTS AND ITS INTERPRETATION

All the simulations have been carried out in MATLAB software package on a 3730 W Squirrel cage Asynchronous motor furnishing different types of static loads [Appendix D].

A 3-phase EGLC for a 3-phase IAG is designed. From the design data, volt and ampere rating of the diode rectifier bridge and IGBT switch is selected to be 900

V and 9.7 A. The value of R_{dld} and C_{dcl} are selected to 103 Ω and 151 μF for the simulation study under balanced three –phase resistive consumer load. A 3-phase Y-connected asynchronous machine (AM) of 3.73 kW, 460 V, 60 Hz, 4 poles is used as IAG [Appendix D]. The IAG is driven by a prime-mover (dc machine). Initially the IAG is simulated without any kind of load and EGLC to generate peak voltage at no load with the aid of delta connected capacitor bank.

5.5.1 Performance Assessment of IAG Subjected to 3-Phase Balanced/Unbalanced Resistive Consumer (unity power factor) load without any controller

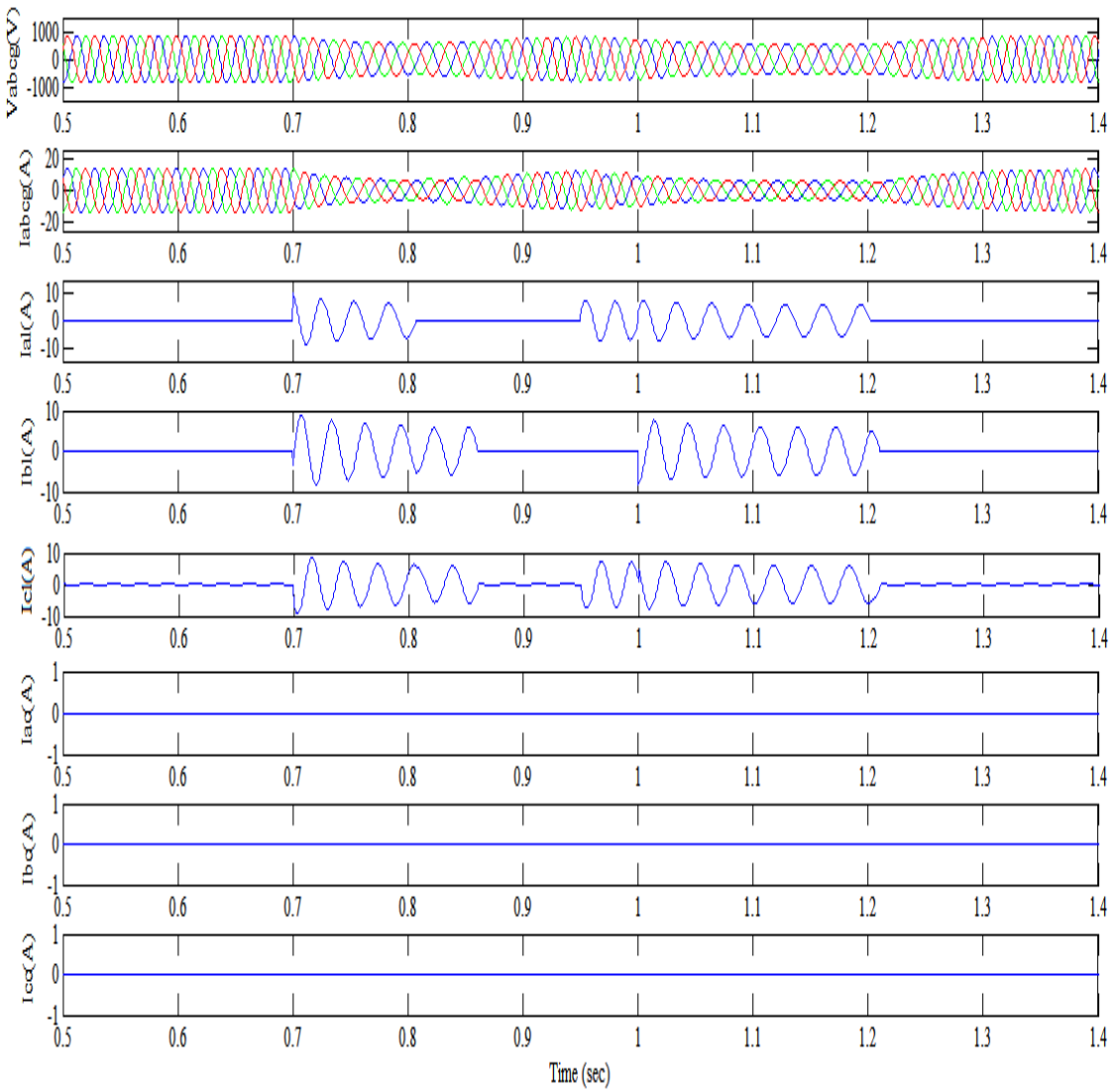

Fig. 5.2 Performance characteristics of IAG without controller with IAG voltage (V_{abcg}), IAG currents (I_{abcg}), resistive load currents (I_{al}, I_{bl}, I_{cl}) and EGLC currents (I_{ac}, I_{bc}, I_{cc})

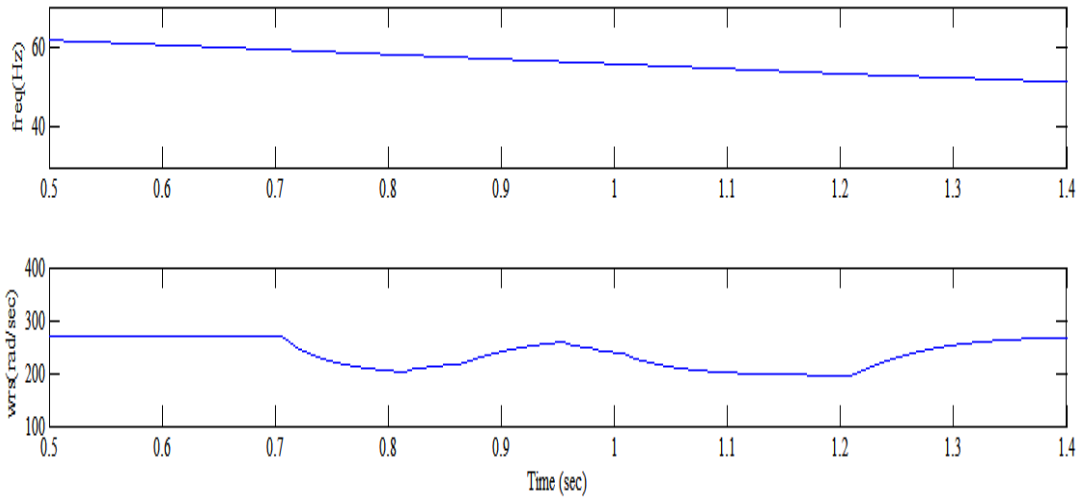

Fig. 5.3 Performance characteristics of IAG without any controller with frequency and speed

Fig. 5.2 shows the various transient performance characteristics of IAG voltages (V_{abcg}), IAG currents (I_{abcg}), resistive load currents (I_{al}, I_{bl}, I_{cl}) and EGLC currents (I_{ac}, I_{bc}, I_{cc}).

It is inferred from the simulated outcomes shown in Fig. 5.2 and Fig. 5.3 that when a 3-phase balanced/unbalanced load is inserted in the circuit from 0.7-1.2 sec, the generator voltage and its frequency drop. Hence, the need of some controller is realised which can support both IAG voltage and its frequency under varying load.

5.5.2 Performance Assessment of IAG-EGLC System Subjected to no load 3-Phase Balanced/Unbalanced Resistive Consumer (unity power factor) Load

Fig. 5.4 shows the various transient performance characteristics of IAG voltages (V_{abcg}), IAG currents (I_{abcg}), resistive load currents (I_{al}, I_{bl}, I_{cl}) and EGLC currents (I_{ac}, I_{bc}, I_{cc}).

It is visualised that IAG is subjected to the operating conditions of load (balanced as well as unbalanced) ranging from 0.7 to 1.2 sec. It is also visualised that prior to 0.7 sec, the whole of the generated power of IAG is delivered to the EGLC.

It is observed from the simulated results depicted in Fig. 5.4 that when the three-phase balanced resistive full-load is introduced in the system from operating time 0.7-0.8 sec, the consumers load rises and the EGLC load declines almost to zero

value. It signifies that power is delivered from three-phase EGLC to the balanced three-phase consumer load. Thus IAG feels constant load on it. Hence EGLC supports IAG voltage and its frequency.

It is also observed that when IAG is subjected to unbalanced resistive load from operating time 0.85-1 sec with the removal OFF of one phase at 0.8 sec. Under these operating conditions, consumer load current declines and the EGLC currents rises. It signifies that power is delivered from unbalanced consumer load to the three-phase EGLC. Hence the EGLC maintains constant load on the IAG and hence is able

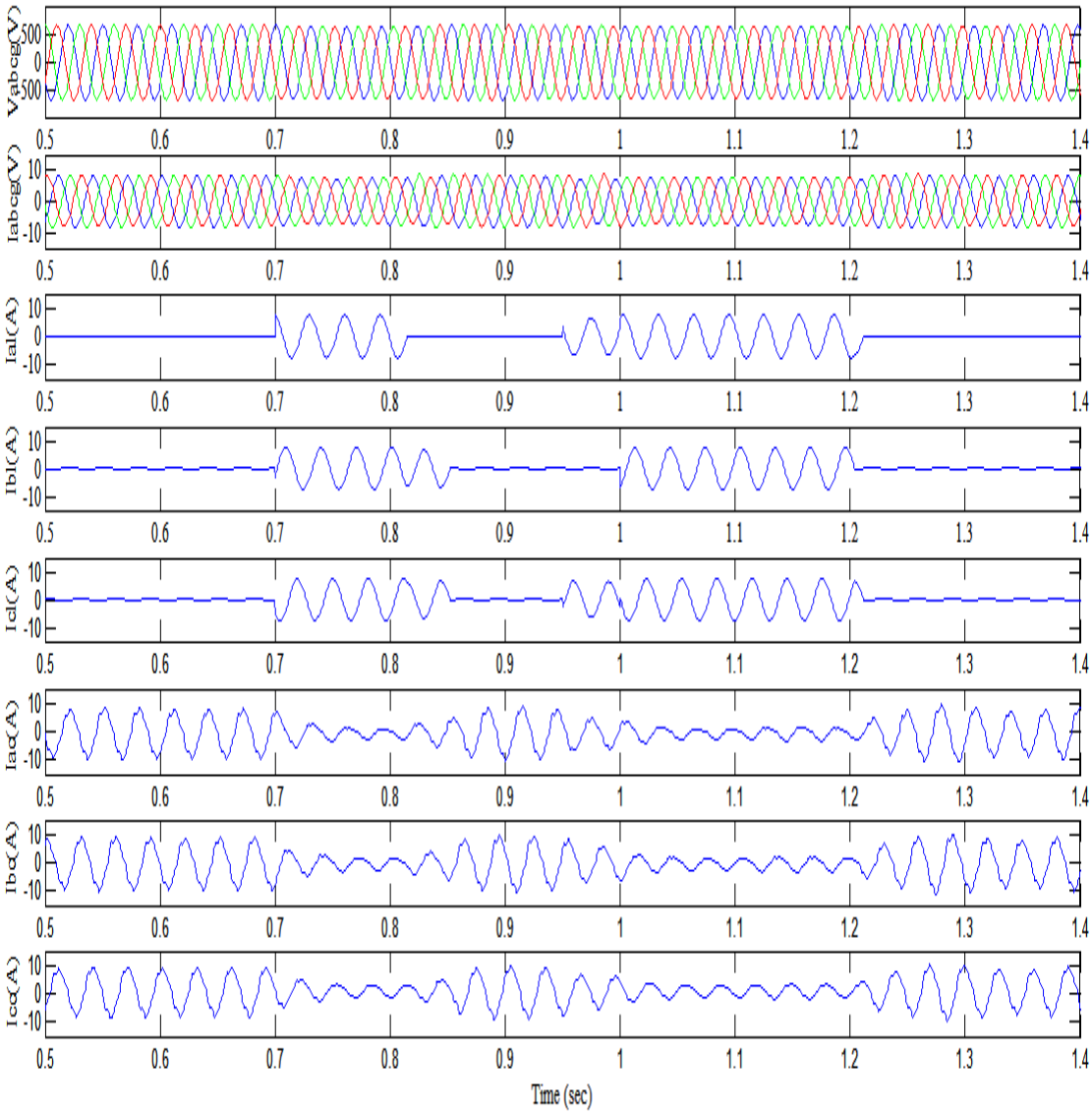

Fig. 5.4 PI controller based performance characteristics of IAG-EGLC system subjected to resistive load with IAG voltage (V_{abcg}), IAG currents (I_{abcg}), load currents (I_{al}, I_{bl}, I_{cl}) and EGLC currents (I_{ac}, I_{bc}, I_{cc})

to support generator voltage and its frequency. The load on the IAG is once again balanced from 1-1.2 sec by reconnecting the phases of load. With the removal OFF the complete three-phase balanced resistive consumer load at 1.2 sec, load current becomes zero and EGLC current increase which signifies that power is delivered from consumer load to EGLC.

Hence, it is inferred from the simulated outcomes that the generator voltage, current, frequency, speed and power are supported by the IAG over the entire operating range of varying load (balanced as well as unbalanced) as illustrated in Fig. 5.4 and Fig. 5.5.

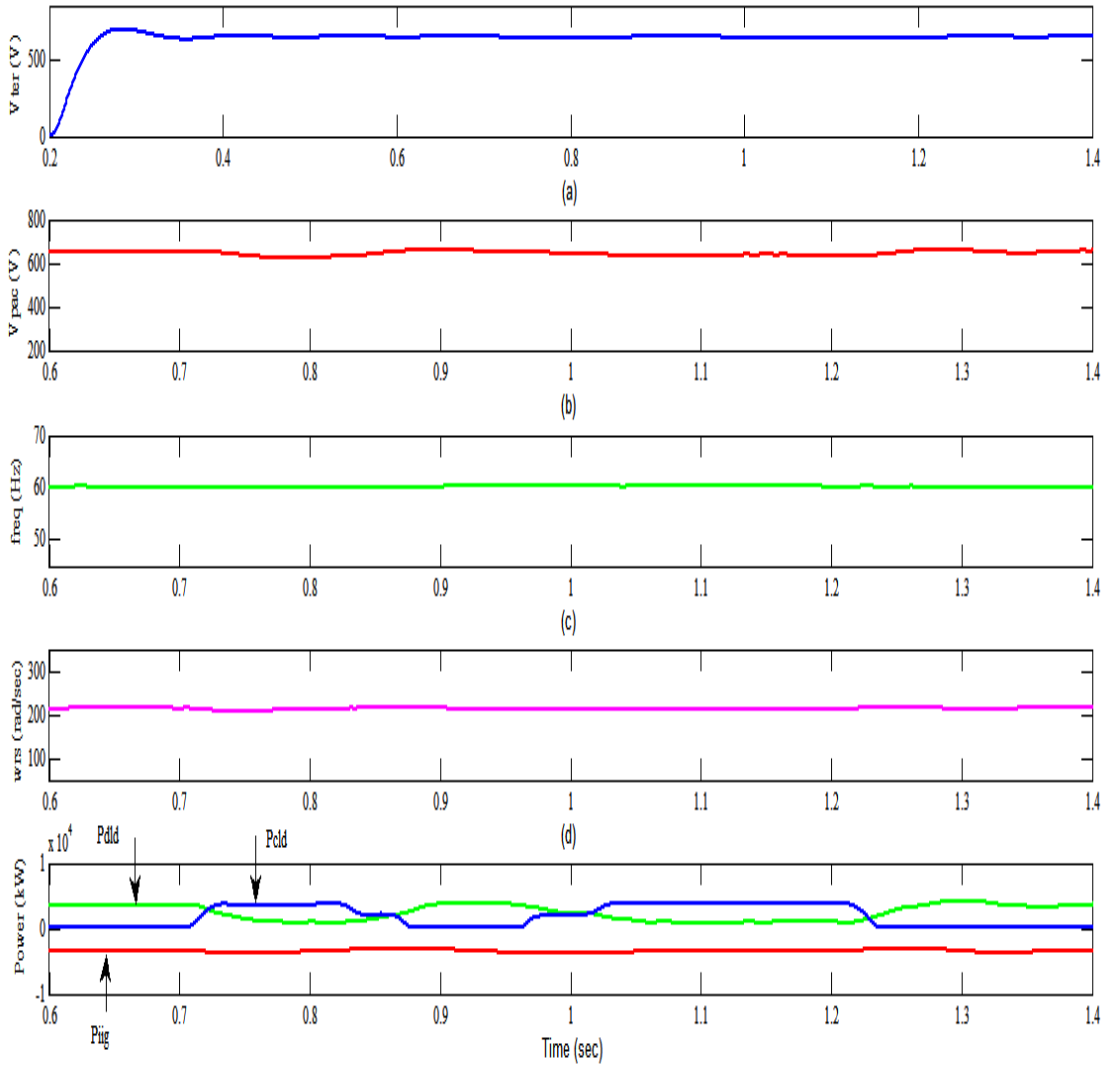

Fig. 5.5 PI controller based performance characteristics of IAG-EGLC system subjected to resistive load using the IAG ac voltage magnitude (V_{ter}) , its peak ac voltage (V_{pac}), its frequency (freq), its speed (w_{rs}), IAG power (P_{iag}), consumer power (P_{cld}) and dump power (P_{dld}) .

5.5.3 Performance Assessment of IAG-EGLC System Subjected to 3-Phase Balanced/Unbalanced Reactive Consumer (lagging power factor) Load

Fig. 5.6 shows the various transient performance characteristics of IAG voltages (V_{abcg}), IAG currents (I_{abcg}), reactive load currents (I_{al}, I_{bl}, I_{cl}) and EGLC currents (I_{ac}, I_{bc}, I_{cc}).

The IAG-EGLC system is initially started without any kind of load on the system**.** The whole of the IAG load acts on the EGLC. This is depicted by the whole of the current flowing or passing through the EGLC and current flowing through the load is zero. A 3-phase reactive balanced load is

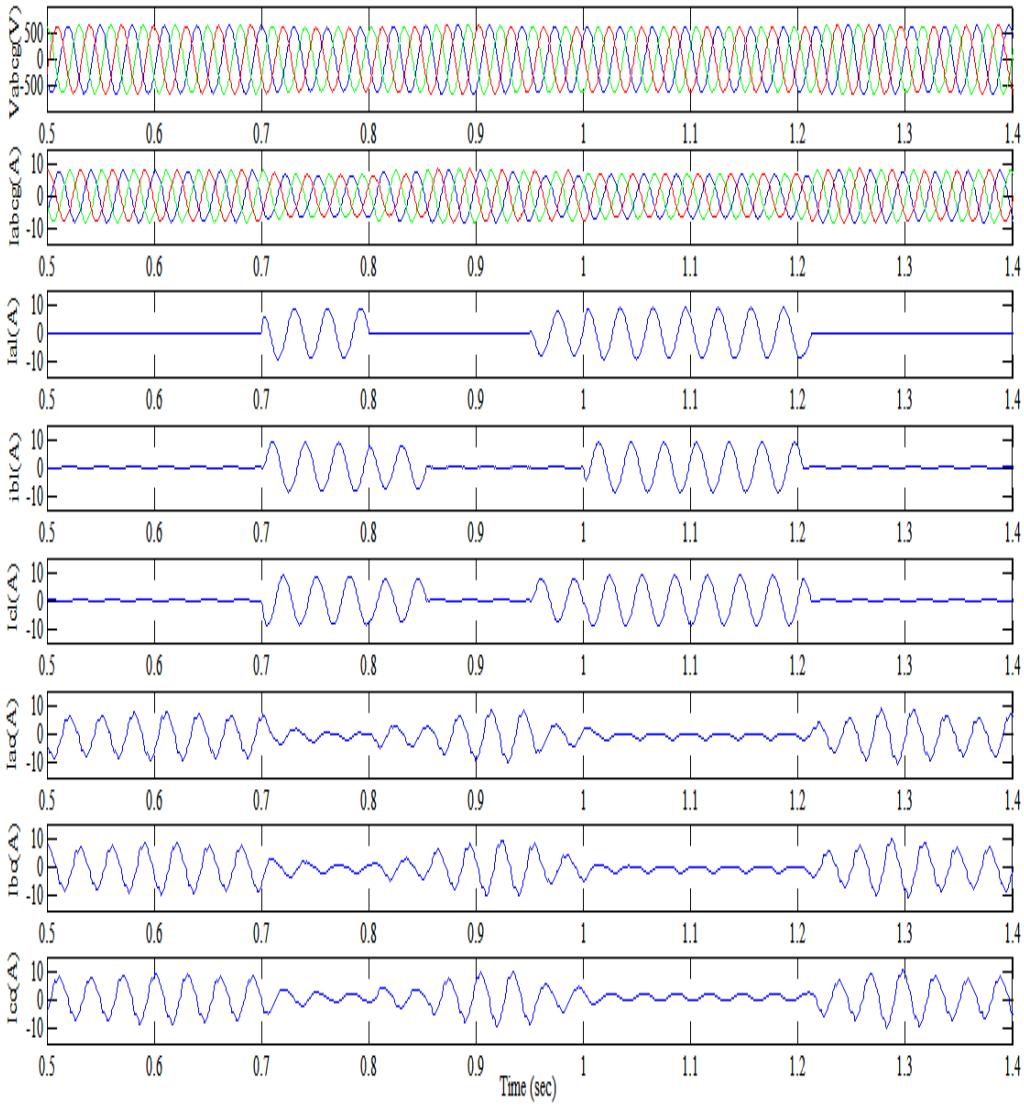

Fig. 5.6 PI controller based pperformance characteristics of IAG-EGLC system subjected to pure reactive load with IAG voltage (V_{abcg}), IAG currents (I_{abcg}), load currents (I_{al}, I_{bl}, I_{cl}) and EGLC currents (I_{ac}, I_{bc}, I_{cc}).

introduced in the circuit at the operating time range from 0.7-0.8 sec. This is indicated by rise in load currents and drop in EGLC currents and now the difference of the generated and the load current starts passing through the EGLC to just balance the IAG system.

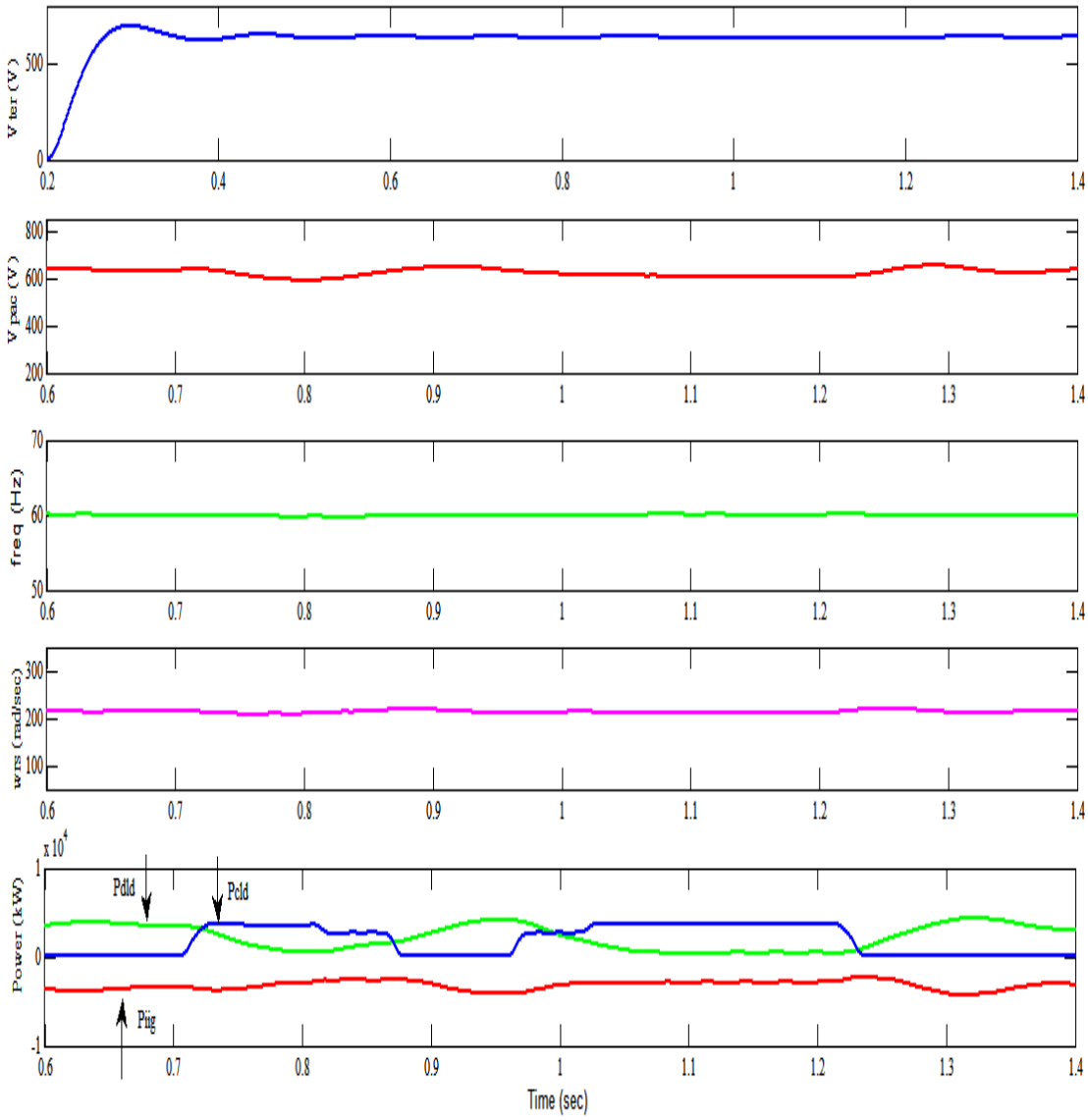

Fig. 5.7 PI controller based performance characteristics of IAG-EGLC system furnishing pure reactive load with the IAG ac voltage magnitude (V_{ter}) , its peak ac voltage (V_{pac}), its frequency (freq), its speed (w_{rs}), IAG power (P_{iag}), consumer power (P_{cld}) and dump power (P_{dld}).

Hence the EGLC maintains constant load on the IAG and hence is able to support generator voltage and its frequency as illustrated in Fig. 5.6 and Fig. 5.7. During the unbalanced operating condition from 0.8-1 sec the EGLC current rises to balance the IAG system. During balanced operating condition from 1-1.2 sec, the load

current rises and the EGLC current declines to almost zero value to balance the IAG system. Hence, it is concluded that during the complete operating condition of load from 0.7-1.2 sec, the EGLC maintains constant load even when IAG is subjected to varying reactive load and hence supports IAG voltage and its frequency.

Hence, it is inferred from the simulated outcomes that the generator voltage, current, frequency, speed and power are supported by the IAG over the entire operating range of varying load (balanced as well as unbalanced) as illustrated in Fig. 5.6 and Fig. 5.7.

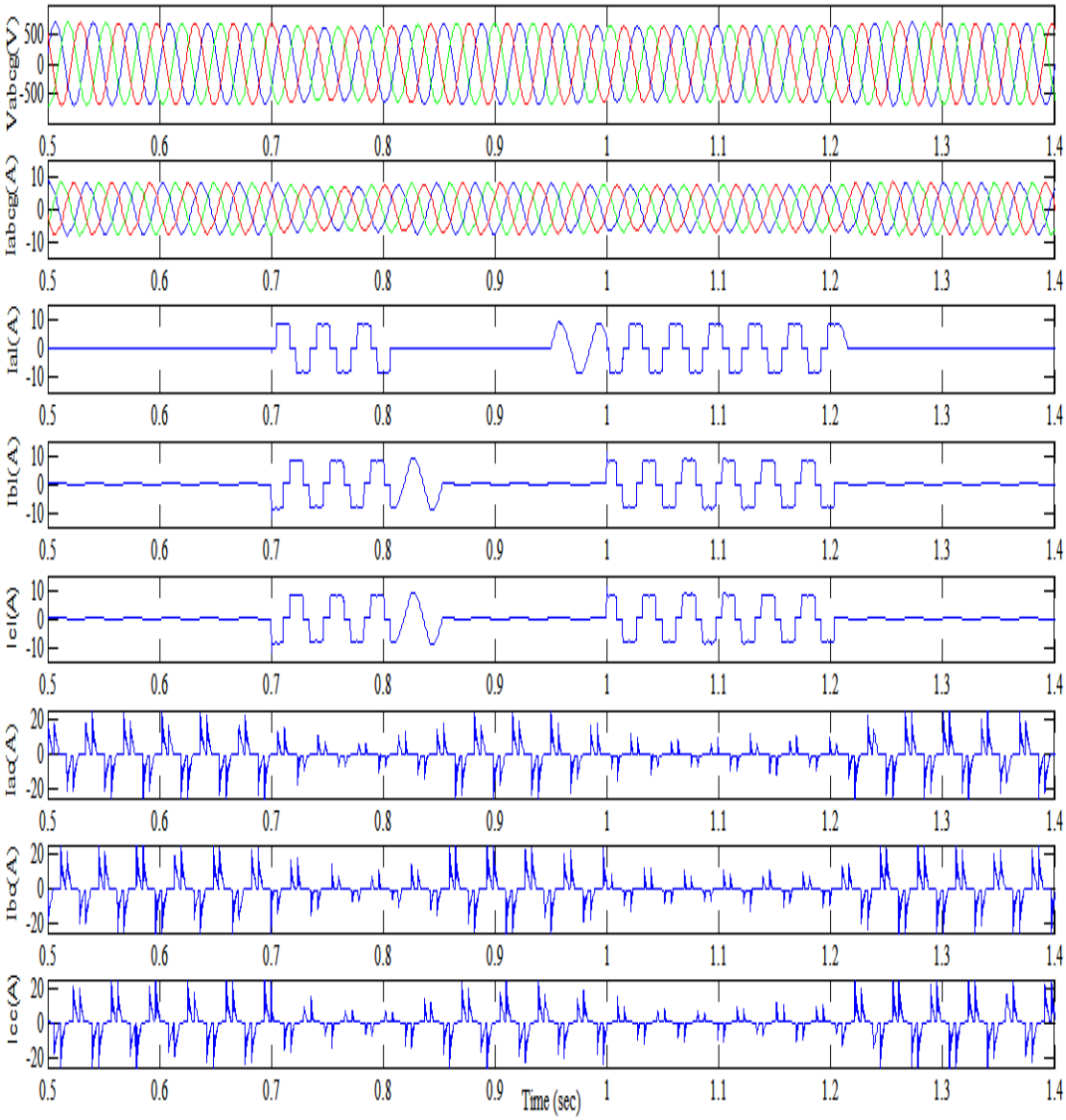

Fig. 5.8 PI controller based pperformance characteristics of IAG-EGLC system furnishing non-linear load with IAG voltage (V_{abcg}), IAG currents (I_{abcg}), load currents (I_{al}, I_{bl}, I_{cl}) and EGLC currents (I_{ac}, I_{bc}, I_{cc})

5.5.4 Performance Assessment of IAG-EGLC System Subjected to 3-Phase Balanced/Unbalanced Non-linear Load

It is visualised that the generator voltage and current are pure sinusoidal and free from harmonics. It means that the proposed controller eliminates the harmonics from generator voltage and current and makes the whole system healthy. The speed of the IAG is constant throughout the whole operating period of balanced/unbalanced load which shows that the EGLC is providing support to IAG voltage, its frequency and power depicted in Fig. 5.8 and Fig. 5.9.

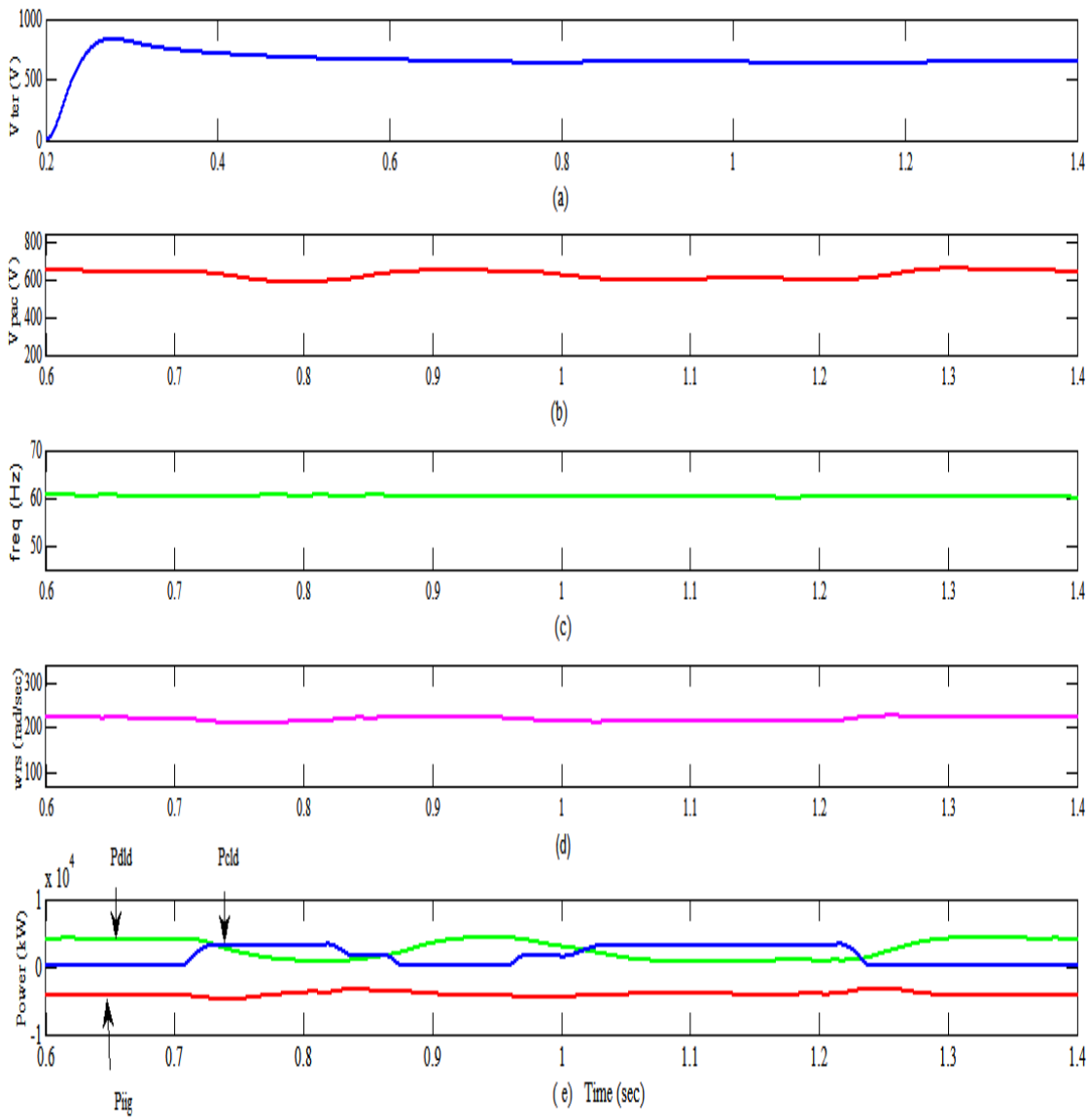

Fig. 5.9 PI controller based performance characteristics of IAG-EGLC system furnishing non-linear load with the IAG ac voltage magnitude (V_{ter}) , its peak ac voltage (V_{pac}), its frequency (freq), its speed (w_{rs}), IAG power (P_{iag}), consumer power (P_{cld}) and dump power (P_{dld}).

5.6 SUMMARY

From the simulated results, it has been concluded that the developed EGLC supports both voltage and frequency of IAG when subjected to varying balanced/unbalanced consumer (resistive/reactive/non-linear load). An EGLC controller has been designed and developed in MATLAB/SIMULINK for the three-phase IAG. Based on the designed procedure described in this chapter, volt and ampere rating of the diode bridge rectifier and IGBT switch, value of resistance R_{dld} and capacitance C_{dcl} of the 3-phase EGLC for the three-phase IAG can be estimated for electrical power generation in far-flung off-grid sites.

CHAPTER 6

DETAILS OF FUZZY LOGIC CONTROLLER (FLC)

6.1 GENERAL

Fuzzy means the things that are not logical or clear or are vague. Any process or event or function that is ever changing or keeps on changing cannot be defined or specified appropriately in terms of true or false type situation. These things are defined or specified more appropriately in terms of fuzzy logic. The concept of fuzzy logic was first explored by Lotfi A. Zadeh in 1965 in his research paper entitled “fuzzy set”. He is contemplated as the father of fuzzy logic (FL). It is a kind of mathematical tool that handles uncertainty, vague or imprecise data based problems associated with the real life. The FL approach can be tested and validated using hardware set-up, software package or using both. It outputs a definite conclusion after processing imprecise, noisy, ambiguous, vague or incomplete data at its input side.

6.2 DIFFERENCE BETWEEN CONVENTIONAL AND FL BASED CONTROL METHODS

FL operates on rule based system of If X and Y then Z approach to solve control problems rather than modeling a system mathematically. It is an empirical approach that totally works on an operators experience rather than the technical knowhow of the system. It basically resembles or mimics the human behavior decision making aspect at a faster rate. E.g. temperature control of steam in a boiler is formulated as “BT=600F”, “T<1100F” or 200C<TEMP<210C. Then using the FL the same temperature problem can be formulated in terms like IF (process steam is too cold) AND (process steam is getting colder) THEN (add some heat to the process) or IF (process steam is too hot) AND (process steam is heating rapidly) THEN (cool the process steam slowly).Though the terms used here are imprecise or vague but yet provide the complete description of the process that must actually takes place or happens.

6.3 SALIENT FEATURES OF FUZZY LOGIC (FL)

The distinguishing features of fuzzy logic controllers are described below:

1. Inherent robustness is the chief advantage of FLas it does not need any precise or accurate or noise free data to process it and yields smooth output with varying inputs.
2. The FL controller operates according to rules defined by the operator based on human experience and yields the controlled and smooth output. To attain performance enhancement these user formulated rules can be tweaked and modified easily. More sensors can be added to the existing system simply by generating or formulating new rules governing the output.
3. FL controllers are not restricted to only feedback sensed inputs and control outputs. Moreover it is not necessary to evaluate the rate of change of various parameters in terms of error i.e. temp error, voltage (ac or dc) error etc for its implementation. Any data sensed by the sensor in terms of system action and reaction is sufficient enough for its implementation. It concludes that some that some inexpensive and imprecise sensors are required and hence reduces the system complexity and the overall system cost.
4. As FL controllers operates on rule-based criteria, so any number of inputs (1 to 8 or more) can be processed to generate or produce any number of output (1 to 4 or more). In case of more number of inputs and outputs, the rule-base of the system adds complexibility. In this case it is preferable to break the whole control system into small sub parts. Then these small sub parts of the control system collectively operate the system but now with limited tasks or responsibility than whole control system.
5. FL controllers can effectively handle the system having non-linearity or non-linear control systems as the mathematical modeling of such systems is difficult to accomplish or sometimes difficult to formulate such systems using the concept of mathematics.

6.4 FUZZIFICATION PROCESS

It is a well known fact that the input to a fuzzy inference system (FIS) must be fuzzy input or linguistic variable input. These linguistic values are normally represented by the degree of the membership in the fuzzy set. The method of converting the measured numerical quantities (crisp value) into linguistic variables (fuzzy value) is known as fuzzification. During fuzzification, different types of membership functions can be used and the degree of membership is also evaluated.

6.5 MEMBERSHIP FUNCTION DETAILS

The concept of membership function was first explored by Lofti A. Zadeti in 1965 in his first research paper entitled “fuzzy sets”. Membership function signifies fuzziness regardless of the nature of elements in fuzzy set whether continuous or discrete. The membership function can be depicted graphically also. The rules defining fuzziness graphically are also fuzzy in nature. The membership function represents the level of truth or certainty in fuzzy logic. But there are certain standard forms of MF that are used and maintained universally over years. Membership function (MF) is defined as a graph depicting the variation of input against the membership value of 0 to 1. The three basic characteristics or features of MF are depicted in Fig.6.1 and are described as under:

CORE: It is defined as the region of MF having value 1 e.g. for any fuzzy set $\widetilde{B}$, the core of MF is that part or region of universe that belongs to whole membership of the fuzzy set. Hence, the core include all the elements of y of the universe of information such that

$$\mu_{\tilde{B}}(x) = 1$$

SUPPORT: The support of MF is defined as the region having value greater than 0. e.g for any fuzzy set $\tilde{B}$, the support of MF is that part or region of universe that belongs to non zero membership of the fuzzy set. Hence, the support include all the elements of y of the universe of information such that

$$\mu_{\tilde{B}}(x) > 0$$

BOUNDARY: The boundary of the MF is defined as the region having value between 0 and 1. For example, for a fuzzy set $\tilde{B}$, the boundary of MF is that part or region of universe that belongs to non zero but incomplete membership in fuzzy set $\tilde{B}$. Hence, the support include all the elements of y of the universe of information such that

$$1 > \mu_{\tilde{B}}(x) > 0$$

6.6 OVERVIEW OF FUZZY INFERENCE SYSTEM (FIS) [115]

It basically includes fuzzy rule based system, fuzzy expert system and fuzzy models etc. It is basically the key point or it plays the key role in fuzzy logic system.

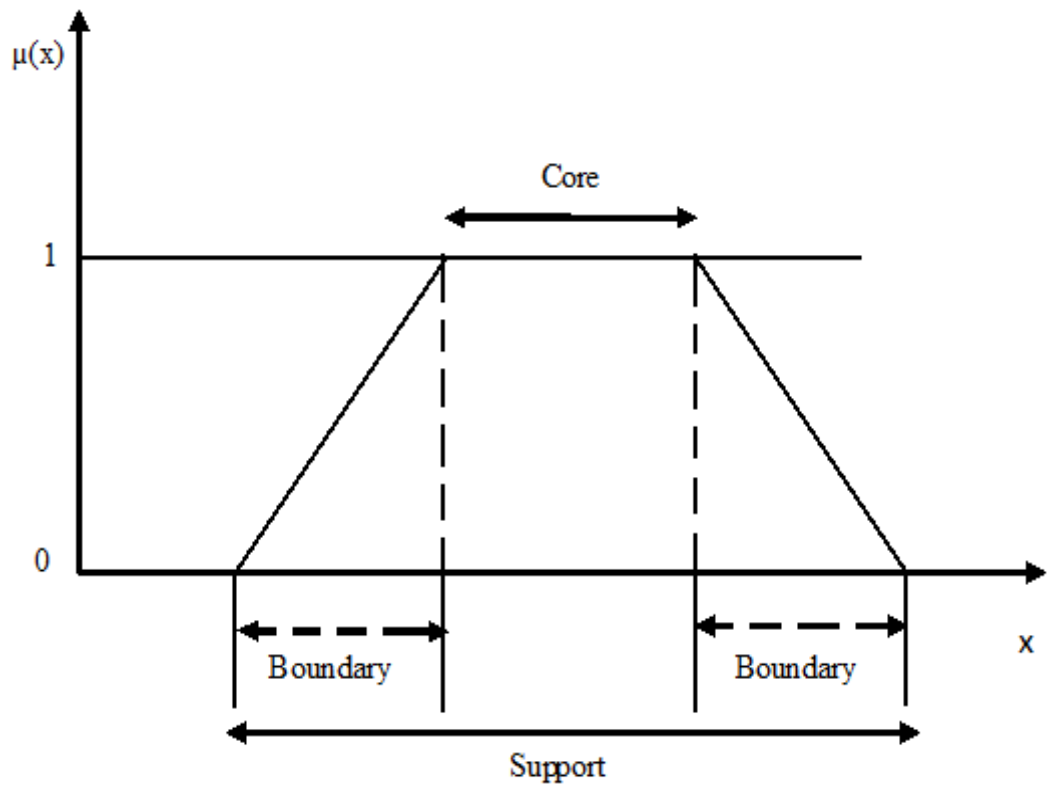

Fig. 6.1 Representation of features of membership function (core, support and boundaries)

It primarily provides the decision making FIS basically works on 'IF-----THEN' rules using "OR" or "AND" as connectors for providing necessary decision rules. The fuzzy set or crisp set may be applied as the input to the FIS but its output always results into a fuzzy set. Whenever this FIS is operating like a controller then it is essential to have crisp set output only. Hence there is felt a need of defuzzification unit for the purpose of converting the fuzzy set variables into crisp set variables.

6.6.1 Schematic Diagram and Working Principle of FIS

The block diagram representation of FIS is depicted in Fig. 6.2.

It consists of the following blocks:

1. A rule base: It basically comprises of various IF----THEN statement based fuzzy rules.
2. A data base: It basically defines the MFs of fuzzy set.
3. Decision making unit (DMU): It basically provides the decision and accordingly executes the operation on the rules.

4. Fuzzification interface unit (FIU): This unit basically converts the crisp input quantities into fuzzy quantities.
5. Defuzzification interface unit (DIU): This unit basically helps in converting the fuzzy quantities back into crisp quantities

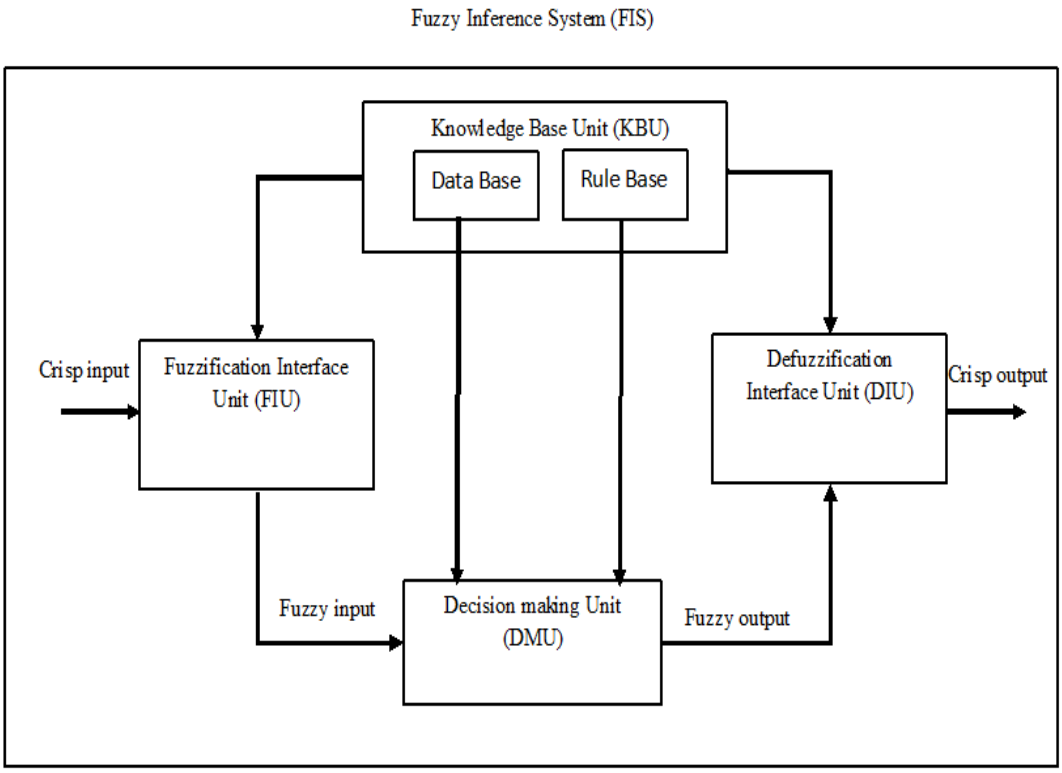

Fig. 6.2 Schematic diagram of FIS structure

6.6.2 Different Types of FIS

FIS are basically of two types i.e. Mamdani type FIS and Sugeno type or TSK type FIS. These two types of FIS differ only in the consequent part of the fuzzy rules. In Mamadani type FIS, basically fuzzy sets are treated as rule consequences whereas in TSK type FIS, linear functions of the input variables are treated as or taken as rule consequents. Mamdani type FIS are widely applicable and acceptable in all universal approximations than TSK type FIS.

6.3.3 Mamdani Type FIS

This system was proposed by E. Mamdani in the year 1975. The proposed system emerges or is based from the formulation of fuzzy rules obtained from a system consisting of steam engine and boiler unit. In such systems, the output MF are desired

to be fuzzy set. Each output variable after aggregation process results into a fuzzy set. Hence the need of defuzzification unit is realized at the output side. The step-wise procedure to compute or evaluate output is discussed below:

STEP-1: Create a set of fuzzy rules using IF – THEN statement using AND/OR connectors.

STEP-II: Select input membership functions (MFs) to make all the inputs of FIS system fuzzy.

STEP-III: Combine all the fuzzified inputs (T-norms) based on fuzzy rules to evaluate the rule strength. Here fuzzy "and" is used to combine all the fuzzified inputs to establish rule strength

STEP-IV: Combining the rule strength and the output MFs to determine the consequent part of the fuzzy rule. The consequent part of the fuzzy rule can be evaluated by two methods:

- Firstly by combining the rule strength completely using fuzzified inputs.
- Secondly by clipping the output membership function (MF) distribution obtained.

STEP-V: Next combine all the consequent part of the fuzzy rules to get a fuzzy output distribution. Here fuzzy "or" is used to obtain the fuzzy output distribution.

STEP-VI: Lastly a defuzzified output (a crisp output) distribution is obtained (if crisp output is required otherwise skip step VI).

A two fuzzy input and two rule based Mamdani type FIS depicted in fig.6.3. In fig minimum operation is preferred for evaluating the rule strength and then the output MF is treamed at this evaluated value of rule strength. Finally the output is evaluated using maximum operator.

The two types of defuzzification techniques are:

CENTRE OF MASS: This technique helps in finding the centre of mass of the output distribution to find one crisp value for the output. The centre of mass is evaluated as

$$z = \frac{\sum_{j=1}^{q} z_j u_c(z_j)}{\sum_{j=1}^{q} u_c(z_j)}$$

Here z is the centre of mass and u_c is the membership in class c at value z_j.

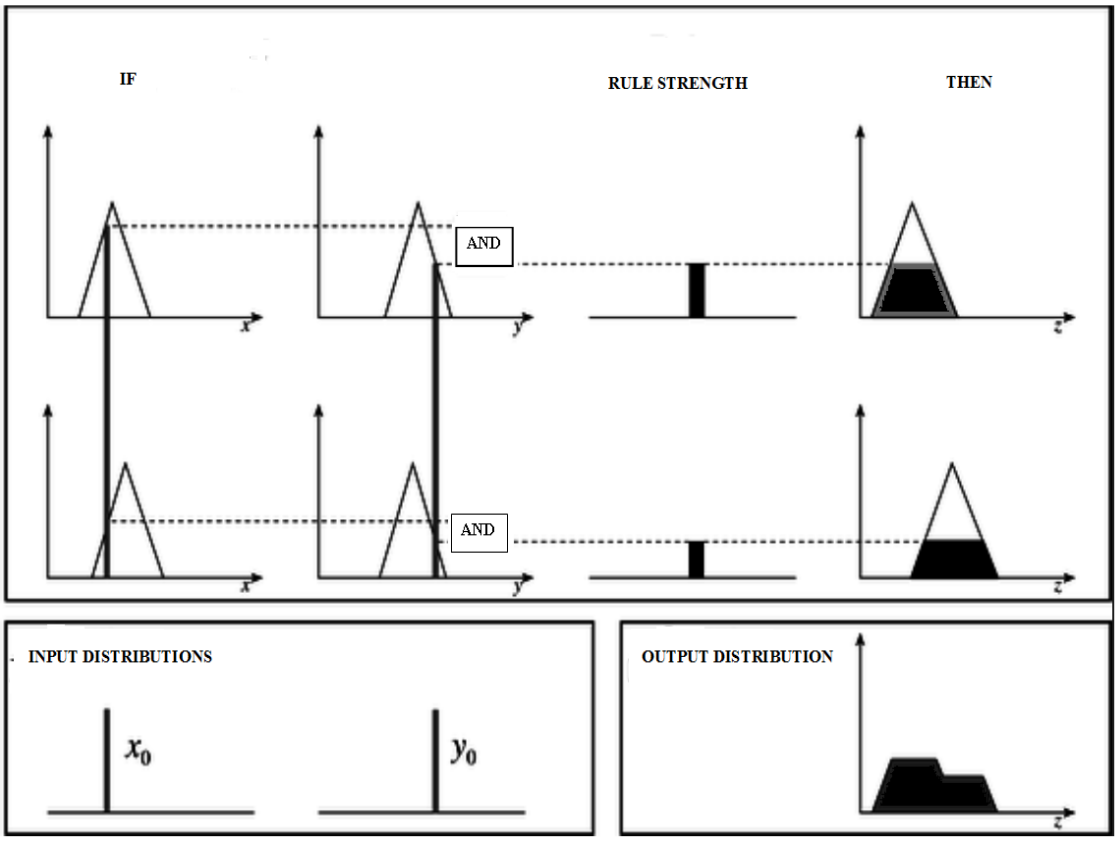

Fig. 6.3 Mamdani type FIS with two fuzzy inputs and two rules

MEAN OF MAXIMUM: This technique helps in finding the mean of maxima of the output distribution to find one crisp value of the output. The mean of maximum is evaluated as:

$$z = \sum_{j=1}^{l} \frac{z_j}{l}$$

Here z is the mean of maximum, z_j is the point at which MF is maximum and l is the number of times the output distribution reaches the maximum level.

6.6.4 Takagi-Sugeno and Kang Type FIS (TSK Type FIS)

This method was recommended in 1985 by Takagi-Sugeno and Kang. The format representation of the fuzzy rule of a TSK type FIS is given by

IF x is A and y is B THEN z=f(x, y)

Here A and B are fuzzy sets in the antecedents and z=f(x, y) is a crisp function in the consequent. Generally f(x, y) represents the polynomial relating with input variables x and y. If f(x, y) represents the first degree order polynomial, then z represents first degree order Sugeno fuzzy type model or TSK type model.

$$z=bx + cy + d$$

If f represents a constant, then z represents zero degree order TSK type model. A zero degree order sugeno fuzzy type model or TSK type model is considered equivalent to a network based on radial function subjected to certain minor constraints e.g.

$$z=bx + cy + d \ (b = c = 0)$$

This can be considered as a special case of Mamdani type FIS in which each rule consequent is represented by a fuzzy singleton.

If input 1= x and Input 2=y, then the firing strength of the rule w_i using AND as connectors is evaluated as

$$w_i = \text{And Method}(F_1(x)F_2(y))$$

Here $F_1(x)$ and $F_2(y)$ represent the membership function for inputs 1 and 2.

The overall output of the system is given by the weighted average of all rule outputs and is evaluated as

$$\text{Final output} = \frac{\sum_{i=1}^{n} w_i z_i}{\sum_{i=1}^{n} w_i}$$

Here n is the number of rules and z represents output level

The step-wise procedure to compute or evaluate output is discussed below:

STEP-I: Fuzzifying the inputs

STEP-II: Applying the fuzzy operator

The implementation of step-1 and step-II are exactly same. The major difference between the Mamdani and Sugeno type FIS is that in case of Sugeno type FIS the output MFs are functions are either constant or linear.

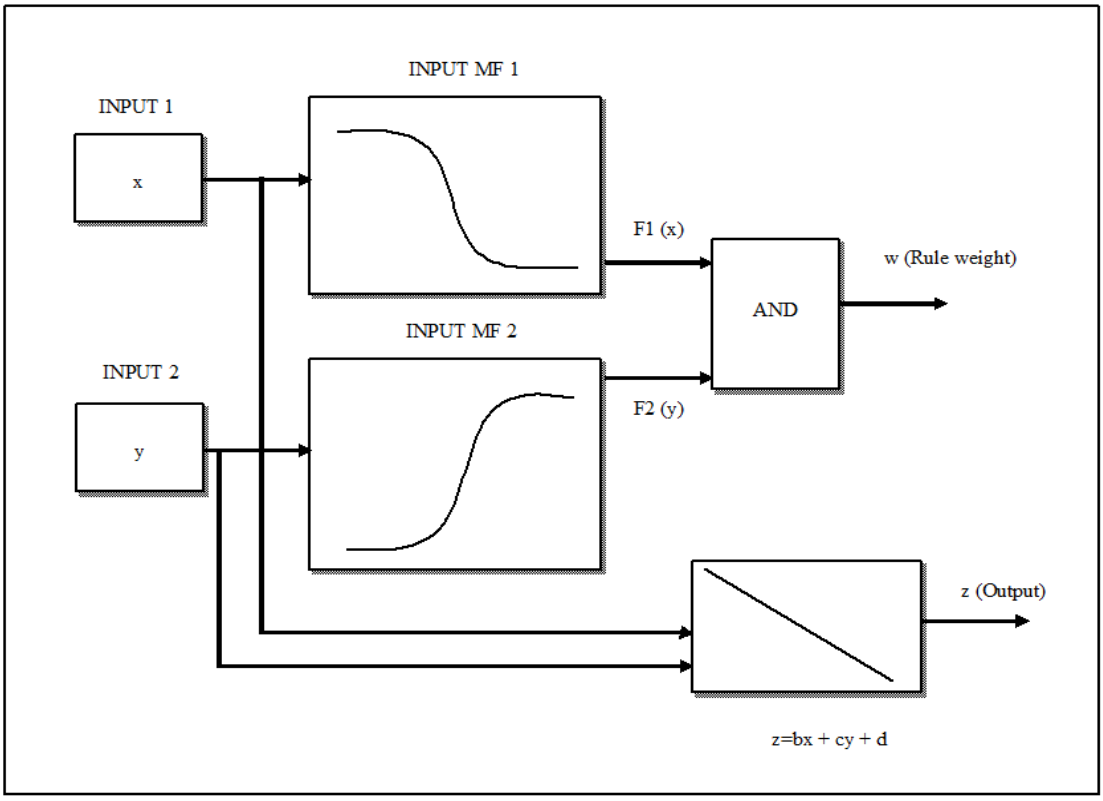

Fig. 6.4 Sugeno type FIS Rule for a first order model

In Fig. 6.4 each rule has a numerical or crisp output and the overall system output is obtained by weighted average of all rules outputs and thus eliminates the diffuzification process as is required in Mamdani type FIS.

6.7 COMPARISON BETWEEN MAMDANI AND SUGENO TYPE FIS

The comparison made between the two FIS techniques is discussed below:

1. The major difference between the Mamdani and Sugeno type FIS is related with the type of output membership function. In Sugeno type FIS, the output membership function are either constant or linear.

2. The two types of FIS have different consequent part of the fuzzy rule and hence their aggregation and defuzzification techniques are different.
3. In case of non-triangular or non-trapezoidal membership functions or fuzzy inputs, the configuration of Sugeno type FIS is smaller than Mamdani type FIS.
4. The Sugeno type controllers have more adjustable parameters in the consequent part of the fuzzy rule and the number of these adjustable parameters increases exponentially with increase in number of input variables.
5. The Sugeno type controllers work more efficiently with the various mathematical techniques i.e. linear techniques, optimization techniques and adaptive techniques.
6. Construction and implementation of Mamdani type FIS is much easier than Sugeno type FIS.

6.8 ADVANTAGES OF MAMDANI TYPE FIS

1. It has globally and widely accepted.
2. It is well suited for mimicking the human behavior.
3. It is intuitive in nature

6.9 ADVANTAGES OF SUGENO TYPE FIS

1. It is proven to be computationally efficient and fast.It is compact in size because of reduced configuration and works efficiently with various mathematical techniques i.e. linear techniques (PID control), adaptive techniques and optimization techniques. The adaptive technique helps in customize the membership function according to ones need and hence it helps the fuzzy system to model the data in a better way.
2. It is preferred for carrying out mathematical analysis.
3. It has guaranteed or ensured continuity of output surface.

6.10 SUMMARY

In the real life situation, we normally deal with imprecise, vague or uncertain and incomplete data. This data when processed through conventional PI controllers does not provide controlled and smooth output. The fuzzy logic makes use of this data and after processing through FLC controllers provides requisite, smooth and controlled

output. FL is basically a logic that handles uncertainty and system non linearity with ease without any complexibility. It proves quite efficient when it is not possible to model any system or lacks of technical knowhow. This chapter emphasis on the implementation aspects of two types of FIS i.e. Mamadani and Sugeno type FIS for the performance enhancement of the system. It is observed that Mamdani type FIS is globally acceptable whereas the Sugeno type FIS works efficiently with linear, optimization and adaptive techniques.

CHAPTER 7

TRADITIONAL PI AND FL BASED ELECTRONIC GENERATOR LOAD CONTROLLER (EGLC) FOR AN ISOLATED ASYNCHRONOUS GENERATOR (IAG)

7.1 GENERAL

Distributed or ON-site power generation has proven to be more reliable and economical in recent years than the OFF-site generation due to its cost, complexity of national grid system, reduced reliability and transmission losses. Thus, a distributed power generation system is an alternative or an enhancement of the existing traditional electric power system. Thus a suitable and feasible independent isolated system using regionally obtainable energy sources like small hydro, wind, biomass become a preferred option. As these energy sources systems are attainable in far-off areas they must be reliable, sturdy, cost effective and manageable by regional communities. The unskilled community must handle the complete system comprises of prime mover, ac generator and its related controller. The Isolated Asynchronous Generator (IAG) is the most preferred and suitable option due to single excitation, cost effective, simple construction, ruggedness, brushless rotor, requires little or no maintenance, self-protection under short-circuit conditions and its off-the shelf availability. Due to the latest research on non conventional energy sources and grid OFF systems, the IAG becomes one of the most important and favored renewable sources of energy [55-60, 63, 64, 67, 68, 70, 73, 74, 75-88]. For power rating below 100kW, uncontrolled turbines driving IAG are recommended. These turbines keep the hydropower potential constant and hence solicit the IAG output power to be retain constant at different operating conditions of consumer loads. This necessitates, an EGLC where a complementary nature load is connected in shunt or across the consumer load so that the total active power consumed is retain constant.

Various types of voltage and frequency controllers (VFC's) for IAG have been developed and are reported in literature along-with its advantages and disadvantages [60, 63, 64, 67, 68, 70, 73-74, 76-88]. The IAG can be used for constant power applications and for variable power applications. In constant power applications, prime mover rotational speed, value of excitation capacitor and the consumer load are kept constant and thus known as a single point operation. For variable power

applications, rotation of the prime mover is kept fixed but the value of excitation capacitance increases with load. For constant power application, generated power and consumer output power must be fixed for stable operation of three-phase IAG. Input power is maintained constant with the help of uncontrolled pico-hydro turbine but power output may not be constant due to varying consumer load. Most of the VFC's reported in literature employed traditional PI type controllers because of their simple design. The major drawback was in attaining the optimal performance. But, today different types of intelligent controllers are grabbing the attention of researcher [87-88]. Fuzzy logic based Mamdani type approach is discussed and implemented in this chapter because such controller can handle non-linearity, noisy signals and also do not require mathematical model of the system. In this chapter, first time an initiative is taken to adjudge the performance of an IAG using both PI and FL based controller to support both voltage and frequency under balanced and unbalanced load operating conditions.

7.2 OVERVIEW ABOUT SIMULATION MODEL OF THE GENERATING UNIT AND THE CONTROLLER

The complete diagram of the three-phase EGLC-IAG system is depicted in Fig.7.1. The whole system is a build by integrating various elements: Asynchronous machine (AM), delta connected capacitor bank, three-phase load and EGLC. First, a delta connected capacitor bank is connected across the stator terminals of the machine to generate the rated voltage at no load then the asynchronous machine is run above the synchronous speed of the motor with the help dc machine. The EGLC consists of various components: six-pulse diode bridge rectifier, an IGBT type high frequency (1 kHz) operated chopper switch, a filtering capacitor (C), a complementary load resistance (R_{dld}). The diode based bridge rectifier provides dc output voltage. The output dc voltage has the distortion, which should be filtered and therefore a capacitor filter is used to smoothen the dc output voltage. An IGBT type high frequency chopper switch provides the variable dc voltage across the R_{dld}. Initially the consumer load and the EGLC are kept OFF and the IAG is self-excited at no-load. After successful voltage build-up of 650 V, the EGLC consumes the whole of the generated power. When both the consumer load and the chopper is switched ON, the current flows through the R_{dld} and consumes the difference between the generated power and consumer load power and thus result in a constant load on the IAG and hence constant

voltage and frequency at the balanced/unbalanced consumer load. Thus the IAG retains the power balance in the system.

For the proper operation of IAG, the suitable value of capacitors is connected to generate rated voltage at desired power [60, 63, 64, 67, 68, 70, 73-74, 76-88].The input power of the IAG is held constant at varying consumer loads. Thus, IAG supplies power to both the consumer load and R_{dld} in shunt. When one load is consuming more power than the other load will be consuming less power so that the total power is constant. It means that both loads are complementary in nature. The power balance for an IAG is attained using EGLC. The dump load power of EGLC may be used for various types of lighting loads, low power applications in remote off grid areas.

In this way, power generated by IAG is utilised in a better and efficient way. Thus, makes the whole generating system more efficient and reliable.

7.3 CONTROL TECHNIQUES

7.3.1 Design of Traditional PI Controller

The control circuit of EGLC is based upon calculation of the magnitude of the three-phase terminal ac voltage of IAG given by

$$V_{ter} = \left\{\frac{2}{3}\left(V_{as}^2 + V_{bs}^2 + V_{cs}^2\right)\right\}^{\frac{1}{2}} \tag{7.2}$$

This voltage is then compared with the ac reference voltage of 650V. The output of this comparator is the error voltage and its expression is given by

$$V_{eac} = V_{terf} - V_{ter} \tag{7.3}$$

This error in ac voltage is then processed through a discrete PI controller. The output of the PI controller is given by

$$I_{(x)} = I_{(x-1)} + K_{pac}\left\{V_{eac(x)} - V_{eac(x-1)}\right\} + K_{iac}V_{eac(x)} \tag{7.4}$$

Where V_{eac} signifies the error in terminal ac voltage in (5.3) and $I_{(x)}$ signifies the output control signal at the xth time. $I_{(x-1)}$ signify the output control signal at the $(x-1)^{th}$ time. K_{pac} and K_{iac} are the proportional and integral gains of the discrete PI controller. The output of the PI controller is now compared with the saw tooth type

high frequency waveform (1 kHz) to generate Pulse width modulated gate driving signal of varying duty cycle for the chopper switch illustrated in Fig.7.1 and Fig. 7.2. The optimised or properly tuned values of K_{pac} and K_{iac} are 32.4 and 1.24 to obtain better performance under both steady and transient conditions.

7.3.2 Design of FL Approach Based Controller

In order to obtain better results pertaining to performance, the PI controller is replaced by a fuzzy logic controller block. In this chapter, Mamdani type FL a.c terminal voltage controller is developed and illustrated in Fig.7.3. The FL approach based controller consists of four processes or stages: fuzzification process, rule base, fuzzy interface link and defuzzification process. The fuzzification process is required for the conversion numerical input variable to a linguistic variable. The fuzzy interface link consists of simple input-output relationship. Input data is managed by FI link to produce output data using Mamdani type fuzzy interface algorithim. The defuzzification process converts the fuzzy set output into a crisp value. The centre of area method is used for this process.

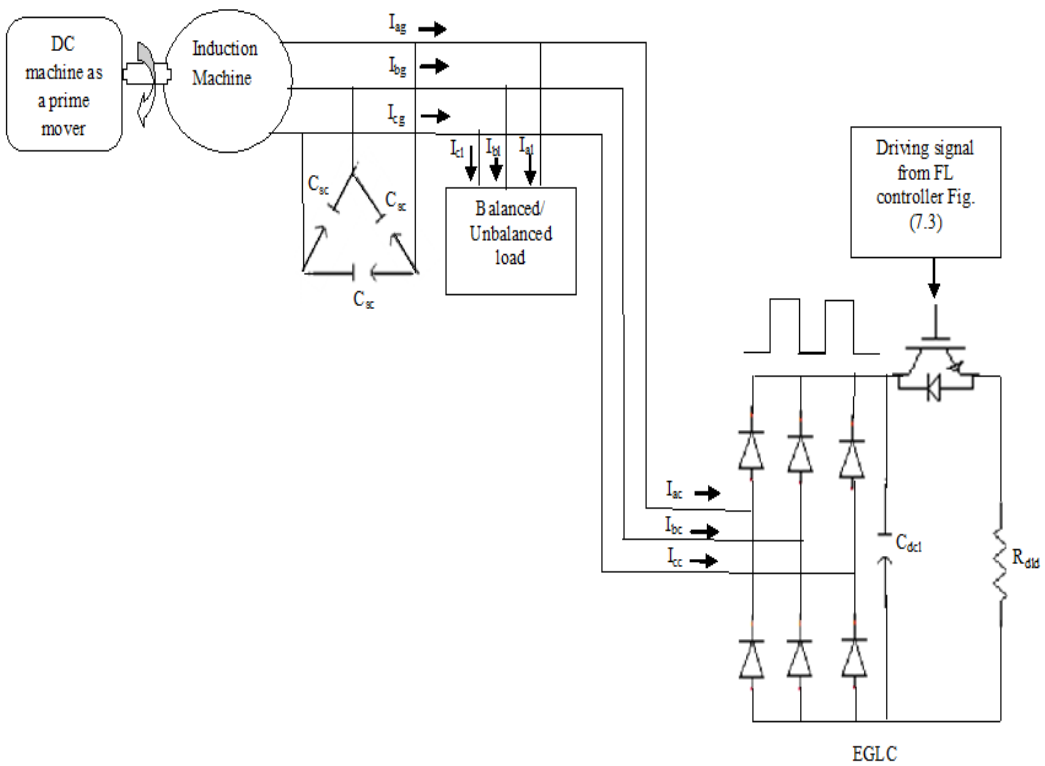

Fig. 7.1 Schematic diagram of IAG with EGLC

In Table.3, LNE, MNE, SNE, ZE, SPO, MPO, LPO are considered as large negative large, medium negative, small negative, zero, small positive, medium positive and large positive. The 49 rules are formed using If – then rules and are given in Table. 3.

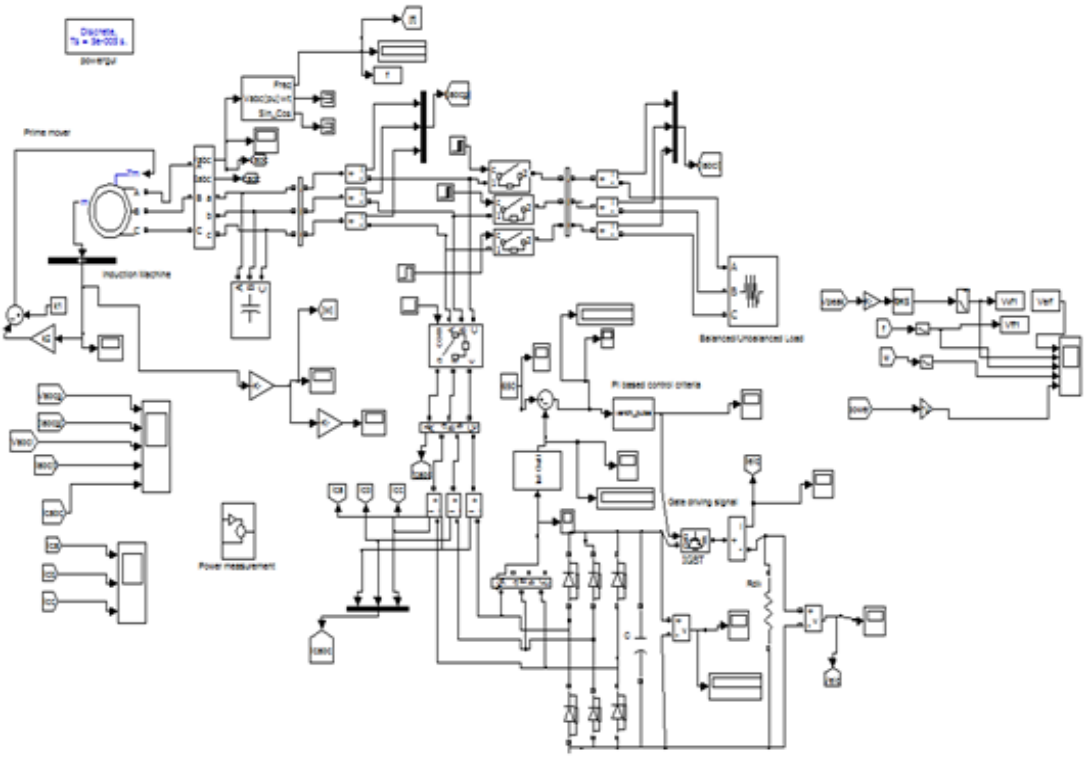

Fig. 7.2 Simulink model of the generating unit along with EGLC for terminal ac voltage (V_{ter}) control using traditional PI

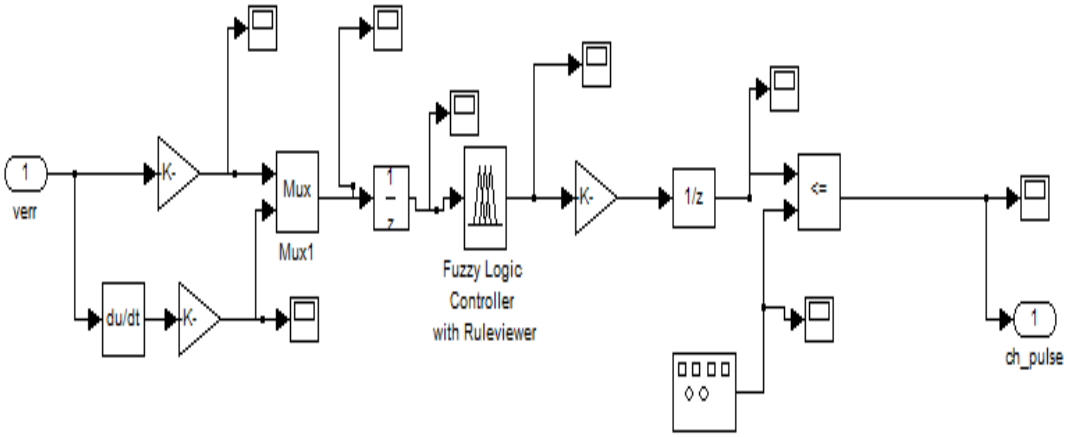

Fig. 7.3 Magnitude of terminal ac voltage (V_{ter}) control using FL based criteria

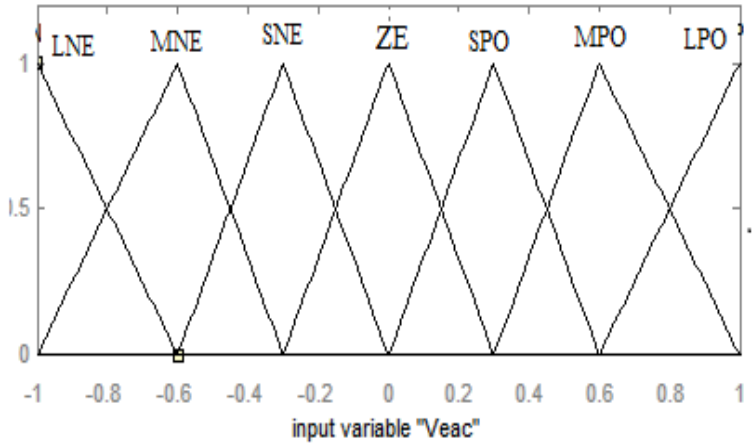

(a)

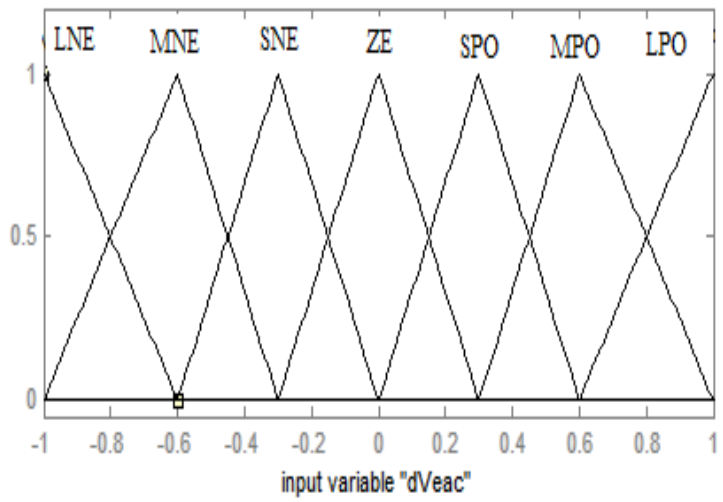

(b)

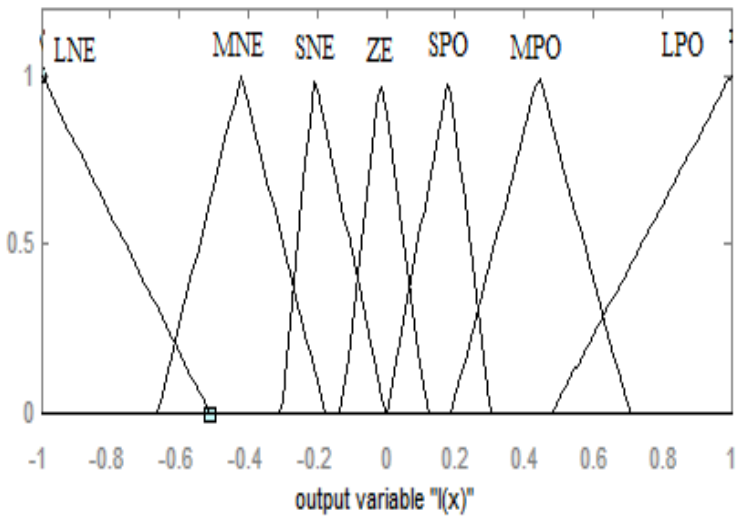

(c)

Fig. 7.4 Triangular membership function for inputs and output

Table 3: Rules defining relationship between inputs and output

V_{eac} / dV_{eac}	LNE	MNE	SNE	ZE	SPO	MPO	LPO
LNE	LNE	LNE	MNE	SPO	SPO	MPO	MPO
MNE	LNE	MNE	MNE	SPO	SPO	MPO	MPO
SNE	MNE	MNE	SNE	MPO	SPO	ZE	MPO
ZE	MNE	MNE	SNE	MPO	SPO	MPO	LPO
SPO	MNE	SNE	ZE	MPO	MPO	MPO	LPO
MPO	SNE	SNE	ZE	MPO	MPO	SPO	LPO
LPO	SNE	SNE	ZE	MPO	MPO	SPO	LPO

The variable error voltage V_{eac} and change in error voltage dV_{eac} signifies the inputs of FL approach based controller. The seven triangular membership functions are used for V_{eac}, dV_{eac} and output variable $I_{(x)}$ [Fig. 7.4]. The variation range for the fuzzy variable i.e. V_{eac}, dV_{eac} and $I_{(x)}$ is kept from -1 to 1 only. This needs scaling of both input and output variables within the specified range. Thus, the scaling factors for the variables V_{eac}, dV_{eac} and $I_{(x)}$ are 0.012, 0.001 and 0.29 respectively.

7.4 SIMULATED OUTCOMES OF PI AND FL BASED CONTROLLER

The generating unit along-with EGLC is modelled and tested in MATLAB SIMULINK using Simpower system Blockset [Fig. 7.2]. The system is constituted using various blocks: asynchronous machine block, circuit breakers, three phase load, Universal bridge block, capacitors for creating capacitor bank, IGBT based chopper switch. All the simulations have been carried out on a Squirrel cage asynchronous motor [Appendix E] in stationary reference frame including the effect of saturation. All the simulation testing is performed using discrete mode having sample time (50e-6), Discrete solver mode (Forward Euler), simulation time (2 seconds), relative

tolerance 1e-3), time tolerance (10*128*eps) and ode45 (Stiff/TR-BDF2) solver. A three-phase EGLC for a three-phase IAG is simulated and tested. A three-phase star-connected asynchronous machine is used as IAG. The IAG is driven by a dc machine [Appendix E]. To generate rated voltage i.e. 650 V at no-load, three-phase capacitor bank of appropriate value is connected across the machine stator terminals.

7.4.1 Simulation Based Performance Outcomes of IAG-EGLC System with Three-Phase Balanced/Unbalanced Resistive Load

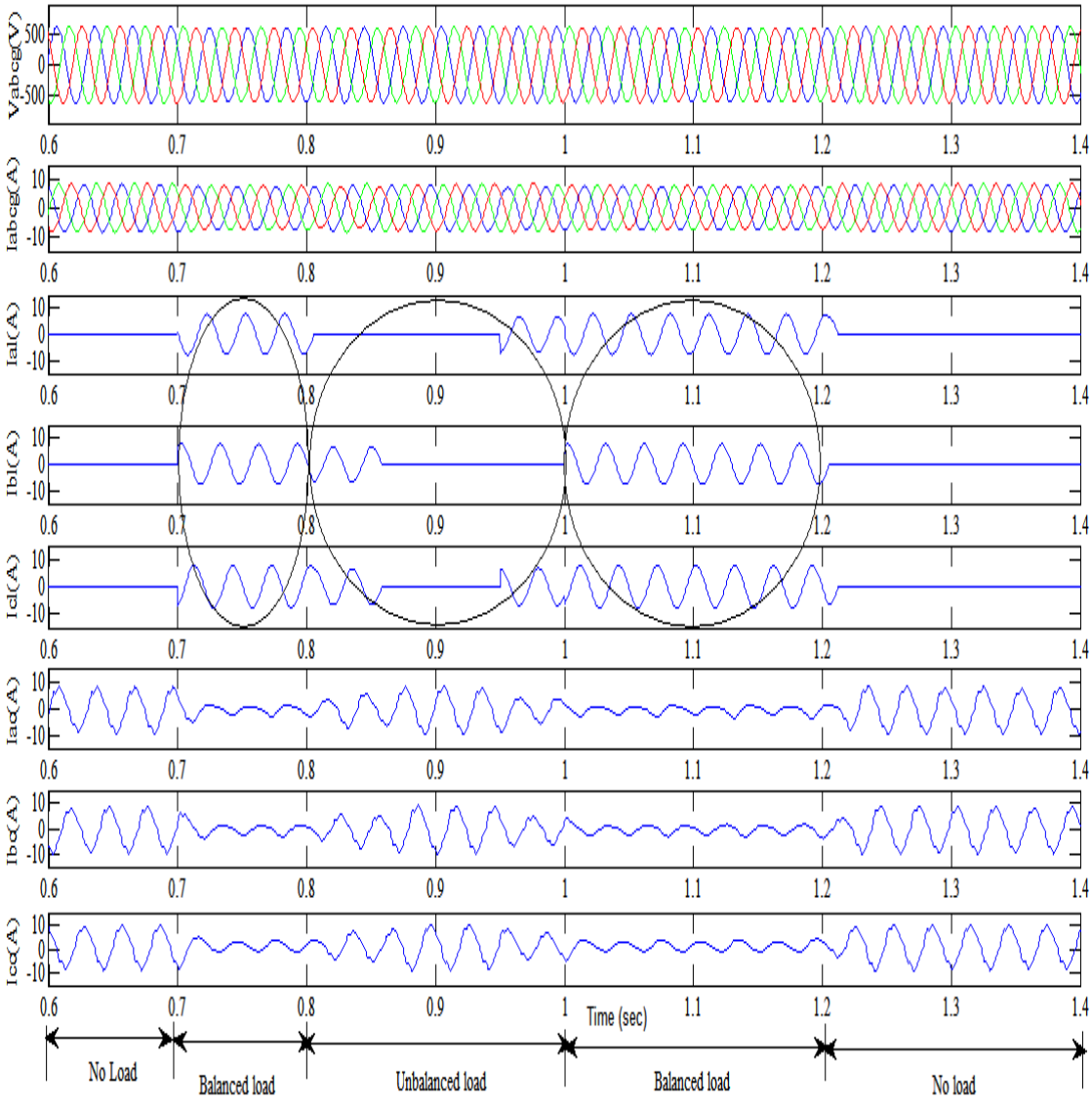

Fig. 7.5 Simulated transient characteristics waveforms of voltage generated by three-phase IAG (V_{abcg}), three-phase IAG currents (I_{abcg}), per-phase resistive load currents (I_{al}, I_{bl}, I_{cl}), per-phase EGLC currents (I_{ca}, I_{cb}, I_{cc}) under balanced and unbalanced resistive load using FL controller.

Fig. 7.5 indicates the FL controller based transient performance characteristics of three-phase IAG voltage (V_{abcg}), three-phase IAG currents (I_{abcg}), per-phase resistive load currents (I_{al}, I_{bl}, I_{cl}), per-phase EGLC currents (I_{ac}, I_{bc}, I_{cc}) furnishing R load .

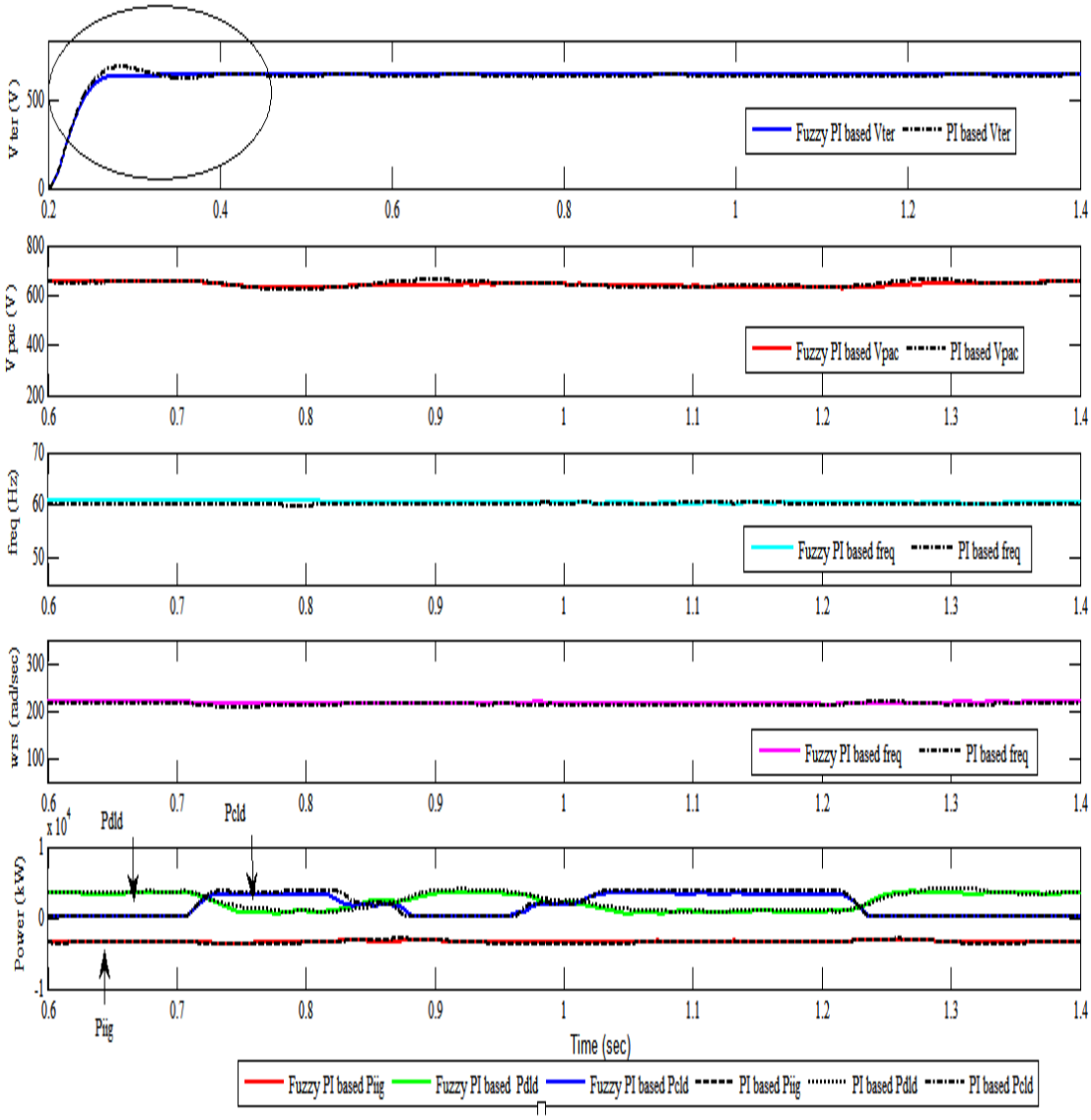

Fig. 7.6 Comparison of the simulated results of magnitude of terminal ac voltage (V_{ter}) , peak value of generated ac voltage (V_{pac}), frequency (freq) , rotational speed (w_{rs}), power generated by IAG (P_{iig}), consumer load power (P_{cld}) and dump load power (P_{dld}) for pure resistive load using both PI and FL.

A 3-phase balanced resistive full load is inserted between phase to phase from 0.7 sec to 0.8 sec. During this time interval, the load currents raises and the EGLC currents die down to zero value [Fig. 7.6]. Hence, during this period power is

conveyed from EGLC to IAG. The unbalanced load condition is created by separating one phase at 0.8 sec and another phase at 0.85 sec. The unbalanced load duration

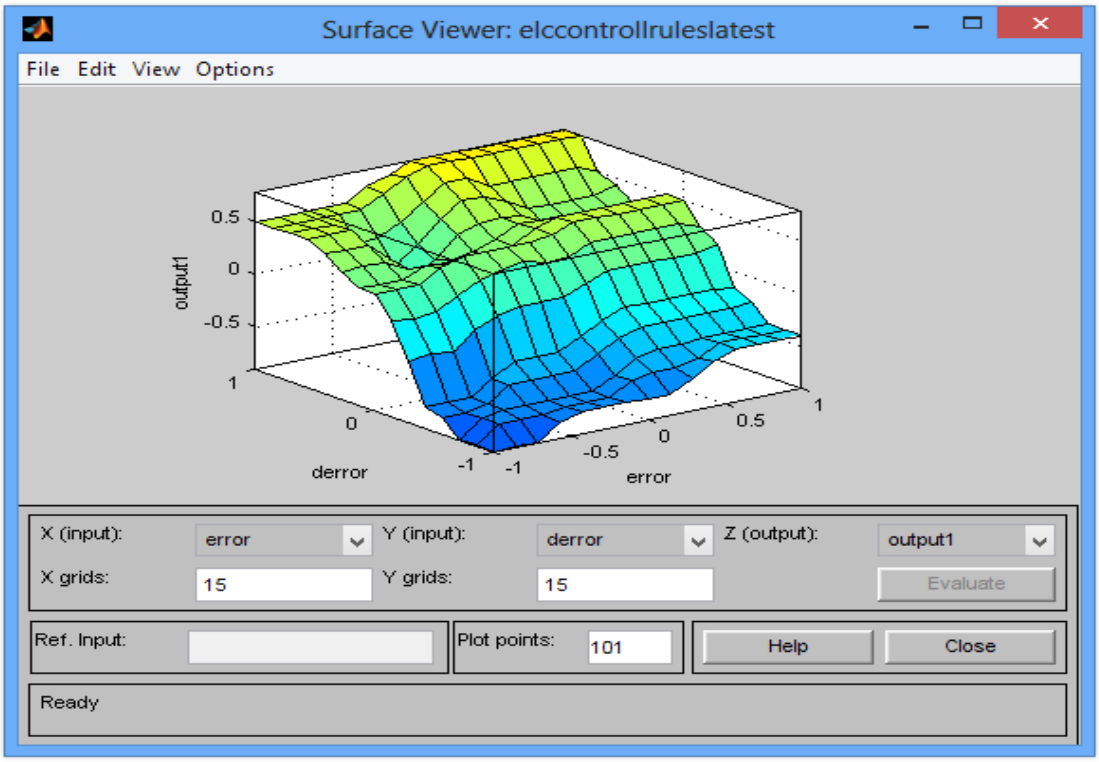

Fig. 7.7 Surface viewer window of Mamdani type FIS file for resistive load.

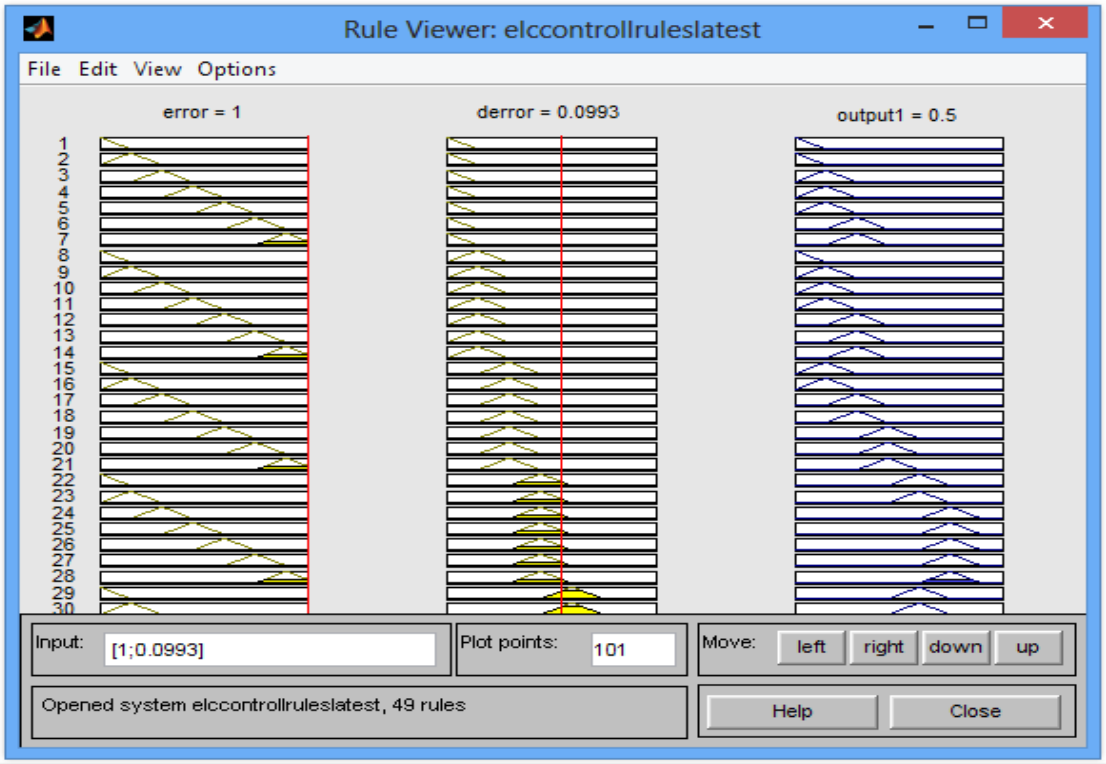

Fig. 7.8 Rule viewer window of Mamdani type FIS file for resistive load

ranges from 0.8-1sec.Throughout, the aforementioned range, the load currents decreases and EGLC currents increase. Hence, the power is conveyed from load to EGLC. The balanced load condition is again achieved by reinserting one phase at 0.9 sec and the other at 1 sec. Thus, from time range 1-1.2 sec load is balanced and load currents raises but during this aforementioned range, the EGLC currents die down to zero.

Hence, during this period power is again conveyed from EGLC to IAG. It is clearly noticed here that the power is conveyed from EGLC to IAG under balanced conditions and from IAG to EGLC during unbalanced load conditions so that IAG power remains constant. Hence voltage, frequency and power of IAG are supported by EGLC under both balanced and unbalanced load conditions. Moreover, the voltage is perfectly sinusoidal under balanced and unbalanced conditions [Fig. 7.5 and Fig. 7.6].

Fig. 7.6 also indicates the comparison of simulated results of amplitude of terminal ac voltage V_{ter}, the peak value of generated ac voltage V_{pac}, frequency (freq), speed (w_{rs}), IAG power, consumer load power and dump load power due to both PI and FL controllers. It is clearly visualized from the results outcomes; the response of ac voltage V_{ter} is notably faster in FL in comparison to traditional PI. Moreover, at the time of load insertion and separation there is smooth and fine control in case FL in comparison to traditional PI.

The performance relating to rise time, settling time and overshoot are considerably lower in FL than PI controller as mentioned in Table 4. Also, the performance relating to THD values of IAG voltage and current are considerably lower in FL than PI controller as mentioned in Table 5. The surface viewer and rule viewer window of Mamdani type FIS for resistive load is illustrated in Fig. 7.7 and Fig. 7.8.

7.4.2 Simulation Based Performance Outcomes of IAG-EGLC System with Three-Phase Balanced and Unbalanced Reactive Load

Fig. 7.9 indicates the FL controller based transient performance characteristics of three-phase IAG supplying 0.8 p.f lagging R-L load. The 3-phase reactive balanced load is incorporated through circuit breakers to the generator terminals at 0.7 sec. This

results in rise in load currents and drop in EGLC currents to balance the IAG system. With the separation of one phase at 0.8 sec and another phase of load at 0.85 sec, the load becomes unbalanced and hence EGLC currents of two phases increase for balancing the IAG system.

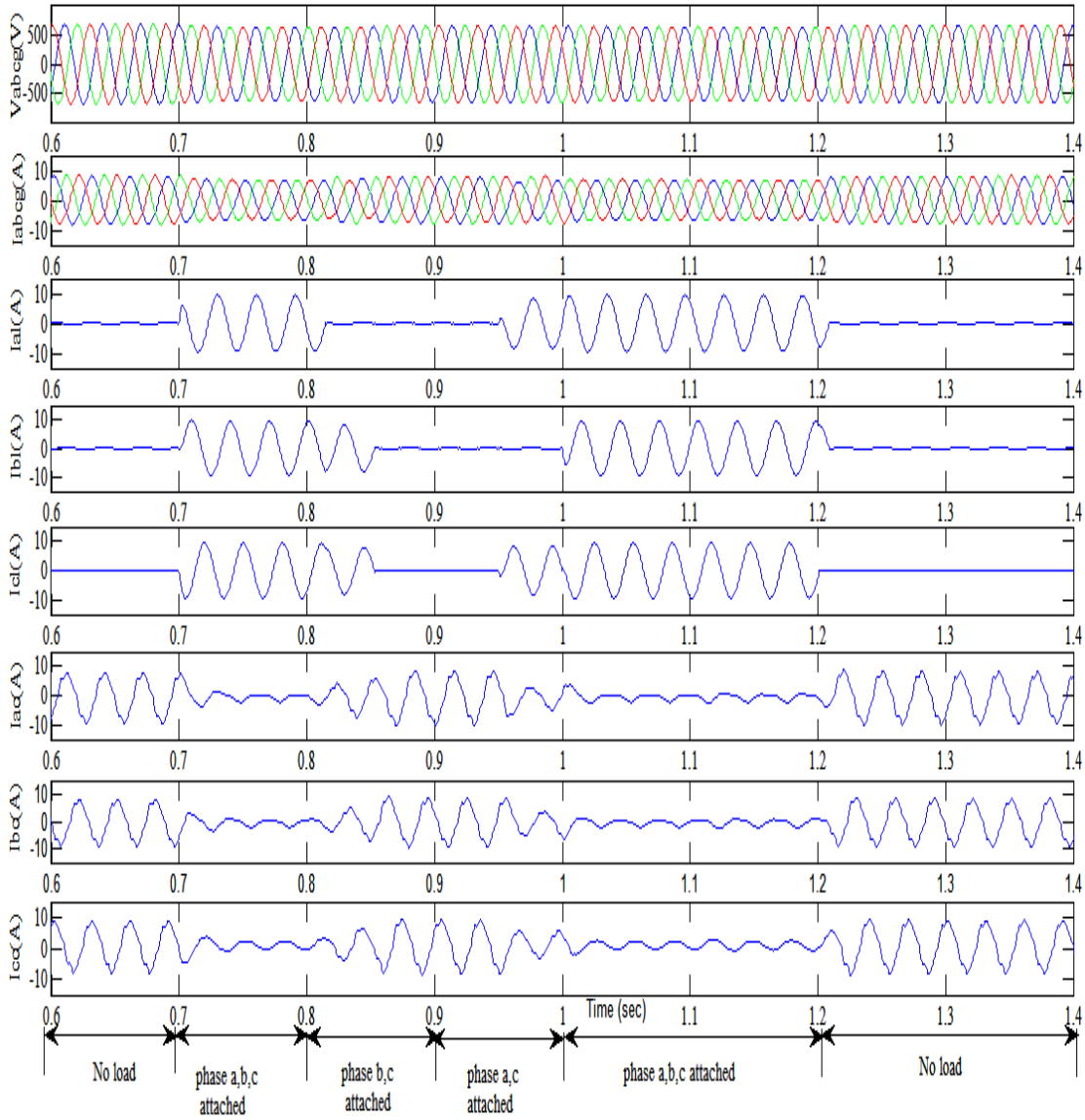

Fig. 7.9 Simulated transient characteristics waveforms of voltage generated by three-phase IAG (V_{abcg}), three-phase IAG currents (I_{abcg}), per-phase reactive load currents (I_{al}, I_{bl}, I_{cl}), per-phase EGLC currents (I_{ac}, I_{bc}, I_{cc}) under balanced and unbalanced reactive load using FL controller.

At 0.95 sec one-phase and at 1 sec another phase of load is reinserted at IAG terminals. Under such situation, EGLC currents die down to zero value to make IAG system balanced. It means that the controller current increases and decreases when the

consumer load decreases and increases respectively. It shows that both the consumer load current and dump load current are complementary in nature. Because of the complementary nature of load and controller current, the load on the generating unit is held constant. Hence the voltage, current, frequency, rotational speed and the generated power of the IAG remains constant even at varying load conditions [Fig. 7.9 and Fig. 7.10]. In reactive load situation, generator voltage is constant and is perfectly sinusoidal which shows that EGLC is working as a voltage supporter and load balancer

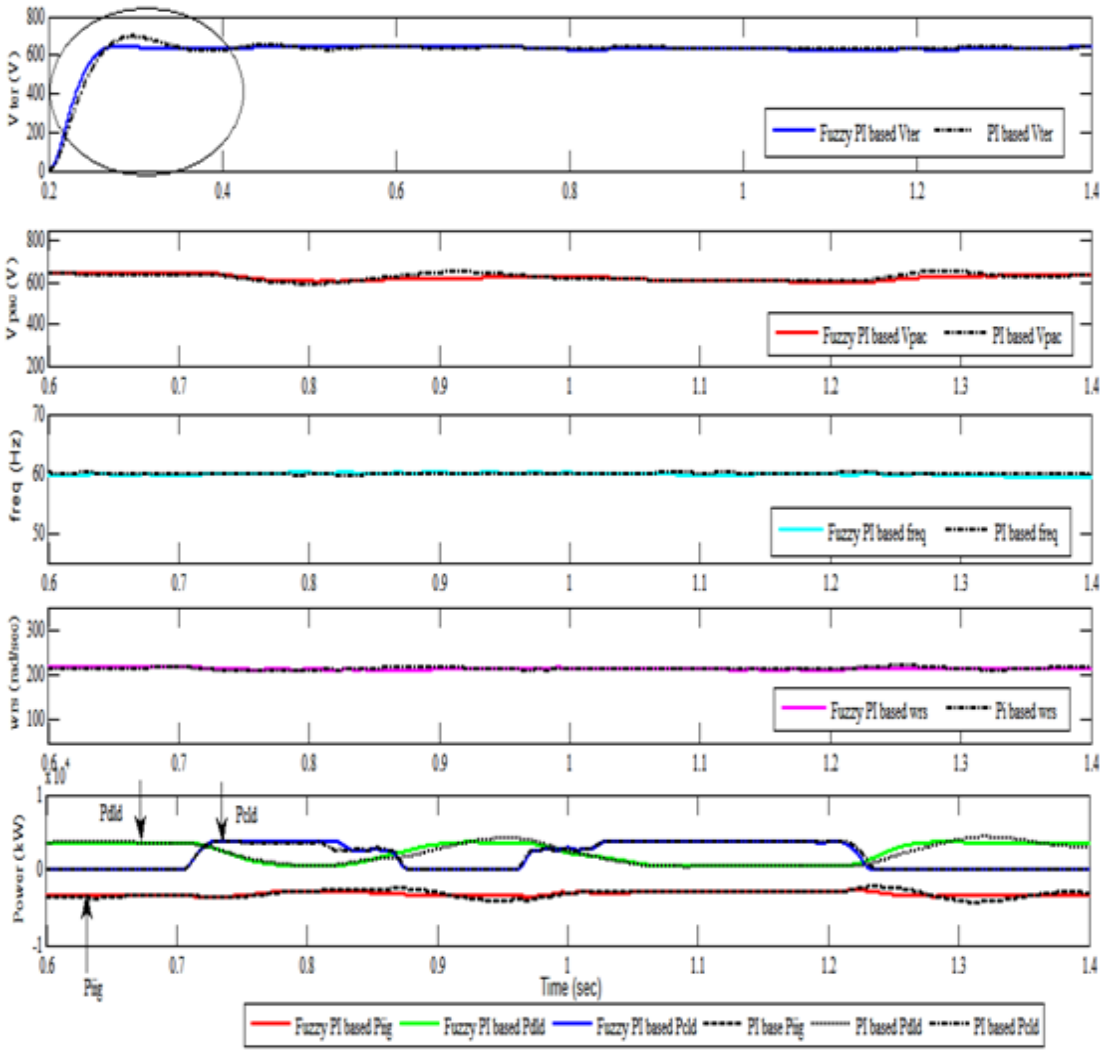

Fig. 7.10 Comparison of simulated results of magnitude of terminal ac voltage (V_{ter}), peak value of generated ac voltage (V_{pac}), frequency (freq) , rotational speed (w_{rs}), power generated by IAG (P_{iig}), consumer power (P_{cld}) an dump load power (P_{dld}) for resistive-inductive load using both PI and FL controllers.

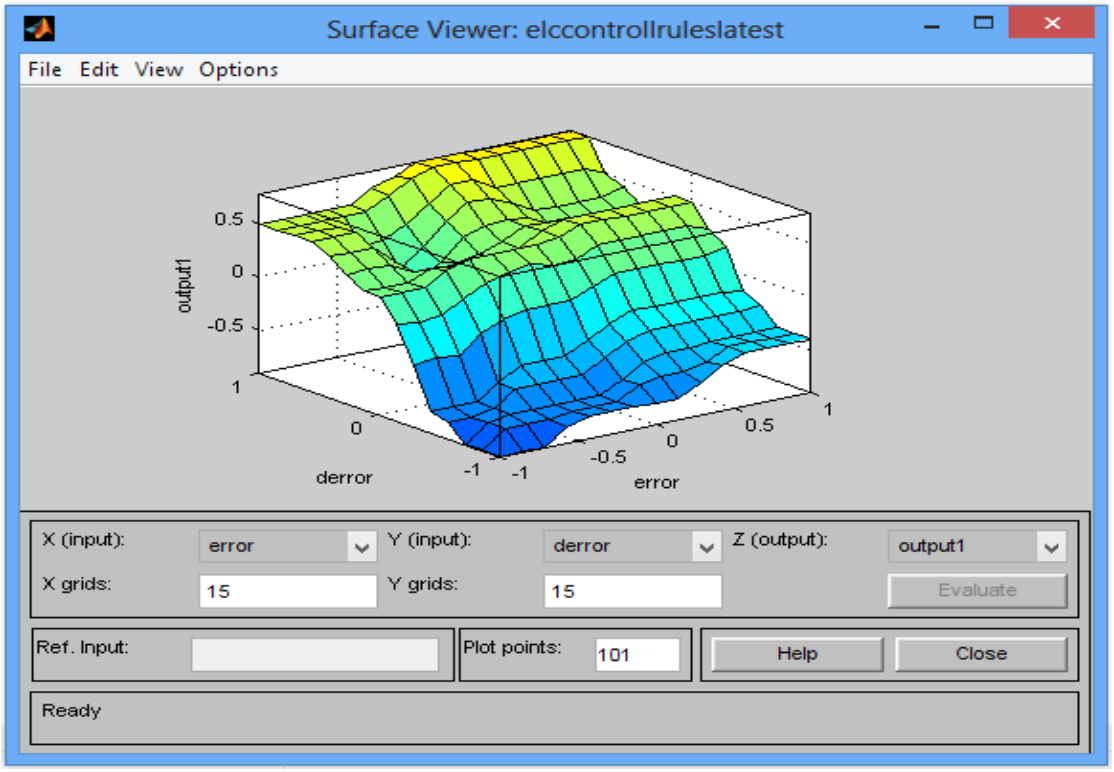

Fig. 7.11 Surface viewer window of Mamdani type FIS file for reactive load

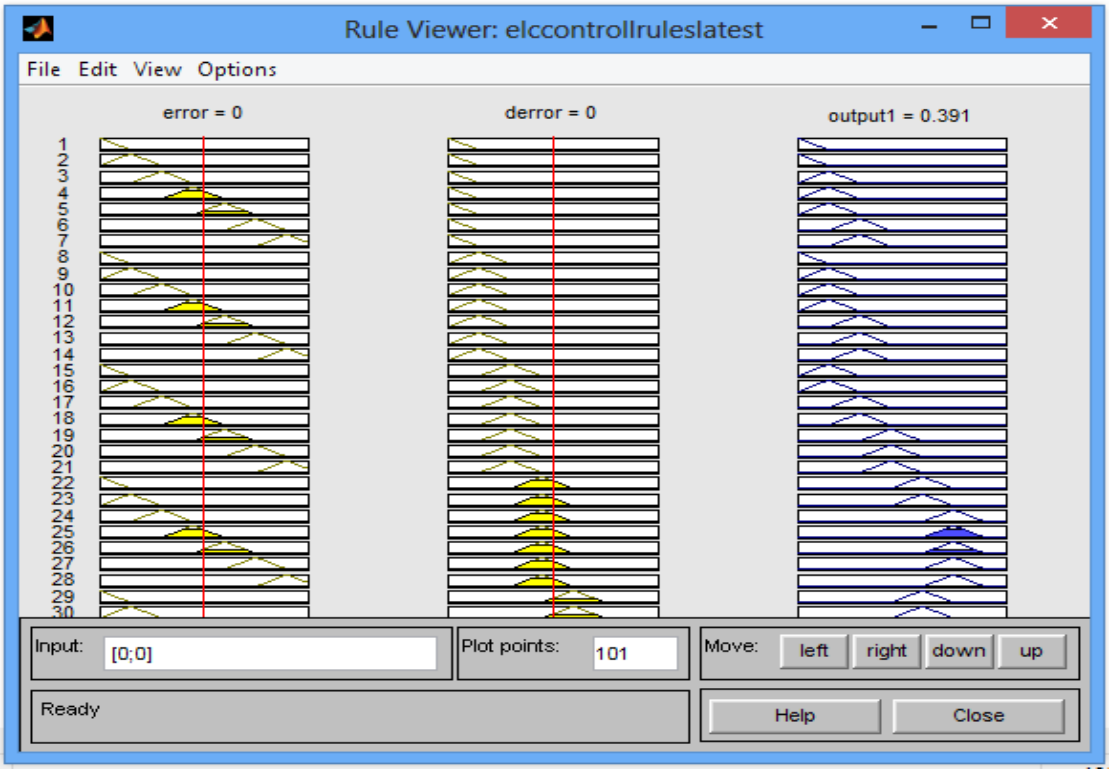

Fig. 7.12 Rule viewer window of Mamdani type FIS file for reactive load

Fig. 7.10 also indicates the comparison of simulated results of amplitude of terminal ac voltage (Vt_{er}), the peak value of generated ac voltage V_{pac}, frequency (freq), speed (w_{rs}), IAG power, consumer load power and dump load power due to both PI and FL controllers.

In Fig. 7.10 (a), the response of ac voltage V_{ter} attained using FL controller is remarkably faster than PI controller. The settling time for V_{ter} due to PI is 0.45 sec whereas due to FL controller is 0.34 sec [Table 4].

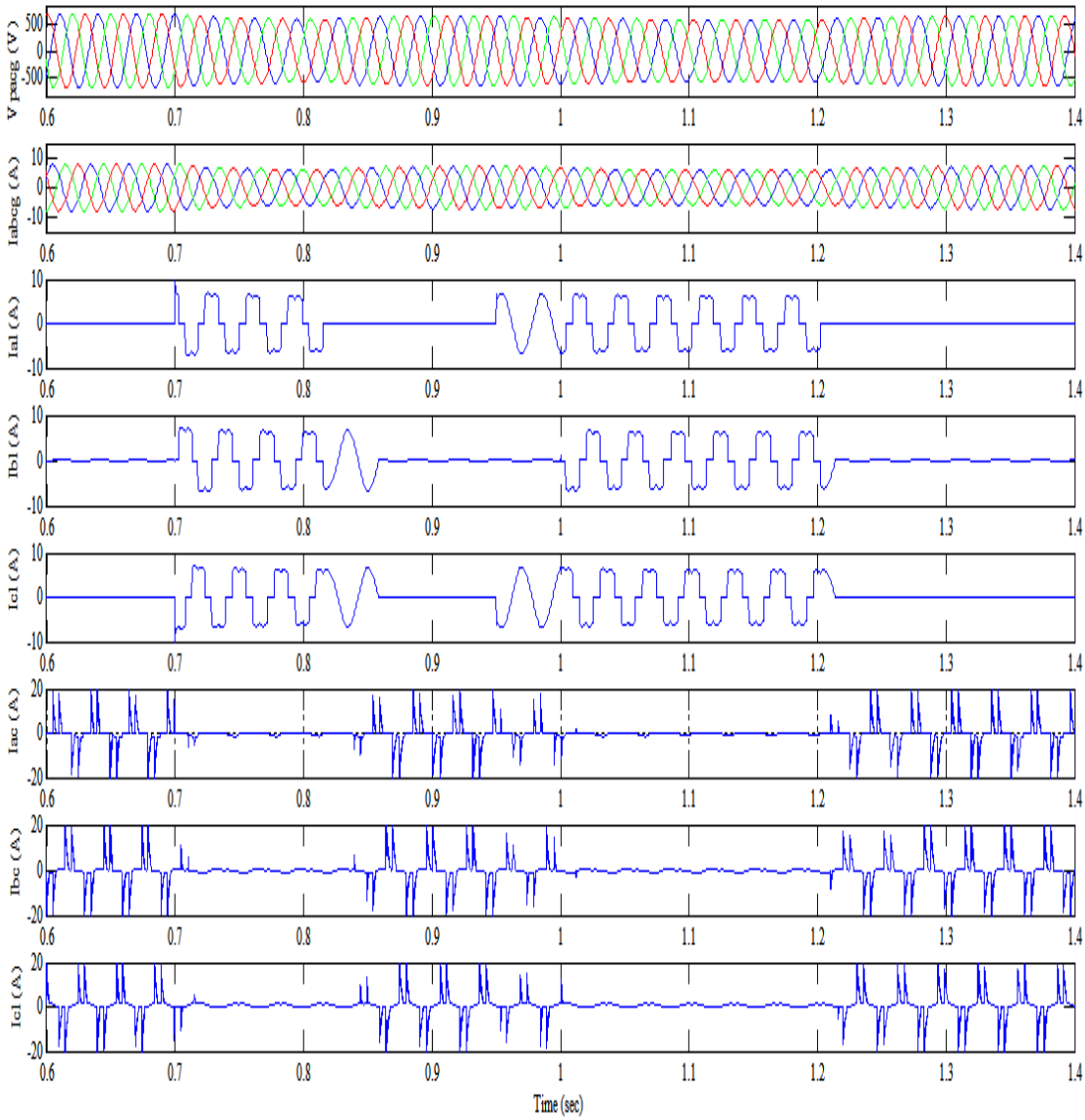

Fig. 7.13 Simulated transient characteristics waveforms of voltage generated by three-phase IAG (V_{abcg}), three-phase IAG currents (I_{abcg}), per-phase non-linear load currents (I_{al}, I_{bl}, I_{cl}), per-phase EGLC currents (I_{ac}, I_{bc}, I_{cc}) under balanced and unbalanced nonlinear rectifier load using FL controller.

From Fig. 7.10, it is observed that the amplitude of terminal ac voltage, peak value of generated ac voltage, frequency, rotational speed and power generated by the IAG are constant.

Also, the performance relating to THD values of IAG voltage and current are considerably lower in FL than PI controller as mentioned in Table 5. The surface viewer and rule viewer window of Mamdani type FIS for reactive load is illustrated in Fig. 7.11 and Fig.7.12

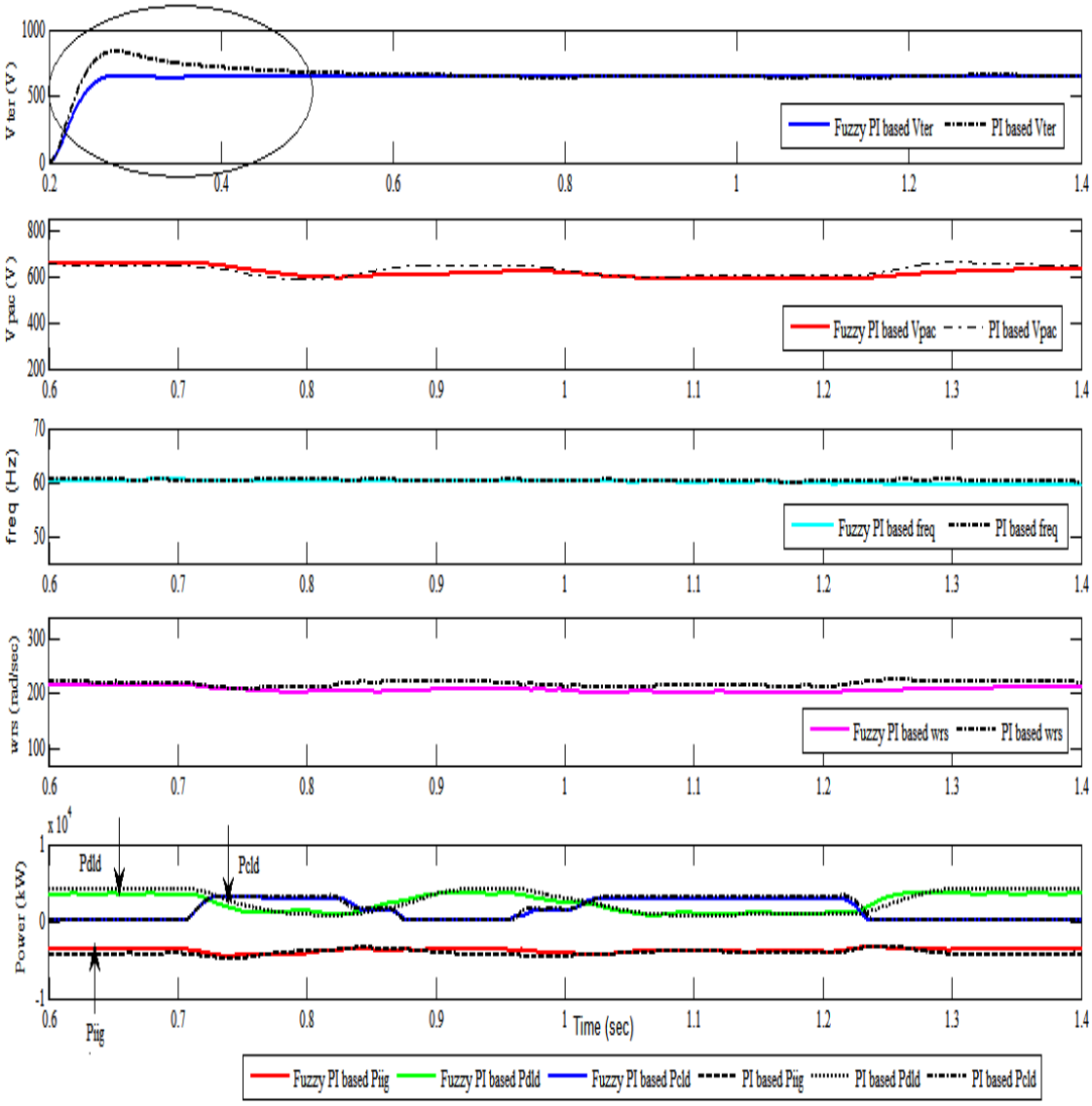

Fig. 7.14 Comparison of magnitude of terminal ac voltage (V_{ter}), peak value of generated ac voltage (V_{pac}), frequency (freq), rotational speed (w_{rs}), power generated by IAG (P_{iag})

7.4.3 Simulation Based Performance Outcomes of IAG-EGLC System with Three-Phase Balanced/Unbalanced Non-Linear Load

Fig. 7.13 indicates the FL controller based transient performance characteristics of three-phase IAG voltage (V_{pabcg}), three-phase IAG currents (I_{abcg}), per-phase resistive load currents (I_{al}, I_{bl}, I_{cl}), per-phase EGLC currents (I_{ac}, I_{bc}, I_{cc}) furnishing non-linear rectifier load .consumer power (P_{cld}) and dump load power (P_{dld}) for non-linear rectifier load using both PI and FL controllers.

The non-linear rectifier load is formed by using three-phase diode rectifier with resistive load and capacitive type filter at its DC end side. At 0.7 sec, a balanced non-linear load is inserted then the EGLC currents are reduced within a cycle for regulating the power, frequency and these becomes non-linear for eliminating harmonic currents. On separation of one phase of the load at 0.85 sec, the load becomes unbalanced but the IAG currents remain balanced, which shows the load balancing aspect of the controller. It is noticed from table.6, the THD values of V_{pa} and I_{ag} using FL under different loads is significantly less than PI based control criteria. The THD values are also less than the earlier published research.

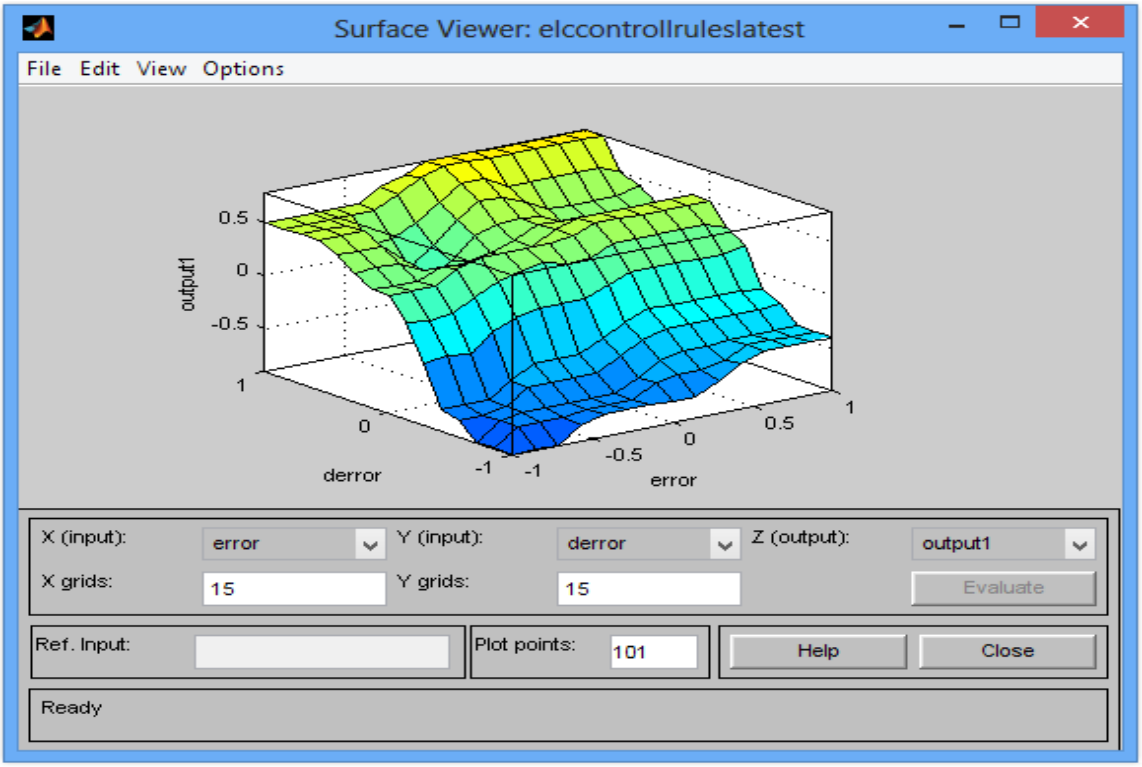

Fig. 7.15 Surface viewer window of Mamdani type FIS file for non-linear load

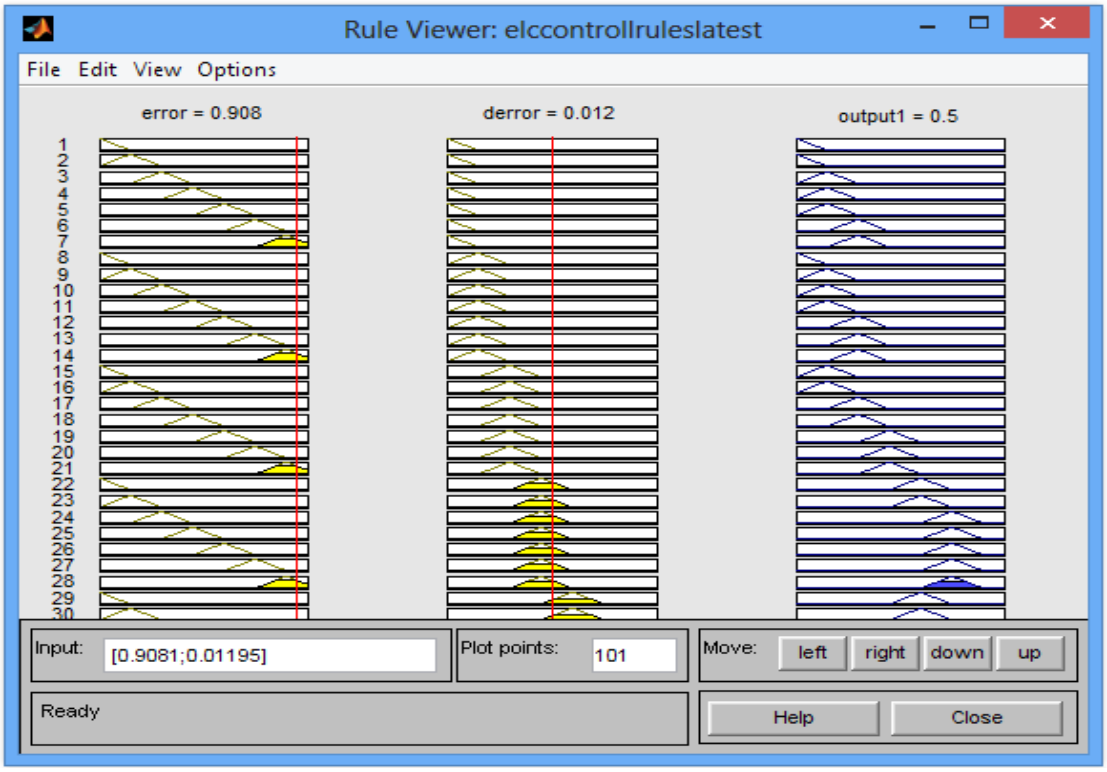

Fig. 7.16 Rule viewer window of Mamdani type FIS file for non-linear load

The speed of the IAG is constant throughout the whole generating processes which show that the IAG is generating constant voltage, frequency and power as depicted in Fig. 7.13 and Fig. 7.14. The surface viewer and rule viewer window of Mamdani type FIS for non linear load is illustrated in Fig. 7.15 and Fig.7.16.

Fig. 7.14 indicates the comparison of simulated results obtained using PI and FL method for magnitude of terminal ac voltage, peak value of generated voltage (V_{pac}), frequency (freq), rotational speed (w_{rs}), power generated by IAG (P_{iag}) and consumer power (P_{cld}) and load power (P_{dld}) for non-linear rectifier load. The results obtained by using both methods are quite satisfactory and comparable in terms of performance. But the response of ac voltage V_{ter} due to FL is notably faster and smoother than traditional PI controller as depicted in Fig. 7.14 (a). Fig.7.17 indicates the THD values of IAG voltage (V_{pa}), IAG current (I_{ag}), consumer load current (I_{al}) under balanced and unbalanced load conditions using Powergui FFT Analysis Tool. It is concluded from the figure, the THD of V_{pa} and I_{ag} is lower than the limit of 5 % mentioned in IEEE-519 standard document [72].

Table 4: Performance of EGLC regarding or relating to rise time, settling time and overshoot

Load Type	Controller type	Rise time (sec)	Settling time (sec)	Overshoot
Resistive Load	PI controller	0.0434	0.3681	7.7549
	Fuzzy PI controller	0.0426 ↓	0.2687 ↓	0.6121 ↓
Reactive Load	PI controller	0.0450	0.4605	9.1064
	Fuzzy PI controller	0.0418 ↓	0.2861 ↓	0.0170 ↓
Non-linear Load	PI controller	0.0478	0.8023	28.1646
	Fuzzy PI controller	0.0419 ↓	0.6142 ↓	0.0045 ↓

Table 5: Performance relating to THD value of IAG voltage and current

Load Type	Controller type	THD values in %	
		IAG voltage (V)	IAG current (A)
No Load	No controller	8 %	5.04 %
Resistive Load	PI controller	1.42	3.57
	Fuzzy PI controller	**1**	**2.71**
Reactive Load	PI controller	1.54	3.93
	Fuzzy PI controller	**1.25**	**2.75**
Non-linear Load	PI controller	2.26	4.09
	Fuzzy PI controller	**1.29**	**2.87**

The comparison of THD values of IAG voltage and current under different loads using both methods is depicted in Table 5.

FFT Window FFT Analysis

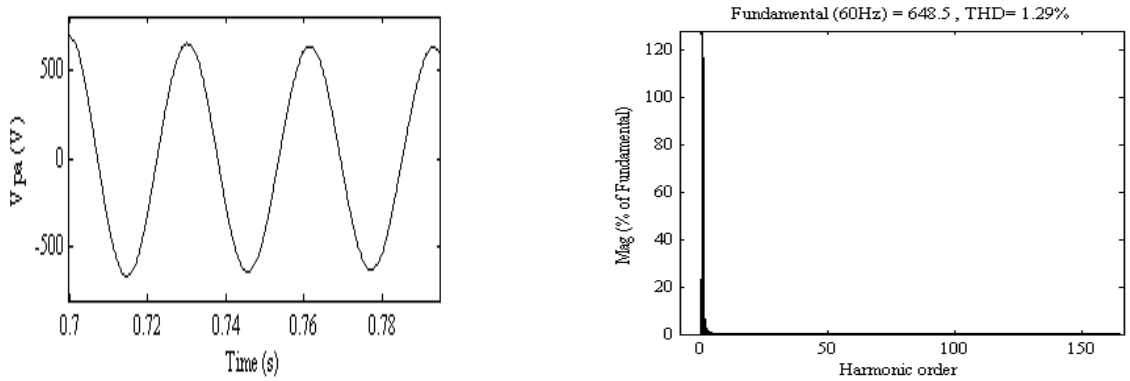

(a)

FFT window FFT Analysis

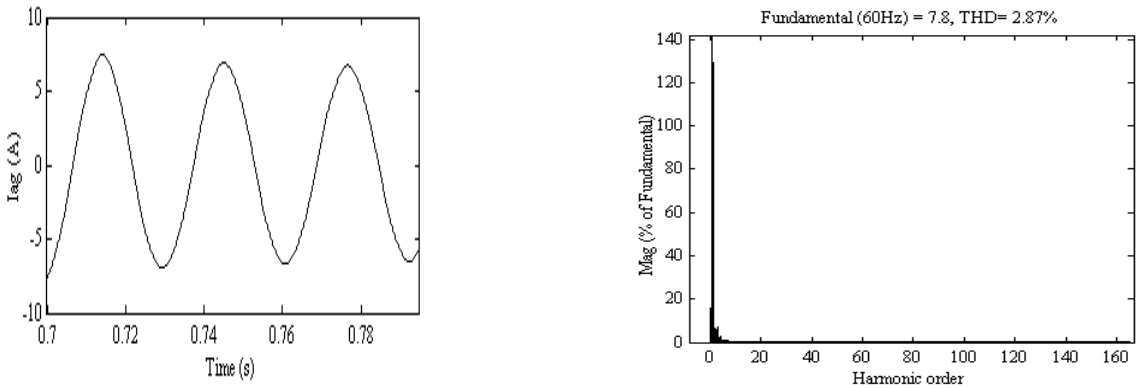

(b)

FFT window FFT Analysis

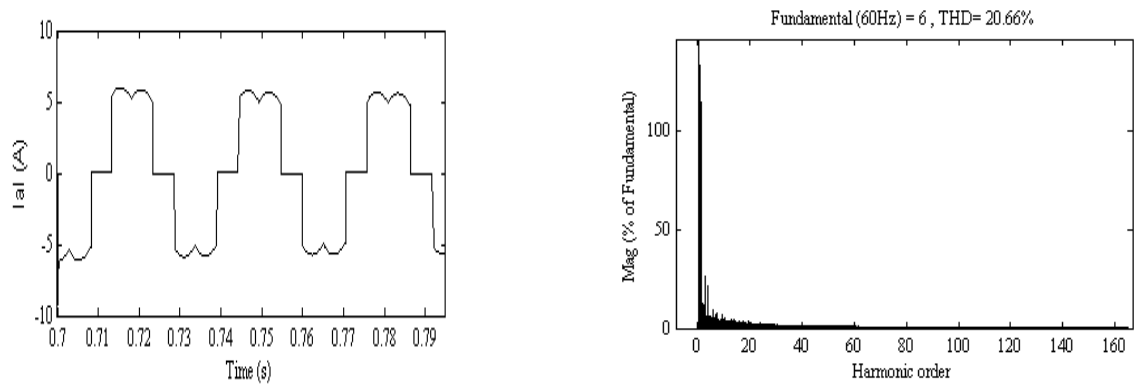

(c)

Fig. 7.17 FFT window and FFT analysis of (a) IAG voltage V_{pa} (b) IAG current I_{ag} and (c) Consumer load current I_{al} under both balanced and unbalanced load.

7.5 SUMMARY

The complete performance of the system under both transient and steady state are adjudged using both traditional PI and Mamdani based FL for EGLC. The performance relating to voltage, frequency, speed and power etc are analyzed and compared using both methods.

Table 4 shows that FL type controller provides better performance pertaining to rise time, settling time and overshoots. Table 6 shows that the THD values of the IAG voltage and current using FL based controller are less than traditional PI based controller. These values also lies within the range mentioned in IEEE 519 standard document [72]. Thus FL based EGLC behaves as a load balancer, voltage and frequency supporter and a THD reducer. Hence, performance enhancement of IAG is achieved using FL based EGLC than the PI controller. But in Mamdani based FL, this enhancement in performance is achieved at the cost of an increase in computational needs. However, the computational needs are lesser in PI controller. Such types of intelligent systems are cost effective and can also be used for electrification purposes in remote and grid isolated areas or for pico - hydro based applications.

CHAPTER 8

HARDWARE IMPLEMENTATION OF PWM IC-3524 BASED (EGLC) FOR AN IAG MEETING ELECTRIFICATION OF RURAL SITES

8.1 GENERAL

Energy is the basic need for the social and economical development of a country. Energy consumption of a nation is the direct way of accessing the index of development and it is only 500 W for India which is lower than the developed countries like America, U.S etc. In developing countries like India around 1/3 of the country population resides in villages or rural areas and they even do not have any access to electricity. In such areas, grid extension may not be possible and feasible due to some technical constraints, financial constraints and cost effectiveness. India is glorified with plenty of sustainable renewable energy sources in such off-grid areas. Due to continuous degradation, depletion and cost hike of conventional energy sources in early 1970's, researchers promoted the renewable energy technologies for electrical power generation (EPG) using isolated asynchronous generators (IAG). The IAG driven by these renewable energy sources (RES) is emerged as a viable and cost effective alternative. Using such systems, power generation capacity can be raised and can efficiently meet the increased energy needs in future. It is a well known fact that more power generation leads to more power consumption and cost per kWh decreases and hence the people residing in remote areas can access the electricity at the lowest possible rates. Now a day, micro-generation technologies are preferred for low power generation. It includes wind turbine, solar power photovoltaic or a combination of these technologies. It is promoted as an alternative source of renewable energy technology. India is the first country in the world to establish a Ministry of non-conventional energy resources called MNRE (Ministry of new renewable energy). India set a target of accomplishing 40% of its total power generation from non fossil fuel by 2030.

Therefore, the concept of distributed generation using RES to cater the single-phase load requirements in rural off grid areas has proved a viable and cost effective

option. The installed units of such generating systems are usually handled by local communities or by village panchayats. These generating systems are simple, robust, maintenance free operation, no operating personnel. So, the unskilled people can handle the plant.

The steady state and transient state performance analysis of 3-phase IAG feeding balanced and unbalanced is discussed in several papers. Various phase balancing schemes are discussed and implemented to obtain balanced sinusoidal voltages under unbalanced conditions [19, 40, 42, 49, 51].

It is observed that IAG is subjected to poor voltage and frequency regulation under varying load situation [19, 40, 42, 49 and 51]. So, there is felt a need of some controller which can provide voltage and frequency support under varying loads condition. A numerous number of papers are covering the analysis; design and implementation of three-phase ELC for three-phase IAG feeding single phase load [55, 88, 74, 66, 67, 76, 75, 60, 58, 65, 70, 82, 77, 62, 64, 68, 81, 63, 65, 85, 82, 83, 89, 90, 84, 92].

D. Henderson [88] explianed the original work related to the development of microprocessor opearted binary weighted electronic load controller (ELC). D. K Palwalia et.al [89] proposed a DSP based voltage and frequency regulator for a 3-phase IAG driven by an unregulated micro-hydro turbine and feeding 1-phase load. V. Verma et.al [90] explored a VSC based voltage and frequency regulator for an IAG operating under varying load. S. Gao et.al [91] proposed an efficient and low cost microcontroller (dsPIC30F6010) based electronic load controller (ELC) for voltage regulation of 3-phase IAG feeding 1-phase load.

In this chapter the analysis, design and the practical implementation of a PWM IC-3524 based voltage and frequency controller for a three-phase IAG feeding 1-phase load has been detailed. The proposed controller can be recommended as a cost effective voltage regulator for micro hydro systems in rural sites. This paper highlights (ii) Constant load based control of IAG using PWM IC-3524 (iii) PWM generation (iv) Design methodology for 1-phase ECLC (v) Results (vi) Discussion.

8.2 CONSTANT LOAD BASED CONTROL OF AN IAG USING PWM IC-3524

A three-phase delta connected asynchronous machine is used as an asynchronous generator. The asynchronous machine is driven mechanically above synchronous speed with the help of dc machine A C-2C capacitor configuration is opted here to obtain single-phase supply for supplying single-phase loads. An autotransformer is used here to step-down the ac voltage from a level of 380 V to 230 V as depicted in Fig. 8.1. This 230 V acts as an input to both the consumer load (lamp load) and dump load. The designed IC-3524 based controller is fabricated using Protel System Design Software [Fig. 8.2]. The electronic components used are

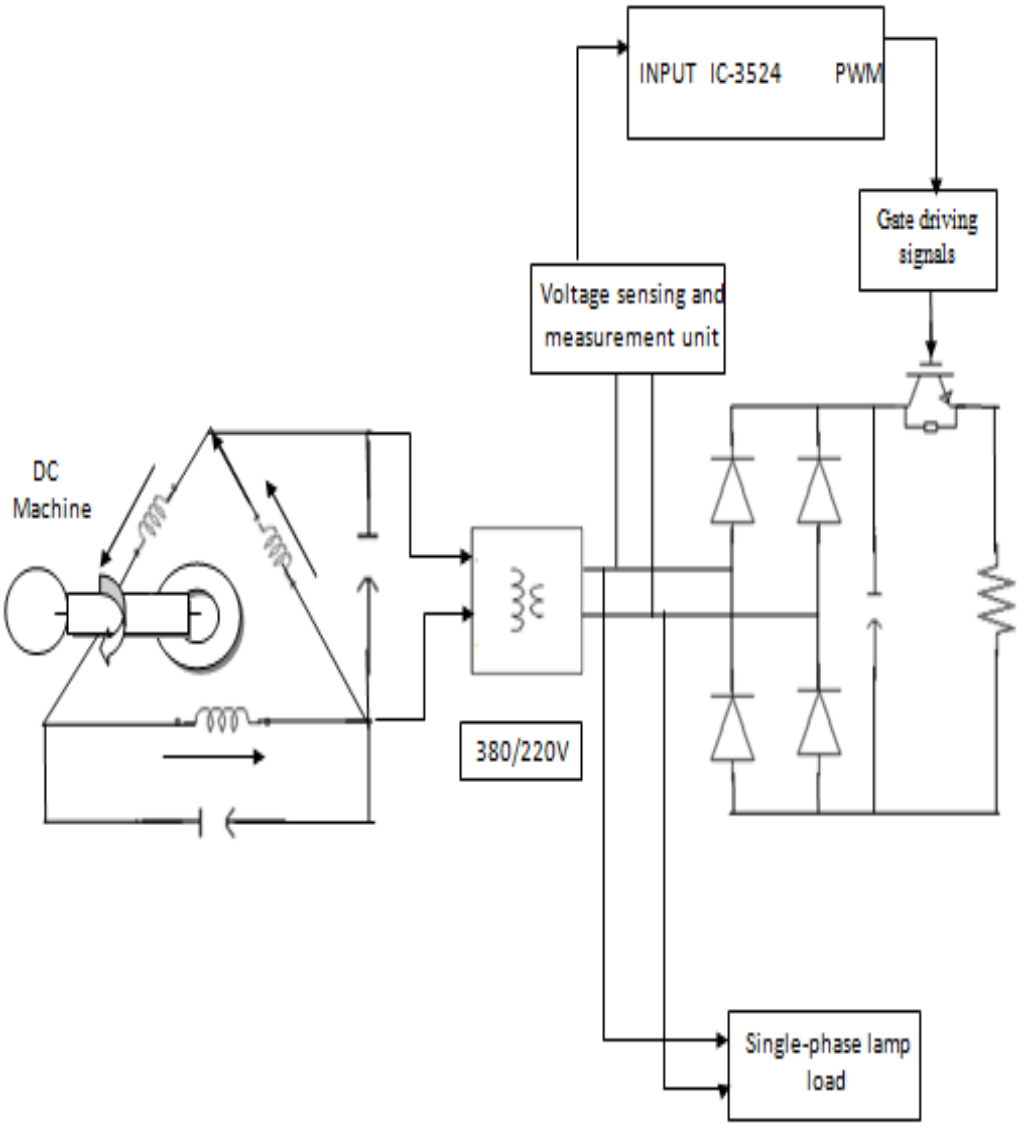

Fig. 8.1 Schematic diagram of three-phase IAG feeding single-phase load with EGLC

uncontrolled diode rectifier, chopper (IGBT type) switch, opto-coupler, IC-3524, transistors.

8.3 PWM GENERATION

The PWM based IC-3524 operates at a frequency determined by resistance R and capacitance C. The inbuilt 5V regulator acts as a reference voltage inside the IC. This 5V voltage is divided outside the IC using resistor divider circuit and this voltage is treated as a reference input voltage to inbuilt error amplifier. The output voltage is first sensed and then compared with the reference voltage. The error in voltage is first amplified then compared with the ramp voltage for generating the PWM signal or driving signal. This PWM signal is then fed to transistor T_1 and transistor T_2 through

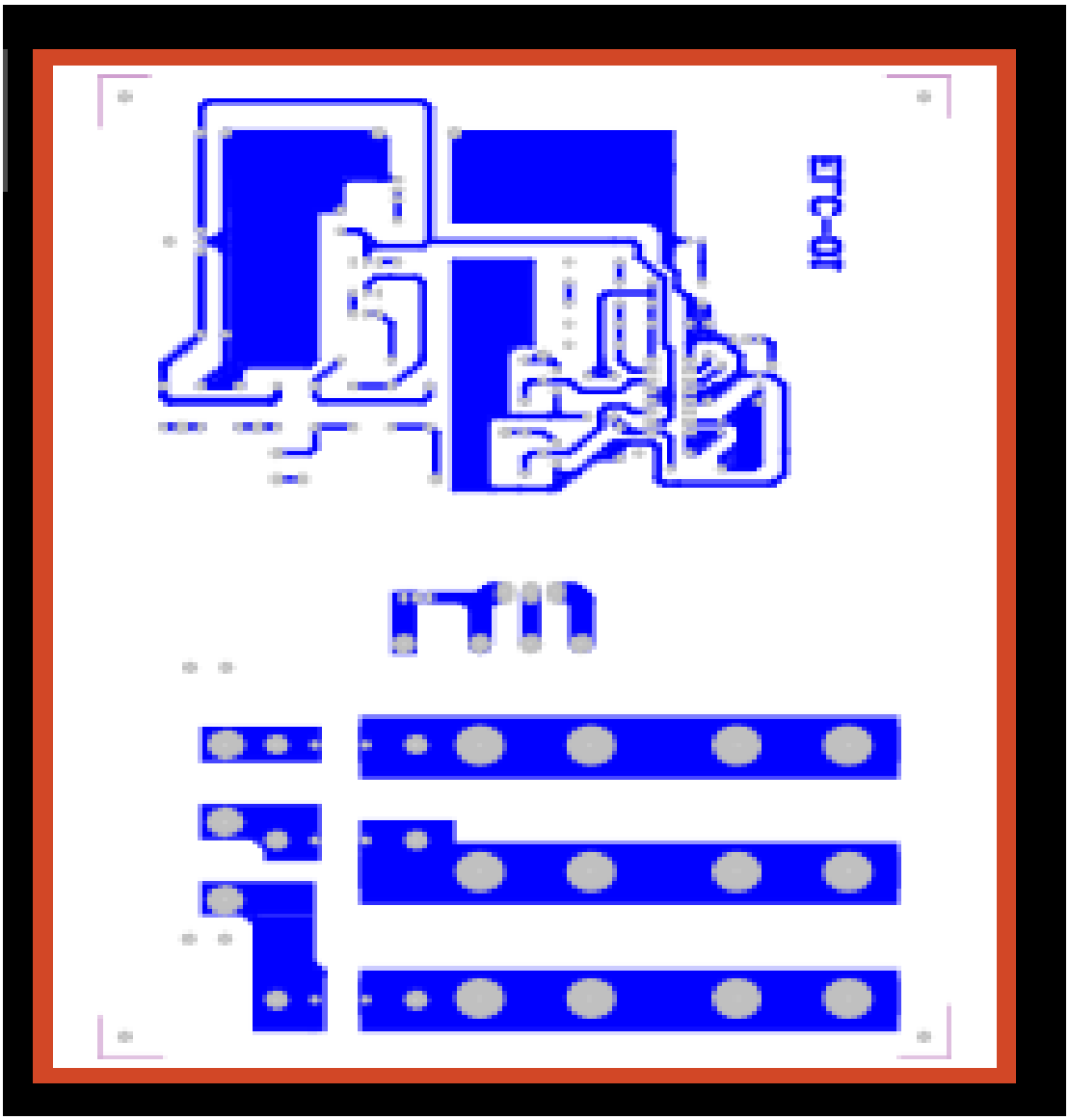

Fig. 8.2 PCB layout of the control circuit

flip-flops. The oscillator output pulse also acts as an inhibiting pulse i.e. both the transistors T_1 and T_2 are never in ON state simultaneously. The duration of this pulse is controlled by the value of C. Pin no. 11 and 14 are connected to the transistors T_1 and T_2 for driving 12-0-12 V primary and 220 V secondary. When pin no. 14 is high, upper transistor is ON and positive train of pulses is obtained. When pin no. 11 is high, lower transistor is ON and negative train of pulses is obtained. This train of pulses is fed to the IGBT Gate driver IC 3120 and is then fed to the IGBT switch of the EGLC.

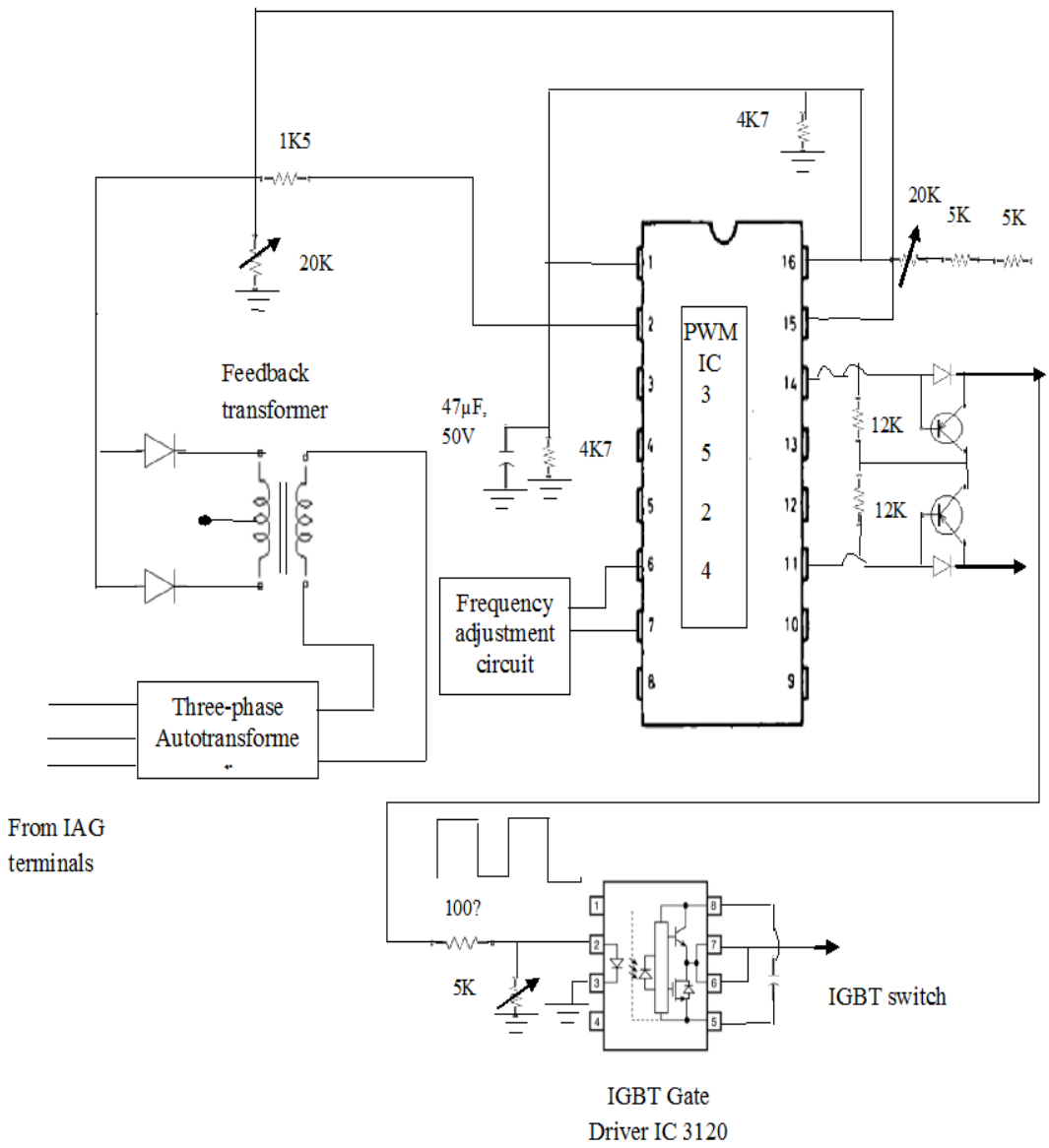

Fig. 8.3 Hardware diagram of the control circuit

8.4 HARDWARE IMPLEMENTATION OF 1-Φ EGLC FOR 3-PHASE IAG

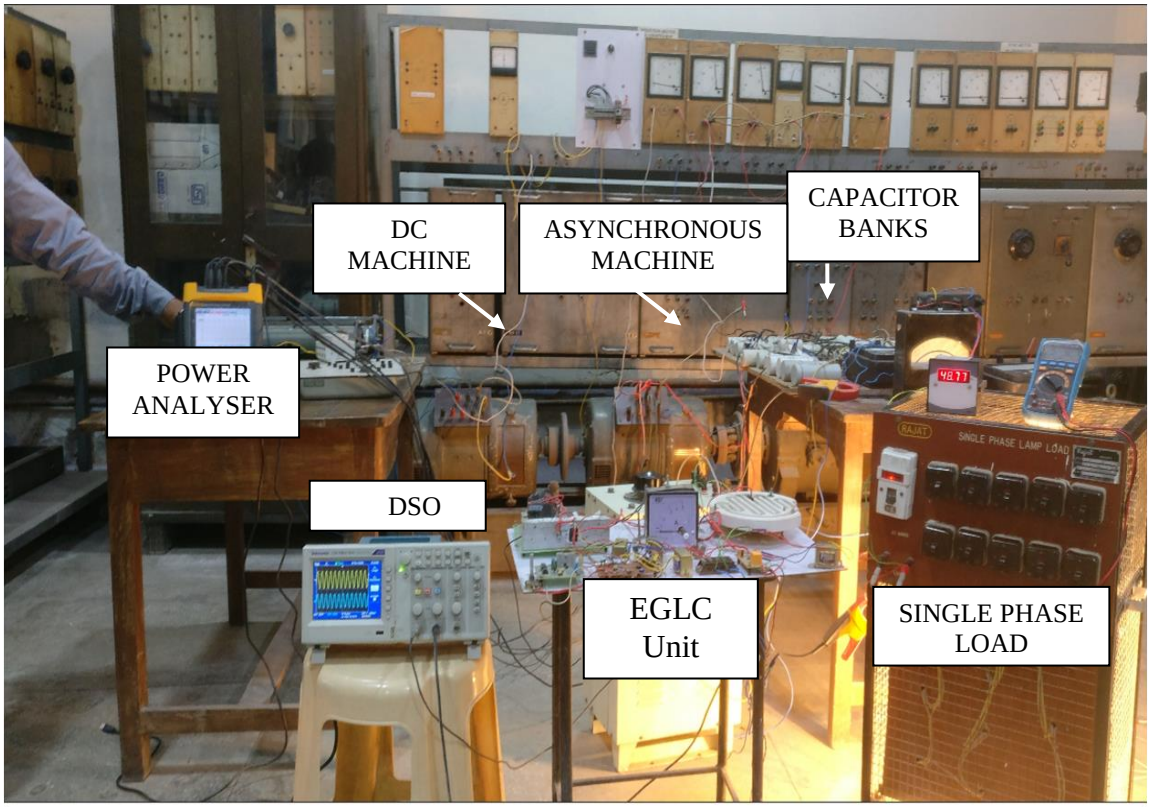

Photo 3 Photograph of the complete generating unit along with EGLC unit

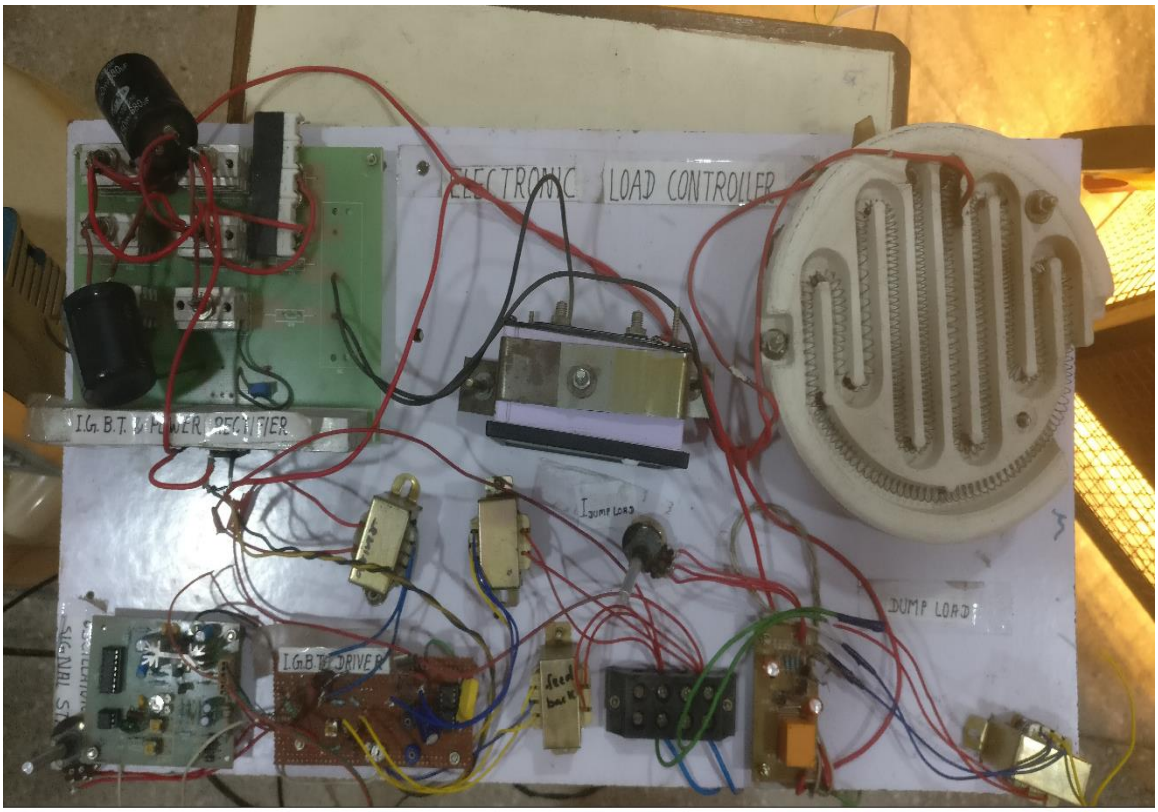

Photo 4 Photograph of the Electronic Generator load controller (EGLC)

The hardware part of the whole generating system integrated with the EGLC unit consists of: a three-phase asynchronous machine, a dc machine acting as a prime-mover, set of three-phase capacitor banks, a single phase resistive load, voltmeters, ammeters, wattmeters, mulltimeters, tachometer, power analyzer, DSO, 10:1 attenuator probe, frequency meter and EGLC unit.

8.5 DESIGN METHODOLOGY FOR 1-Φ EGLC

The voltage rating of the uncontrolled rectifier and IGBT type chopper switch will be the same and dependent on the r.m.s ac input voltage and average value of the output dc voltage. The average value of dc voltage is calculated as

$$V_{dco} = \frac{\left(2\sqrt{2}\ V_{cl}\right)}{\pi} = (0.9)V_{cl}$$

Where V_{cl} is the r.m.s value of the input voltage of the uncontrolled rectifier of an EGLC. For the 1.2 kW rating load, the average value of dc voltage

$$V_{dco} = (0.9) * 240 = 216V$$

An overvoltage of 10% of the rated voltage is considered for the transient condition and hence, the r.m.s ac input voltage will be (264V) with a peak value of

$$V_{Pk} = \sqrt{2} * 264 = 373.296V$$

This peak voltage will appear across the components of EGLC. The current rating of the uncontrolled rectifier and chopper is decided by the active component of input ac current and is calculated as

$$I_{aca} = \frac{P_{cl}}{V_{cl}}$$

where P_{cl} is the power rating of single-phase load. The active current of an AG may be calculated as

$$I_{aca} = \frac{1200}{240} = 5\ A$$

The single-phase uncontrolled rectifier current waveform has a distortion factor of 0.9; the input ac current (peak value) of EGLC may be obtained as

$$I_{dac(peak)} = \frac{I_{aac} * 2}{0.9} = \frac{5 * 2}{0.9} = 11.11\ A$$

So, for the uncontrolled rectifier, the maximum voltage may be 373.296 V and peak current may be 11.11 A. The commercial available rating of an uncontrolled rectifier and chopper switch is 600 V and 30 A. Therefore, rating of the uncontrolled rectifier and chopper switch has been decided to be 600V and 30 A.

The rating of the dump load resistance R_{dl} is calculated by

$$R_{dld} = \frac{(V_{dco})^2}{P_{rated}} = \frac{(216)^2}{1200} = 38.88\Omega$$

The value of the dc-link capacitance of the EGLC varies with the ripple factor (RF). The relation between the value of the dc link capacitance and ripple factor for a single-phase uncontrolled rectifier is

$$C_{dcl} = \left\{\frac{1}{(4fR_{dld})}\right\}\left\{1 + \frac{1}{(\sqrt{2}RF)}\right\}$$

If 20% ripple factor is permitted in the average value dc-link voltage then the filtering capacitance is calculated as

$$C_{dcl} = \left\{\frac{1}{(4 * 50 * 38.88)}\right\}\left\{1 + \frac{1}{(\sqrt{2} * 0.2)}\right\} = 583\ \mu F$$

Table 6: Designed values of various elements of EGLC

Power rating of motor (W)	Voltage rating of the uncontrolled bridge rectifier (V)	Current rating of the uncontrolled bridge rectifier (I)	Voltage rating of the IGBT operated chopper switch (V)	Current rating of the IGBT operated chopper switch (I)	Rating of Dump load resistance (Ω)	Rating of filtering capacitor (μF)
3730	600V	30A	600V	30A	38.88	583

8.6 EXPERIMENTAL AND ANALYTICAL INVESTIGATIONS

8.6.1 Transient Result Outcomes Interpretation on Three-Phase IAG and Single-Phase Load Side

Fig. 8.4 (a) and (b) depicted the three-phase generated voltage and capacitor current and the unbalance in both voltage and current. When a three phase IAG is feeding a

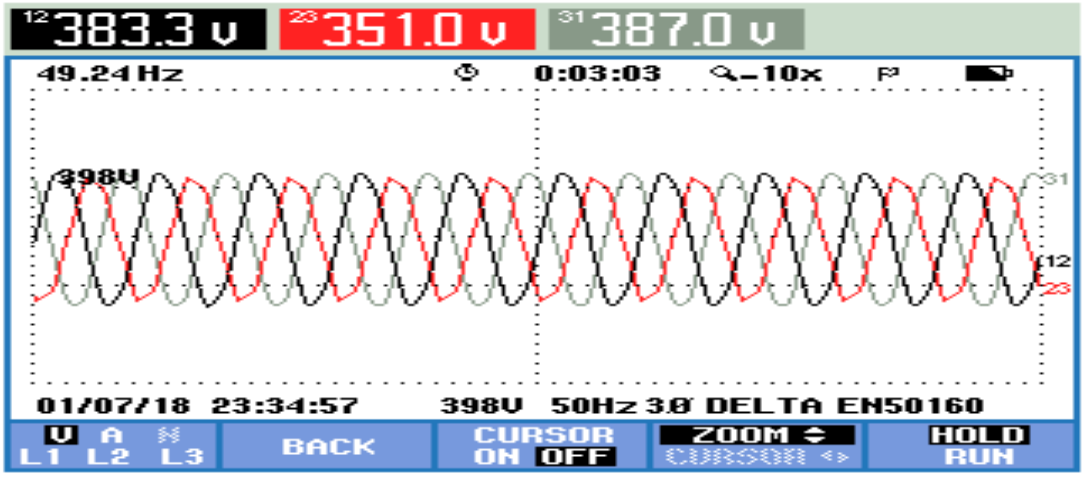

(a)

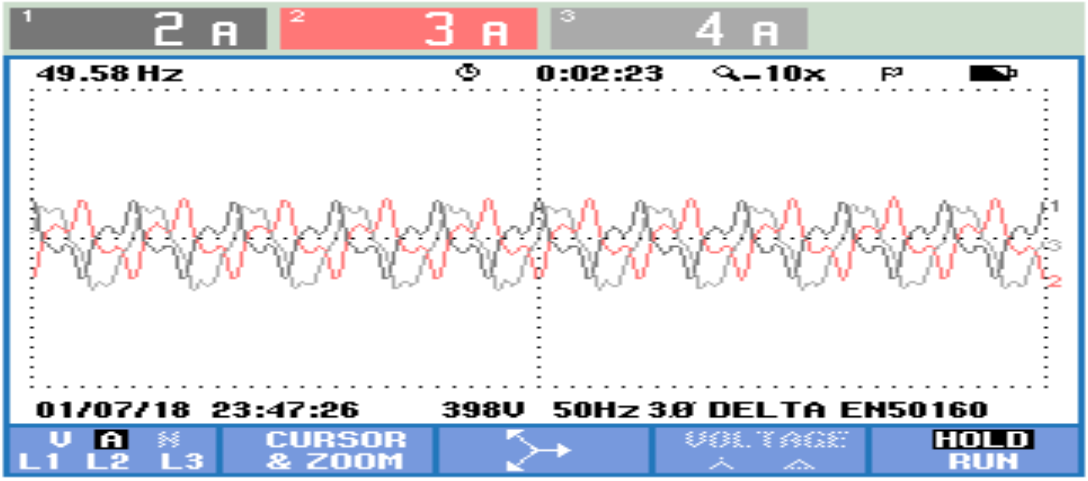

(b)

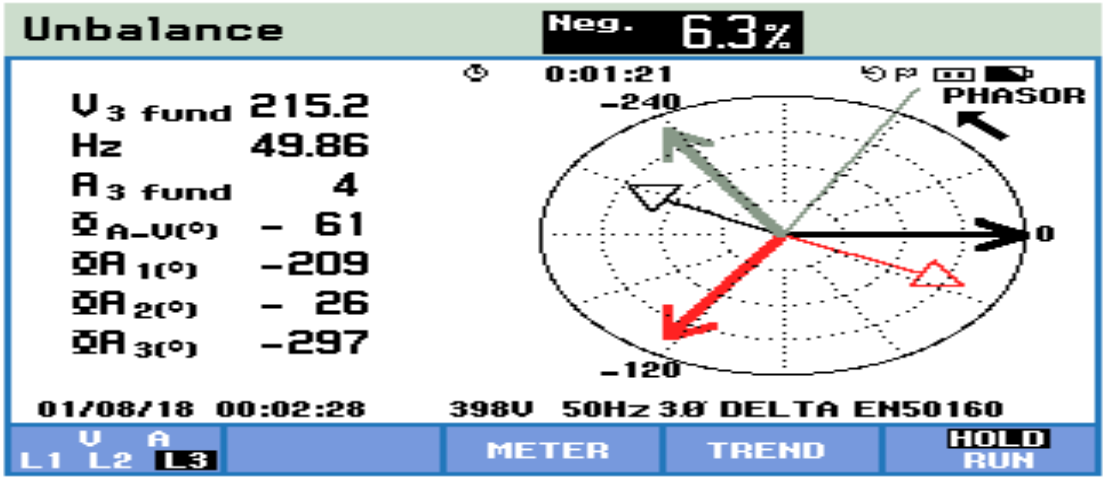

(c)

Fig. 8.4 (a) Waveform of three-phase generator voltages (b) three-phase genearted current (c) voltage unbalance on single-phase side under no-load conditions.

single-phase load, an unbalance occurs in three-phase generated voltages and currents of the IAG. To avoid or minimize this unbalance a C-2C capacitor connection is suggested [19, 40, 42, 49 and 51]. A voltage of 380 V is generated with the help of a delta-connected IAG at no load first. Then to feed single-phase load a capacitor connection of type C-2C is used here. The voltage across capacitor C is first fed to autotransformer for stepping down to 230 V for single-phase load. An unbalance of 6.3 % is observed in generated voltage and current as depicted in Fig. 8.4 (c).

Fig. 8.5 depicted the single-phase ac voltage fed to the single-phase uncontrolled rectifier under no load situation. A voltage of 228 V and frequency 50 Hz is applied to the uncontrolled rectifier.

Fig. 8.6 depicted the PWM generation at different duty cycles (24.7, 32.6 and 49.6) for driving the IGBT type chopper switch so that the dump load is connected in the circuit and current starts flowing through the dump load.

Fig. 8.7 depicted the saw tooth waveform for required for modulation purpose for attaining PWM pulses for driving the IGBT type chopper switch.

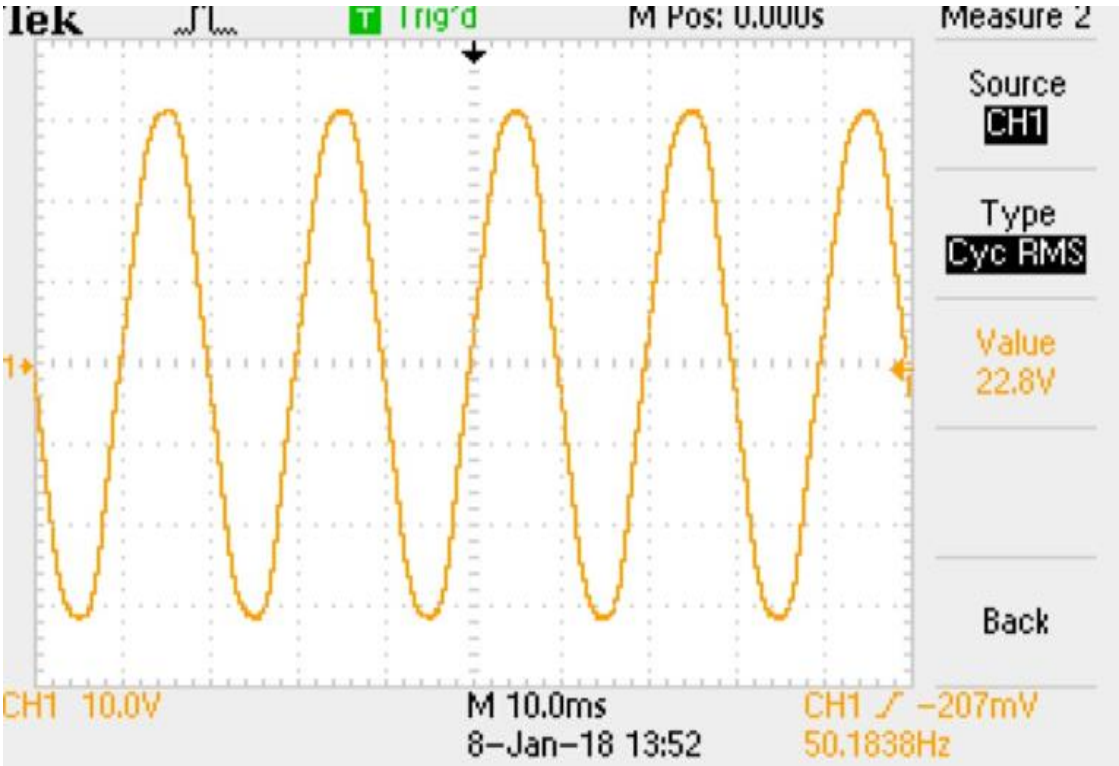

Fig. 8.5 Single-phase voltage (228 V) fed to EGLC

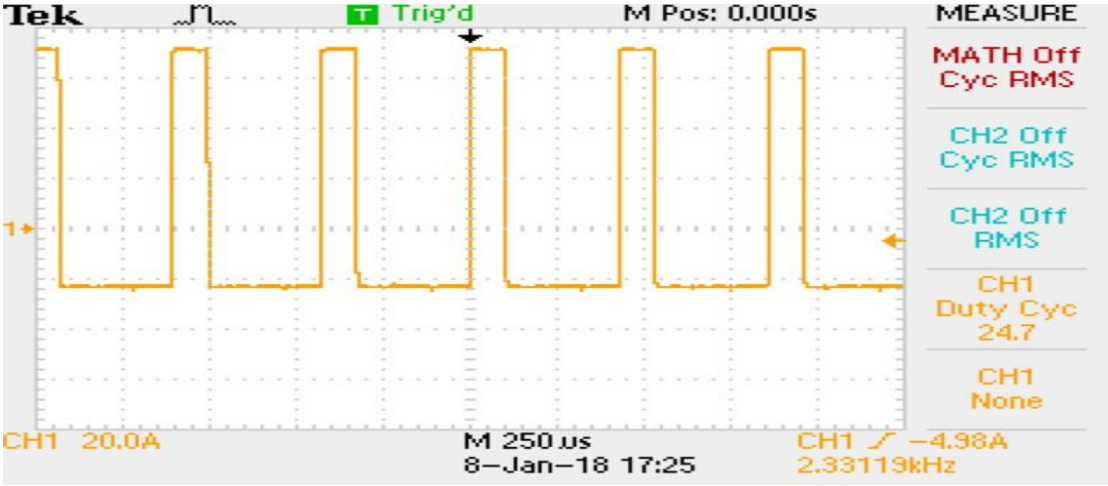

(a)

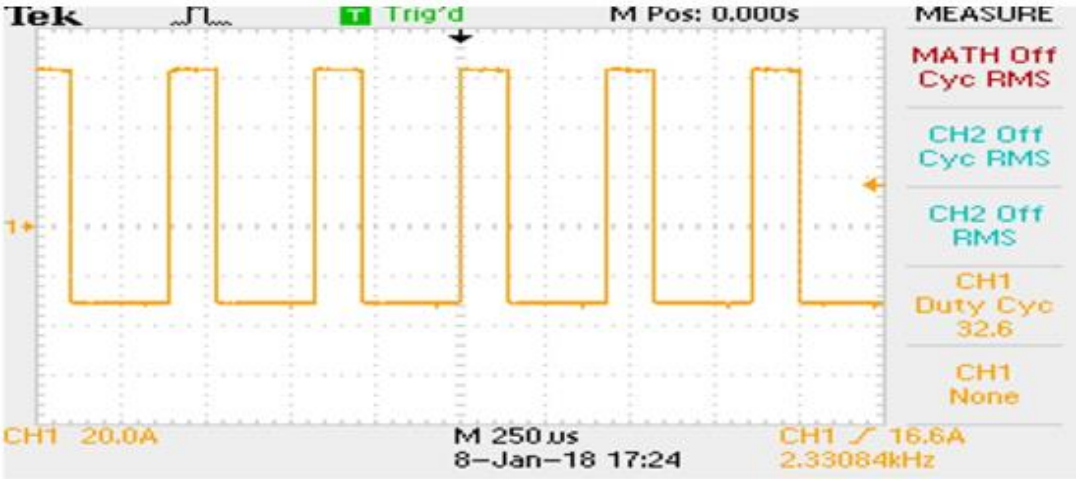

(b)

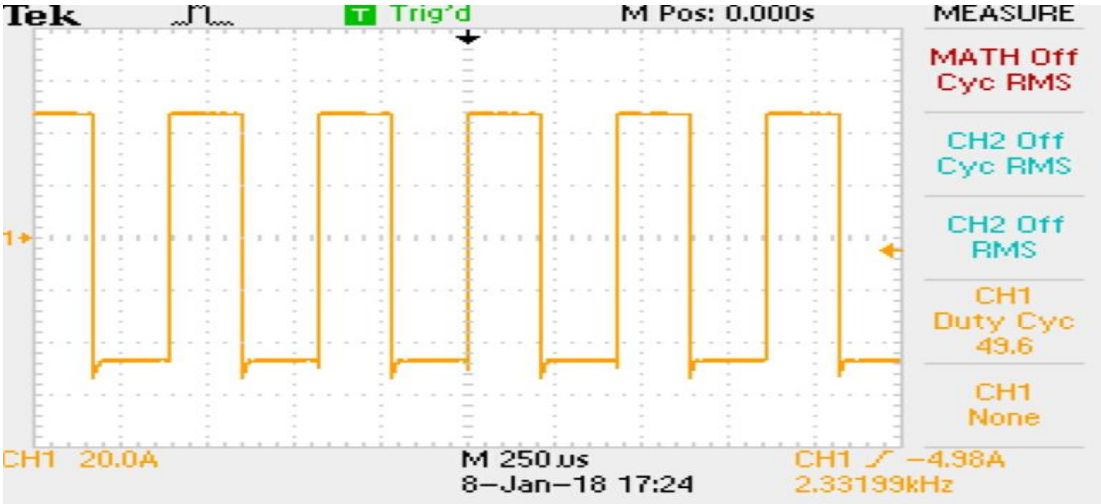

(c)

Fig. 8.6 PWM generation of different duty cycle (a) Duty cycle 24.7, (b) Duty cycle 32.6 and (c) Duty cycle 49.6

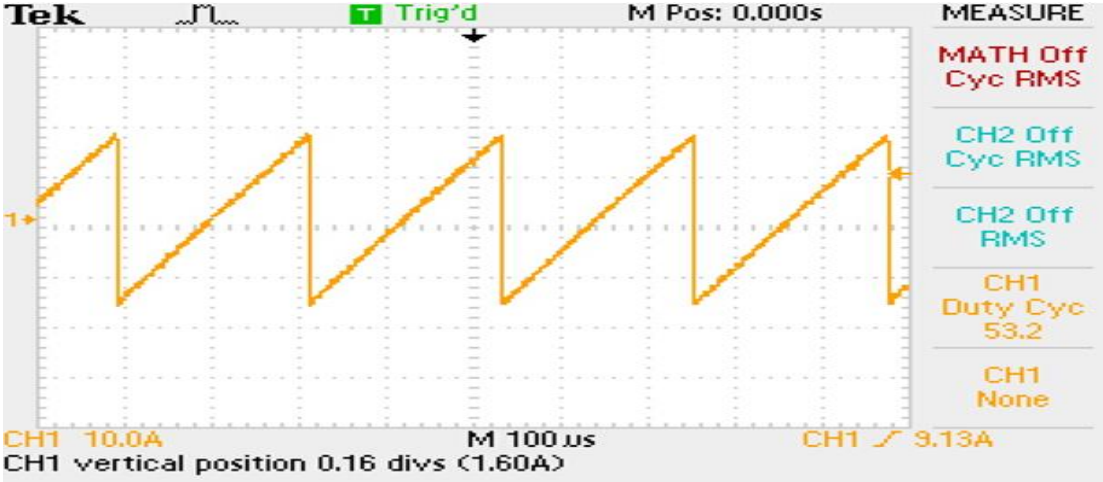

Fig. 8.7 Sawtooth waveform

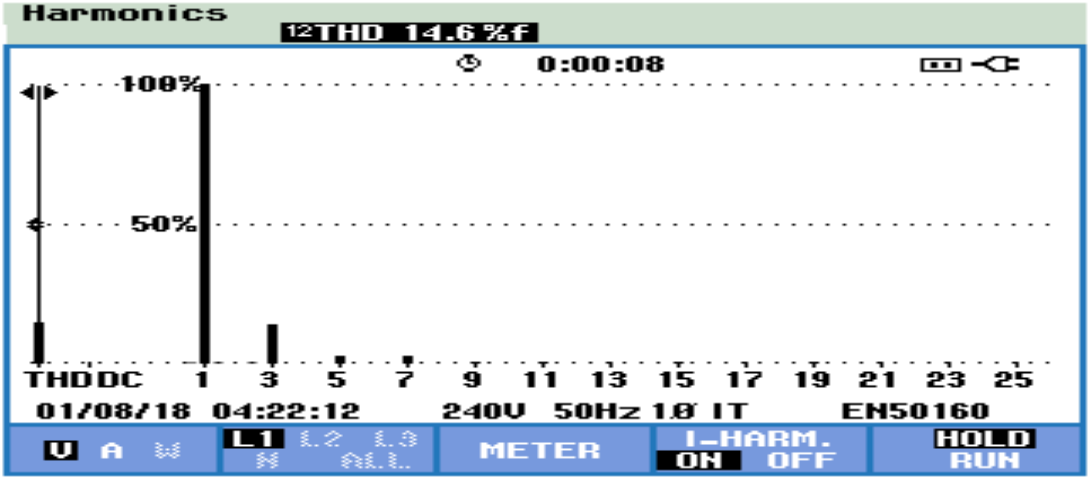

(a)

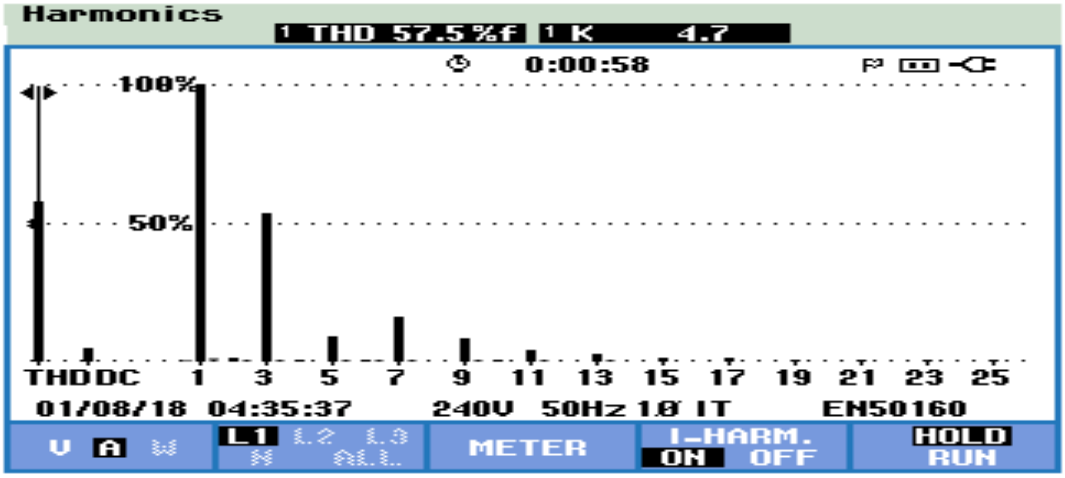

(b)

Fig. 8.8 (a) THD in IAG-EGLC voltage under zero consumer load (b) THD in IAG-EGLC current under zero consumer load.

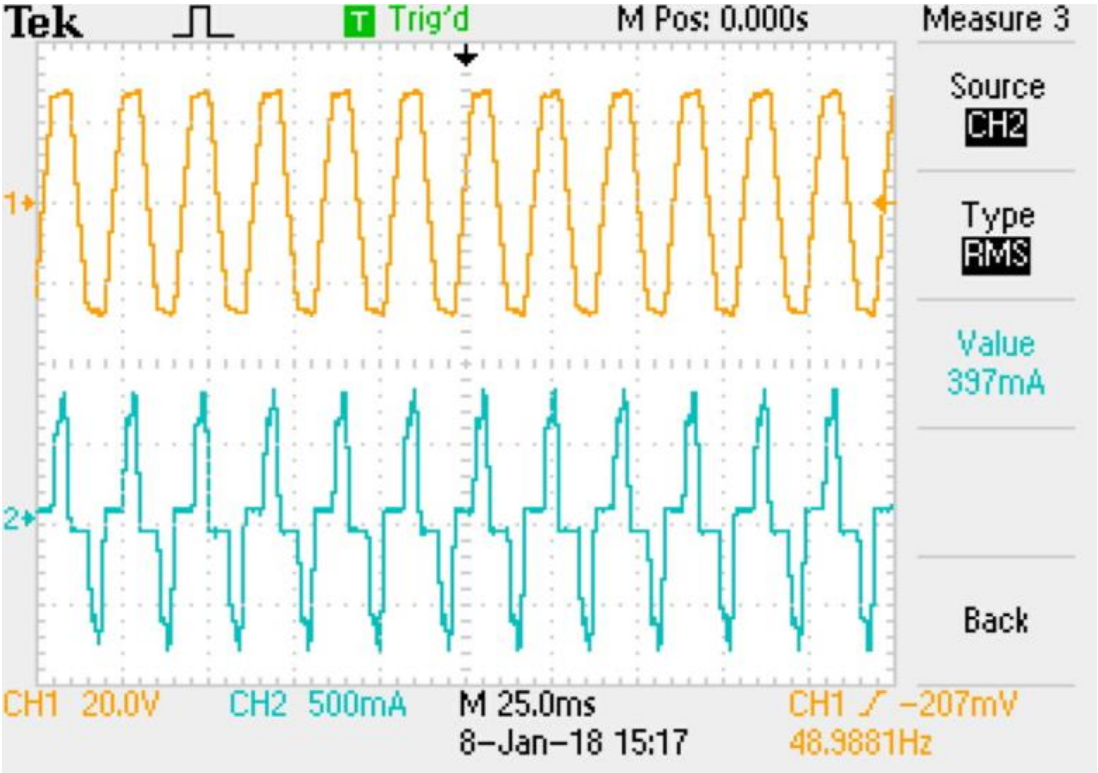

Fig. 8.9 Top: Single-phase voltage fed to EGLC (228V) at zero consumer load, Bottom: Current flowing through EGLC at zero consumer load

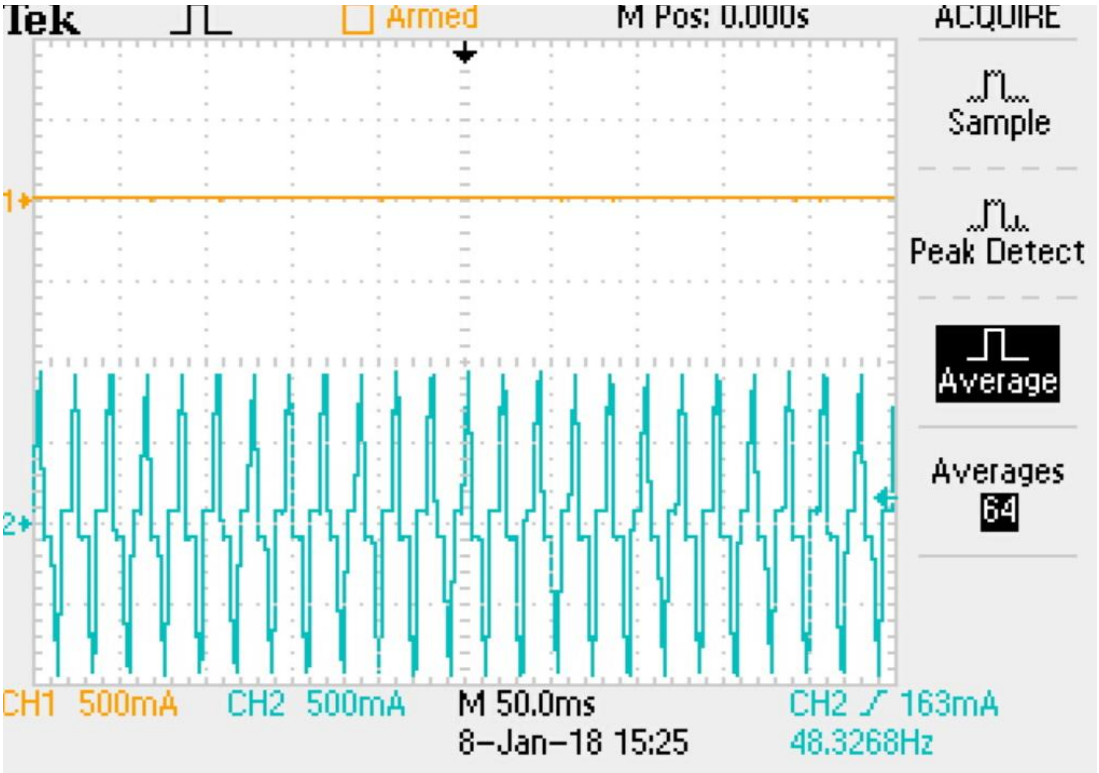

Fig. 8.10 EGLC current under zero consumer load

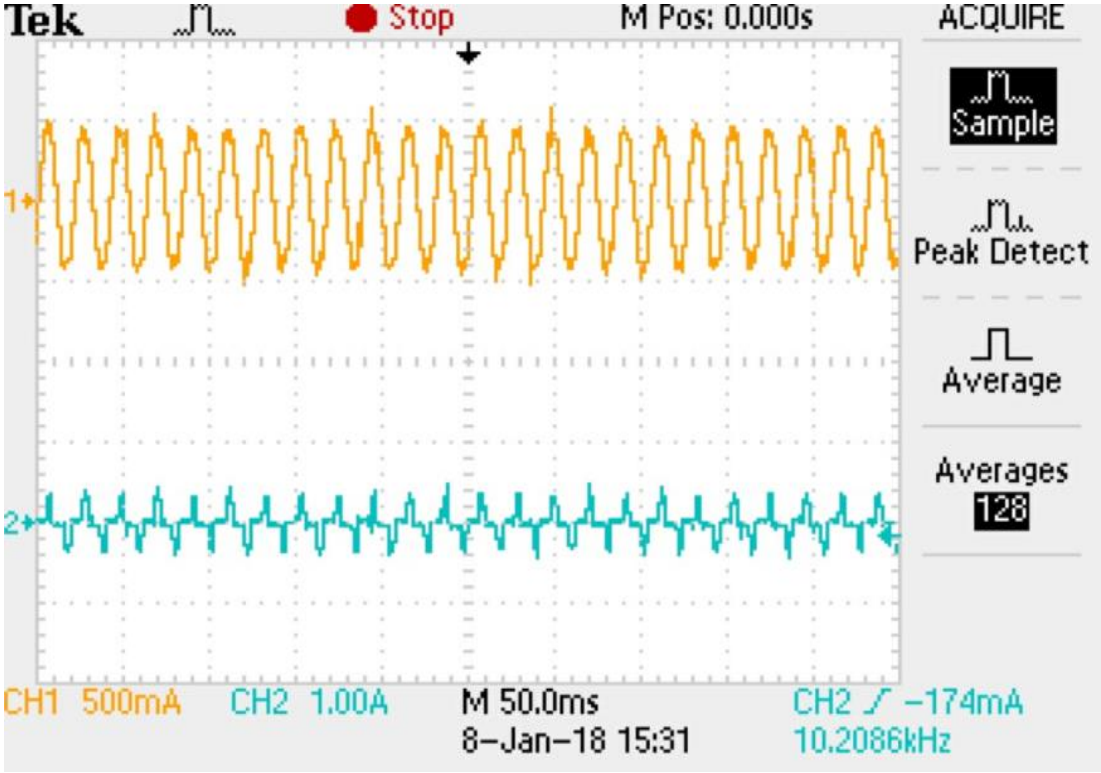

Fig. 8.11 Consumer current under 1.2kW consumer load under zero EGLC current

Fig. 8.8 depicted the Total Harmonic Distortion values in IAG-EGLC voltage and current under zero consumer loads. It is observed that the THD in generated voltage is 14.6% and the IAG current is 57.5% under zero consumer loads

Fig. 8.9 dpicted the single-phase voltage fed to the single phase rectifier and the driving signals are fed to the controller with zero consumer load.

Now the whole of the generated current is passing through the EGLC. This situation is depicted in Fig. 8.10. Now the consumer load is switched on in steps from 0 W to 1.2 kW. As the consumer load is inserted into the circuit and is increased, the current in the controller starts decying. It means when the consumer load current is increasing, then the current in the controller starts decaying so that the total load on the generator is held constant [Fig. 8.11] This constant load attributes to the constant load voltage [Fig. 8.12] and frequency operation of the IAG when administered or dealed to varying load.

Fig. 8.13 depicted the variation of load current, dump load current and the generator current with the power out across 1-phase unity power factor load. The load current raises as the load is varied from 0W to 1.2 kW and the dump load current

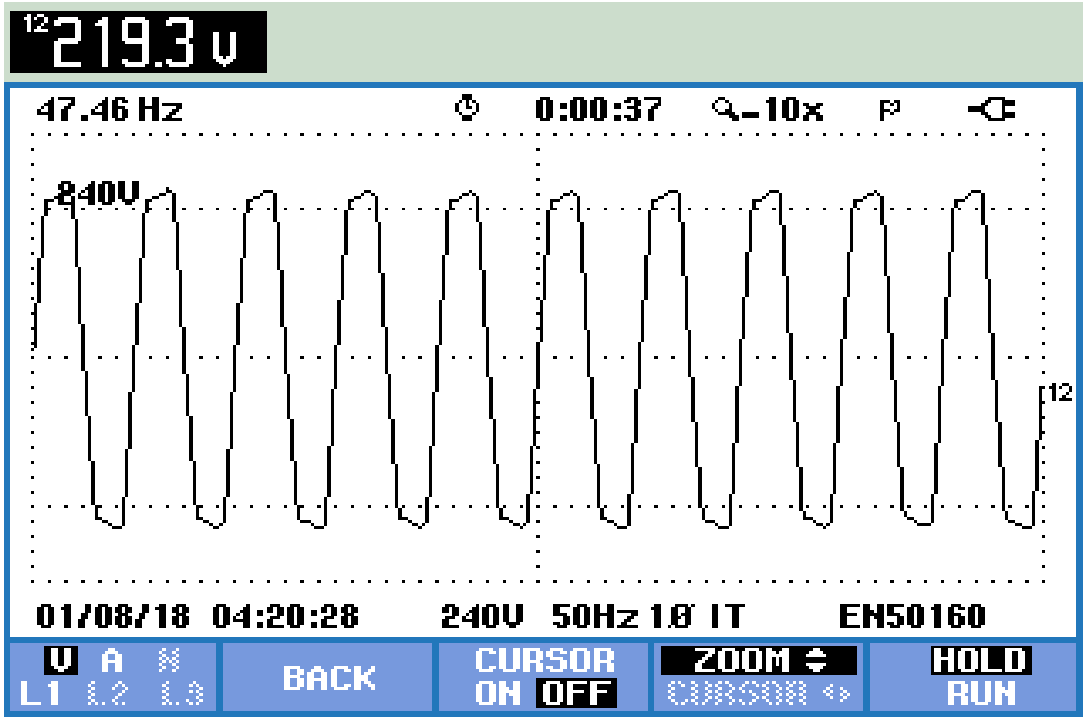

Fig. 8.12 Single-phase load voltage of IAG with EGLC

8.6.2 Steady State Result Outcomes Interpretation on Single-Phase Load Side with Controller

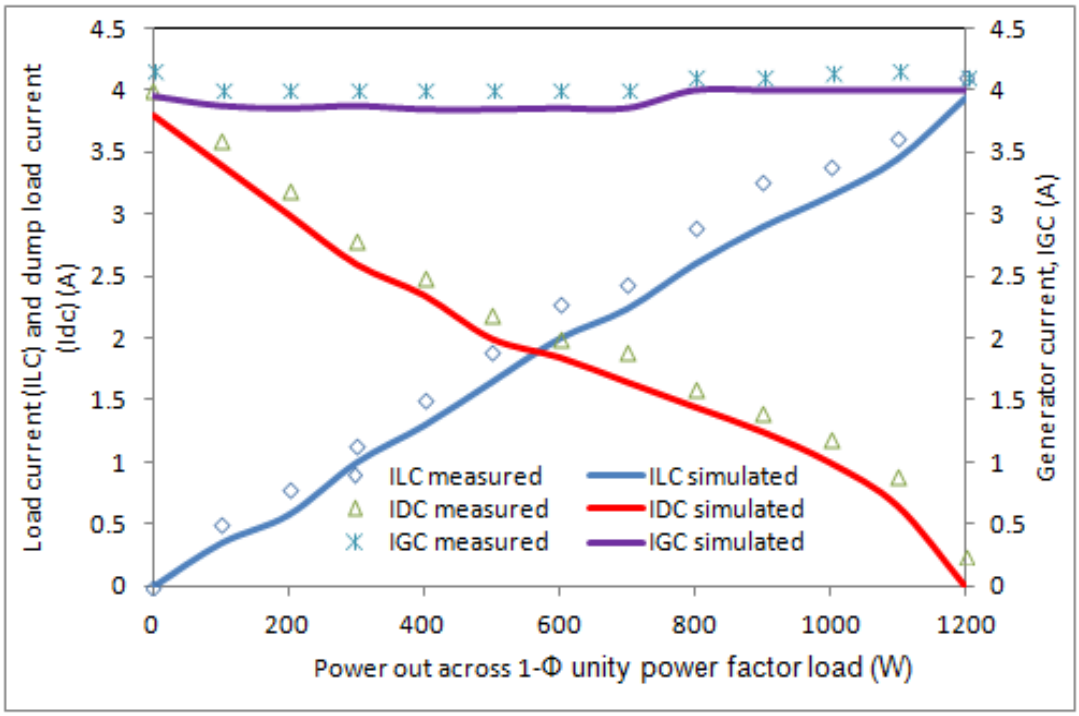

Fig. 8.13 Variation pattern of load current, dump load current and generator current with power output

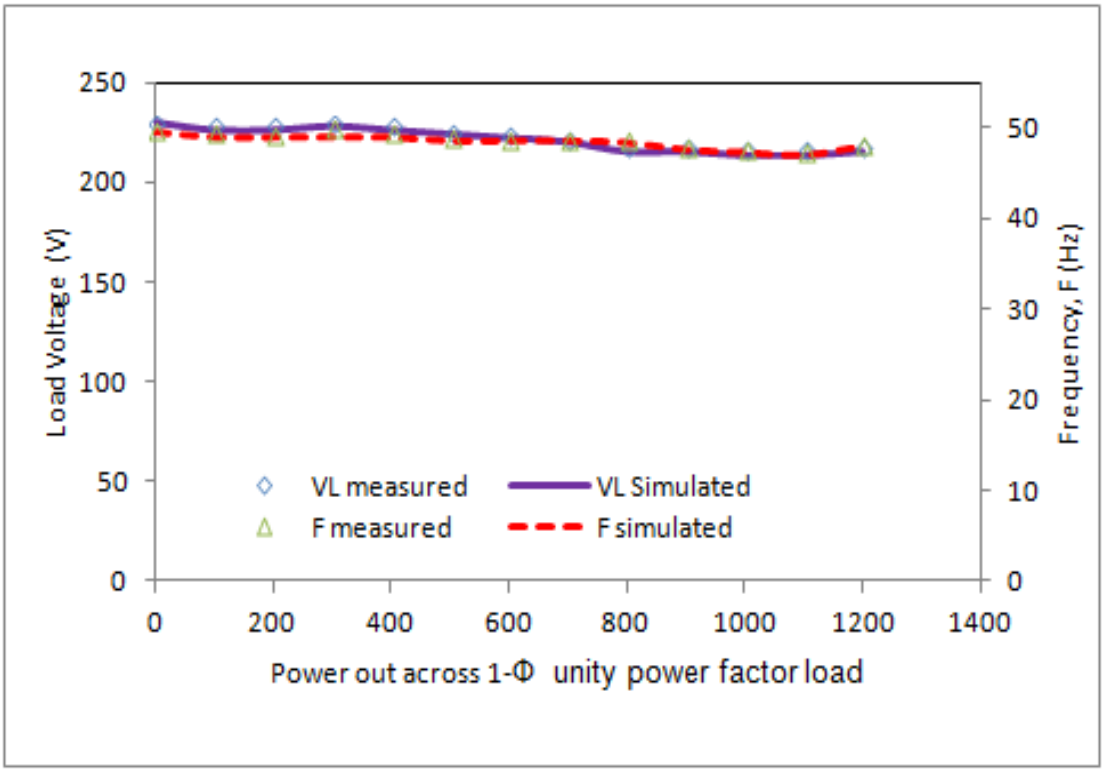

Fig. 8.14 Variation pattern of load voltage and frequency with power output

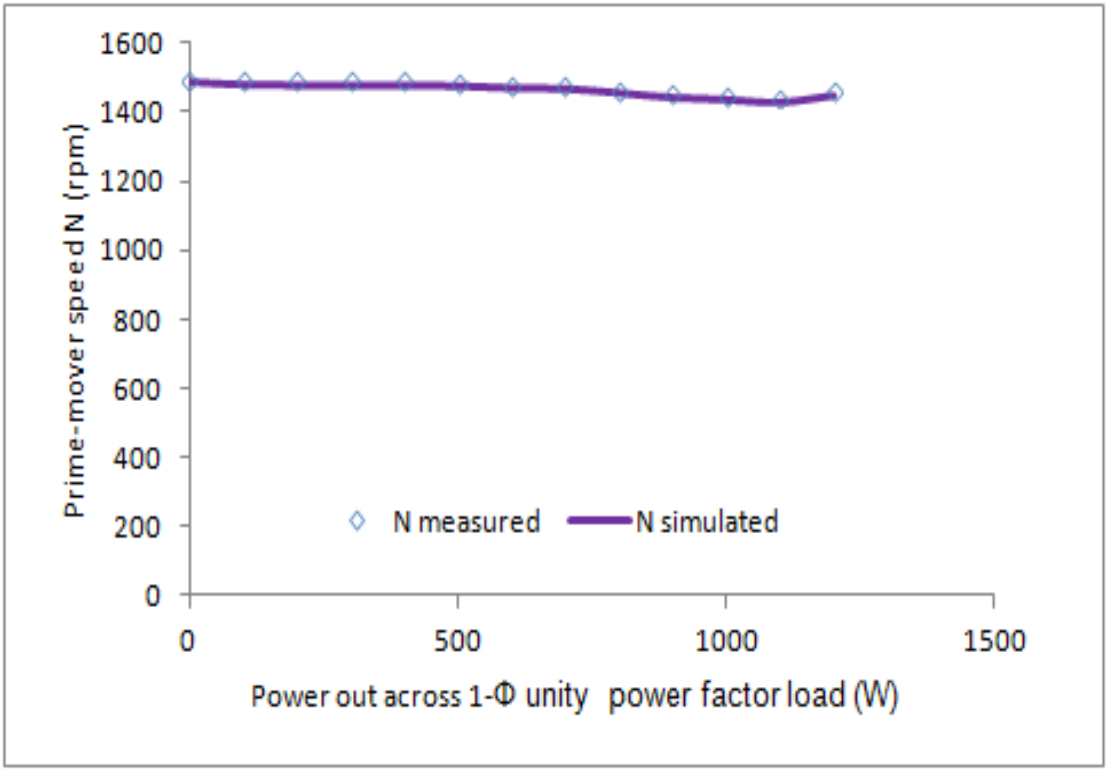

Fig. 8.15 Variation pattern of prime-mover speed with power output

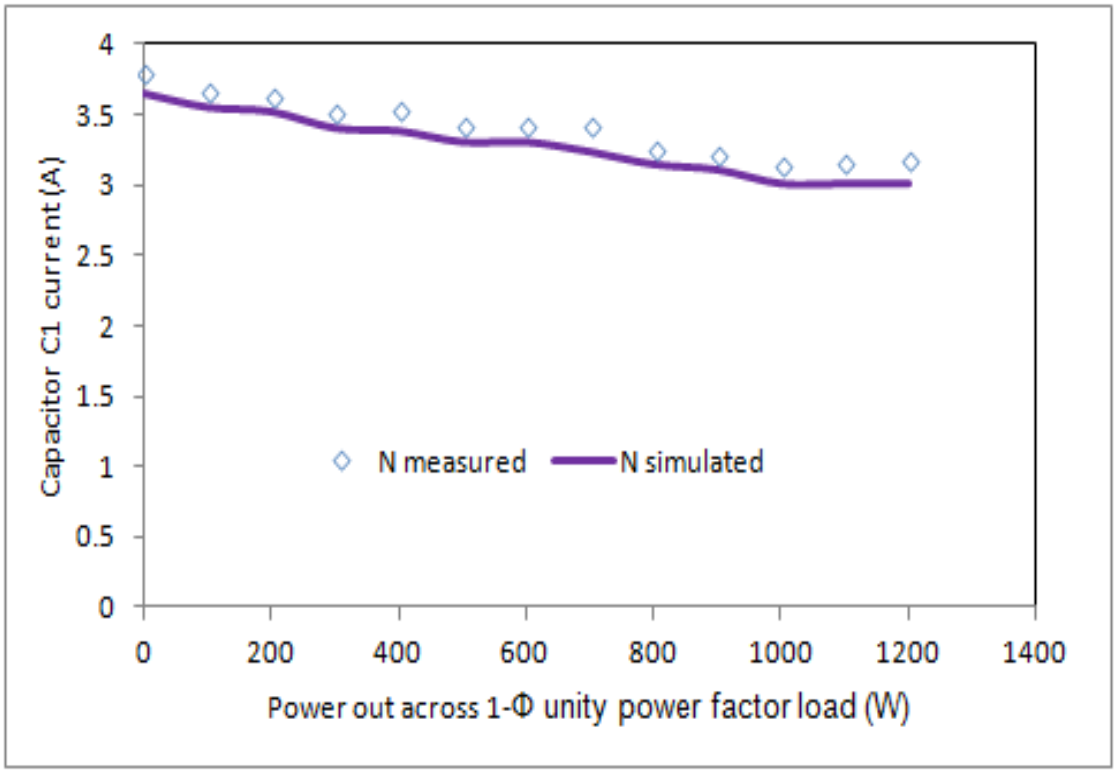

Fig. 8.16 Variation pattern of capacitor current with power output

decays and decays to almost zero at a load of 1.2 kW. This controller current is complementary type and helps in retaining constant load on the generator. Hence voltage and frequency of the generator is constant as depicted in Fig. 8.14.

The prime-mover speed is almost retained constant throughout the operation under varying load conditions [Fig. 8.15]. There is slight decrease in capacitor current with load as desired and is depicted in Fig. 8.16.

Fig. 8.17 depicted the Total Harmonic Distortion values in IAG-EGLC voltage and current under 1.2 kW consumer loads. It is observed that the THD in generated voltage is reduced to 7.3% and the IAG current is 22.2% under 1.2 kW consumer load.

8.7 SUMMARY

A PWM based IC -3524 is explored in this chapter for the generation of driving signals for IGBT based chopper switch.

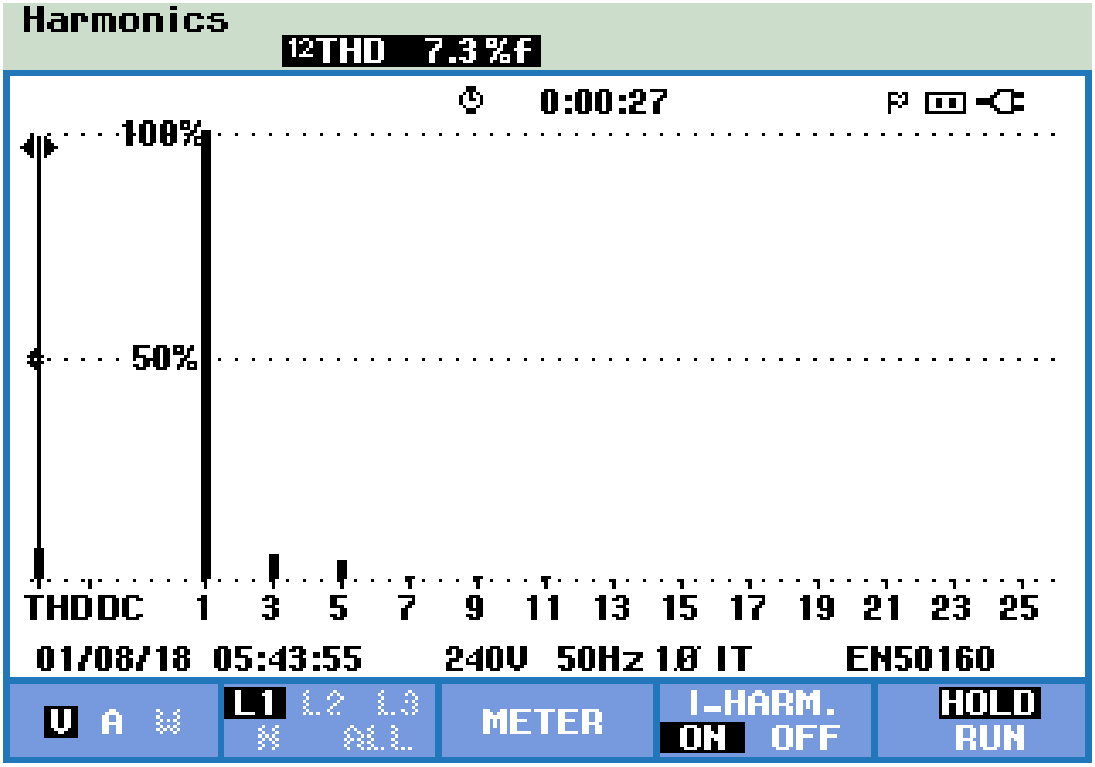
Harmonics
12THD 7.3%f
0:00:27
100%
50%
THDDC 1 3 5 7 9 11 13 15 17 19 21 23 25
01/08/18 05:43:55 240V 50Hz 1Ø IT EN50160
V A W
L1 L2 L3
N ALL
METER
I-HARM.
ON OFF
HOLD
RUN

(a)

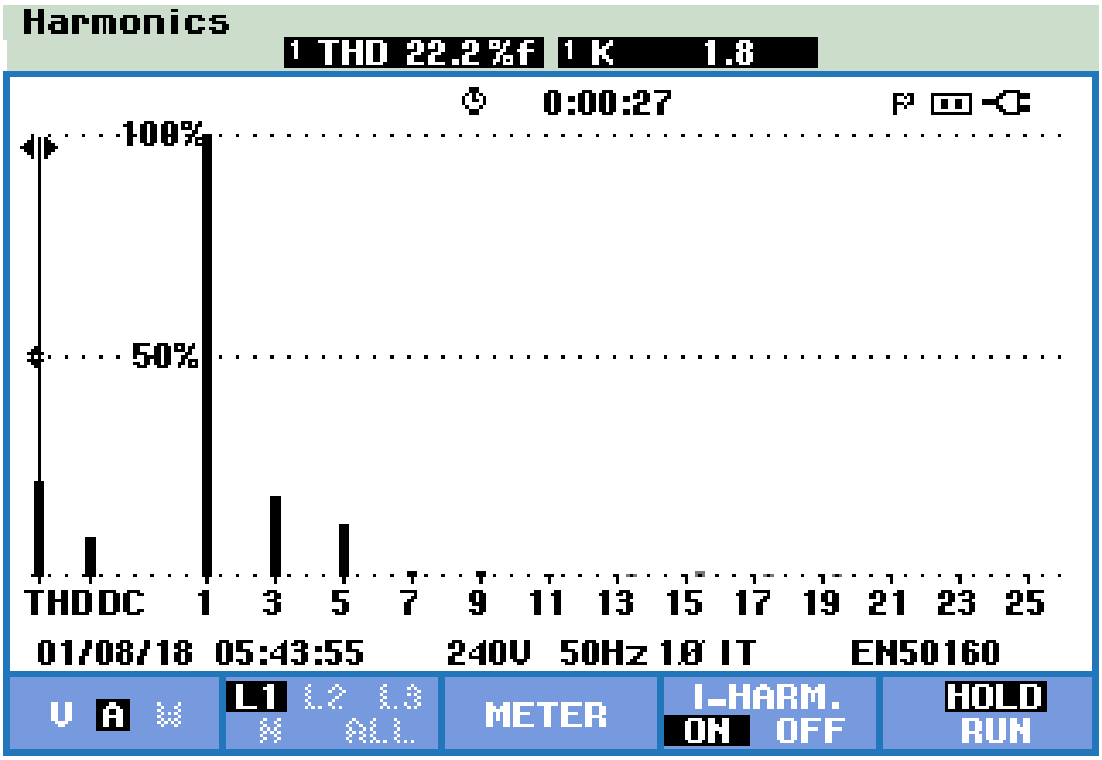
Harmonics
1 THD 22.2%f 1 K 1.8
0:00:27
100%
50%
THDDC 1 3 5 7 9 11 13 15 17 19 21 23 25
01/08/18 05:43:55 240V 50Hz 1Ø IT EN50160
V A W
L1 L2 L3
N ALL
METER
I-HARM.
ON OFF
HOLD
RUN

(b)

Fig. 8.17 THD in voltage and current of IAG-EGLC under 1.2 kW load

The voltage control aspect of an IAG is based on constant load on the IAG. The load on the generator has been maintained constant using dump load in shunt with single-phase load. From experimental investigations the following inferences are made:

- From table 1, the case study 3 revealed that a C-2C capacitor connection of 50-100μF provide a supply system with better voltage regulation and minimum phase unbalance as desired.

- It provided a desirable voltage and frequency support to the IAG but with a THD value of 7.3% and 22.2% in generated voltage and current which is little bit high than the prescribed ranges in IEEE-519 std. Thus the proposed controller supports both voltage and frequency of IAG but with little less power quality of voltage and current.

- The controller cost is approximately less than 5000 Rs. Its cost is very-very less as compared to the various existing microcontroller and DSP based ELC's. A single IC operation proves to be sufficient for voltage and frequency support of IAG. Thus an IAG with this IC based EGLC can electrify the rural communities with desirable voltage and frequency support with minimum cost of generation, electrification and voltage and frequency support.

- The IAG-EGLC system is shown practically to deliver 32% (1.2 kW) of the rated power (3.73 kW) to the single-phase load due to some laboratory hardware constraints.

CHAPTER 9

IMPLEMENTATIONOF FUZZY LOGIC (FL) AND PI BASED 3-LEGGED VSI CONTROLLER FOR AN ISOLATED ASYNCHRONOUS GENERATOR (IAG)

9.1 GENERAL

Now a day renewable technologies are used for small off-grid applications such as in remote and rural areas. Due to the environmental concerns and diminution of conventional energy sources, renewable energy sources such as biomass, wind, solar and small or mini/micro hydro are grabbing the attention of researchers. Traditionally, synchronous generator using conventional energy sources have been used for electrical power generation. But at present an IAG using non-conventional or renewable energy sources are being used for electric power production due to certain advantages over synchronous generator. These advantages are operational simplicity, no need of synchronization, no issue of hunting, brushless and rugged rotor construction, minimum maintenance cost, good dynamic behavior and ability to generate power even under different speeds [93-97] .The major disadvantage of an IAG is reactive power consumption, its voltage and frequency variation with load and speed. Hence, a lot of research is done on the development and implementation of voltage and frequency control of an IAG at varying loads [60, 76, 98-114]. The design aspects of such controllers have been given little attention in literature [106]. To maintain constant terminal voltage at varying load, an attempt has been made using fixed capacitor topology, thyristor controlled reactor (TCR), saturable type reactors and short shunt type connections [97-99]. The drawback of these controllers is that the voltage control is discrete and hence injects harmonics on the generation side of the system. With the advancement of solid state power electronics devices, FACTS device are becoming more popular now a days as these devices are more environment friendly and helps to deliver the electrical power more economically, reliably and efficiently. The biggest constrained in using SVC is large size capacitors and reactors [100-101]. The non-linear loads introduce harmonics into the system and make the load current discontinues in nature. Hence once again the need of controller is realized to reduce the harmonics injected into the system and can make voltage and frequency

regulation better. In almost all the published literature, mainly CPI controllers are employed for reactive and active power control to obtain voltage and frequency support. The main aspiration behind its use is its simplicity. But on the counterpart, there is difficulty in achieving the fine tuning of the gains to obtain desired performance particularly when more than one PI controllers are used. The second biggest drawback is encountered when the system is having non-linearity.

Keeping in view all the facts discussed above, first time two types of FL based controllers are recommended and tested for a 3-legged VSI. This chapter is systematically covered as (i) Introduction (ii) Overview of Generating System and 3-legged VSI (iii) Modeling of template based control scheme for a 3-legged VSI for terminal voltage and frequency regulation (iv) FL based design of Mamdani and Sugeno type controller for ac and dc voltage control (v) Design of 3-legged VSI Controller for simulation testing (vi) Discussions on obtained simulated results (vii) Conclusions

9.2 OVERVIEW OF GENERATING SYSTEM AND 3-LEGGED VSI

The whole generating or energy conversion system depicted in Fig. 9.1 and 9.2 entails of three main components: An IAG, 3-legged VSI and consumer load. An IAG entails of three-phase asynchronous machine, prime mover and 3-phase delta connected capacitors. The capacitors of appropriate value are connected across the terminals of an IAG to obtain rated voltage at rated speed under zero load conditions. These capacitors are permanently connected (long time rated) to the machine terminals to supply wattless (var) power to the generator and the consumer load. The increased requirement of wattless (var) power is supplied by the VSI under changing consumer load conditions. The VSI based controller generates lagging or leading current in order to keep the ac voltage constant with change in consumer load. It fetches active power from the generator for capacitor charging at dc end side. The output of the 3-legged VSI is AC and is connected to the IAG terminals through filter L. A capacitor across the DC side is as an energy storage device and acts as a dc voltage source on the input side of VSI.

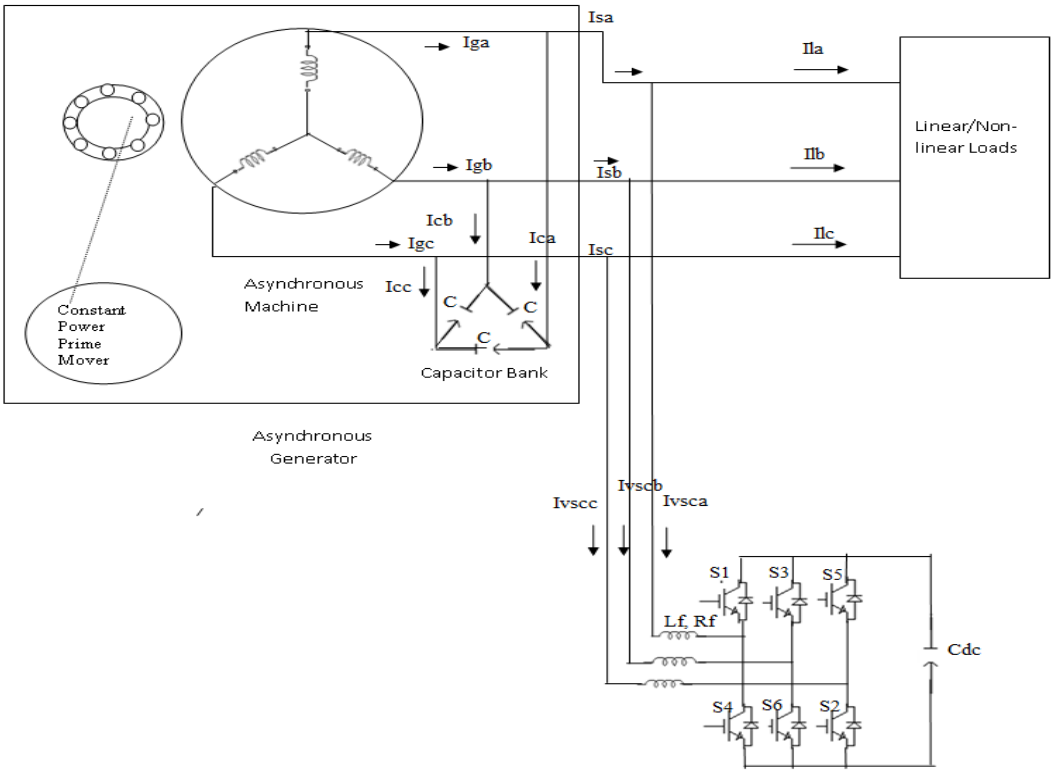

Fig. 9.1 Schematic diagram of IAG with 3-legged CC-VSI

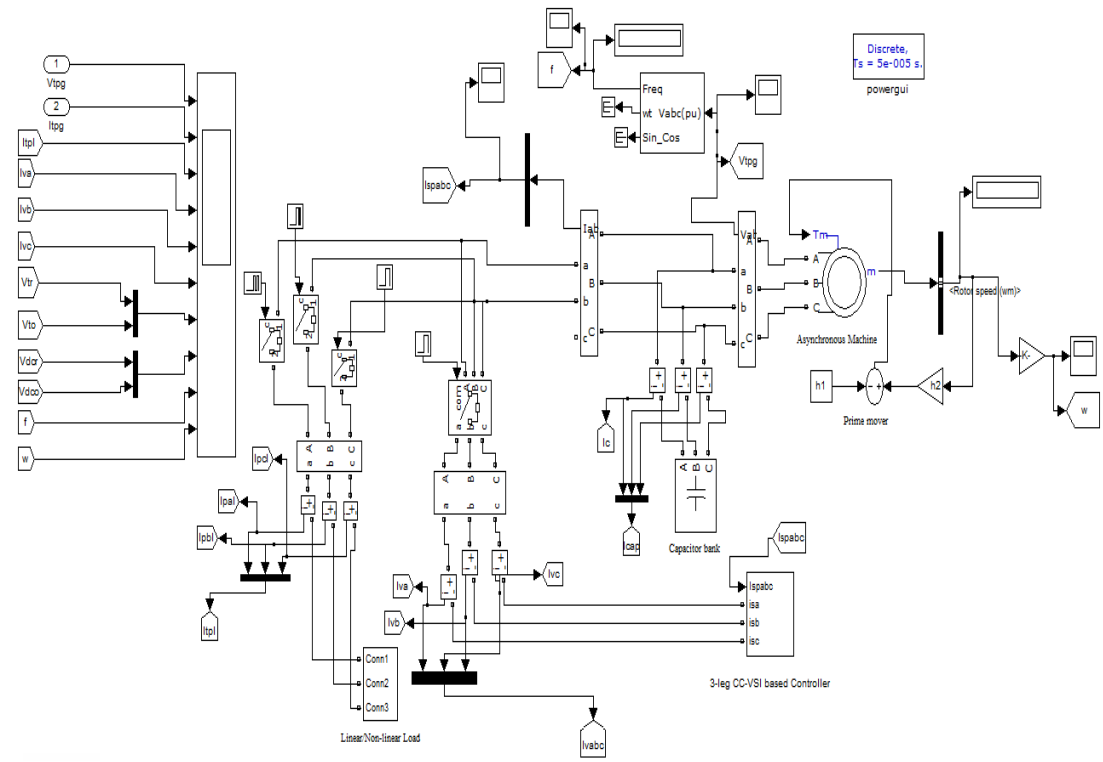

Fig. 9.2 Block diagram representation of the whole generating system with a 3-legged VSI Controller.

9.3 MODELING OF TEMPLATE BASED CONTROL SCHEME FOR A 3-LEGGED VSI FOR TERMINAL VOLTAGE AND FREQUENCY REGULATION [104, 106, 107, 108]

A template based control strategy is addressed here to control the generated ac voltage of an IAG. It is based on the production of reference supply currents. The per-phase voltage of phase a, b and c (v_{apg}, v_{bpg} and v_{cpg}) are sinusoidal quantities and its amplitude (V_{abcg}) is evaluated as

$$V_{abcg} = \left\{\frac{2}{3}\left(v_{apg}^2 + v_{bpg}^2 + v_{cpg}^2\right)\right\}^{\frac{1}{2}} \tag{9.1}$$

The unit amplitude templates (u_{apt}, u_{bpt}, u_{cpt}) are three-phase sinusoidal quantities and these templates in line or phase with v_{apg}, v_{bpg}, v_{cpg} are evaluated as

$$u_{apt} = \frac{v_{apg}}{V_{to}} \tag{9.2}$$

$$u_{bpt} = \frac{v_{bpg}}{V_{to}} \tag{9.3}$$

$$u_{cpt} = \frac{v_{cpg}}{V_{to}} \tag{9.4}$$

The quadrature unit amplitude templates (w_{aqt}, w_{bqt}, w_{cqt}) are also sinusoidal quantities and are evaluated from the from the quadrature transformation of u_{apt}, u_{bpt} and u_{cpt} as

$$w_{aqt} = \frac{-u_{bpt}}{\sqrt{3}} + \frac{u_{cpt}}{\sqrt{3}} \tag{9.5}$$

$$w_{bqt} = \frac{\sqrt{3}}{2} u_{apt} + \frac{(u_{bpt} - u_{cpt})}{2\sqrt{3}} \tag{9.6}$$

$$w_{cqt} = \frac{-\sqrt{3}}{2} u_{apt} + \frac{(u_{bpt} - u_{cpt})}{2\sqrt{3}} \tag{9.7}$$

9.3.1 90º Phase Shift Part of Reference Supply Currents

The error in generated ac voltage $V_{acer(m)}$ at the mth sampling instant is:

$$V_{acer(m)} = V_{tr(m)} - V_{to(m)} \tag{9.8}$$

$V_{tr(m)}$ represents the amplitude of the reference generated ac voltage and $V_{to(m)}$ is the amplitude of the output generated ac voltage across the IAG terminals at m^{th} instant of time.

This error in generated ac voltage is fed to CPI controller 1 and its output current $\left(I^*_{stq(m)}\right)$ for retaining generated ac voltage constant at the mth instant is formulated as:

$$I^*_{stq(m)} = I^*_{stq(m-1)} + k_{pav}\left\{V_{acer(m)} - V_{acer(m-1)}\right\} + k_{iav}V_{acer(m)} \tag{9.9}$$

k_{pav} , k_{iav} are the constants of proportional and the integral gain of the conventional PI controller 1.

$V_{acer(m)}$ represents the error in generated ac voltage at mth instant, $V_{acer(m-1)}$ is the error in generated ac voltage at (m-1)th instant.

The 90° phase shift part of the reference supply currents of each phase are obtained as

$$i^*_{spaq} = I^*_{stq}w_{aqt}; \tag{9.10}$$

$$i^*_{spbq} = I^*_{stq}w_{bqt}; \tag{9.11}$$

$$i^*_{spcq} = I^*_{stq}w_{qct} \tag{9.12}$$

9.3.2 In - Phase Part of Reference Supply Currents

The error in dc capacitor voltage $V_{dcer(m)}$ at the mth instant is:

$$V_{dcer(m)} = V_{dcr(m)} - V_{dco(m)} \tag{9.13}$$

$V_{dcr(m)}$ represents the reference dc capacitor voltage and $V_{dco(m)}$ is the output value of dc capacitor voltage

This error in dc capacitor voltage is fed to conventional PI controller 2 and its output current $\left(I^*_{std(m)}\right)$ for retaining dc capacitor voltage constant at the mth instant is expressed as:

$$I^*_{std(m)} = I^*_{std(m-1)} + k_{pdv}\left\{V_{dcer(m)} - V_{dcer(m-1)}\right\} + k_{idv}V_{dcer(m)} \tag{9.14}$$

k_{pdv} and k_{idv} represents the proportional and integral gains constant of conventional PI controller 2.

Various in phase parts of reference supply currents of each phase are evaluated as:

$$i^*_{sad} = I^*_{std}u_{apt}; \tag{9.15}$$

$$i^*_{sbd} = I^*_{std}u_{bpt}; \tag{9.16}$$

$$i^*_{scd} = I^*_{std}u_{cpt}; \tag{9.17}$$

9.3.3 Total Reference Supply Currents

The total reference supply current of each phase is of supply current is evaluated as:

$$i^*_{sat} = i^*_{spaq} + i^*_{sad} \tag{9.18}$$

$$i^*_{sbt} = i^*_{spbq} + i^*_{sbd} \tag{9.19}$$

$$i^*_{sct} = i^*_{spcq} + i^*_{scd} \tag{9.20}$$

9.3.4 PWM Current Controller (Hysteresis Controller)

The various gate drive signals for the IGBT's devices of the 3-legged CC-VSI are generated from the PWM based controller.

The supply currents are first sensed (i_{spa}, i_{sbp} and i_{spc}) and then the errors in supply currents of each phase are evaluated as:

$$i_{saerr} = i^*_{sat} - i_{spa} \tag{9.21}$$

$$i_{sberr} = i^*_{sbt} - i_{spb} \tag{9.22}$$

$$i_{scerr} = i^*_{sct} - i_{spc} \tag{9.23}$$

If the error in supply current signal of phase 'a' after amplification is found to be more / less than the triangular shape wave (10 kHz) then IGBT device SW1 is closed / open and IGBT device SW4 is open / closed and the switching function SF value is fixed to one / zero.

Same kind of logic applies to phase 'b' and 'c' of VSI. The complete layout of the whole control strategy [Eq. (9.1) – Eq. (9.23)] for ac and dc voltage control is depicted in Fig. 9.3.

9.4 FL BASED DESIGN OF MAMDANI AND SUGENO TYPE CONTROLLER FOR AC AND DC VOLTAGE CONTROL

In FL based controller, the conventional PI controllers 1 and 2 [Eq. (9.9) and Eq. (9.14)] are interchanged by Mamdani and Sugeno type fuzzy controller. These controllers have two inputs and one output. The two inputs are error in voltage (ac and dc) and the rate of change of error voltage (ac and dc). The MF for both the inputs and output are Gaussian for Mamdani type FL controller is shown in Fig. 9.4. The variation range for both the inputs and outputs is from -1 to 1. The mapping of input

and output MF is established through 49 rules based on if-then statement given in Table 8. In this table: NBG, NMM, NSL, ZR, PSL, PMM, PBG are negative big, negative medium, negative small, zero, positive small, positive medium and positive big parts of membership function (MF). The various FIS properties of Gaussian MF in Mamdani type FIS are: And method: min, Or method: max, Implication: min, Aggregation: max and defuzzification method: centroid. The scaling factor for the V_{acer}, CV_{acer} and output are -0.116, 0.011 and 0.01. The scaling factors for the V_{dcer}, CV_{dcer} and output are -0.0114, -0.001 and 1.

In case of Sugeno type FL controller, triangular MFs are employed for both the inputs and singleton membership function for the output. The variation range for both the inputs and outputs are from 0 to 1.The mapping of input and output MF in this type of controller is again established through 49 rules based on if-then statement given in Table 8. The various FIS properties of triangular and singleton MF in Sugeno type FIS are: And method: prod, Or method: probor, Implication: min, Aggregation:

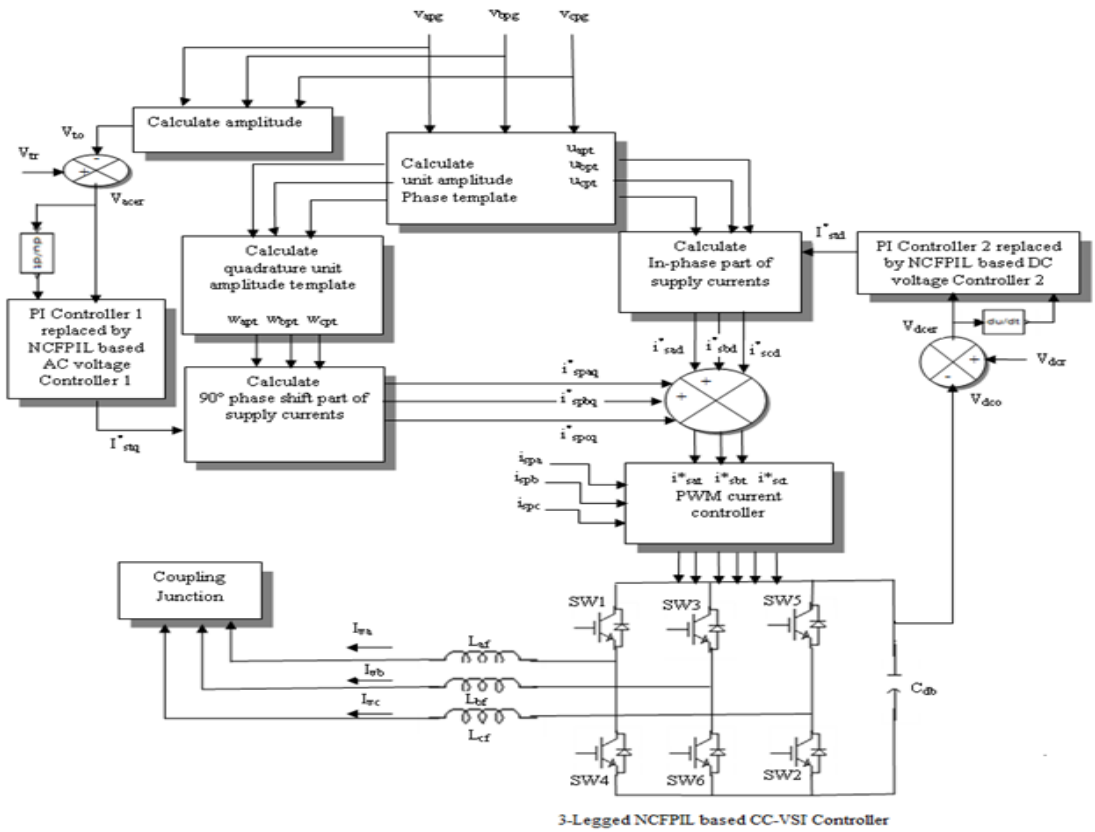

Fig. 9.3 Complete Layout of the control strategy of a FL based 3-legged VSI Controller

max and Defuzzification method: wtaver. The scaling factor for the V_{acer}, CV_{acer} and output are -0.05, -0.011 and -0.1. The scaling factors for the V_{dcer}, CV_{dcer} and output are -0.5, -0.001 and -0.5.

9.5 DESIGN OF 3-LEGGED VSI CONTROLLER FOR SIMULATION TESTING

The detailed design procedure of a 3-legged VSI for a 3- phase 3- wire distribution system is discussed in this section. The kVAR rating required should be 140-160% of rated generated power for supplying the wattless (var) power to the lagging 0.8 p.f load [104]. So, the kVAR rating of the VSI required for an IAG of 3.73 kW, 460 V is approximately 5 kVAR (140%) [Appendix E]. Therefore, the apparent power (S_{ap}) in kVA [104] is evaluated as

$$S_{ap} = \sqrt{P_{ap}^2 + Q_{ap}^2} = 6\text{kVA} \tag{9.24}$$

So, the current rating of the 3-legged VSI

$$S_{ap} = \sqrt{VI_s} = 6\text{kVA} \tag{9.25}$$

The peak value of this current is

$$I_s = 7.53\text{A} \tag{9.26}$$

The value of current ripple through filter inductor L (selecting 5% of max value of current)

$$I_{Lripplepk-pk} = 0.53245\text{A} \tag{9.27}$$

The value of filter inductor L, dc capacitor C_{db} can be evaluated by selecting modulation index as (m_i) "1" and carrier frequency (f_s) as 10 kHz.

The dc voltage for VSI can be evaluated by using Eq. (9.28)

$$V_{db} = \sqrt[2]{2}\left(V/\sqrt{3}\right)/m_i = 750\text{V} \tag{9.28}$$

The selected value of dc voltage is 750V.

The filtering inductance of each line for VSI can be by estimated using Eq. (9.29)

$$L_{af} = L_{bf} = L_{cf} = \left(\sqrt{3}\right)m_i V_{db}/12af_s\, i_{cr(p-p)} = 17\text{mH} \tag{9.29}$$

The selected value of filtering inductance is 17mH.

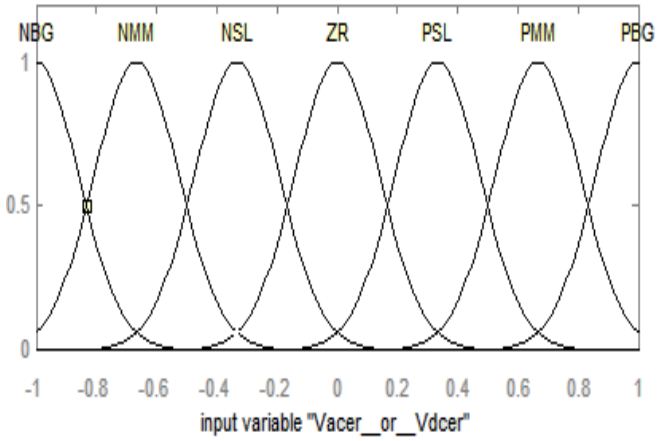

(a)

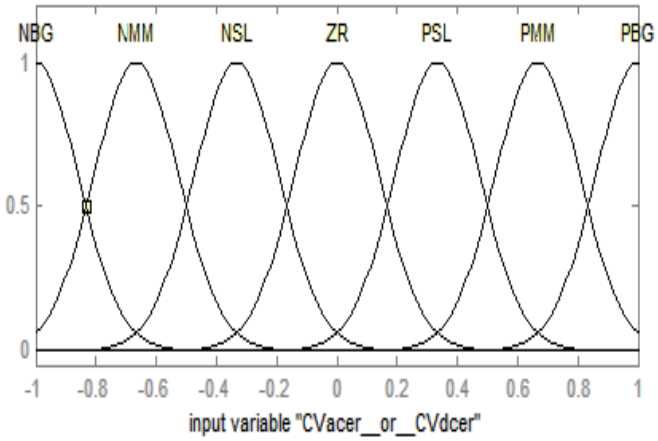

(b)

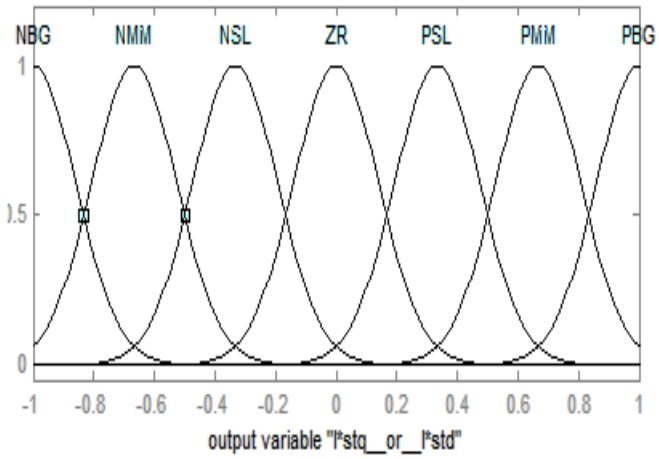

(c)

Fig. 9.4 Membership function representation (a) input variable error in ac or dc voltage (V_{acer} or V_{dcer}) (b) input variable change in ac or dc voltage (CV_{acer} or CV_{dcer}) (c) output variable currents (I^*_{stq} or I^*_{std})

Table 7: Mapping representation of inputs and output membership functions through if- then rule-base

V_{acer} /V_{dcer} / CV_{acer} /CV_{dcer}	NBG	NMM	NSL	ZR	PSL	PMM	PBG
NBG	NBG	NBG	NMM	NSL	ZR	PSL	PMM
NMM	NBG	NBG	NMM	NSL	PSL	PMM	PBG
NSL	NBG	NBG	NMM	NSL	PSL	PMM	PBG
ZR	NBG	NMM	NSL	ZR	PSL	PMM	PBG
PSL	NBG	NMM	NSL	PSL	PMM	PBG	PBG
PMM	NBG	NMM	NSL	PSL	PMM	PBG	PBG
PBG	NMM	NSL	ZR	PSL	PMM	PBG	PBG

The dc capacitance can be evaluated by using Eq. (9.30)

$$V_{db\ ripple} = 1/C_{db} \int i_c\, dt = I_{avg}/(2wC_{db}) \tag{9.30}$$

Where I_{avg} is the average value of current flowing through the 3-legged VSI. Its value may be evaluated by taking the average current of single-phase nature load to be 90% of the peak value of compensator current.

$$I_{avg} = 0.9 * 7.53 = 6.777A \tag{9.31}$$

Consider voltage ripple in V_{db} of order 2% then

$$V_{db\ ripple} = 2\%\ of\ V_{db} = 15V \tag{9.32}$$

Then C_{db} can be evaluated by using Eq. (9.30)

$$C_{db} = 600\mu F \tag{9.33}$$

The selected value of C_{db} is 2000 µF for the system under consideration.

9.6 DISCUSSIONS ON OBTAINED SIMULATED RESULTS

The FL based 3-legged VSI has been designed and tested for an IAG of rating 5 HP, 460V, 60Hz [Appendix E]. The simulated results accomplished after simulations testing under different operating conditions are manifested in Figs. 9.5-9.14.

9.6.1 Performance of an IAG-VSI System Furnishing Pure Linear Resistive (R) Load

Fig. 9.5 from top to bottom manifests the simulated results outcomes of the three-phase generated ac voltages (V_{abcg}), three-phase generated currents (I_{abcg}), per-phase load currents (I_{al}, I_{bl}, I_{cl}), per-phase VSI currents (I_{va}, I_{vb}, I_{vc}), the amplitude of the output generated ac voltage along-with its reference value (V_{to} - V_{tr}), the dc output capacitor voltage along-with its reference value (V_{dco} - V_{dcr}), an IAG frequency (f) and an IAG speed (w).

At 0.6 sec, a three-phase balanced delta connected full load is applied between phase to phase, a few drop in the ac and dc voltage of the 3-legged VSI is observed but recovers quickly due to the proper controlling action of the FL based VSI controller 1 and 2. During balanced load region i.e from 0.6 to 0.8 sec, load current rises and VSI currents in all the 3-phases drops to maintain constant load on the IAG terminals. Hence, this controller is competent enough to support both voltage and its frequency. At 0.8 sec, one phase of the three-phase balanced load is opened or disconnected from an IAG terminal. It is concluded that the FL based 3-legged VSI controller is able to regulate the 3-phase IAG voltage even during the situation of unbalanced consumer load conditions. At 0.9 sec, another phase of the load is disconnected from an IAG terminal. At 0.95 sec, one phase of the load is connected again and at 1.055 sec another phase of the load is reconnected and the system again becomes balanced. A rise and drop in the dc voltage from the reference dc voltage is observed at the point of disconnecting and connecting of the load. This shows that the dc capacitor across 3-legged VSI is charging and discharging when the load is balanced /unbalanced. Thus, the 3-legged VSI based controller is capable of balancing the load the generator even under the situation of unbalanced load conditions on the system. Hence, the controller is intelligent enough to support both the voltage and frequency of an IAG throughout the operating conditions as depicted in Fig. 9.6 and

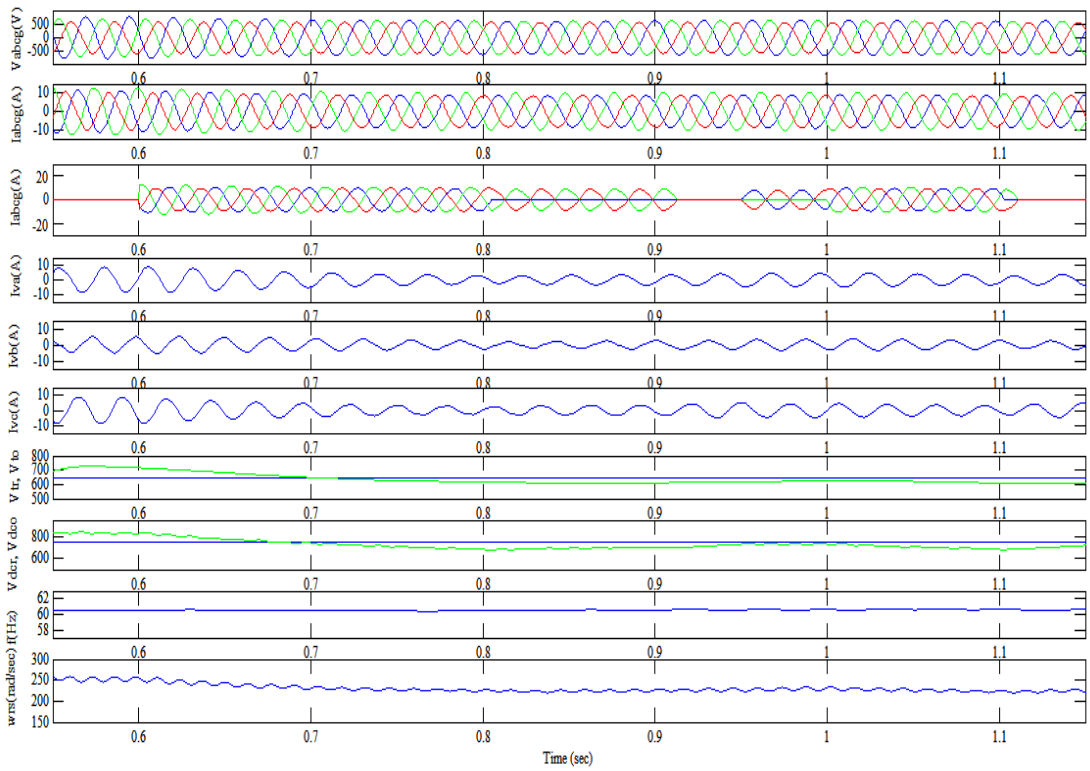

Fig. 9.5 Performance of an IAG furnishing resistive load using conventional PI based controller.

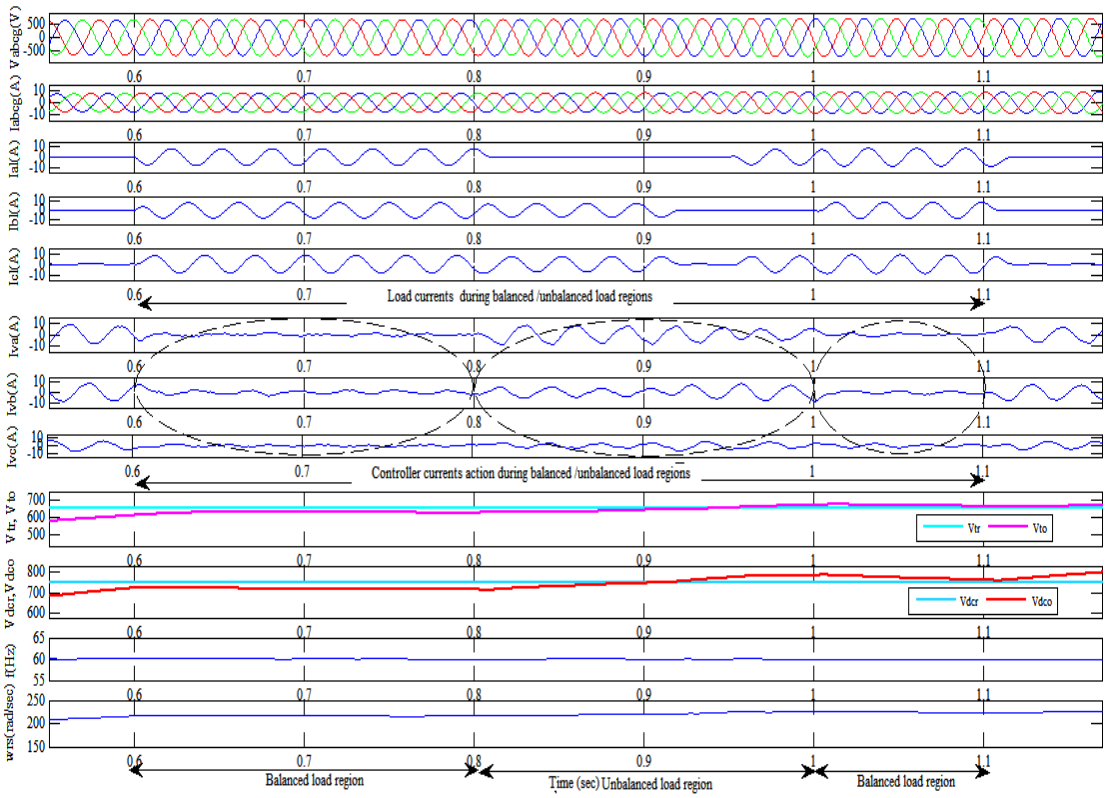

Fig. 9.6 Performance of an IAG furnishing resistive load using FL based Mamdani type fuzzy logic controller.

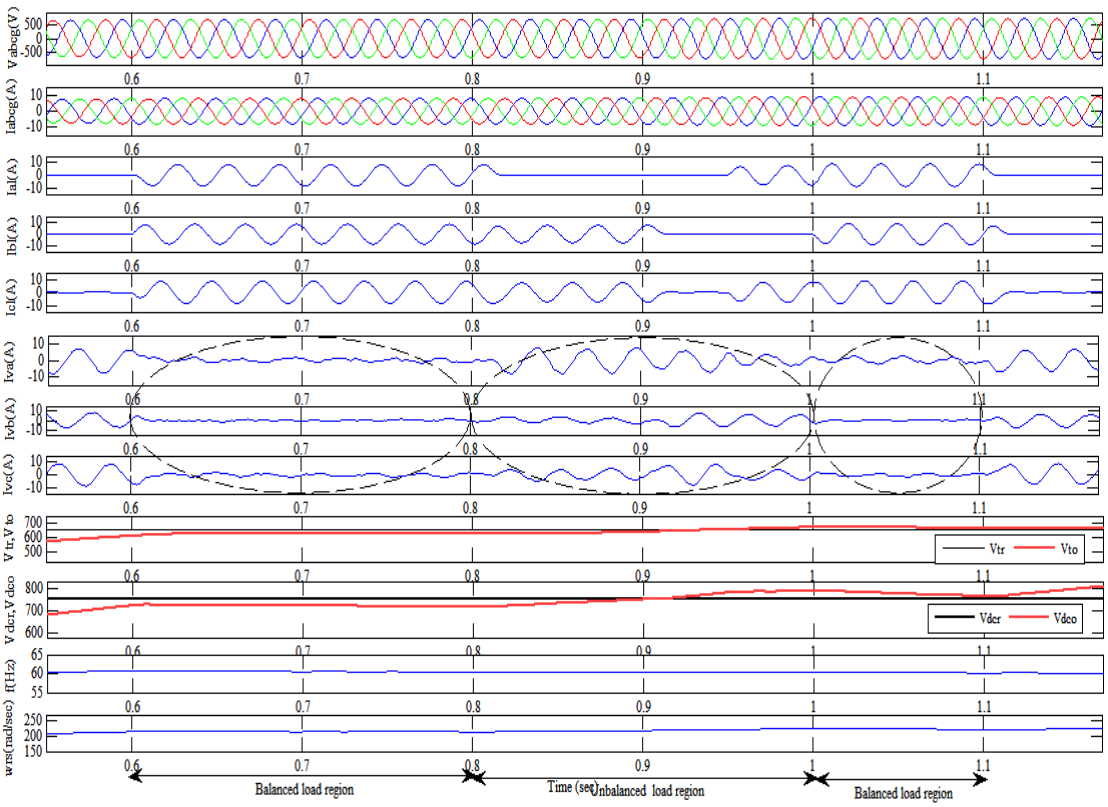

Fig. 9.7 Performance of an IAG furnishing resistive load using FL based Sugeno type fuzzy logic controller.

Fig. 9.7. The same simulated outcomes are also accomplished using Sugeno type fuzzy logic controller as illustrated in Fig. 9.7. The performance enhancement in terms of voltage regulation (ac and dc voltage), THD value, settling time, rise time is superior to conventional PI [Table 3 and Fig. 9.14].

9.6.2 Performance of an IAG-VSI system furnishing linear resistive-inductive (R-L) load

Fig. 9.8 manifests the simulated results outcomes of an IAG furnishing reactive load. At 0.6 sec, an IAG is loaded with a three-phase balanced reactive load R-L load current increases and controller reactive current decreases to maintain constant load on the generator. At 0.8 sec, one phase of the load is removed, creating unbalance, at 0.9 another phase of the load is removed. During unbalanced load region, unbalanced currents flow through the controller to maintain constant load on the generator. At 0.95 and 1.055 sec another phases of the load are again connected, again the system

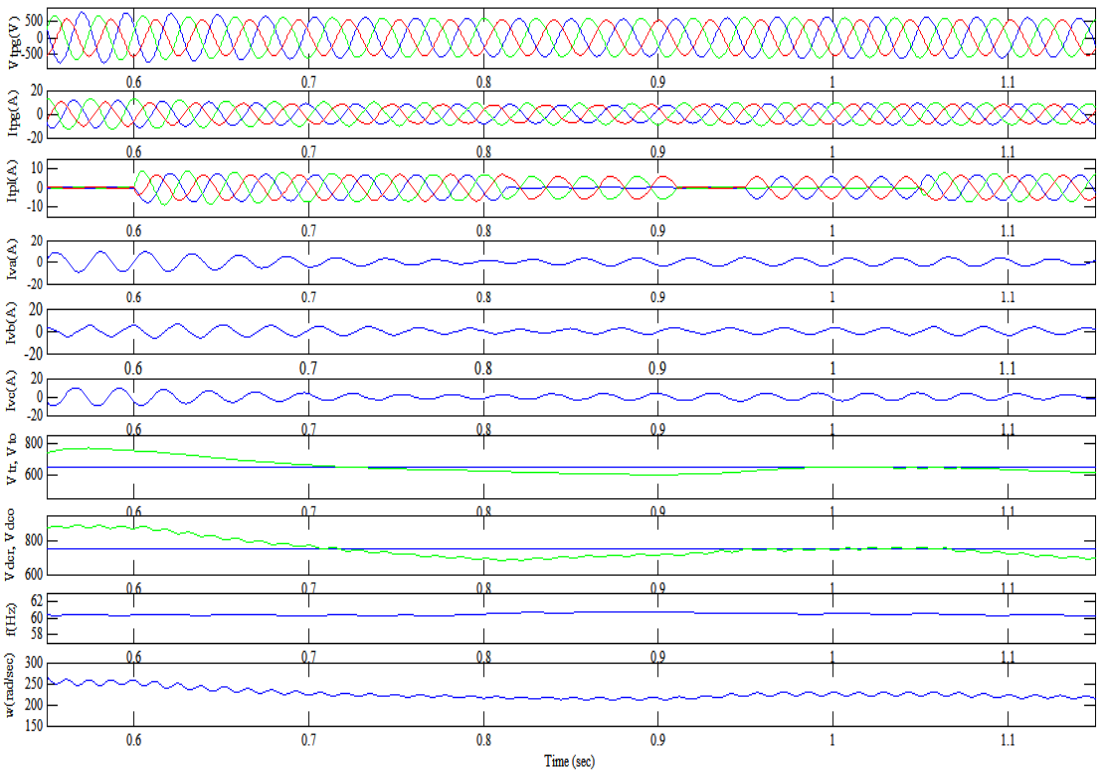

Fig. 9.8 Performance of an IAG furnishing reactive load using conventional PI based controller.

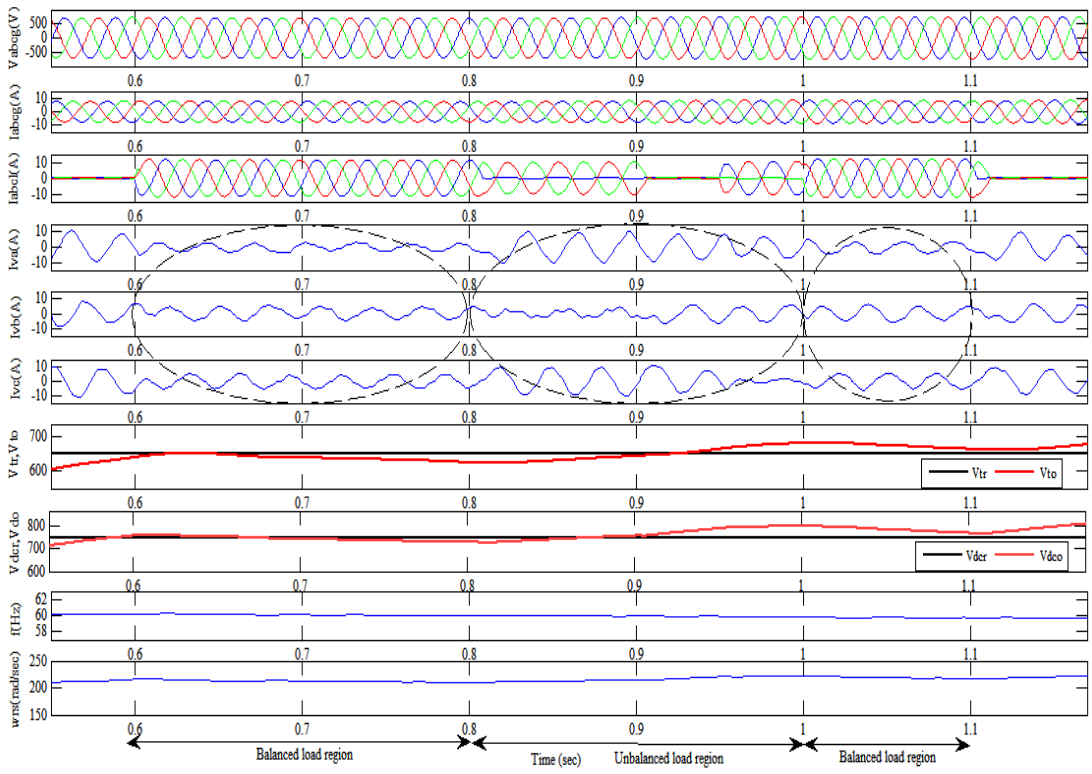

Fig. 9.9 Performance of an IAG furnishing reactive load using FL based Mamdani type fuzzy logic controller.

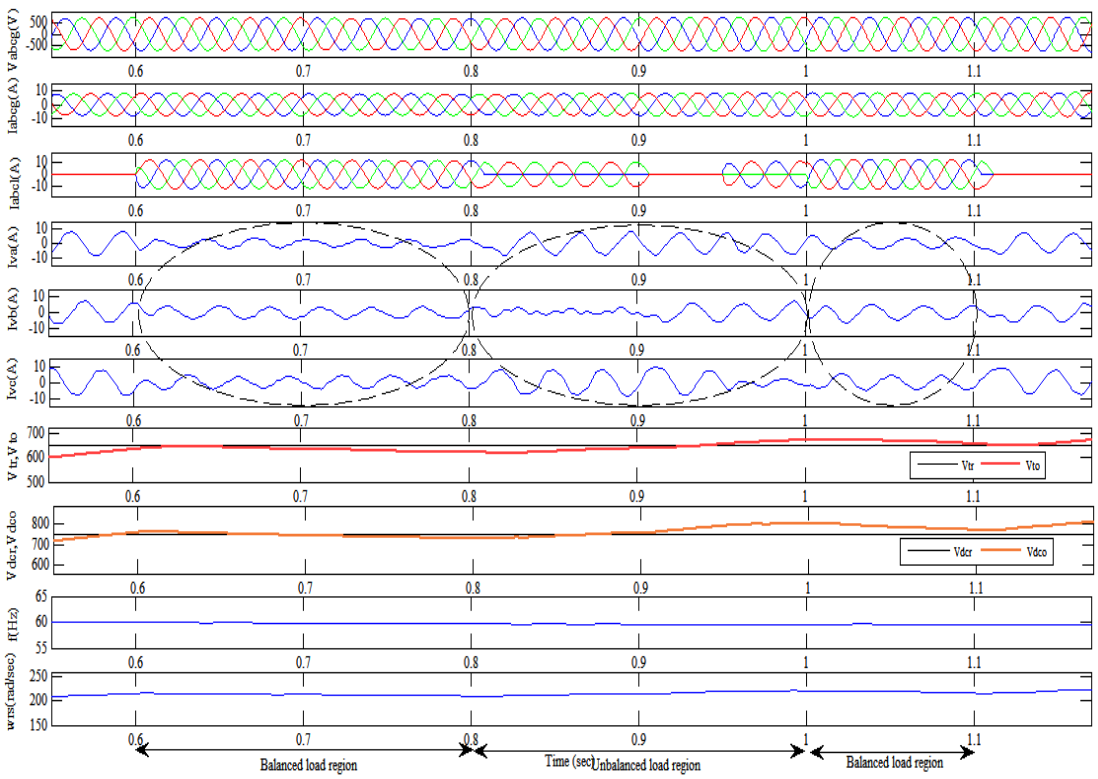

Fig. 9.10 Performance of an IAG furnishing reactive load using FL based Sugeno type fuzzy logic controller.

becomes balanced. During the complete operating region of switch ON and switch OFF the load, it is inferred that the generated ac voltage, generated ac current, frequency and speed are constant. The same performance characteristics accomplished under same operating region using Mamdani and Sugeno type Fuzzy logic controller is depicted in Fig. 9.9 and Fig. 9.10. From the accomplished simulated outcomes, it is inferred that performance enhancement is better in FL based controller than CPI controller [Table 9 and Fig. 9.14].

9.6.3 Performance of an IAG-VSI System Furnishing Non-Linear Rectifier Load

Fig. 9.11 manifests the performance of an IAG system furnishing non-linear rectifier load. The ac current of the FL controller is discontinuous in nature. These discontinuous currents inject harmonics into the system and pollute the system. The 3-legged VSI controller eliminates harmonics of the system and makes the system healthy. Hence the generated ac voltages and the generated currents are free from harmonics. Moreover, the generated ac voltage and current are constant, sinusoidal, balanced and harmonic free even under unbalanced load. So, the controller behaves

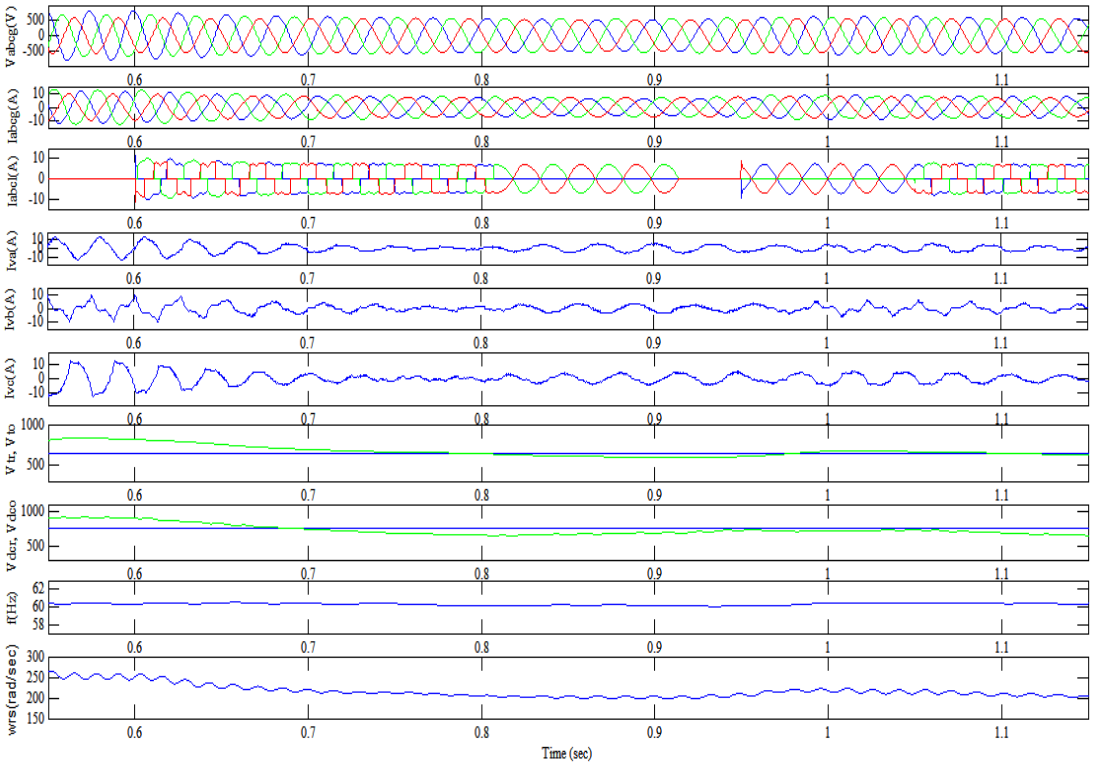

Fig. 9.11 Performance of an IAG furnishing non-linear load using conventional PI controller

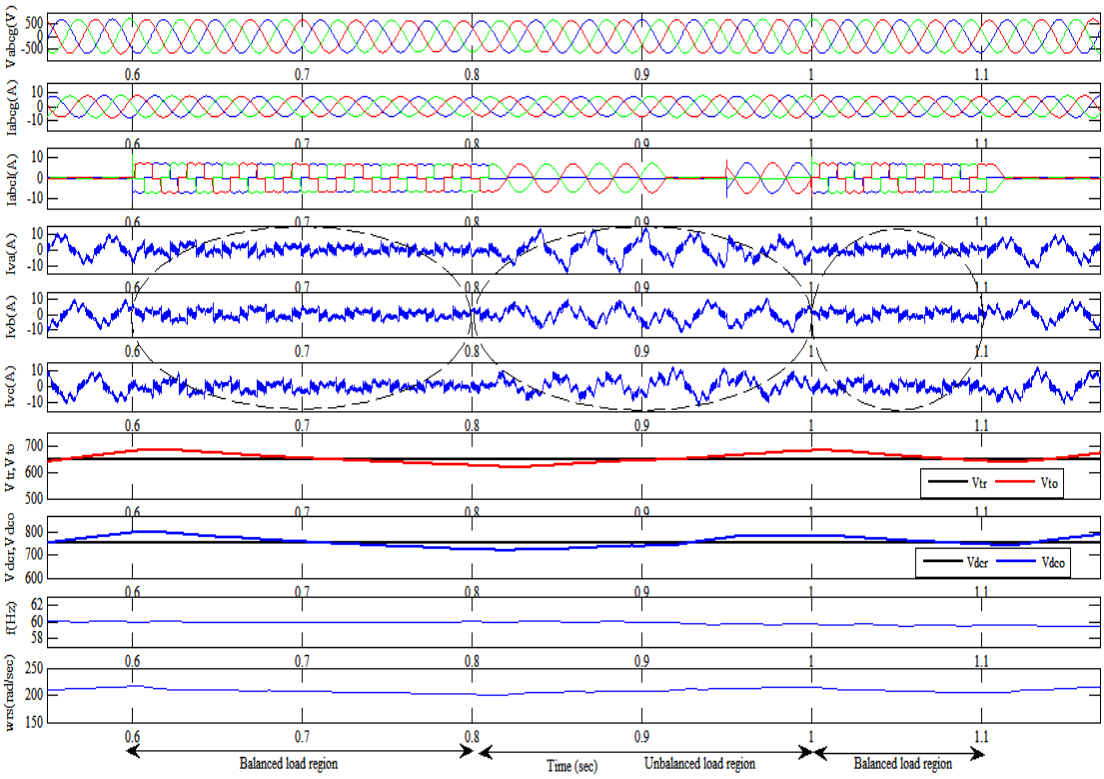

Fig. 9.12 Performance of an IAG furnishing non-linear load using FL based Mamdani type fuzzy logic controller.

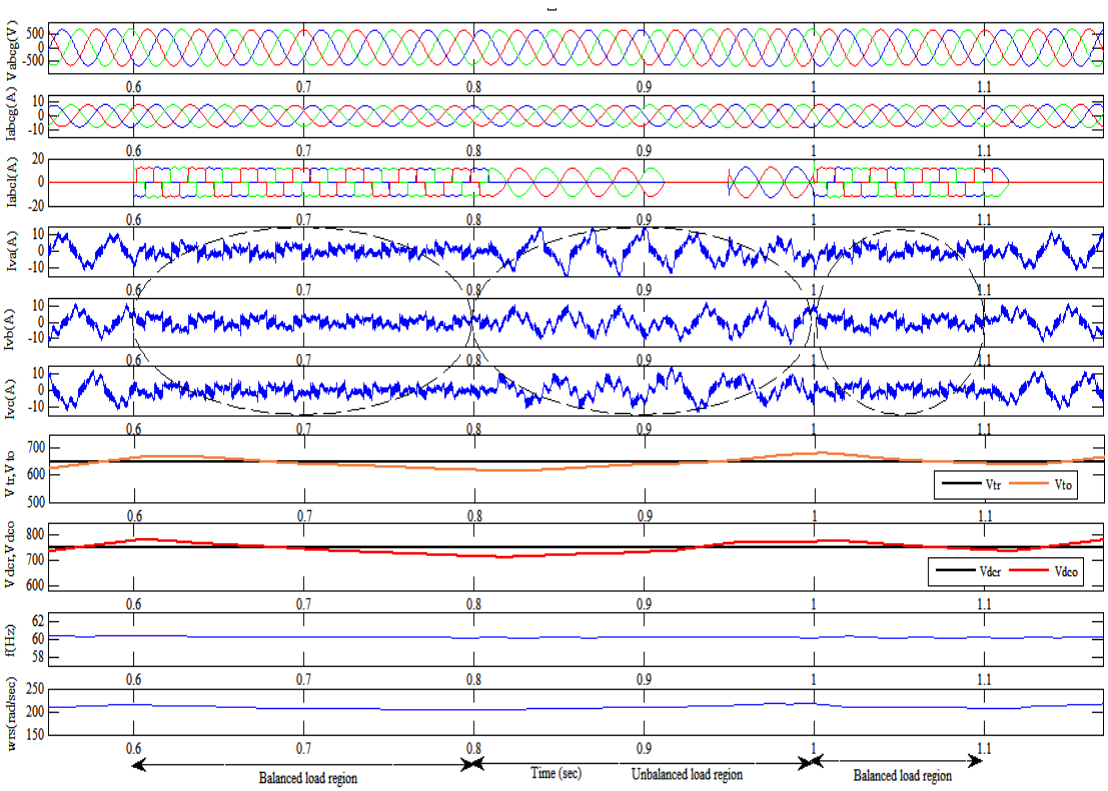

Fig. 9.13 Performance of an IAG furnishing non-linear load using FL based Sugeno type fuzzy logic controller.

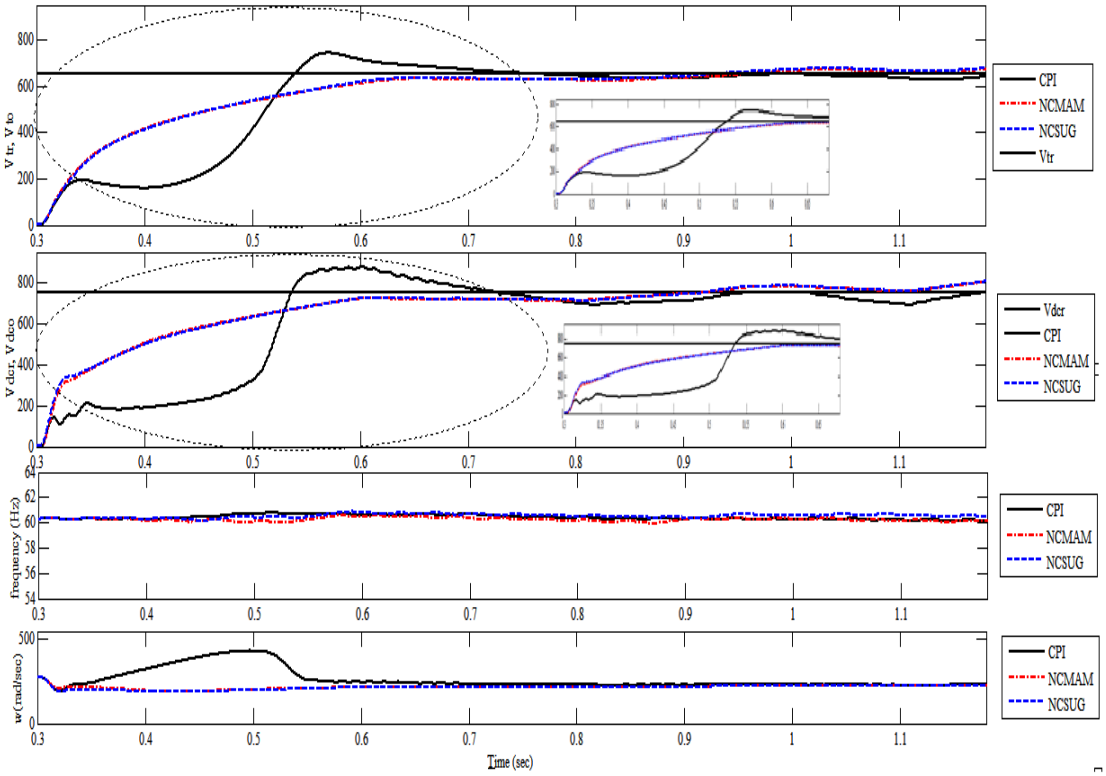

Fig. 9.14 Comparison of Performance characteristics of an IAG using conventional PI and FL (Mamdani and Sugeno) based controller.

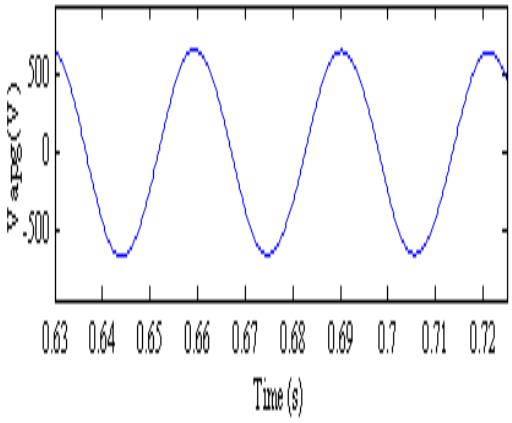

(a) Generated voltage signal

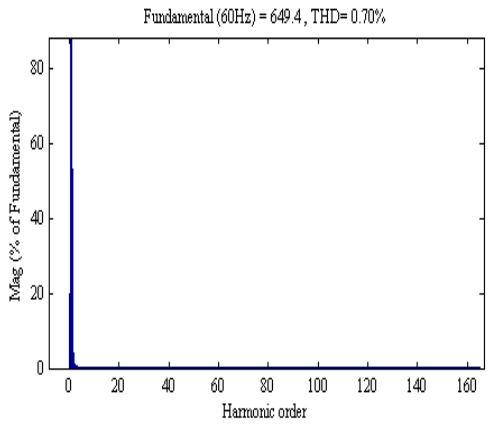

(a) THD value of generated current signal

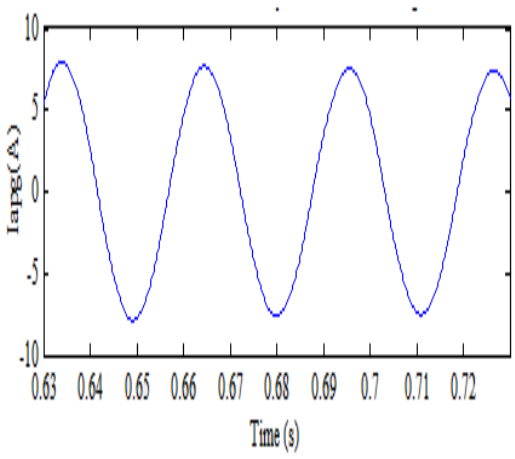

(b) Generated current signal

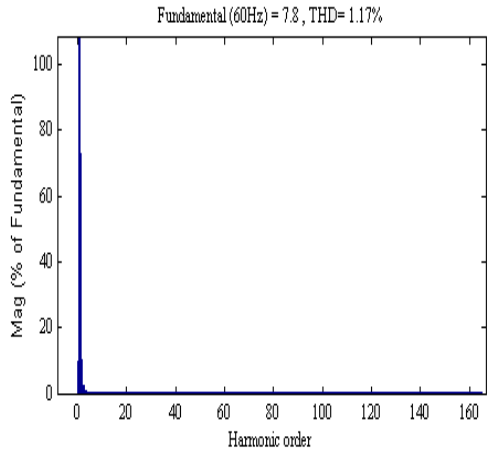

(b) THD value of generated current signal

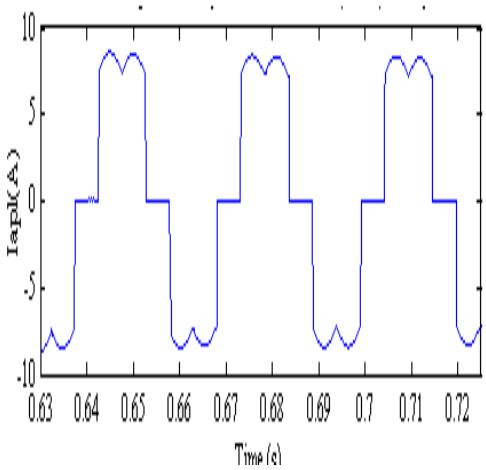

(c) Non-linear load current signal

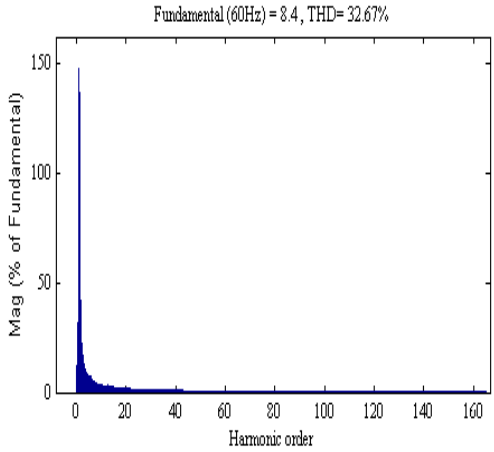

(c) THD value of the non-linear load current signal

Fig. 9.15 THD value of the (a) generated voltage (b) generated current and (c) non-linear load current.

like a load balancer, voltage supporter and harmonic eliminator. The same performance characteristics under same operating region are also accomplished using Mamdani and Sugeno type fuzzy logic controller [Fig. 9.12 and Fig. 9.13].In case of an IAG with FL based 3-legged VSI controller, the generated voltages and currents have THD values of 0.7 and 1.17 as given in Table 9 and is delineated in Fig. 9.15.

It is inferred from Table 9 that the THD related with the generated ac voltage and current are lower in case of FL based controller. Also, the THD values falls in the range defined in IEEE-519 standards [72].

Table 8: THD and voltage regulation of generated voltage and current

Type of Controller	Type of load	THD of Generated Voltage(V)	THD of Generated Current(A)	Voltage regulation (%)
PI	Resistive Load	1.31	2.41	6.1% for ac 5.33% for dc
	Reactive Load	1.47	3.62	
	Non-linear load	1.55	3.74	
FL	**Resistive Load**	**0.57**	**0.94**	**3.07% for ac** **2.67% for dc** **Superior voltage regulation**
	Reactive Load	**0.65**	**1**	
	Non-linear load	**0.70**	**1.17**	

9.7 SUMMARY

A template based control algorithm using two types of FL controllers has been modeled and tested in MATLAB software package for a 3-legged VSI controller. The design procedure of the VSI has also been described in this manuscript. It is inferred from simulated outcomes and Table 9 that superior voltage and frequency regulation is accomplished using the recommended FL based controller (both Mamdani and Sugeno type FIS) than PI based controller. Moreover, the THD of the generated ac voltage and current is significantly reduced and lies within the acceptable bounds defined in IEEE 519 guide. Thus, the enhancement in performance characteristics in terms of rise time, settling time, voltage regulation, frequency regulation, THD value is accomplished as illustrated in Fig. 9.14 and

Table 9. Thus, an IAG –VSI system is a perfect supply option to furnish any type of static load in remote or OFF-grid areas. In future work, an ANFSI based 3-legged VSI controller will be developed for further enhancement in performance characteristics of an IAG.

CHAPTER 10

CONCLUSIONS

10.1 GENERAL

Energy scanty is restraining industrial expansion and economic advancement of country like India. Under the situation of energy crises, the idea of installing new power plant is eluctably reliant on the import of highly volatile nature fossil fuels. Hence it is imperative to overcome the problem of energy crises through judicious utilization of abundantly and freely available renewable energy potential in the form of solar energy, wind energy, small hydro plants, biomass energy etc. Sustainable nature renewable energy sources play a vital role in the industrialization and economic development of a country like India.

Based on the energy consumption criteria, India ranked at sixth position in the world. Since 1947, India has drastically increased its installed power capacity from about 1362 MW to about 112,058 MW. The increased installed capacity can be met by two ways: (i) either by installing more and more new power plants (ii) by judicious utilization of freely available renewable energy sources. The second option proves to be cost effective and viable for electrical power generation using these RES.

Renewable energy sources prove to be environmentally friendly and maintain the environment clean and pollution free. Researchers and energy experts believed that the renewable energy potential if utilized efficiently can brighten the future. Hence, the researchers are promoting the techniques of the optimum utilization of these energy sources for electrical power generation using IAG. Hence the understanding, analysis and control aspects of such system are critical for the development of a community, nation or a country.

10.2 DISCUSSION ABOUT THE OVERALL WORK

As discussed earlier, the performance analysis of IAG subjected to balanced/ unbalanced nature load under steady state and transient state is the primary analyses which need to be carried out prior to designing of control strategy of controllers for voltage and frequency support. In almost all the prevailing literature, this analysis is

based on problem identification and formulation using equivalent circuit represented either in admittance or impedance form. The problem formulation finally results into two non-linear type equations. Then these non-linear equations are solved using various numerical techniques (N-R, secant and golden section method) to evaluate the values of two unknowns for accomplishing the performance of IAG subjected to steady state. Though these techniques prove quite efficient and are preferred option for accomplishing the steady state performance of the IAG. But these techniques lack flexibility, involves extraneous calculations in evaluating the various coefficients concerned with higher degree polynomial, model specific, prone to errors and time consuming.

In the present work, a MATLAB oriented optimization technique "fsolve" is preferred and recommended to solve non-linear equations to evaluate the values of X_{mg} and F_y for accomplishing the performance of 3-phase IAG dealing with 3-phase load under steady state conditions. It is a built-in user friendly function of MATLAB optimization toolbox and does not requisite any kind of mathematical manipulations; detailed knowledge of MATLAB software and its debugging; handles complexity with flexibility and ease in less computational time. The following interpretations have been made:

- It is interpreted from the accomplished experimental and analytical outcomes that the performance related with the generator voltage, its frequency and capacitor current corresponding to no load situation on IAG relies mainly on the speed and capacitor C_{sc}. These performances are highly influenced by the variation of both parameters. The close association of analytical and experimental outcomes has been noticed and validated the accuracy and feasibility of the suggested scheme. Also the transient phenomenon of three-phase voltage build up (380V) profile and capacitor current corresponding to no load situation of IAG is captured using power analyzer.

- Corresponding to resistive load situation on IAG, it is interpreted that the performance under steady state situation related with the generator voltage, load current and capacitor current has been highly affected by both power dispatched to the load and capacitor C_{sc}. On the other hand, the generator current and frequency are highly unaffected by the power dispatched to the

load but is highly affected by the value of C_{sc}. It has been observed that both the theoretical and analytical outcomes are very closely resembled for higher values of C_{sc}. For smaller values of C_{sc}, small deviations between the analytical and experimental outcomes of some performance characteristics have been noticed. But these deviations have been shown lying inside the defined bounds.

A MATLAB based routine "fsolve" is also explored to evaluate the performance under steady state situation of three-phase IAG furnishing single-phase load in unattended and unapproachable off-grid located remote communities. The following inferences have been made:

- The optimization technique 'fsolve' and the theory of symmetrical components has been suggested for evaluating the values of X_{mg} and F_y for accomplishing the steady-state performance of the 3-phase IAG furnishing 1-phase loads in off-grid sites.

- From experimental case studies, it has been concluded that a C- 2C capacitor connection across a 3-phase IAG gives a supply system having less phase unbalance and noiseless operation of the generator. It supports load voltage when IAG is rotated mechanically by a constant speed prime mover. Such capacitor scheme helps the 3-phase IAG in furnishing single-phase load requirement in off-grid sites.

It has been observed that IAG voltage and its frequency drops when subjected to load under transient and steady state. For attaining better performance, the devices must operate at rated voltage, so there realized the need of voltage controllers for IAG under varying load conditions.

Most of the voltage and frequency controllers discussed in literature based on conventional PI controllers owing to its simple design methodology. The main constrain was in accomplishing the fine tuned values of gains to achieve the desired performance. A Mamdani type FIS based EGLC is designed, tested and realized because such controller efficiently deals with non-linearity, noisy signals and does not requisite mathematical knowledge (modeling) of any system. In this thesis first time an attempt is made to accomplish the performance of an IAG using both conventional

PI and FL (Mamadani FIS) type controller to provide the voltage and frequency support to IAG corresponding to balanced/ unbalanced load. The following inferences have been made:

- It has been observed that a Mamdani type FIS based EGLC controller provides better voltage and frequency support to IAG under varying load than the conventional PI based controller. It has been observed that the THD content in voltage and current of IAG using Mamdani type FIS based EGLC are lower than conventional PI type controller.

- The FL based EGLC works like a load supporter, voltage and frequency supporter and a THD minimiser of IAG. Hence, enhancement in performance of IAG is accomplished using FL based EGLC than the PI based controller. Such types of FL based EGLC systems prove economical and can also be adopted for electrifying the remote off-grid sites.

- A hardware of PWM based IC -3524 is designed and installed in laboratory for voltage support to 3-phase IAG furnishing 1-phase load.

The non-linear loads introduce harmonics into the system and make the load current discontinues in nature. Hence once again the need of controller is realized to reduce the harmonics injected into the system along-with voltage and frequency support. In almost all the published literature, mainly conventional PI controllers are employed for voltage and frequency support of IAG. The main aspiration behind its use is its simplicity. But on the counterpart, there is difficulty in achieving the fine tuning of the gains to obtain desired performance especially when the control algorithm or strategy requisites more than one PI controllers. The second biggest drawback is encountered when the system is having uncertainty and non-linearity. Keeping in view all the facts discussed above, first time two types of Mamdani and Sugeno type FL based controllers have been recommended and tested for a 3-legged VSI. In the present work, a template based control algorithm using two types of FL controllers has been modeled, designed and tested in MATLAB software package for a 3-legged VSI controller. The following inferences are made from simulated outcomes:

- It has noticed that the superior voltage and frequency regulation is achieved using both Mamdani and Sugeno type FL controllers than PI based controller.

- Moreover, the THD content in the IAG voltage and its current is considerably reduced and lies within the acceptable bounds defined in IEEE 519 guide. Thus, the enhancement in performance characteristics of IAG in terms of rise time, settling time, voltage regulation, frequency regulation, THD value has been accomplished using FL controllers Thus, an IAG –VSI system can be regarded as a perfect supply option to furnish any type of static load in remote or OFF-grid areas.

10.3 SCOPE FOR FUTURE WORK

In the present work, the performance enhancement of IAG is achieved using fuzzy logic approach based EGLC and three-legged VSI controller. In future work, an ANFSI based EGLC and 3-legged VSI controller will be developed for further enhancement in performance characteristics of an IAG.

The difficulties faced during the experimental work are:

- Loss of residual magnetism in the core at lower values of operating speeds.
- Implementation of IC-3524 based control strategy for an IAG.

The hardware implementation of the control circuit of the controller can be realized using DSPACE and Controller HIL (C-HIL) Typhoon HIL. The Controller HIL (C-HIL) testing can be performed using Typhoon ultra high fidelity Typhoon HIL Simulator.

REFERENCES

[1]. R. Krishan, “Electric motor drives: Modelling, analysis and control,” Prentice Hall Company, New Jersey, 2001.

[2]. K. L. Shi, T. F Chan, Y. K Wong and S. L Ho, “Modeling and simulation of the three-phase induction motor using SIMULINK,” International Journal of Electrical Engineering Education, vol. 36, pp. 163-172, 1999.

[3]. M. L de Aguiar and M.M Cad, “The concept of complex transfer functions applied to the modeling of induction motors,” IEEE Power Engineering Society Winter Meeting, vol. 1, pp. 387-391, 2000.

[4]. P. C Krause, O. Wasynczuk and S.D Sudhoff, “Analysis of electric machinery and drive systems”, IEEE Press, A John Wiley and Sons. Inc. Publication, Second Edition, 2002.

[5]. P. C Krause and C. H Thomas, “Simulation of symmetrical induction machinery ” , IEEE Transaction on Power Apparatus and Systems, vol. PAS-84, No. 11, pp. 1038-1053, Nov1965.

[6]. Lee, R.J., Pillay, P., and Harley, R.G., “D, Q Reference frame for the simulation of induction motors”, Electric Power Systems Research Journal, vol. 8, pp.15-16, October 1984.

[7]. B. K Bose, “Modern power electronics and ac drives”, Prentice Hall, 2002.

[8]. B. Ozpineci and L. M Tolbert, “Simulink implementation of induction machine model-A modular approach”, IEEE International Conference Electric Machine and Drives, pp.728-734, 2003.

[9]. B. C Doxey, “Theory and application of the capacitor-excited induction generator”, The Engineer, 29, pp. 893-897, 1963.

[10]. R. Holland, “Appropriate technology-rural electrification in developing countries,” IEE Review, vol. 35, No. 7, pp. 251-254, July 1989.

[11]. M. G Say, Alternating Current Machines, Wiley, 1976.

[12]. S. S Murthy, O. P Malik and A. K Tandon, “Analysis of self-excited induction generators,” IEE Proceedings, Part C, vol. 129, No. 6, pp. 260-265, 1982.

[13]. A K AI Jabri and A. I Alolah, “Limits on the performance of the three phase self-excited induction generators,” IEEE Transaction on Energy Conversion, vol. 5, No. 2, pp. 350-356, June 1990.

[14]. N. H Malik and S. E Hague, “Steady state analysis and performance of an isolated self-excited induction generator,” IEEE Transaction on Energy Conversion, vol. EC-1, No. 3, pp. 134-139, 1986.

[15]. S. P Singh, B. Singh and M. P Jain, “Performance characteristics and optimum utilization of a cage machine as capacitor excited induction generator,” IEEE Transaction on Energy Power Conversion, vol.5, No.4, pp. 679-685, 1990.

[16]. M. H Haque, “A novel method of evaluating performance characteristics of a self-excited induction generator,” IEEE Transaction on Energy Conversion, vol. 24, No. 2, pp. 358-364, 2009.

[17]. A.H A.L-Bahrani, and N. H Malik, “Steady state analysis and performance characteristics of a three-phase induction generator self-excited with a single capacitor,” IEEE Transaction on Energy Conversion, vol. 5, No. 4, pp. 725-732, Dec 1990.

[18]. M. H Haque and A. L Maswood, “Determination of excitation capacitance of a three-phase self-excited induction generator,” IEEE Power and Energy Society General Meeting, 1-6, 2012.

[19]. S. S Murthy, B. Singh, S. Gupta and B. M Gulati, “General steady- state analysis of three-phase self-excited induction generator feeding three-phase unbalanced load/single-phase load for stand-alone applications,” IEE Proceedings - Generation Transmission and Distribution, vol. 150, No.1, pp. 49-55, 2003.

[20]. A.H A.L-Bahrani and N. H Malik, “Steady-state analysis of parallel operated self-excited induction generators,” Proc. IEE, Part C, vol. 140, No.1, pp. 49-55, 1993.

[21]. A.H A.L-Bahrani and N. H Malik, “Voltage control of parallel operated self-excited induction generators,” IEEE Transaction on Energy Conversion, vol. 8, No. 2, pp. 236-242, June 1993.

[22]. A. H A.L- Bahrani, “Analysis of self-excited induction generators under unbalanced conditions,” Electric Machines and Power Systems, vol. 24, Issue. 2, pp.117-129, 1996.

[23]. N. H Malik and A. L Bahrani, “Influence of the terminal capacitance on the performance characteristics of self-excited induction generator,” Proc. IEE, vol. 137, No. 2, pp. 168-173, 1990.

[24]. Y.H.A Rahim, “Excitation of isolated three-phase induction generator by a single capacitor,” IEE Proc, vol. 140, No. 1, pp. 44-50, 1993.

[25]. K. S Sandhu and S. K Jain, “Operational aspects of self-excited induction generator using a new model,” Electrical Machines and Power Systems, vol. 27, No. 2, pp. 169-180, 1999.

[26]. T. F Chan, “Analysis of self-excited induction generators using an iterative method,” IEEE Transactions on Energy Conversion, vol. 10, No. 3, pp. 502-507, 1995.

[27]. K. S Sandhu, “Iterative model for the analysis of self-excited induction generators,” Electrical Power Components and Systems, vol. 31, No. 10, pp. 925 - 939, 2003.

[28]. A. L. Alolah and M. A. Alkanhal, “Optimization based steady state analysis of three-phase self-excited induction generator,” IEEE Transaction on Energy Conversion, vol. 15, No.1, pp. 61-65, 2000.

[29]. D. Joshi, K. S Sandhu, and M. K Soni, “Constant voltage and constant frequency operation of a self-excited induction generators,” IEEE Transaction on Energy Conversion, vol. 21, No. 1, pp. 228-234, 2006.

[30]. T. F Chan, “Analysis of a single phase self-excited induction generator,” Electrical Machines and Power Systems, vol. 23, No. 2, pp. 149-162, 1995.

[31]. T. F Chan, “Self-excited induction generators driven by regulated and unregulated turbines,” IEEE Transaction on Energy Conversion, vol. 11, No. 2, pp. 338-343, June 1996.

[32]. L. Quazene and G. Mcpherson, “Analysis of the isolated induction generator,” IEEE Transaction on Power Apparatus and Systems, vol. PAS-102, No. 8, pp. 2793-2798, Aug 1983.

[33]. J. L Bhattacharya and J. L Woodward, “Excitation balancing of a self-excited induction generator for maximum power output,” IEE Proc., vol. 135, No. 2, pp. 88-97, 1988.

[34]. L. Wang and C.H Lee, “Long –shunt and short-shunt connections on dynamic performance of a SEIG feeding an induction motor load,” IEEE Transactions on Energy Conversion, Vol.15, No. 1, pp. 1-7, March 2000.

[35]. B. Singh, R. B Saxena, S. S Murthy and B. P Singh, “A single-phase self-excited induction generator for lighting loads in remote areas,” International Journal on Electrical Engineering Education, vol. 25, pp. 269-275, 1988.

[36]. S. S Murthy, H. C Rai and A. K Tandon, “A novel self-excited self-regulated single-phase induction generator, Part II: Experimental Investigation,” IEEE Trans. Energy Conversion, vol. 8, No. 3, pp.383-388, September 1993.

[37]. T. F Chan, “Analysis of a single-phase self-excited induction generator,” Electrical Machines and Power Systems, vol. 23, Issue.2, pp. 149-162, 1995.

[38]. Y. H. A Rahim, A.I Alolah and R.I Al-Mudhaiheem, “Performance of single phase induction generators,” IEEE Transaction on Energy Conversion, vol. 8, No. 3, pp. 389-395, September 1993.

[39]. B. Singh and L. B Shilpkar, “Steady-state analysis of single-phase self-excited induction generator,” IEE Proceeding of Generation, Transmission, and Distribution, vol. 146, No. 5, pp. 421-427, September 1999.

[40]. T. F Chan and L. L Lai, “Steady-state analysis and performance of a single-phase self-regulated self-excited induction generator,” IEE Proceeding of Generation, Transmission and Distribution, vol. 149, No. 2, pp. 233-241, March 2002.

[41]. T. F Chan and L. L Lai, “Steady-state analysis and performance of a stand-alone three-phase induction generator with asymmetrically connected load impedances and excitation capacitances,” IEEE Transaction on Energy Conversion, vol. 16, No.4, pp. 327-333, December 2001.

[42]. S. N Mahto, S. P Singh and M. P Sharma, “Capacitors required for maximum power of a self-excited single-phase induction generator using a three-phase machine,” IEEE Transaction on Energy Conversion, vol. 23, No. 2, pp. 372–381, June 2008.

[43]. T. F Chan, L. L Lai, “Capacitance requirements of a three-phase induction generator self-excited with a single capacitance and supplying a single-phase load,” IEEE Transaction on Energy Conversion, vol.17, No. 1, March 2002.

[44]. A. I Alolah and M. A Alkanhal, “Excitation requirements of three phase self excited induction generator under single phase loading with minimum unbalance,” in Proceedings of IEEE Power Engineering Society Winter Meeting, Singapore, Jan. 23–27, pp. 257-259, 2000.

[45]. Y. J Wang and S.Y Huang, “Analysis of a stand-alone three-phase self-excited induction generator with unbalanced load using a two-port network model,” IET Electrical Power Application, vol. 3, Issue.5, pp. 445–452, January 2009.

[46]. T. F Chan and L. L Lai, “Phase balancing for a self-excited induction generator,” in Proceedings of International Conference on Electric Utility Deregulation, Restructuring and Power Technologies, London, UK, pp. 602-607, April 2000.

[47]. L. Wang and C. M Cheng, “Excitation capacitance required for an isolated three-phase induction generator under single-phasing mode of operation,” in Proceedings of International Conference of Power Engineering Society Winter Meeting, Columbus, USA, pp. 1403-1407, 2001.

[48]. T. F Chan, “Performance analysis of a three-phase induction generator self-excited with a single capacitance,” IEEE Trans. on Energy Conversion, vol.14, No.4, pp. 894–900, December 1999.

[49]. T. F Chan and L. L Lai, “A novel single-phase self-regulated self-excited induction generator using a three-phase machine,” IEEE Trans. on Energy Conversion, vol.16, No. 2, pp. 204-208, June 2001.

[50]. T. F Chan and L. L Lai, “Single-phase operation of a three-phase induction generator with the Smith connection,” IEEE Transaction on Energy Conversion, vol. 17, No. 1, pp. 47-54, 2002.

[51]. T. F Chan and L. L Lai, “A novel excitation scheme for a stand-alone three-phase induction generator supplying single-phase loads,” IEEE Trans. Energy Conversion, vol. 19, No.1, pp. 136-142, March 2004.

[52]. T. F Chan and L. L Lai, “Phase balancing for an induction generator operating on a single phase power system,” IEEE Conference, pp. 167-170, 2000.

[53]. S. N Mahato, M. P Sharma and S. P Singh, “Transient performance of a single-phase self-regulated self-excited induction generator using a three-phase machine,” Electric Power System Research, pp. 839-850, 2007.

[54]. Y. J Wang and M. H Lee, “A method for balancing a single-phase loaded three-phase induction generator,” Energies, pp. 3534-3549, 2012.

[55]. J. M Elder, J. T Boys and J. L Woodward, “Integral cycle control of stand-alone generators,” IEE Proc, vol. 132, Pt C, No. 2, pp. 57-66, 1985.

[56]. R. Bonert and S. Rajakaruna, “Self-excited induction generator with excellent voltage and frequency control,” IEE Proceeding of Generation, Transmission and Distribution, vol. 145, No. 1, pp. 33-39, 1998.

[57]. R. C Bansal, “Three-phase self-excited induction generators: An overview,” IEEE Transactions on Energy Conversion, vol.20, No.2, pp.292-299, June 2005.

[58]. B. Singh, S. S Murthy and S. Gupta, “Analysis and implementation of an electronic load controller for a self-excited induction generator,” IEE Proceeding of Generation, Transmission and Distribution, vol.151, No.7, pp. 51-60, January 2004.

[59]. B. Singh, S. S Murthy and S. Gupta, “Analysis and design of electronic load controller for a self-excited induction generators,” IEEE Transaction on Energy Conversion, vol.21, No. 1, pp. 285-93, 2006.

[60]. T. S Chandra and P.M Bishnu, “Voltage regulators for self-excited induction generator,” IEEE Transactions on Energy Conversion, vol. 20, No. 4, pp. 460-463, April 2004.

[61]. S. Gao, S. S Murthy, G. Bhubaneswar and M. S. L Gayathri, “Design of microcontroller based electronic load controller for a self-excited induction generator supplying single-phase loads,” Journal of Power Electronics, vol.10, No.4, pp. 444-449, 2010.

[62]. J. M Ramirez and Emmanuel Torres M, “An Electronic load controller for self-excited induction generators,” IEEE PES General Meeting, June 24-28, 2007.

[63]. E. G Marra and J.A Promilo, “Induction- Generator- based system providing regulated voltage with frequency constant,” IEEE Trans. Ind. Electron, Vol. 47, No. 4, pp. 908-914, 2010.

[64]. B Singh, G. K Kasal and S Gairola, “Power quality improvement in conventional electronic load controller for an isolated power generation,” IEEE Transactions on Energy Conversion, vol. 23, No. 3, pp. 764-773, Sept. 2008.

[65]. S. Mbabazi and J. Leary, “Analysis and design of electronic load controllers for micro-hydro systems in the developing world,” University of Sheffield, E-Futures, March 2010.

[66]. B. Singh, S. S Murthy and S. Gupta, “Transient analysis of self-excited induction generator with electronic load controller (ELC) for single-phase loading,” National Power System Conference (NPSC), 2002, Dec 27-29, pp. 393- 402.

[67]. B. Singh, S. S Murthy and S. Gupta, “Transient analysis of self-excited induction generator with electronic load controller (ELC) supplying static and

dynamic loads", in Fifth International Conference on Power Electronics and Drive System, PEDS 2003, vol.1, pp. 771-776.

[68]. S. N Mahato, S. P Singh and M. P Sharma, " Transient performance of a three-phase self-excited induction generator supplying single-phase load with electronic load controller," in Electrical Systems for Aircraft, Railway and Ship Propulsion (ESARS), 2010, 19-21.

[69]. B. Singh, S. S Murthy, Madhusudan, Manish Goel, A. K Tandon, "A steady state analysis on voltage and frequency control of self-excited Induction Generator in micro-hydro system," in IEEE Conference, 2006.

[70]. B. Singh, S. S Murthy and S. Gupta, "An electronic voltage and frequency controller for single-phase self-excited Induction Generators for pico hydro applications," in International Conference on Power Electronics and Drive Systems, 2005, vol. 1, pp. 240-245.

[71]. M.H. Rashid, Power Electronics Circuits, Devices and Applications, Pearson/Prentice- Hall: Singapore, 2004.

[72]. IEEE Guide for harmonic Control and Reactive Compensation of Static Power Converters, IEEE Standard 519, 1992.

[73]. S. C Kuo and L.Wang, P.M, "Analysis of voltage control for a self-excited induction generator using a current-controlled voltage source inverter (CC-VSI)," Proc. Inst. Elect. Eng., Transm. Distrib, *v*ol. 148, No.5, pp. 431-438, Sept 2001.

[74]. E.Suarez and G. Bortolotto, "Voltage frequency control of a self-excited induction Generator," IEEE Transaction on Energy Conversion, *v*ol. 14, pp. 394-40, Sept 1999.

[75]. S.S Murthy, B. Singh, A. Kulkami, R. Sivarajan and S. Gupta, " Field experience on a Novel Pico-hydel System using Self-Excited Induction Generator with Electronic Load Controller," Power Electronics and Drive Systems, 2003, PEDS 2003. The fifth International Conference, Vol. 2, pp. 842-847, 17-20, Nov. 2003.

[76]. B. Singh, S. S Murthy and S. Gupta, "An improved Electronic Load Controller for Self-Excited Induction Generator in Micro-Hydel Applications", Industrial Electronics Society, 2003, IECON' 03, The 29th Annual Conference of the IEEE, Vol. 3, pp.2741-2746, November 2003.

[77]. I. Serbian, C Ion, C. Marinescu and M. N Cirstea, “Electronic Load Controller for Stand-Alone Generating Units with Renewable Energy Sources,” Power Engineering Society General Meeting, IEEE, pp. 1-8. November 2006.

[78]. B. Singh, A. Chandra, G. K Kasal and K-AI-Haddad, “A Frequency Based Electronic Load Controller for an Isolated Asynchronous Generator feeding 3-phase 4-wire loads”, IEEE International Symposium, pp. 1513-1518, June 30 2008-July 2 2008.

[79]. B. Singh and V. Rajagopal, “Electronic Load Controller for Islanded Asynchronous Generator in Pico Hydro Power Generation,” Power Electronics Specialists Conference, PESC IEEE, pp. 2057-2063, 2008.

[80]. V. Rajagopal and B. Singh, “Electronic Load Controller using IcosΦ Algorithm for Standalone Induction Generator”, IEEE Conference, pp.1-6, 2010.

[81]. E. Torres, F. Chan, J. Ramirez and A. Cowo, “ A PWM control for Electronic Load Controller for Self-Excited Induction Generator based in IGBT series inverted switch”, pp. 61-66, IEEE Conference 2010.

[82]. S.S Murthy, Ramrathnam and M.S.L Gayathri, “A Novel Digital Control Techniques of Electronic load Controller for SEIG based Micro- Hydel Power Generation”, Power Electronics, Drives and Energy Systems, 2006, PEDES 2006, International Conference, pp. 1-5, 12-15 December 2006.

[83]. D. K Palwalia and S. P Singh, “Design and implementation of induction generator controller for single-phase self-excited induction generator,” in third IEEE Conference on Industrial Electronics and Applications ICIEA 2008, pp. 400-404, 3-5 June 2008, Singapore.

[84]. S.S Murthy, G. Bhubaneswar, S. Gao and M.S.L Gayathri, “Performance Analysis of a Self-Excited Induction Generator with Digitally Controlled Electronic Load Controller for Micro Hydel Power Generation,” Power India Conference, 2008, POWERCON 2008. Join International Conference, pp. 1-6, 12-15 Oct 2008.

[85]. S. Gao, S. S Murthy, G. Bhubaneswar and M.S.L Gayathri, “Design of a microcontroller based electronic load controller for a self-excited induction generator supplying single-phase loads”, Journal of Power Electronics, Vol. 10, no.4, pp. 444-449, July 2010.

[86]. S. Sharma and B. Singh, "Fuzzy proportional-integral regulators for stand-alone wind energy conversion system," IEEE Conference ICPCES, pp.1-8, January 2011.

[87]. Y. Sofian and M. Iyas, "Design of Electronic load Controller for a Self-Excited Induction Generator using Fuzzy Logic method based Microcontroller", International Conference on Electrical Engg and Informatics, IEEE, Bandung, Indonesia, 17-19 July 2011.

[88]. D. Henderson, "An advanced electronic load governer for control of micro hydroelectric generation ," IEEE Trans. Energy Convers., Vol.13, No. 3, pp.300-304, 1998.

[89]. D. K Palwalia and S. P Singh, "Digital signal processor based controller design and implementation for self-excited induction generator," Journal of Electrical Power Components, 36 (10), pp. 1130-1140, 2008.

[90]. V. Verma, P. Pant and B. Singh, "VSC supported active load control for SEIG under load perturbations," IEEE Conference IICPE, 28-30 Jan 2011, New Delhi, India.

[91]. S. Gao, G. Bhuvaneswari, S. S Murthy and U. Kalla, "Efficient voltage regulation scheme for three-phase self-excited induction generator feeding single-phase load in remote locations," IET Renewable Power Generation, Vol.8, Issue.2, pp.100-108, 2014.

[92]. S. S Murthy, R. Rose and B. Singh, "Experience in the development of micro-hydel grid independent power generation scheme using induction generators for Indian conditions," IEEE TENCON International Conference, pp. 461-465, 1998.

[93]. S. S Murthy and B. Singh, "Capacitive var controllers for induction generators for autonomous power generation," IEEE Conference, pp. 679-685.

[94]. S. K Jain, J. D Sharma and S.P Singh, "Transient performance of three-phase self-excited induction generator during balanced and unbalanced faults," IEE Proceeding of Generation, Transmission and Distribution, 149, pp. 50-57, 2002.

[95]. M. B Brennen and A. Abbondanti, "Static exciter for induction generators," IEEE Transactions on Industrial Applications, vol. IA-13, No. 5, pp. 422-428, 1977.

[96]. R. K Mishra, B. Singh and M. K Vasantha, “Voltage regulator for a self-excited cage induction generator,” Electrical Power System Research, 24, pp. 75-83, 1992.

[97]. L. Shridhar, B. Singh and C. S Jha, “Transient performance of the self-regulated short shunt self excited induction generator,” IEEE Transaction on Energy Conversion, vol. 10, No. 2, pp. 261-267, 1985.

[98]. T. Ahmed, E. Hiraki, M. Nakaoka and O. Noro, “Three- phase self excited induction generator driven by a variable sped prime mover for clean renewable energy utilizations and its terminal voltage regulation characteristic by static var compensator,” IEEE IAS Annual Meeting, Conference on Industry Applications, pp. 693-700, 2003.

[99]. T. Ahmed, K. Nishida and M. Nakaoka, “Static var compensator based voltage regulator of single-phase self-excited induction generator,” IEEE IAS Annual Meeting Conference on Industry Application, pp. 2069-2076, 2004.

[100]. B. Singh and L. B Shilpakar, “Analysis of a novel solid state voltage regulator for a self-excited induction generator,” IEE Proceeding on Generation Transmission Distribution, vol. 145, No. 6, pp. 647-655, 1998.

[101]. S. C Kuo and L. Wang, “Analysis of voltage control for a self-excited induction generator using a current controlled voltage source inverter (CC-VSI),” IEE Proceeding on Generation Transmission Distribution, 148, pp.431-438, 2001.

[102]. S. C Kuo, L. Wang , “Analysis of isolated self excited induction generator feeding a rectifier load,” IEE Proceeding on Generation Transmission Distribution, vol. 149, No.1, pp. 90- 97, 2002.

[103]. B. Singh, S. S Murthy and S. Gupta, “STATCOM based voltage regulator for self-excited induction generator feeding non-linear loads,” IEEE Transactions on Industrial Electronics, vol. 53, No. 5, pp. 1437-1451, 2006.

[104]. B. Singh, S. S Murthy, S. Gupta, “Analysis and design of STATCOM based regulator for self-excited induction generators,” IEEE Transaction on Energy Conversion, vol.19, pp. 783 -790, 2004.

[105]. M. Bašić, D. Vukadinović and M. Polić, “Fuzzy logic vs. Classical PI voltage regulator for a self-excited induction generator,” Mathematical Applications in Science and Mechanics, pp. 189-194, 2013.

[106]. B. Singh, S. S Murthy, S. Gupta, “Modelling and analysis of STATCOM based voltage regulator for self-excited induction generator with unbalanced loads,” IEEE Conference, 2003.

[107]. B. Singh, S. S Murthy, S. Gupta, “ A solid state controller for Self-excited Induction Generator for voltage regulation, Harmonic compensation and load balancing,” Journal of Power Electronics, Vol.5, No.2, pp.109-119, 2005.

[108]. B. Singh, S. S Murthy and S. Gupta, “Modelling of STATCOM based voltage regulator for self-excited induction generator with dynamic loads,” IEEE Conference, 2006.

[109]. Y. K Chauhan, S. K Jain and B. Singh, “Performance of self-excited induction generator with cost effective static compensator,” Maejo International Journal of Science and Technology, Vol. 6, No. 1, pp. 12-27, 2012.

[110]. T. Ahmed, O. Noro, E. Hiraki and M. Nakaoka, “Terminal voltage regulation characteristics by static var compensator for a three-phase self-excited induction generator”, IEEE Transactions on Industry Applications, Vol. 40, No.4, pp. 978-987, 2004.

[111]. S. Tiwari, S. Gupta, S. Jain and B. Singh, “Fuzzy logic controller based SAPF for isolated asynchronous generator,” Journal of Electrical Engineering, Vol. 15, No. 1, pp. 79-89, 2015.

[112]. A. Banerji, S. K Biswas and B. Singh, “Voltage and frequency controller for an autonomous asynchronous generator,” International Journal of Electrical Engineering and Informatics, Vol. 6, No. 2, pp. 250-265, 2014.

[113]. S. Sharma and B. Singh, “Fuzzy proportional-Integral regulators for stand-alone wind energy conversion system,” IEEE Conference ICPCES, 2010.

[114]. A. Banerji, S. K Biswas and B. Singh, “Fuzzy logic based window operation of DSTATCOM for an autonomous asynchronous generator,” International Journal of Electrical Engineering and Informatics, Vol. 3, No. 4, pp. 401-413, 2011.

[115] S. N Sivanandam and S. N Deepa, “Principle of soft computing,” Second edition, Wiley India, 2011.

APPENDIX-A

MACHINE - I DATA

Rated Power	3 HP
Rated Line to Line Voltage	220V
Rated Frequency	60Hz
Number of poles, P	4
Stator Resistance, R_{st}	0.435 ohm
Stator Leakage Reactance, X_{lst}	0.754 ohm
Rotor Resistance, R_{ro}'	0.816 ohm
Rotor Leakage reactance, X_{lro}'	0.754 ohm
Moment of inertia, J	0.089 Kg-m^2
Magnetizing reactance, X_{mg}	26.13 ohm

MACHINE - II DATA

Rated Power	2250HP
Rated Line to Line Voltage	2300V
Rated Frequency	60Hz
Number of poles, P	4
Stator Resistance, R_{st}	0.029 ohm
Stator Leakage Reactance, X_{lst}	0.226 ohm
Rotor Resistance, R_{ro}'	0.022 ohm
Rotor Leakage reactance, X_{lro}'	0.226 ohm
Moment of inertia, J	63.87 Kg-m^2
Magnetizing reactance, X_{mg}	13.04 ohm

APPENDIX B

The various constants in Eq. (3.6) and Eq. (3.7) are mathematically attained as:

$$\left.\begin{aligned}
M_1 &= -2X_l R_{lo} \\
M_2 &= -X_l^2 R_{lo} \\
M_3 &= 2X_l R_{lo} \\
M_4 &= X_l^2 R_{lo} \\
M_5 &= X_{sc}(R_{lo} + R_{st} + R_{ro}) \\
M_6 &= X_{sc}X_l(R_{lo} + R_{st} + R_{ro}) + R_{st}R_{lo}R_{ro} \\
M_7 &= -X_{sc}(R_{st} + R_{lo}) \\
M_8 &= -X_l X_{sc}(R_{st} + R_{lo})
\end{aligned}\right\} \quad \text{(A-1)}$$

$$\left.\begin{aligned}
N_1 &= 2X_l X_{sc} + R_{lo}(R_{st} + R_{ro}) \\
N_2 &= R_{lo}X_l(R_{st} + R_{ro}) + X_l^2 X_{sc} \\
N_3 &= (R_{st}R_{lo} + 2X_l X_{sc}) \\
N_4 &= -X_l(R_{st}R_{lo} + X_l X_{sc}) \\
N_5 &= -X_{cs}R_{ro}(R_{lo} + R_{st})
\end{aligned}\right\} \quad \text{(A-2)}$$

ASYNCHRONOUS MACHINE DATA

The hardware structure embody a delta connected three-phase asynchronous machine of 380/660V, 8.2/4.75A, 50Hz, 3.73 kW, 4-pole, 1450 rpm. The various electrical parameters of the machine are evaluated as:

$$V_{bv} = 380 \text{ V}$$

$$I_{bv} = \frac{8.2}{\sqrt{3}} = 4.7344 \text{ A}$$

$$Z_{bv} = \frac{V_{bv}}{I_{bv}} = 80\ \Omega$$

$$f_{bv} = 50 \text{ Hz}$$

$$N_{bv} = 1500 \text{ rpm}$$

$$X_{le} = X_{lst} = X_{lro} = 0.08215 \text{ p.u}$$

$$R_{st} = 0.045 \text{ p.u}$$

$$R_{ro} = 0.052 \text{ p.u}$$

In order to measure the variation of V_{gp}/F_y at different X_{mg} the asynchronous machine was whirled at synchronous speed by the D.C shunt motor. Fig. 3.4 presented the experimental results relating the non-linear variation of V_{gp}/F_y and X_{mg} due to saturation of the machine. For the analysis purpose, the variation under the saturated region can be linearised using the approximate curve in Fig. 3.4 & may be expressed in Eq. (3.16)

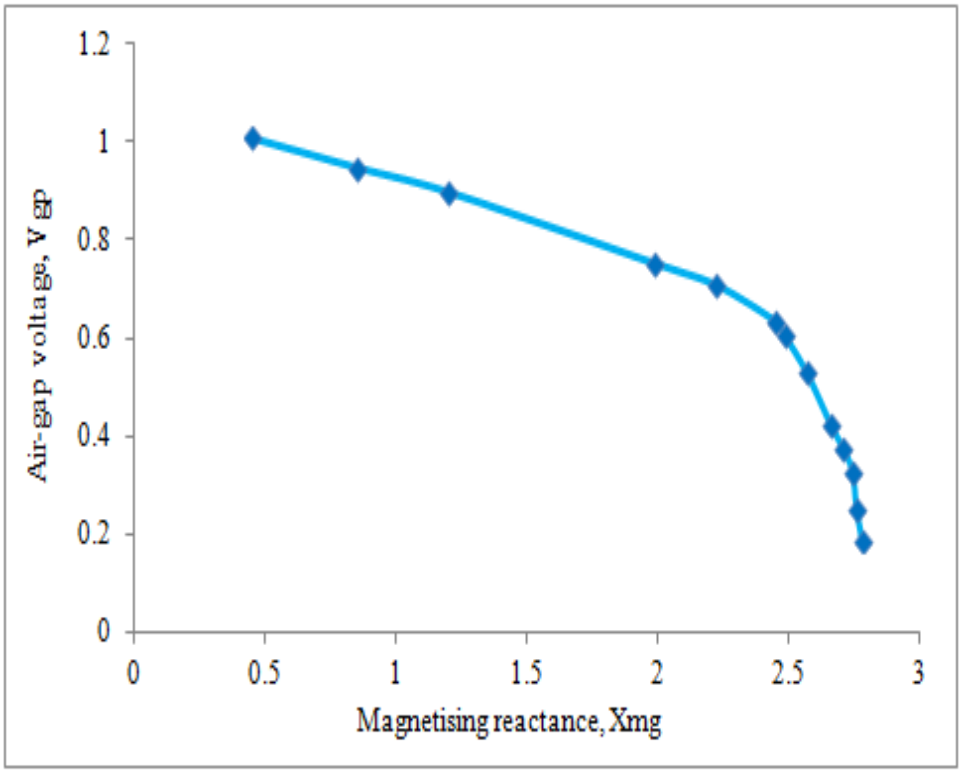

Fig. B.1 Variation of magnetizing reactance (X_{mg}) with air gap voltage (V_{gp}/F_y) for a three-phase asynchronous machine at synchronous speed

$$\left.\begin{aligned} V_{gp}/F_y &= -0.1819X_{mg} + 1.1044 \quad X_{mg} \le 2.4474 \\ &= -1.014X_{mg} + 3.1243 \quad 2.4474 < X_{mg} \le 2.7054 \\ &= -2.5191X_{mg} + 7.1987 \quad 2.7054 < X_{mg} \le 2.78 \\ &= \quad 0 \qquad\qquad\qquad\qquad 2.78 < X_{mg} \end{aligned}\right\} \quad (3.16)$$

PRIME MOVER DATA

A 3/2/9.6 kW, 220/170V, 1500 rpm, 17.4A dc machine

RESISTIVE LOAD DATA

A 3-phase, 3kW, 440 V, 7A resistive load is attached to IAG.

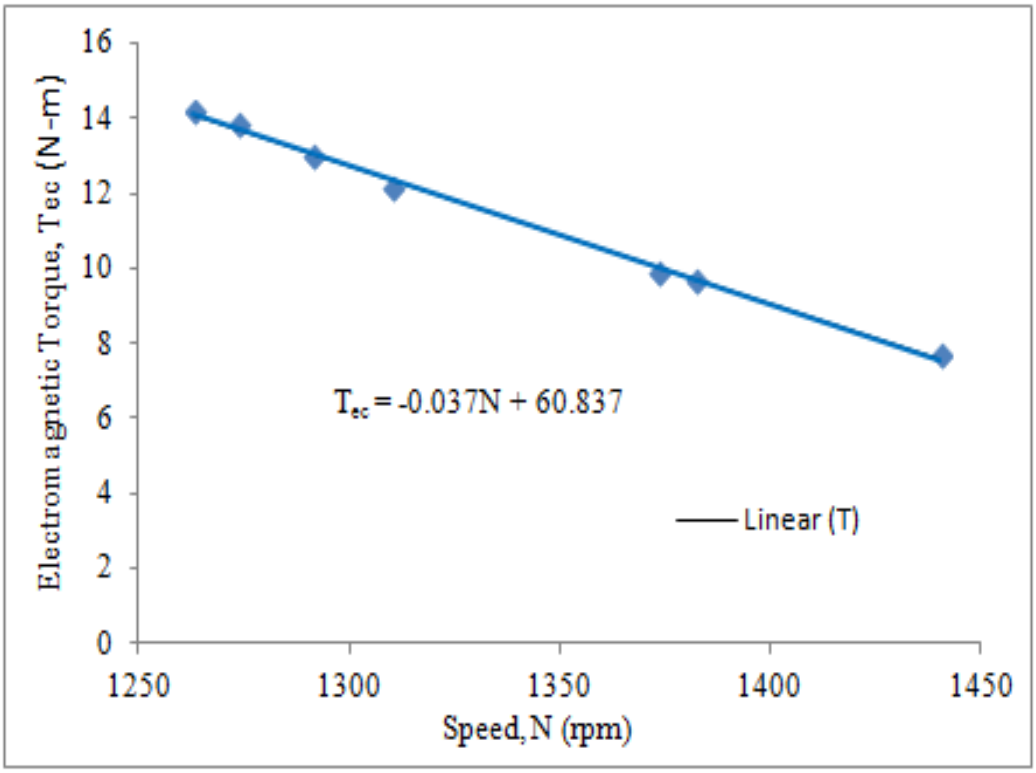

Fig. B.2 Torque (T_{ec}) - speed (N) characteristics of the prime mover.

APPENDIX-C

The various constants of Eq. 4.24 (a) and Eq.4.24 (b) are given below:

$$S_1 = 2G_L X_l - 4G_L X_l + \varkappa_5 R_s - \varkappa_4 U_2$$

$$S_2 = X_l[G_1 X_l - 3G_L X_l + \varkappa_5 R_s - \varkappa_4 U_2]$$

$$S_3 = vR_r[\varkappa_5 - \varkappa_4] - vS_1$$

$$S_4 = U_3 - vS_2$$

$$S_5 = 2\varkappa_5 X_l - 4\varkappa_4 X_l + G_L U_2 - G_1 R_s + 3$$

$$S_6 = X_l[\varkappa_5 X_l - 3\varkappa_4 X_l + G_L U_2 - G_l R_s] + 3X_l$$

$$S_7 = vR_r(G_L - G_1)$$

$$S_8 = U_4 - vS_6$$

Here

$$U_1 = R_s + R_r/2$$

$$U_2 = U_1 + R_s$$

$$G_l = T_1 U_1 + 2T_2 X_1$$

$$\varkappa_5 = -T_2 U_1 + 2T_1 X_l$$

$$U_3 = vR_r[3 + G_L U_2 - G_1 R_s - 3\varkappa_4 X_l + \varkappa_5 X_l]$$

$$U_4 = vR_r[\varkappa_4 U_2 - \varkappa_5 R_s + 3G_L X_l - G_l X_l]$$

APPENDIX- D

A 3-phase star connected asynchronous machine of rating 5 HP, 460 V, 60 Hz, pole pairs 2 for the simulation study and testing. The other technical details are:

D. 1 Various Electrical Parameters in Per-Unit (P.U)

R_{st} = 0.01965

X_{lst} = 0.03969

R_{ro}' = 0.019087

X_{lro} = 0.03969

X_{mg} = 1.3534

Inertia factor, JF = 0.09526

Friction factor, FF = 0.05479

D. 2 Saturation Characteristics in p.u

$L_{mg} = 1.1799$	$I_{mg} < 0.212$
$L_{mg} = 0.0814\, I_{mg}^2 - 0.5533 I_{mg} + 0.9943$	$0.212 < I_{mg} < 4.576$
$L_{mg} = 0.1159$	$4.563 < I_{mg} < 6.476$
$L_{mg} = 0$	$I_{mg} > 6.4763$

D. 3 PI Based Controller Gains

Optimal values of gains

K_{pac} = 32.4

Ki_{ac} = 1.24

D. 4 Prime Mover Characteristics in p. u

$T_{shaft} = a_1 - a_2 * w_{rs}$

a_1=2.36, a_2=1.011

APPENDIX- E

E. 1 Capacitor Bank Data

Excitation capacitance = 32.5 kVAR / phase

E. 2 Prime Mover Data

$$T_{shaft} = a_1 - a_2 * w_{rs}$$

a_1 = 1970; a_2 = 10.4

E. 3 Parameters of 3-Legged VSI

L_f = 17 mH, C_{db} = 2000 µF

PI Controller 1 Gains, K_{pav} = 0.115; K_{iav} = -0.051

PI Controller 2 Gains, K_{pdv} = 0.069; K_{idv} = -0.031

Switching frequency (f_s) = 10 kHz

Hysteresis band = ± 0.02

SCHOLAR BRIEF PROFILE OF THE RESEARCH

Ms. Shakuntla received the B.Tech degree in Electrical Engineering from MDU Rohtak (Haryana) in 1997 and M.E degree in Power Systems from Punjab Engineering College, Chandigarh in 2004. Since 2007, she is the part of YMCA University of Science & Technology as Assistant professor in the Department of Electrical Engineering. She is pursuing Ph. D in the field of Electrical Machines. She has more than 15 international and national publications in the area of electrical machines and asynchronous generators.

LIST OF PAPERS PUBLISHED OUT OF THESIS

SNO	Title of the paper along-with volume, Issue No, year of publication.	Publisher	Impact factor	Referred or Non-referred	Whether you paid any money or not for publication	Remarks
1	Dynamic D-Q axis modeling of three-phase asynchronous machine using MATLAB, Vol.2, Issue8, August 2013	IJAREEIE	5.621		-	
2	Electronics based Dump load Controller for an Grid Isolated Asynchronous Generator (GIAG), Vol.2, August 2015	International Journal on Emerging Technologies, Research Trend	3.1		Free	
3	Traditional PI and FPIL Based VFCU for an Isolated Induction Generator (IIG), Vol.9, No.12, Dec 2017	International Journal of Intelligent Systems and Applications, MECS	GIF=0.743	Referred	Free	Scopus
4.	Analytical and Experimental Investigations of Shunt Capacitor-Stimulated Induction Generator (SCSIG), Vol.4, 2018.	International Journal Series in Engineering Science	0.452	Referred	Free	SCI
5	Optimization Based Performance Evaluation of 3-Phase CEIG Feeding 1-Phase Load for Rural Sites	Science direct Procedia Computer Science				Scopus

LIST OF PAPER COMMUNICATED

SNO	Title of the paper along-with volume, Issue No, year of publication.	Publisher	Impact factor	Referred or Non-referred	Whether you paid any money or not for publication	Remarks
1.	Implementation of NCFPIL and CPI Based 3-legged VSI Controller	Journal of Engineering Science and Technology, Kavala Institute of Technology, Greece	SJR= 0.16		Free	Scopus

SUMMARY

I. GENERAL

The per-phase equivalent circuit approach of the asynchronous machine is only helpful for attaining the steady state condition analysis. In various types of adjustable speed drives, the machine constitutes an element within a feedback loop and therefore the analysis of the machine is also considered under transient state condition. The control scheme in case of high performance drive control such as vector or field oriented control is based on the dynamic d-q model of the machine. Such models can be described in different reference frames i.e. stationary or synchronously rotating frames [1-4].

An asynchronous machine can be operated as an asynchronous generator through self-excitation phenomenon. Such generators are termed as self-excited induction generator (SEIG) or Isolated Asynchronous Generator (IAG) [5]. An IAG is particularly preferred for electrification purpose in grid isolated remote areas using renewable energy sources, such as wind and mini-hydro turbines [6, 7].

An isolated asynchronous generator (IAG) is found to be the most preferable and economical option to generate electrical power in remote areas using locally available abundant renewable energy sources, such as wind and mini-hydro turbines. In early 1970's due to concerns regarding increase in prices of fossil fuel and its continuously depleting nature, the generation of electrical energy from the sustained, safe and pollution-free renewable energy sources has gained momentum. An IAG has emerged as a suitable candidate of such energy sources. It is because of its certain distinguishing advantages over a conventional synchronous generator as a source of isolated power supply.

Even though an IAG is very suitable for wind and mini-hydro plants, it can also efficiently be used with prime movers driven by other energy sources, such as diesel, biogas, natural gas, gasoline, etc. These advantages facilitate IAG operation in isolated mode for supplying local load. In remote locations or hilly areas, electrical energy from local resources can be inexpensive compared to grid operated systems.

The per-capita of energy consumption of a particular country is the direct indication of the economic development or growth of that country. It is estimated by the energy engineers that by the 21st century fossil fuels will be depleting or diminishing. The significance or relevance of non-conventional energy sources was recognized in India in 1970's. For people living in remote areas such type of generating systems prove to be more cost effective or economical than extending a power line to the electricity grid. Such types of generating systems are also preferred by the people living in the vicinity of the grid and willing to get independence from the power providers or whose inclination is towards non-polluting energy sources. Energy experts predicted renewable energy as the upcoming energy of future for energy generation. The energy generation using renewable energy techniques is more environmentally friendly and addresses the local demand of energy at the point of need. Use of such generating systems results in reduced transmission losses. This advantage fetches the attention of the researchers towards the use of renewable energy sources. A lot of research is already done but is still a topic of research. Many researchers have analyzed the steady state performance of IAG using equivalent circuit. In the earlier published research work, mainly two methods namely loop impedance and nodal admittance methods have been recommended for the solution of simultaneous non-linear equations. If the self-excited induction generator is loaded with resistive or inductive loads, its terminals voltage drops down by a considerable amount. However, in most of the applications, a constant terminal voltage source is required irrespective of the amount and nature of loads. The constant terminal voltage of this generator with varying loads can be maintained by adjusting the value of capacitor or speed. But the adjustment of speed is not easily possible and will require the complicated control of prime movers. Hence, the easiest way to maintain the constant terminal voltage is to adjust the value of capacitors or by connecting some power electronics or FACTS based controllers in shunt with the consumers load.

2. ANALYSIS OF IAG FEEDING BALANCED /UNBALANCED LOAD

2.1 Performance Analysis of 3-Phase IAG Feeding 3-Phase Load

Many researchers have analyzed the steady state performance of three-phase IAG feeding three-phase load using equivalent circuit. In the earlier published research work, mainly two methods namely loop impedance and nodal

admittance methods have been recommended for the solution of simultaneous non-linear equations [3-24].

A vast number of research papers covered the aforementioned two techniques of evaluating or investigating the performance characteristics of SEIG or an Isolated Asynchronous Generator (IAG) based on equivalent circuit using loop analysis technique [3-16]. The problem formulation consists of two simultaneous non-linear equations in terms of two unknown variables (frequency and magnetizing reactance). These equations are obtained after disintegrating real and imaginary parts of the total loop impedance and equating them individually to zero. Then these equations are evaluated using various numerical techniques like Newton Raphson method, Secant method, Golden section method etc. The solution of these equations yields the value of frequency and magnetizing reactance. With the aid of the attained value of frequency, magnetizing reactance and the magnetization characteristic, the equivalent circuit of an IAG can be completely solved. Hence, the complete performance of an IAG under steady state conditions can be analytically attained.

The steady state and transient analysis is also investigated using admittance method [17-24]. The problem formulation results into an equivalent circuit in terms of admittances. This method accounts the admittance of the air-gap voltage branch node of the equivalent circuit. Two simultaneous non-linear equations in terms of frequency and magnetizing reactance are attained after disintegrating real and imaginary parts of the total admittance and then equating them individually to zero. A higher degree polynomial in frequency is attained after equating the sum of real parts of total admittance equal to zero. Solution of this higher order polynomial outputs the value of frequency. The value of magnetizing reactance can be attained by using the aforementioned value of frequency and equating the sum of imaginary parts of the total impedance equal to zero.

2.2 Performance Analysis of 3-Phase IAG Furnishing a 1-Phase Load

Isolated Asynchronous generators (IAG) may be opted as a single-phase generating unit for feeding single-phase distribution unit [29-34] because of its

very simple protection scheme, low cost and almost maintenance free operation. Such systems suffers from

- Worse performance because these machines were originally designed for motor operation.
- More economical advantages for machine rating less than 5hp only.
- Complicated self-excited phenomenon in 1-phase asynchronous generator owing to the presence of backward rotating field.
- The backward rotating field attributes to the additional rotor losses and hence, the single-phase IAG proves to be less efficient than the corresponding 3-phase IAG.

Above 5 Hp, three-phase IAG is preferred due to economical advantages over single-phase IAG of the same rating. These advantages are low cost, more readily available and have higher efficiency than the equivalent rating single-phase machine. Hence, it thrives the researchers to use three-phase IAG for generating single phase power for feeding single-phase distribution system [35-48]. With passage of time or due to failure of one or two capacitors from the balanced excitation scheme of the machine, the drop in power output and voltage will not be highly affected and the machine continues to be operated as an IAG with the left over capacitors of the excitation scheme. The little bit unbalance in generating voltages and currents is visualized. To minimize these adverse effects, a lot of research has been focused on three-phase IAG feeding 1-phase load. This unbalanced operation is of utmost importance for various remote sites for low power applications where balanced operations are not required. The various applications of IAG in remote sites are 1-phase emergency supplies, as a portable source for construction sites, the isolated line repeaters etc.

2.3 VOLTAGE AND FREQUENCY REGULATION SCHEMES OF IAG FEEDING BALANCED/UNBALANCED LOADS

Various types of voltage and frequency controllers for Isolated Asynchronous Generator (IAG) have been developed and are reported in literature along-with its advantages and disadvantages [49-57]. The IAG can be used for constant power applications and for variable power applications. In constant power applications, prime mover rotational speed, value of excitation capacitor and the consumer load are kept constant and thus known as a single point operation. For

variable power applications, rotation of the prime mover is kept fixed but the value of excitation capacitance increases with load. For constant power application, generated power and consumer output power must be fixed for stable operation of three-phase IAG. Input power is maintained constant with the help of uncontrolled pico-hydro turbine but power output may not be constant due to varying consumer load. Most of the VFC's reported in literature employed conventional PI type controllers because of their simple design. The major drawback was in attaining the optimal performance. But, today different types of intelligent controllers are grabbing the attention of researcher [58].

Hence, a lot of research is also done on the development and implementation of 3-legged VSI based voltage and frequency control of an IAG at varying loads [59-74]. The design aspects of such controllers have been given little attention in literature [72]. To maintain constant terminal voltage at varying load, an attempt has been made using fixed capacitor topology, thyristor controlled reactor (TCR), saturable type reactors and short shunt type connections [59-62]. The drawback of these controllers is that the voltage control is discrete and hence injects harmonics on the generation side of the system. With the advancement of solid state power electronics devices, FACTS device are becoming more popular now a days as these devices are more environment friendly and helps to deliver the electrical power more economically, reliably and efficiently. The biggest constrained in using SVC is large size capacitors and reactors [66-67]. The non-linear loads introduce harmonics into the system and make the load current discontinues in nature. Hence once again the need of controller is realized to reduce the harmonics injected into the system and can make voltage and frequency regulation better. In almost all the published literature, mainly conventional PI controllers are employed for reactive and active power control to obtain voltage and frequency support. The main aspiration behind its use is its simplicity. But on the counterpart, there is difficulty in achieving the fine tuning of the gains to obtain desired performance particularly when more than one PI controllers are used. The second biggest drawback is encountered when the system is having non-linearity.

2. 4 OBJECTIVE OF STUDY / PROBLEM FORMULATION

As the poor voltage and frequency regulation is a major bottleneck in its commercialization. These controllers have been investigated either for a three-phase, 3-wire, or single-phase power applications of SEIG or IAG. Analysis, design and control aspects of self-excited induction generators (SEIG) are dealt in several papers. A crucial aspect in this area is the development of appropriate control mechanism to achieve desired output in terms of voltage, frequency and waveforms at different loads with different types of prime movers.

2.5 METHODOLOGY ADOPTED

- The transient/steady-state analysis of three -phase self-excited induction generator (SEIG) or IAG furnishing 3-phase/1-phase/static or dynamic load with an appropriate controller has been carried out.
- A composite mathematical model of the total system has been developed by combining the modeling of the prime mover, SEIG or IAG, controller and load.
- The dynamic model of the SEIG or IAG using a three phase asynchronous machine has been developed based on stationary reference frame.
- Simulated results have been compared with the experimental results attained on hardware set-up of IAG system.

The following steps have been adopted or followed to achieve the above mentioned objectives:

Step1: Literature survey

Step2: Dynamic d-q modelling of the asynchronous machine

Step3: Experimental and Optimization based analysis of IAG under balanced conditions.

Step4: Analysis of IAG under balanced and unbalanced conditions using symmetrical component theory.

Step5: An electronics generator load controller (EGLC) has been designed and simulated in MATLAB/SIMULINK to support voltage and frequency of an Isolated Asynchronous Generator (IAG) furnishing three-phase balanced and unbalanced consumer load for constant power applications.

Step6: Design and Implementation of conventional PI and fuzzy logic (FL) based EGLC for voltage and frequency support of an Isolated Asynchronous Generator (IAG) subjected to varying consumer load.

Step7: Hardware implementation of Electronic Generator Load Controller (EGLC) for an Isolated Asynchronous Generator (IAG) furnishing single-phase load.

Step8: Design and Implementation of 3-legged PI and Fuzzy logic (FL) based VSI controller for an IAG.

2.6 ORGANISATION OF THE THESIS

The whole work related to thesis is covered in ten chapters.

CHAPTER 1 first briefed about the research topic. Then it covers the brief theory of asynchronous machine and its d-q modelling in different reference frames. This chapter also described the dynamic modelling of 3-phase asynchronous motor in synchronously rotating frame. The influences of the step change in load torque on the motor output variables are examined. Then it discusses the various conditions under which an asynchronous machine starts working as an asynchronous generator along-with its advantages, disadvantages and its applications.

CHAPTER 2 covers the literature review of various issues related to an Isolated Asynchronous Generator (IAG) i.e. self-excitation phenomenon, analysis of IAG furnishing 3-phase and 1-phase load using various techniques. It also highlights the problem of poor voltage and frequency regulation and provides the state of art of various voltage and frequency controllers or regulators available in the past along-with its advantages and disadvantages.

CHAPTER 3 This chapter covers the analytical and optimization based analysis of IAG under balanced conditions. This chapter envisages initially the basic phenomenon of voltage build-up and the steady state analysis of 3-phase IAG furnishing three phase balanced resistive load. This preliminary study forms the foundation or basis of the design of future controllers. The conventional Newton Raphson technique and a MATLAB based optimization technique fsolve is elaborated in detail along-with advantages and disadvantages for attaining the solution of simultaneous non linear equation. The fsolve technique is adopted in this chapter for the solution of non-linear equations due to its advantages over conventional method.

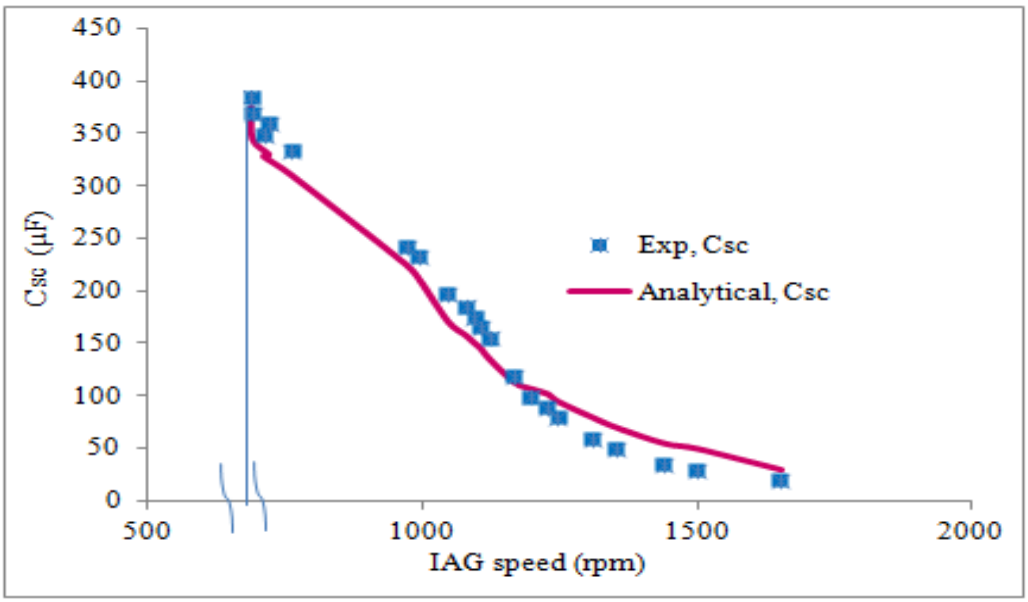

Fig.1 Variation of shunt capacitor excitation (C_{sc}) with speed at no load at constant speed

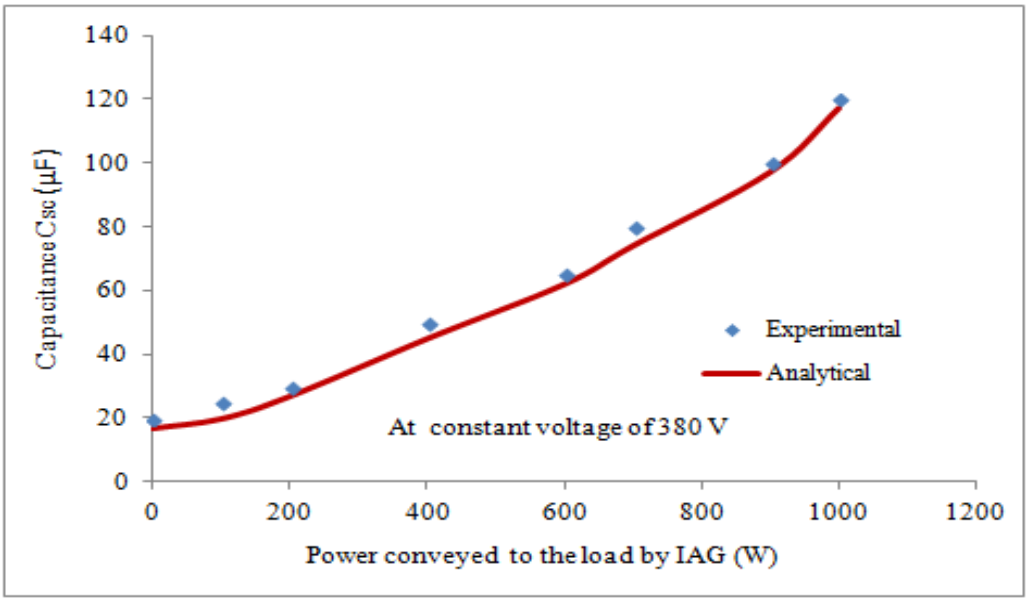

Fig. 2 Variation of Excitation capacitance with power conveyed to the load (W) at constant voltage

The solution of these equations yields the saturated value of magnetizing reactance X_{mg} and frequency F_y. Then the performance can be accessed from equivalent circuit using these values of X_{mg} and F_y. The effect of excitation capacitance on the different performance characteristics under no load and resistive load on the IAG is also investigated here. The experimental results outcomes are investigated on laboratory available asynchronous machine (AM) set of 3.73 kW coupled with a dc shunt machine (prime mover). The analytical and the experimental investigations outcomes

exhibit a very good association. The good association between the two outcomes authenticates the implementation of the proposed technique. The results under transient condition are captured using Fluke-434 Power Quality Analyzer. The variation pattern for capacitance with speed under no load and power delivered to the load is depicted in Fig. 1.and Fig. 2.

CHAPTER 4 In this chapter, analysis of IAG under balanced and unbalanced conditions is carried out using symmetrical component theory. The performance of 3-phase IAG furnishing unbalanced load and 1-phase load is investigated in this chapter. In this chapter, the performance equations describing the behaviour of the IAG under unbalanced operating conditions/single-phase load conditions is attained analytically using the concept of symmetrical component theory and the sequence equivalent circuits.

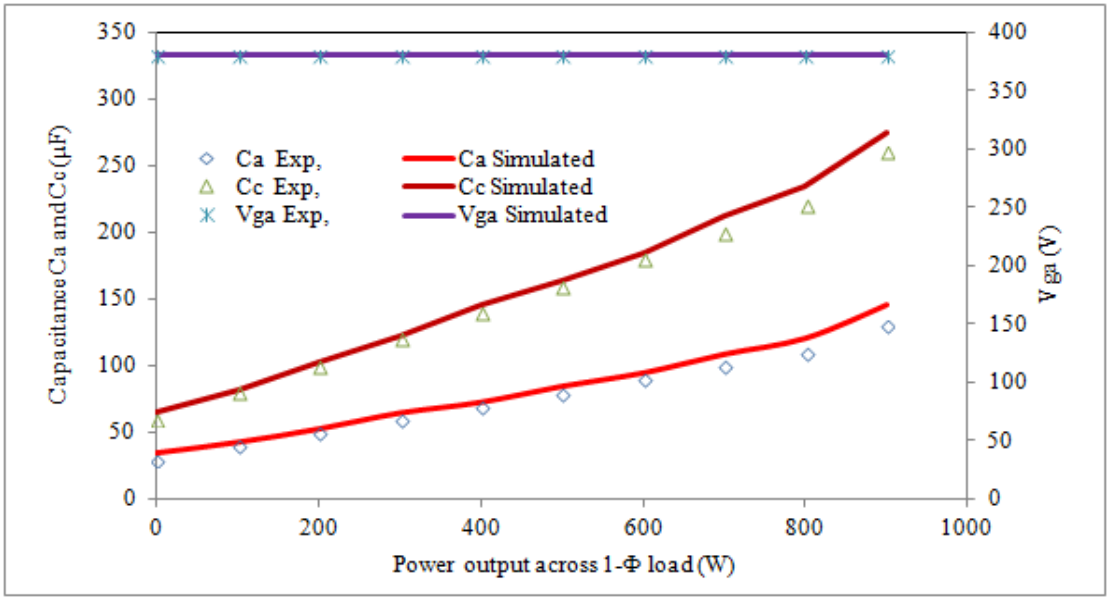

Fig. 3 Variation of capacitance with power output at unity power factor and at constant voltage.

The equation representing self-excitation criteria is a non-linear equation having two unknowns (magnetizing reactance and frequency). The solution of this nonlinear equation using fsolve technique results in the saturated value of magnetizing reactance (X_{mg}) and frequency (F_y). Using these evaluated values of X_{mg} and F_y, the complete performance equations can be accessed from the sequence equivalent circuits. The simulated results are verified experimentally in the laboratory. The results obtained show good degree of resemblance as depicted in Fig. 3.

CHAPTER 5 This chapter covers the design and simulation of an electronics generator load controller (EGLC) in MATLAB/SIMULINK to support IAG voltage and its frequency subjected to 3-phase balanced/unbalanced consumer load for constant power applications. The EGLC comprises of a six-pulse diode based bridge rectifier, IGBT switch, filtering capacitor, PI controller and a dump load (resistive). The transient behaviour of IAG-EGLC system is investigated and studied under different operating conditions to demonstrate the capabilities of EGLC and is illustrated in Fig. 4 and Fig. 5.

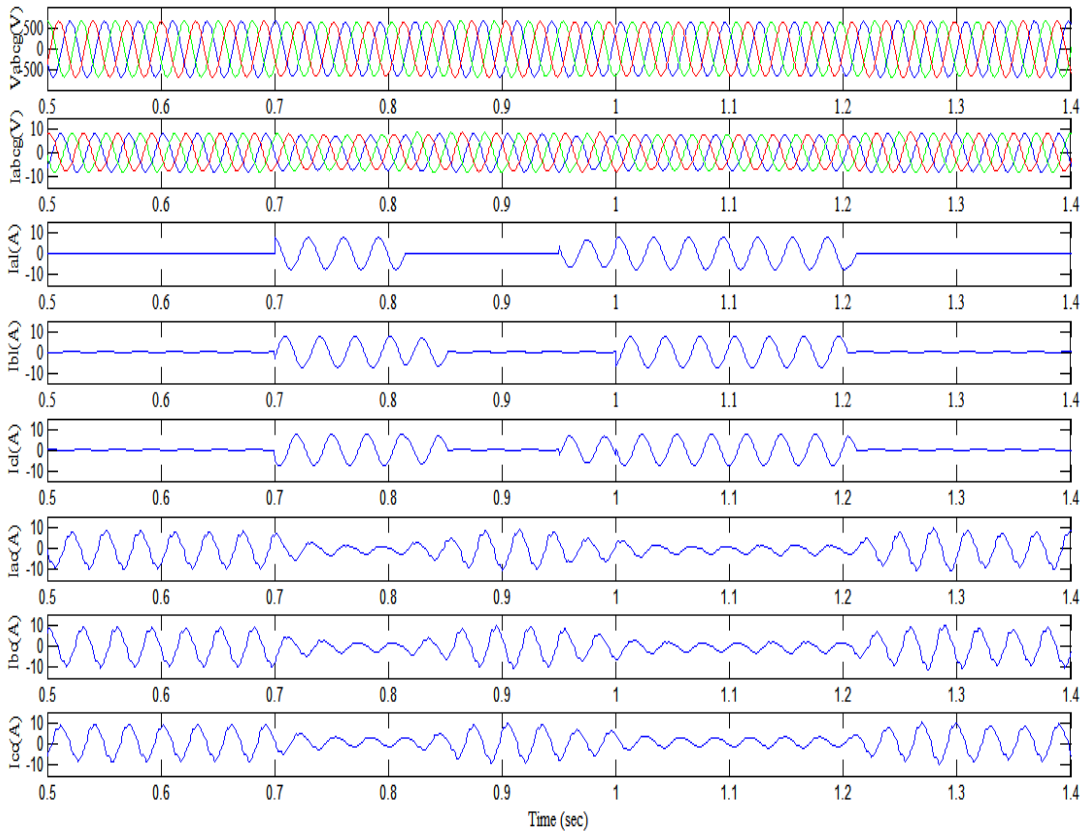

Fig. 4 Performance characteristics of IAG-EGLC system for pure resistive load using PI controller depicting ; the IAG voltage (V_{abcg}), IAG currents (I_{abcg}), load currents (I_{al}, I_{bl}, I_{cl}) and EGLC currents (I_{ac}, I_{bc}, I_{cc})

CHAPTER 6 This chapter covers the basic details regarding the fuzzy logic (FL) based controller approach. It also provides information based on different types of Fuzzy Inference System (FIS) along with its advantages and disadvantages. Two types of FIS i.e. Mamadani and Sugeno type are discussed for the performance enhancement of the system. It is observed that Mamdani type FIS is globally

acceptable whereas the Sugeno type FIS works efficiently with linear, optimization and adaptive techniques.

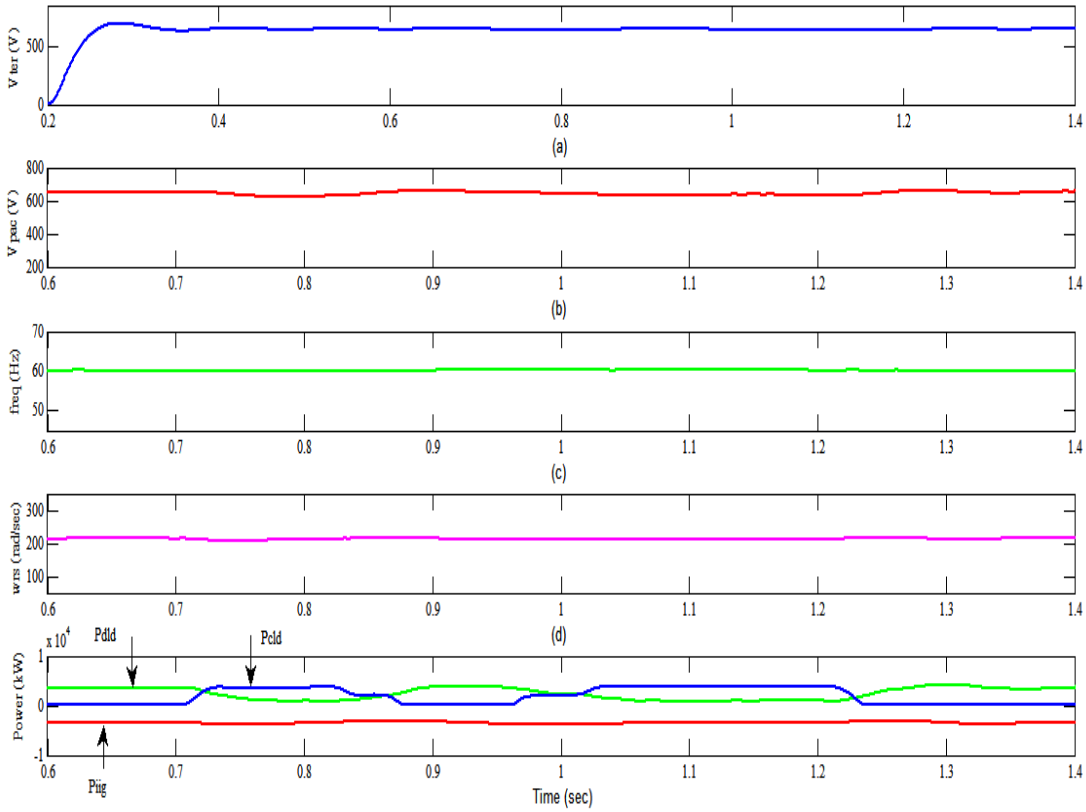

Fig. 5 Performance characteristics of IAG-EGLC system for pure resistive load using PI controller depicting; the IAG ac voltage magnitude (V_{ter}) , its peak ac voltage (V_{pac}), its frequency (freq), its speed (w_{rs}), IAG power (P_{iag}), consumer power (P_{cld}) and dump power (P_{dld}).

CHAPTER 7 This chapter explored the designing, realization and testing of PI and fuzzy logic (FL) based EGLC for an IAG subjected to varying load. The performance of IAG-EGLC system subjected to varying load is accomplished corresponding to transient and the steady. The performance enhancement of IAG is attained relating to rise time, settling time, and overshoot and THD values using the suggested FL based controller as inferred from the results.

CHAPTER 8 explains the hardware implementation of EGLC for an IAG furnishing single-phase loads in the laboratory. The voltage support at consumer terminals is required in remote areas. This voltage support should be provided economically. The study carried out in this chapter emphasis on the designing methodology and

implementation of an EGLC for an asynchronous generator feeding single-phase loads. The driving signals for the IGBT based chopper switch is generated using IC-3524. The generator is providing power to the two loads connected in shunt across each other. The objective of the controller is to maintain constant load or power on the generator during the entire operation of the generator. The outcomes have been verified using a hardware model of the IC-3524 based controller developed in laboratory to testify the expected results. The outcomes have been also evaluated and verified using MATLAB. Both results have been verified and justified its applications for feeding single-phase loads in remote areas as depicted in Fig. 8 and Fig. 9.

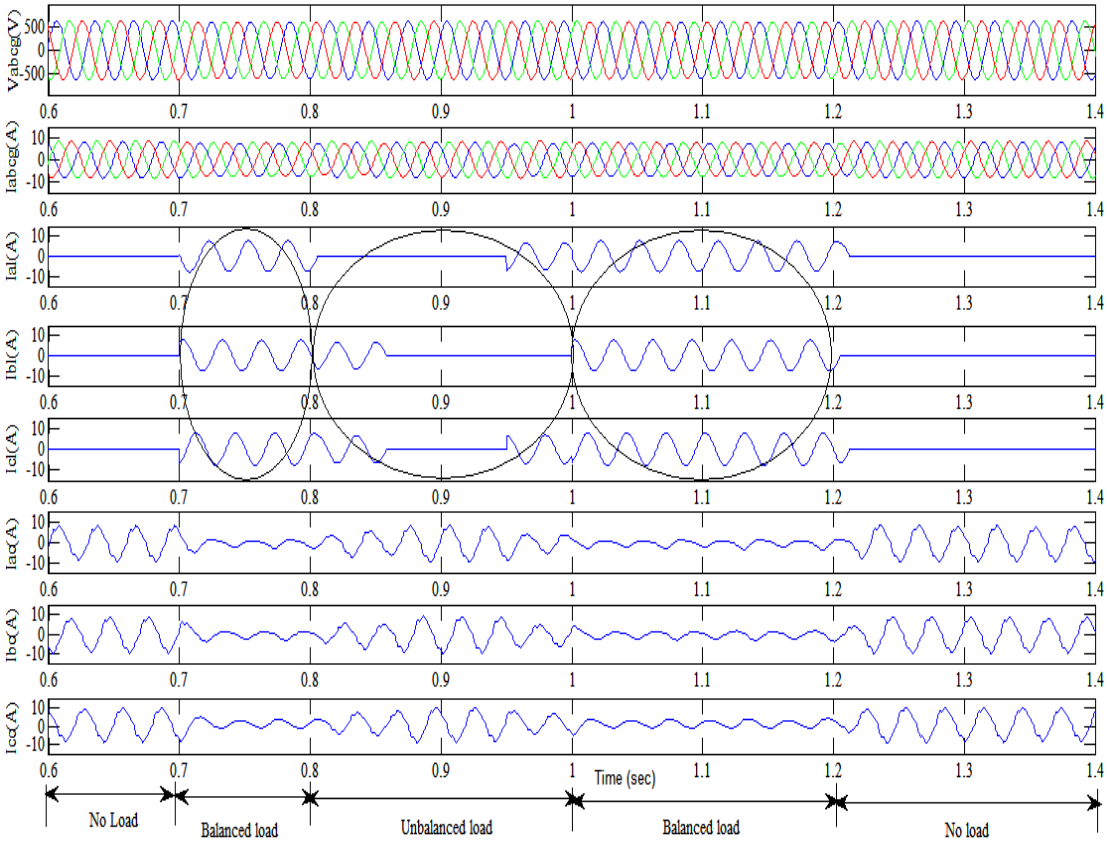

Fig. 6 Simulated transient characteristics waveforms of voltage generated by three-phase IAG (V_{abcg}), three-phase IAG currents (I_{abcg}), per-phase resistive load currents (I_{al}, I_{bl}, I_{cl}), per-phase EGLC currents (I_{ca}, I_{cb}, I_{cc}) under balanced and unbalanced resistive load using FL controller.

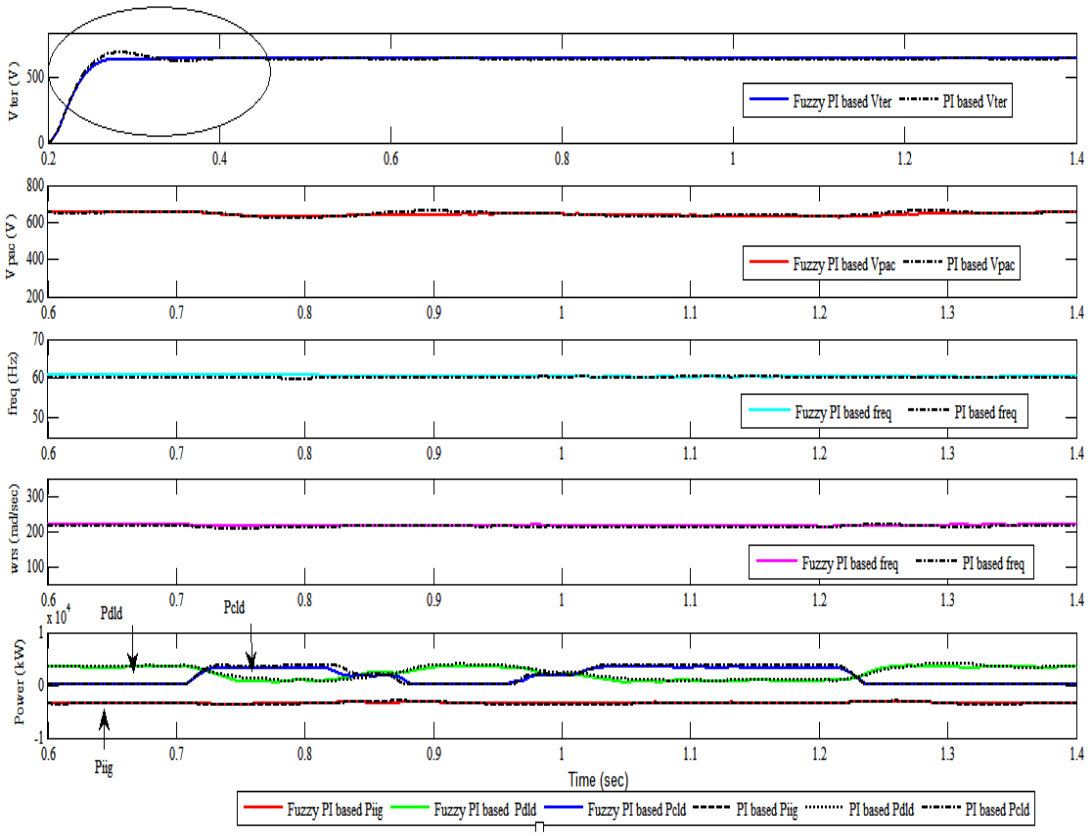

Fig. 7 Comparison of the simulated results of magnitude of terminal ac voltage (V_{ter}), peak value of generated ac voltage (V_{pac}), frequency (freq) , rotational speed (w_{rs}), power generated by IAG (P_{iig}), consumer load power (P_{cld}) and dump load power (P_{dld}) for pure resistive load using both PI and FL.

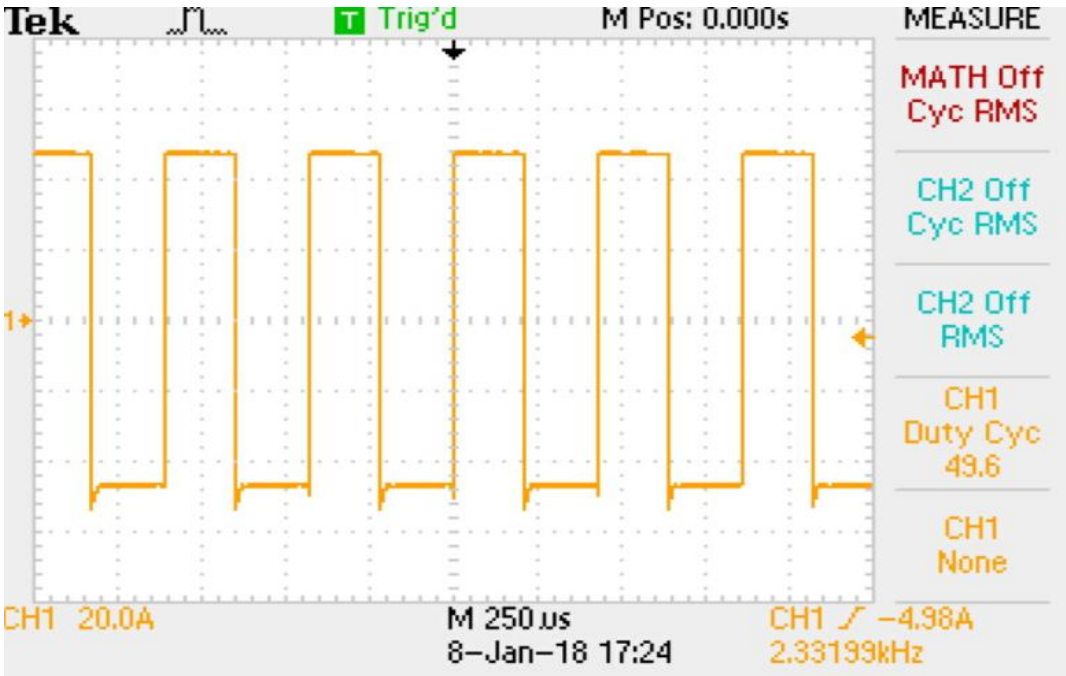

Fig. 8 Gating signal

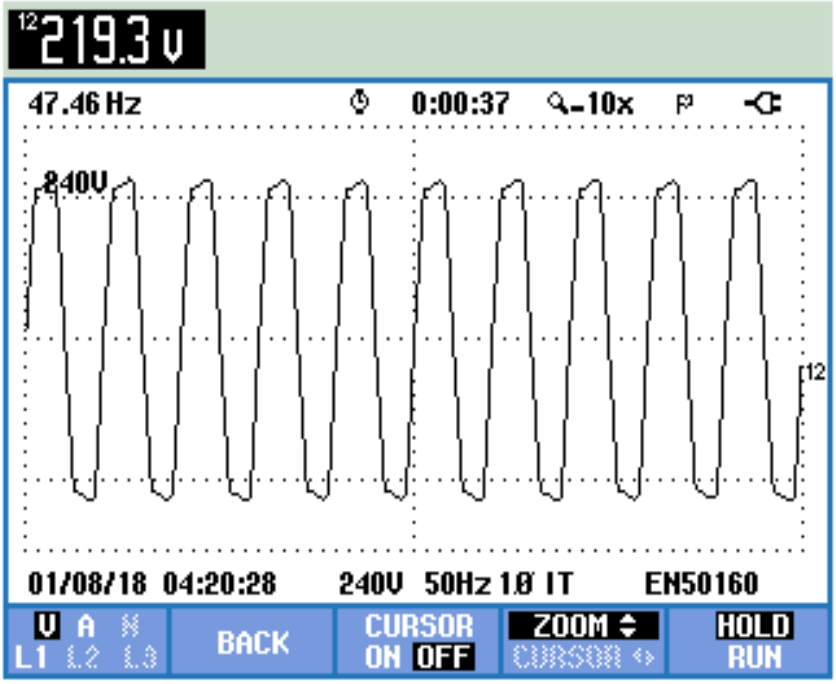

Fig. 9 Single-phase load voltage of IAG with EGLC

CHAPTER 9 In this chapter, two types of Fuzzy logic (FL) controllers (one for ac generated voltage and another for dc capacitor voltage control) are recommended to formulate template based algorithm for yielding reference supply currents. The recommended controller controls both reactive and active (kW) power parallely for retaining the IAG voltage and its frequency at the desired level under varying loads. The designing part of 3-legged VSI controller is also elaborated. The controller used here is formed by integrated various electronic components: 3-legged IGBT type current controlled VSI, high carrier frequency (10 kHz) DC type chopper and a capacitor across 3-legged VSI to filter out ripples in dc voltage. In this chapter, first the simulated outcomes of the performance characteristics are accomplished using Mamdani and Sugeno type FL based controller as illustrated in Fig.10 and Fig.11. Then, the comparison of various outcomes based on conventional PI and FL is made to testify that the recommended controller is superior to the conventional PI method and is well suited for power generation in isolation mode. Here, the whole electrical system and the controller are modelled using Simpower system and Fuzzy logic toolbox of MATLAB (version 7.8) software package.

CHAPTER 10 The various analysis or investigations made in the research work have been concluded in this chapter. It also highlights the scope for future work.

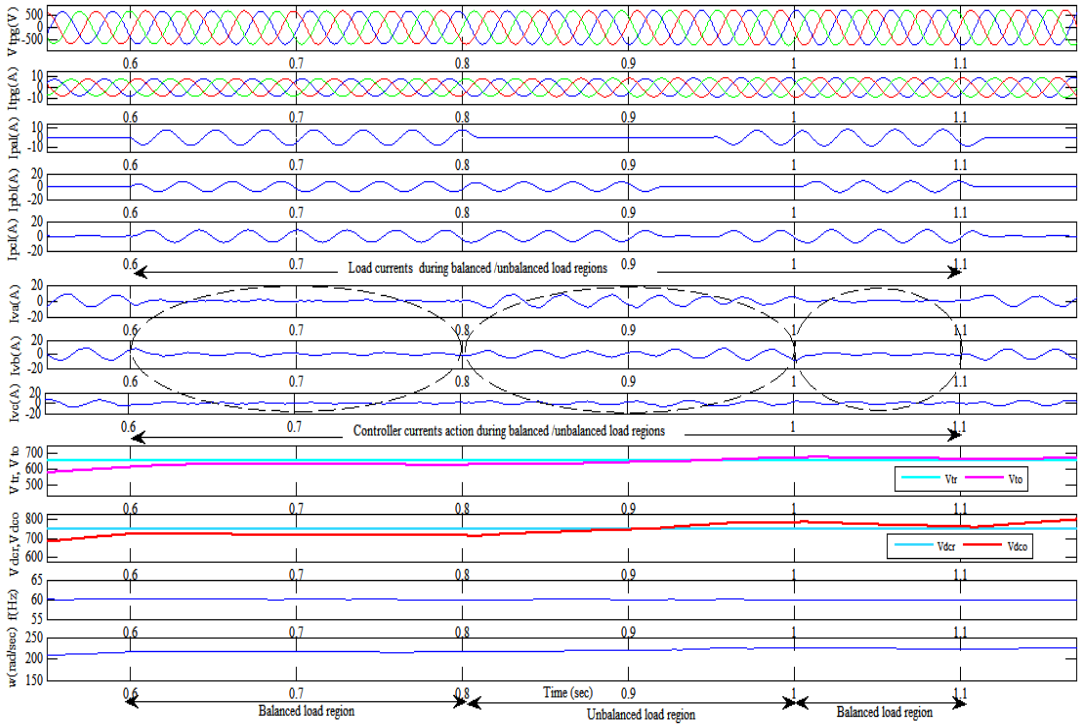

Fig. 10 Performance of an IAG furnishing resistive load using FL based Mamdani type controller.

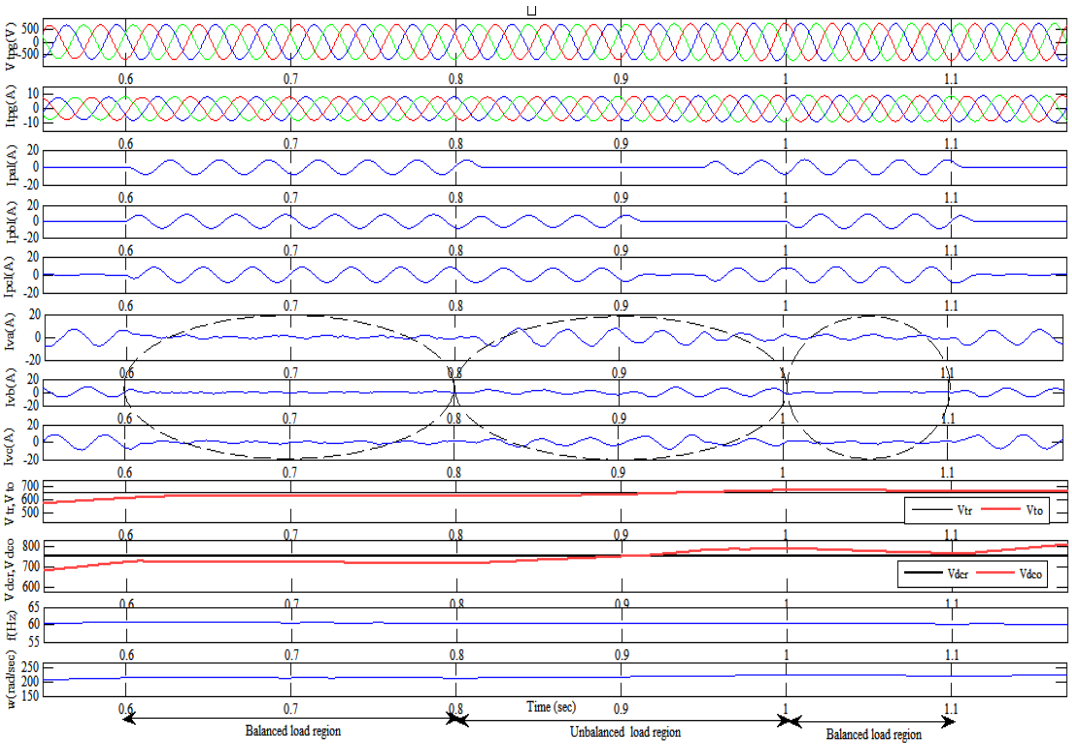

Fig. 11 Performance of an IAG furnishing resistive load using FL based Sugeno type controller

2.7 PROPOSED OUTCOME OF THE RESEARCH AND SCOPE OF FUTURE WORK

As the poor voltage and frequency regulation are the two constraints of IAG under load condition and restricted its use for the commercialization purposes. In almost all the published literature, mainly conventional PI controllers are employed for voltage and frequency support. The main aspiration behind its use is its simplicity.

But on the counterpart, there is difficulty in achieving the fine tuning of the gains to obtain desired performance particularly when more than one PI controllers are used. The second biggest drawback is encountered when the system is having both non-linearity and uncertainty.

The traditional PI and fuzzy logic (FL) based controllers are designed and implemented for EGLC and 3-legged VSI for an IAG for accomplishing its steady state and transient performance. The various performance characteristics related with IAG voltage, its frequency, speed and power etc are analyzed and compared using both methods. It is inferred from the outcomes that fuzzy logic (FL) based controllers enhanced the performance of IAG pertaining to rise time, settling time and overshoots. Also, the THD value of IAG voltage and its current using FL based controller are less than PI based controller. Thus FL based EGLC behaved as a supporter of load, generator voltage and its frequency and a THD minimiser. Hence, performance enhancement of IAG is achieved using FL based EGLC than the PI based controller.

The enhancement in performance characteristics of an IAG with a 3-legged VSI is accomplished using Mamdani and Sugeno type FL based controller. The comparison of various outcomes based on conventional PI and FL proved that the recommended controller is superior to the conventional PI method and is well suited for power generation in isolation mode.

In the present work, the performance enhancement of IAG is achieved using fuzzy logic approach based EGLC and three-legged VSI controller. In future work, an ANFSI based EGLC and 3-legged VSI controller will be developed for further enhancement in performance characteristics of an IAG.

The difficulties faced during the experimental work are:

- Loss of residual magnetism in the core at lower values of operating speeds.
- Implementation of IC-3524 based control strategy for IAG.

The hardware implementation of the control circuit of the controller can be realized using DSPACE and Controller HIL (C-HIL) Typhoon HIL. The Controller HIL (C-HIL) testing can be performed using Typhoon ultra high fidelity Typhoon HIL Simulator.

2.8 REFERENCES

[1]. K.L. Shi, T.F. Chan, Y. K. Wong and S. L. Ho, "Modeling and simulation of the three-phase induction motor using simulink", International Journal of Electrical Engineering Education, vol. 36, pp. 163-172, 1999.

[2]. P.C. Krause, O.Wasynczuk, S.D. Sudhoff, "Analysis of electric machinery and drive systems", IEEE Press, A John Wiley and Sons Inc. Publication, Second Edition, 2002.

[3]. Lee, R.J., Pillay, P., and Harley, R.G., "D, Q Reference frame for the simulation of induction motors", Electric Power Systems Research Journal, Vol. 8, pp. 15-16, October 1984.

[4]. B. Ozpineci, L.M. Tolbert, "Simulink implementation of induction machine model- A modular approach," IEEE Int.Conf. Electric Machine and Drives, pp.728-734, 2003.

[5]. B.C Doxey, "Theory and Application of the capacitor-excited induction generator", The Engineer, 216, pp. 893-897, 1963.

[6]. R. Holland, "Appropriate technology- Rural electrification in Developing countries", IEE Review, Vol. 35, No. 7, pp. 251-254, 1989.

[7]. S. S. Murthy, O.P. Malik and A.K. Tandon, "Analysis of self- excited induction generators", IEE Proceedings, Part C. Vol. 129, No. 6, pp. 260-265, 1982.

[8]. A. K. AI Jabri and A.I. Alolah, "Limits on the performance of the three phase self-excited induction generators", IEEE Trans. on Energy Conversion, Vol.5, No.2, pp.350-356, June 1990.

[9]. N.H. Malik and S.E. Hague, "Steady state analysis and performance of an isolated self-excited induction generator", IEEE Trans. on Energy Conversion, Vol. EC-1, No. 3, pp.134-139, September 1986.

[10]. S.P. Singh, B. Singh and M.P. Jain, “Performance Characteristics and Optimum utilization of a cage machine as Capacitor excited Induction Generator”, IEEE Trans. on Energy Power conversion, Vol. 5, pp. 679-685, 1990.

[11]. M.H. Haque, “A Novel method of Evaluating Performance Characteristics of a self-excited Induction Generator”, IEEE Trans. on Energy Conversion, Vol. 24, No.2, pp. 358-364, June 2009.

[12]. AI-Bahrani, A.H. and Malik, N. H., “Steady state analysis and performance characteristics of a three-phase induction generator self-excited with a single capacitor”, IEEE Trans. on Energy Conversion, Vol. 5, No. 4, pp. 725-732, 1990.

[13]. M. H. Haque and A.I. Maswood, “Determination of excitation capacitance of a three-phase self-excited induction generator”, IEEE Power and Energy Society General Meeting, pp.1-6, 2012.

[14]. S.S. Murthy, B. Singh, S. Gupta and B.M. Gulati, “General steady- state analysis of three-phase self-excited induction generator feeding three-phase unbalanced load/single-phase load for stand-alone applications”, IEE Proc-Gener. Transm. Distrib, Vol. 150, No. 1, pp. 49-55, Jan 2003.

[15]. AI-Bahrani, A.H. and Malik N. H., “Steady-state analysis of parallel operated self-excited induction generators”, Proc. IEE, Part C, Vol. 140, No. 1, pp. 49-55, 1993.

[16]. AI-Bahrani, A.H. and Malik N. H., “Voltage control of parallel operated self-excited induction generators”, IEEE Trans. on Energy Conversion, Vol. 8, No. 2, pp. 236-242, 1993.

[17]. A.H. AI-Bahrani, “Analysis of self-excited induction generators under unbalanced conditions”, Electric Machines and Power Systems, Vol. 24, pp.117-129, 1996.

[18]. N.H. Malik and A.H. Al-Bahrani, “Influence of the terminal capacitance on the performance characteristics of self-excited induction generator”, Proc. IEE, Vol. 137, Part C, No. 2, pp. 168-173, 1990.

[19]. Rahim, Y.H.A., “Excitation of isolated three-phase induction generator by a single capacitor”, IEE Proc., Pt. B., Vol. 140, No. 1, pp. 44-50, 1993.

[20]. K.S. Sandhu and S. K. Jain, “Operational aspects of self-excited induction generator using a new model”, Elec. Mach. Power Syst., Vol. 27, No. 2, pp. 169-180, 1999.

[21]. T.F Chan, “Analysis of self-excited induction generators using an Iterative method”, IEEE transactions on Energy Conversion, Vol. 10, No. 3, pp. 502-507, September 1995.

[22]. K. S. Sandhu, “Iterative model for the analysis of self-excited induction generator”, Elec. Power Comp. Syst. Vol.31, No. 10, pp. 925-939, 2003.

[23]. A. L. Alolah and M. A. Alkanhal, “Optimization-based steady state analysis of three-phase self-excited induction generator”, IEEE Trans. Energy Convers., Vol. 15, No. 1, pp. 61-65, March 2000.

[24]. D. Joshi, K. S. Sandhu, and M. K. Soni, “ Constant voltage and constant frequency operation of a self-excited induction generators”, IEEE Trans. Energy Convers., Vol. 21, No. 1, p. 228-234, March 2006.

[25]. T. F Chan, “Analysis of a single phase self-excited induction generator”, Electrical Machines and Power Systems, pp. 149-162, April 2007.

[26]. T. F Chan , “ Self-excited induction generators driven by regulated and unregulated turbines”, IEEE Trans. Energy Convers., Vol. 11, No. 2, p. 338-342, June 1996.

[27]. L. Quazene and G. Mcpherson, “Analysis of isolated induction generator”, IEEE Trans. Power App. Syst., Vol. PAS-102, No. 8, pp. 2793-2798, Aug. 1983.

[28]. J.L Bhattacharya and J.L Woodward, “Excitation balancing of a self-excited induction generator for maximum power output”, IEE Proc. Part C, Vol. 135, No. 2, pp. 88-97, 1988.

[29]. B. Singh, R. B Saxena, S.S. Murthy and B.P Singh, " A single-phase self-excited induction generator for lighting loads in remote areas”, International Journal on Electrical Engineering Education, Vol. 25, pp. 269-275, 1988.

[30]. T. F. Chan, “Analysis of a Single-Phase Self-Excited Induction Generator”, Electrical Machines and Power Systems, 1993.

[31]. S. S. Murthy, “A novel self-excited self-regulated single-phase induction generator, Part II: Experimental Investigation”, IEEE Trans. Energy Conversion, Vol.8 No.3, pp.377-388, 1993.

[32]. B. Singh and L. B Shilpkar, “Steady-state analysis of single-phase self-excited induction generator”, Proc. Inst. Elect. Power Application, Vol. 146, pp.421-42, 1999.

[33] Y.H.A. Rahim, A.I. Allah and R.I. Al-Mudhaiheem, “Performance of Single-Phase Induction Generators”, IEEE Trans. Energy Conversion, Vol. 8,pp. 389-395, 1993.

[34]. T. F Chan and L. L Lai, “Steady-state analysis and performance of a single-phase self-regulated self-excited induction generator”, IEE Proc. Gener. Transm. Distrib., Vol. 149, No.2, pp.233-241, 2002.

[35]. T. F Chan and L.L Lai, “Steady-state analysis and performance of a stand-alone three-phase induction-generator with asymmetrically connected load impedances and excitation capacitances”, IEEE Trans. on Energy Convers., Vol.16, No. 4, pp. 327-333, 2001.

[36]. S.S Murthy, B. Singh, S. Gupta and B.M Gulati, “ General steady-state analysis of three-phase self-excited induction generator feeding three-phase unbalanced load/single-phase load for stand-alone applications”, IEE Proc. Gener. Transm. Distrib., Vol.150, pp. 49–55, 2003.

[37]. A.H Al-Bahrani and N.H Malik, “Steady-state analysis and performance characteristic of a 3-phase induction generator self-excited with a single capacitor”, IEEE Trans. Energy Convers., Vol. 5, pp.725–732, 1990.

[38]. S.N Mahto, S.P Singh and M.P Sharma, “Capacitors required for maximum power of a self-excited single-phase induction generator using a three-phase machine”, IEEE Trans. Energy Convers., Vol. 23, pp. 372–381, 2008.

[39]. T.F Chan and L.L Lai, “Capacitance requirements of a three-phase induction generator self-excited with a single capacitance and supplying a single-phase load”, IEEE Trans. Energy Convers., Vol. 19, 222, 2004.

[40]. A. I Alolah and M. A Alkanhal , “Excitation requirements of three phase self excited induction generator under single phase loading with minimum unbalance”, in Proceedings of IEEE Power Engineering Society Winter Meeting, Singapore, Jan. 23–27, 2000.

[41]. Y.J Wang and S.Y Huang, “Analysis of a stand-alone three-phase self-excited induction generator with unbalanced load using a two-port network model”, IET Electr. Power Appl., Vol.3, pp. 445–452, 2009.

[42]. T.F Chan and Lai, L.L, “Phase balancing for a self-excited induction generator”, In Proceedings of International Conference of Power Utility Deregulation, Restructuring and Power Technologies, London, UK, pp. 602-607, 2000.

[43]. A.H Al-Bahrani and N.H Malik, “Steady-state analysis and performance characteristic of a 3-phase induction generator self-excited with a single capacitor”, IEEE Trans. Energy Convers., Vol. 5, pp.725–732, 1990.

[44]. T.F Chan, “Performance analysis of a three-phase induction generator self-excited with a single capacitance”, IEEE Trans. Energy Convers., Vol.14, pp. 894–900, 1990.

[45]. L. Wang and C.M Cheng,“Excitation capacitance required for an isolated three-phase induction generator under single-phasing mode of operation”, In Proceedings of International Conference of Power Engineering Society Winter Meeting, Columbus, USA, 27–31, 2001.

[46]. T. F Chan and L.L Lai, “Single-phase operation of a three-phase induction generator with the smith connection”, IEEE Trans. Energy Conversion, Vol.16, No. 2, pp. 47-54, 2002.

[47]. T.F Chan and L.L Lai, “A novel single-phase self-regulated self-excited induction generator using a three-phase machine”, IEEE Trans. Energy Conversion, Vol.17, pp.204-208, 2001.

[48]. T.F Chan and L.L Lai, “A novel excitation scheme for a stand-alone three-phase Induction Generator supplying single-phase loads,” IEEE Trans. Energy Conversion, Vol. 19, No.1, pp. 136-142, 2004.

[49]. B. Singh, S. S. Murthy and S. Gupta, “Analysis and implementation of an electronic load controller for a self-excited induction generator”, IEE Proc. Gener. Transm. Distrib., Vol.151, No.7, pp.51-60, January 2004.

[50]. B. Singh, S.S Murthy and S. Gupta, “Analysis and design of an electronic load controller for a self-excited induction generator”, IEEE Trans. On Energy Conversion, Vol. 21, No.1, pp.285-93, 2006.

[51]. T.S Chandra and P.M Bishnu, “Voltage regulators for self-excited induction generator,” IEEE Transactions on Energy Conversion, Vol. 20, No.4, pp. 460-463, April 2004.

[52]. S. Gao, S.S Murthy, G. Bhubaneswar and M. Sree Lalitha Gayathri, “Design of microcontroller based electronic load controller for a self-excited induction

generator supplying single-phase loads", Journal of Power Electronics, Vol.10, No.4, pp.444-449, 2010.

[53]. Juan M. Ramirez and Emmanuel Torres M., "An Electronic load controller for self-excited induction generators," IEEE PES General Meeting, June 24-28, 2007.

[54]. E.G. Marra and J.A. Promilo, "Induction- Generator- based system providing regulated voltage with frequency constant," IEEE Trans. Ind. Electron, Vol. 47, No. 4, pp. 908-914, 2010.

[55]. R. Bonert and S. Rajakaruna, "Self-excited Induction Generator with excellent voltage and frequency control", IEE Proc. Gener Transm. Distrib., Vol. 145, pp. 33-39, January 1998.

[56]. S.C Kuo and L Wang, P.M., "Analysis of voltage control for a self-excited induction generator using a current-controlled voltage source inverter (CC-VSI)", Proc. Inst. Elect. Eng., Transm. Distrib, Vol.148, pp. 431-438, Sept 2001.

[57] E. Suarez and G. Bortolotto, "Voltage frequency control of a self-excited induction Generator", IEEE Trans. Energy Convers, Vol.14, pp.394-40, Sept 1999.

[58]. Sachin Sharma and Bhim Singh, "Fuzzy proportional-integral regulators for stand-alone wind energy conversion system", IEEE Conference ICPCES, pp. 1-8, January 2011.

[59]. M.B Brennen and A Abbondati , "Static exciter for induction generator", IEEE transactions on Industrial Applications, Vol.13, pp.422-428., 1977.

[60]. R.K Mishra, B. Singh and M.K Vasantha, "Voltage regulator for a self-excited cage induction generator", Electrical Power System Research, Vol. 24, pp. 75-83, 1992

[61]. T.S Chandra and P.M Bishnu, "Voltage regulators for self excited induction generator", IEEE TENCON Conference, p.460-463, 2004.

[62]. L Shridhar, B. Singh and C.S Jha, "Transient analysis of the self-regulated short shunt self excited induction generator", IEEE Transaction on Energy Conversion, Vol.10, pp.261-267, 1985.

[63]. R.K Mishra, B. Singh and M.K Vasantha, "Voltage regulator for a self-excited cage induction generator", Electrical Power System Research, Vol. 24, pp. 75-83, 1992.

[64]. T.S Chandra and P.M Bishnu, “Voltage regulators for self excited induction generator”, IEEE TENCON Conference, pp.460-463, 2004.

[65]. L Shridhar, B Singh and C.S Jha, “Transient analysis of the self-regulated short shunt self excited induction generator”, IEEE Transaction on Energy Conversion, Vol.10, pp.261-267, 1985.

[66]. T Ahmed, E Hiraki, M Nakaoka and O Noro, “Three- phase self excited induction generator driven by a variable sped prime mover for clean renewable energy utilizations and its terminal voltage regulation characteristic by static var compensator”, IEEE IAS Annual Meeting. Conference on Industry Applications, pp. 693 -700, 2003.

[67]. T Ahmed, K Nishida and M Nakaoka, “Static var compensator based voltage regulator of single phase self-excited induction generator. IEEE IAS Annual Meeting Conference on Industry Application, pp.2069-2076, 2004.

[68]. B Singh and L.B Shilpakar, “Analysis of a novel solid state voltage regulator for a self-excited induction generator”, IEE Proceeding on Generation Transmission Distribution, Vol.14, pp.647-655, 1998.

[69]. S.C Kuo and L Wang, “Analysis of voltage control for a self-excited induction generator using a current controlled voltage source inverter (CC-VSI). IEE Proceeding on Generation Transmission Distribution, Vol.148, pp.431- 438, 2001.

[70]. S.C Kuo and L. Wang, “Analysis of isolated self excited induction generator feeding a rectifier load”, IEE Proceeding on Generation Transmission Distribution, Vol.149, pp.90- 97, 2002.

[71]. B Singh, S.S Murthy and S. Gupta, “STATCOM based voltage regulator for self-excited induction generator feeding non-linear loads”, IEEE Industrial Electronics Society Conference, Roanoke Virginia, USA, pp.709-714, 2003.

[72]. B Singh, S.S Murthy and S. Gupta, “Analysis and design of STATCOM based regulator for self-excited induction generator”, IEEE Transaction on Energy Conversion, Vol.19, pp.783-790, 2004.

[73]. B. Singh, S.S Murthy and S Gupta, “STATCOM based voltage regulator for self-excited induction generator feeding non-linear loads”, IEEE Transaction on Industrial Electronics, Vol. 53, pp.1437-1452, 2006.

[74]. M Bašić, D Vukadinović and M Polić, “Fuzzy logic vs. Classical PI voltage regulator for a self-excited induction generator”, Mathematical Applications in Science and Mechanics, pp.189-194, 2013.